Sheffield Hallam University

Capillary electrophoresis in the analysis and characterisation of lubricant additives.

SMITH, John E.

Available from Sheffield Hallam University Research Archive (SHURA) at:

http://shura.shu.ac.uk/20666/

This document is the author deposited version. You are advised to consult the publisher's version if you wish to cite from it.

Published version

SMITH, John E. (2004). Capillary electrophoresis in the analysis and characterisation of lubricant additives. Doctoral, Sheffield Hallam University (United Kingdom)..

Copyright and re-use policy

See http://shura.shu.ac.uk/information.html

Sheffield Hallam University Research Archive
http://shura.shu.ac.uk

Return to Learning Centre of issue
^ e s are charged a, S O p p ^

2 5 JAH 2007

Lf-.OM *r*

REFERENCE

ProQuest Number: 10702003

All rights reserved

INFORMATION TO ALL USERS
The quality of this reproduction is dependent upon the quality of the copy submitted.

In the unlikely event that the author did not send a complete manuscript
and there are missing pages, these will be noted. Also, if material had to be removed,
a note will indicate the deletion.

uest

ProQuest 10702003

Published by ProQuest LLC(2017). Copyright of the Dissertation is held by the Author.

All rights reserved.
This work is protected against unauthorized copying under Title 17, United States Code
Microform Edition © ProQuest LLC.

ProQuest LLC.
789 East Eisenhower Parkway
P.O. Box 1346
Ann Arbor, MI 48106- 1346

Capillary Electrophoresis in the Analysis and Characterisation of Lubricant Additives

John Eric Smith

A thesis submitted in partial fulfilment of the requirements of
Sheffield Hallam University
For the degree of Doctor of Philosophy

December 2004

Collaborating Organisation: Castrol UK Ltd

Candidates Statement

The aim of this work was to assess and develop methodology for the use of nonaqueous capillary electrophoresis with ultraviolet and mass spectrometry detection for the lubrication industry. Methods were developed for two additives, zinc dialkyldithiophosphates and alkylsalicylates. These methods were then applied to the analysis of formulated lubricant products with success.

The work detailed in this thesis was carried out by the author at the School of Science and Mathematics, between October 1999 and October 2002, contributions made by third parties for work in chapter 8 has been acknowledged. Work displayed in this thesis is original except where acknowledged by reference.

John Eric Smith

Abstract

Capillary electrophoresis (CE) has proved to be a very efficient separation method in aqueous media. This work reports developments in nonaqueous capillary electrophoresis (NACE) for samples from the lubricants industry.

Two commonly used additives in lubricants, zinc dialkyldithiophosphate and the metallic detergent alkylsalicylate, were analysed. Method development included selection of solvent, pH*, and electrolyte type and concentration.

Improvements in the separation were obtained by altering the injection conditions and the electric field strength. Hexadimethrine bromide (HDB) was shown to be essential in controlling the electroosmotic flow (EOF), and its concentration was optimised. Best separation was seen when analyte dilution prior to injection was carried out with methanol, resulting in sample stacking.

Analysis of ZDDPs showed that separation occurred through migration of free dithiophosphate ions. Calcium alkylsalicylate showed similar results where the free alkylsalicylate ions migrated. Identification was achieved through peak patterns and relative migration times.

Adequate separation conditions were identified and then coupling of NACE to mass spectrometry was attempted. Direct infusion MS was first utilised with great success in identification of the two additives. Using a solution of methanol and ammonium acetate it was possible to identify free dithiophosphate ions from the ZDDP and free alkylsalicylate ions from magnesium alkylsalicylates. Only the molecular ions were obtained in all instances making identification easier.
NACE-MS was carried out successfully; however, sample dilution and adequate interfacing were problematic.

Analysis of formulated lubricating oil was performed by NACE, NACE-MS and MS. Degradation products were identified for ZDDPs, where sulphur atoms were replaced with oxygen leading to the formation of phosphates.

NACE has been shown to be a technique of potential for the analysis of lubricant additives, and in combination with mass spectrometry it could be very powerful.

Acknowledgements

This work is dedicated to my daughter Caitlin who always puts a smile on my face and to the memories of my grandma and Dr Lee W Tetler.

I would like to thank Dr David Crowther and Dr Duncan Leech for their willingness to take on and help finish this project. I would also like to thank Dr David Crowther for the support he has shown me in my personal life in a turbulent year.

I am also grateful to the technical staff especially Paul Collins and the late Barry Christian for their expertise with ICP and NMR experiments.

During my time I have made some good friends who made the experience less painful Jill, Edward, Peter, Arun (especially the long nights running experiments), Shaun, Boris, Kevin, Mike and Bimal.

On a more personal level I would like to thank my mum and dad for unwavering support. Anthony and Davina whose lives I have invaded, they never complained and always had time to listen, thanks also to my sister and brother. Thanks for putting a smile on my face Nina, Lauren, Lisa, Abbie, Billy and Aidan. Also thanks to Mick (the fastest milkman in town) for lending an ear, I promise I will give it back to you!

I would finally like to thank Sharon who stood by me going to university and then again to do my PhD. I will be eternally grateful for what she sacrificed and also for bringing our daughter into this world.

I love you all.

Contents

Chapter 1

Introduction to Lubrication and Additives

1.0 Friction

When two surfaces are in contact and in opposing motion friction is produced. Friction opposes motion regardless of the material, shape or size of the surfaces in contact. Friction is caused by molecular attraction between two surfaces, interlocking of opposing surface irregularities (asperities, figure 1) and surface waviness. The friction generated between two surfaces in contact depends on the type of friction, pressure applied, nature and condition of the surfaces. The amount of friction present in a system can be seen in the amount of heat generated, rate of wear and the power to maintain motion.

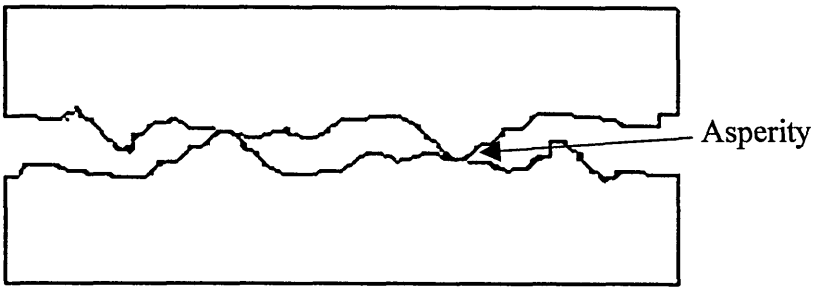

Figure 1.0 A graphic representation of two surfaces in contact showing the unevenness seen on even the smoothest surface.

1.1 Wear

The consequence of friction is wear, wear is essentially the diminishing surface area at a rate that is partly comparable to the amount friction present. However, wear is complicated and a combination of mechanisms may be present, being:

- Adhesive (friction)
- Abrasive (friction)
- Corrosive
- Fatigue

- Fretting

1.2 Lubrication

Lubrication is the science of reducing friction to a minimum, it is used to essentially separate the two surfaces that are in contact. There are various materials used for this purpose and are shown in table 1 below:

Material	Use
Liquids (oil)	Engines
Semi liquids (greases)	Gear boxes
Solids	Brake pads
Gases	Dentists drills

Table 1.0 Shows the different materials used for lubrication and one use.

There are three main types of lubrication in the reduction of friction: being boundary, fluid and mixed.

1.2.1 Boundary lubrication

A protective layer is formed by chemical and physical reactions between the surface and the surrounding lubricant, additives or atmosphere (figure 1.1). Fatty acids form the boundary lubricants, via the formation of a single monolayer of soap. This monolayer is also seen with other long chain hydrocarbon molecules. Boundary lubrication is essential during the starting and stopping of machines.

Figure 1.1 Boundary lubrication.

1.2.2 Fluid film lubrication

A fluid film completely separates two surfaces (figure 1.2). To maintain this separation of the two surfaces the pressure in the lubricating film must equal the load on the two surfaces.

Figure 1.2 Fluid film lubrication.

1.2.3 Mixed lubrication

As the name suggests, mixed lubrication is a mixture of both fluid film and boundary lubrication. It is encountered in gears, ball and roller bearings.

Figure 1.3 Mixed lubrication.

1.2.4 Sources of Lubricating Oil

Lubrication is used to prevent friction and wear of two rubbing surfaces, a typical example is the internal combustion engine. The application and use of lubrication is seen in history, and in nature. Prior to the 19th century and the industrial revolution a commonly used lubricant was animal fat. The growth of the petroleum industry brought about a new source of lubricant stock, crude oil. Modern times have seen the introduction of synthetic lubricants; however, the majority are still petroleum products derived from crude oil. Crude oil fields are found world wide (see table 1.1), where Saudi Arabia has the largest oil reserves in the world as well as the largest oil field in the Al-Ghawar.

Region	Cumulative Production*	Reserves*
North America	202	106
South America	74	93
Western Europe	23	19
Eastern Europe	113	104
Central Asia & Transcaucasia	16	24
Middle East	194	666
Africa	57	32
Oceania and Asia	45	45
TOTAL	**724**	**1,119**

Table 1.1 Shows the regions of oil production (*billions of barrels).

Crude oil has, as its major constituents, carbon (84%) and hydrogen (14%), with other components that include sulphur (1-3%), nitrogen (<1%) and oxygen (<1%); metallic elements (<1%), salts (1%) and decay-resistant organic remains such as siliceous skeletal fragments, wood and spores among others. The hydrocarbon content of crude oil can be grouped into basic chemical series. The paraffinic series consists of saturated straight and branched chain hydrocarbons (C_nH_{2n+2}). The naphthenic series

consists of complex cyclic hydrocarbons (C_nH_{2n}), the aromatic series (C_6H_5-Y) where y is a straight or branched alkyl chain attached to a benzene ring. Other hydrocarbons present are alkenes ($C_2H_{21}O$, dienes and alkynes (C_nH_{2n-2})- In its original state crude oil is not appropriate for use in lubrication due to its many contaminants and its viscosity, and therefore refining of the crude oil provides the oil consistency that is required for lubrication products.

Oil refining separates all the different hydrocarbon chain lengths according to their boiling points, the higher the boiling point the longer the chain length. This method of refining crude oil is called fractional distillation (see figure 1.4 page 6). Using this method a number of products are obtained petroleum gas, naphtha, petrol, kerosene, diesel, lubricating oil, fuel oil and residuals.

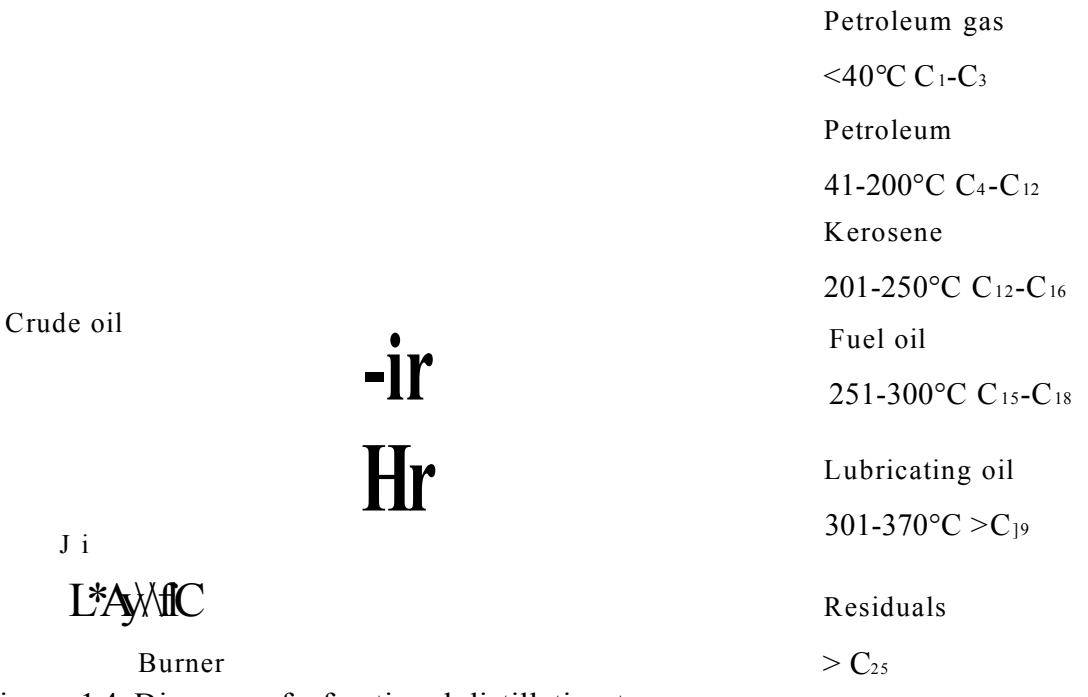

Figure 1.4 Diagram of a fractional distillation tower.

The fractions that make up the lubricating oil or base stock can be naphthenic, aromatic or paraffinic; however, mixtures are mostly used. Once obtained, the base stock is

further processed or cleaned to further remove any unwanted contaminants such as some aromatics, asphalt and naphthenic acid that would otherwise reduce thermal and oxidative stability as well as any wax that would cause the lubricant to solidify at low temperatures. The clean-up processes could incorporate the use of acid treatment followed by a caustic wash, which is then followed by filtration. The removal of wax may be carried out by refrigeration. More recently, solvents and solvent mixtures have been used to clean up lubricant base stock.

An alternate method for refining crude oil is hydrocracking; the crude oil is treated with hydrogen to break up many of the molecules. This method removes very long molecules and reduces the wax content of the subsequent lubricating base stock.

Synthetic base stock is manufactured chemically to possess superior viscosity characteristics at low temperatures as well as improved thermal and oxidative stability. The advantage of using synthetic base stocks is that they can be manufactured to meet specific thermal or physical requirements.

Once the lubricant base stock has been cleaned up, it undergoes blending. Blending mixes various types of refined lubricant base oils with various viscosities and in various proportions, with performance additives to make up a finished lubricant. The blending process ensures that the highest quality and performance lubricant is manufactured. A typical lubricant oil is composed of several different lubricant base oils, these being mineral or synthetic plus several performance additives each contributing a characteristic to the final product.

1.3 Additives

The hydrocarbon base oil is exposed to very harsh conditions. These are high shear stress, high temperatures and chemical attack by fuel combustion products or 'blow-by' gases. Oxidation of hydrocarbon oil produces corrosive products, which result in fine particles being present in the oil. Particles agglomerate or become deposited on the internal surfaces of combustion engines. The agglomerated particles settle into the crankcase, as tar-like deposits, slimy sludge or granules, from where they can then be re-cycled through the engine.

On re-cycling through the engine, oxidation products can be deposited on pistons where a hard material that resembles varnish develops. Also formed are carbonaceous deposits with soot-like appearance that can be deposited on the internal surfaces of an engine impacting on efficiency. The presence of water in the cooler engine parts increases oxidation and produces acids of carboxylic and mineral (sulphuric, nitric and hydrochloric) types. To this end and for improvement of lubricant performance and longevity, lubricant additives are utilised. It is easy to remember that oxidation converts a clean efficient engine into a dirty inefficient engine.

A wide range of additives are available for use within a lubricant; however, not all are used at any one time and the additives chosen are tailored for the role the lubricant has to play. The table below shows the different types of additives available.

Additive type				
Anti-oxidant	Anti-spalling	Radiation protection material	Anti-foaming agents	Fungicide
Anti-stick slip friction modifier	Anti-wear	Bactericide	Wetting agents	Demulsifiers
Detergents	Ashless dispersants	Thickening agent	Running-in improver	Emulsifiers
Extreme pressure	Colour dyes	Film strength	Flow improvers	Tackiness
Coupling agents	Friction modifier	Viscosity index improver	Anti-rust	Anti-corrosion
Pour point depression	Seal expanders	Anti-friction	Anti-oxidants	Anti-rust

Table 1.2 Some of the types of additives available for lubricant products.

Although the table shows a wide range of additives, most of the compounds used can carry out more than one job.

To illustrate the use of these additives, the table below shows some specific equipment and the additives used in lubricating oil, the additive packages used making up some 15 to 20% of the lubricant.

Equipment	Additives used
Petrol engine	Anti-oxidant, corrosion inhibitor, viscosity index improver, detergent/dispersant, anti-wear.
Diesel engine	Anti-oxidant, corrosion inhibitor, detergent/dispersant, anti-wear, anti-foam, basic additive (neutralise acid)
Steam turbines, compressors	Anti-oxidant, corrosion inhibitor, anti-emulsifier.

Table 1.3 The different additive packages used in different equipment.

The work described in this thesis is focused on an anti-wear additive and a detergent additive used in diesel and petrol engines, these being zinc dialkyldithiophosphates and alkyl salicylates, respectively.

1.4 Zinc dialkyldithiophosphates (ZDDPs)

1.4.1 Synthesis of ZDDPs

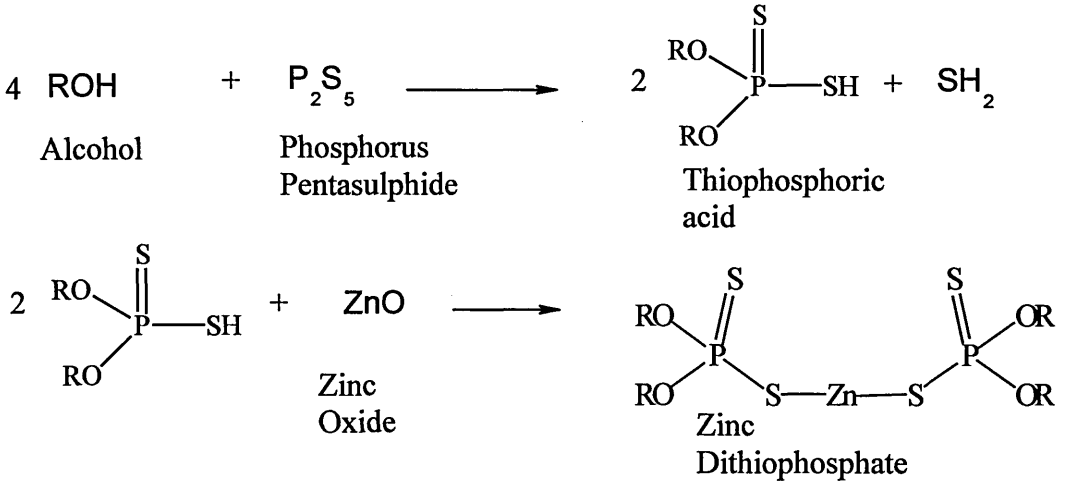

Figure 1.5 The synthesis route of ZDDPs as commonly used in industry.

1.4.2 How zinc dialkyldithiophosphates work

Zinc dialkyldithiophosphates (ZDDPs) are a family of compounds used within the lubrication industry for their anti-wear and anti-oxidant properties.

Under the severe conditions seen within an internal combustion engine blowby gases and oil contain many metal reactive species. These are seen as mineral acids as well as oxygen, water, peroxy radicals and hydroperoxides[1] among many others, which all lead to severe engine wear if not kept under control. As well as the aforesaid effects the friction between two surfaces is another factor that has to be eliminated to prevent wear. ZDDPs are compounds that can play an essential role containing and eliminating both chemical and mechanical forces that result in wear and catastrophic engine failure. The action of ZDDP is very complex and as of yet is not fully understood.

Roberts *et al.* (1997)[2] investigated the three structures that ZDDP can be found in for stability. The three structures were classed as neutral ($Zn[PS_2\ (OR)_2]_2$), dimeric ($Zn_2[PS_2\ (OR)_2]_4$) and basic ($Zn_4[PS_2\ (OR)_2]_6\ O$). They concluded that the basic structure was most stable, this stability results in slower reaction rates and as such longer times are required for producing anti-wear films and its antioxidant properties.

In 1967 Dickert Jr and Rowe[3] studied the thermal decomposition of a ZDDP; at 155°C a glass like insoluble solid was formed that was difficult to characterise. The vapours given off were propylene, a mercaptan and hydrogen sulphide. The reactions followed an induction period where little reactivity occurred; this induction could be shortened by the addition of an acid leading to suggestions that there was an autocatalytic character to the decomposition of ZDDP. The decomposition of hydroperoxides by ZDDP was also studied, ZDDP decomposed hydroperoxide forming the basic ZDDP (anti-oxidant properties), dithiophosphate and alcohol. Thiophosphoric acid ($(RO)_2\ PS_2H$ ~pKa 1)[4] a ZDDP decomposition product decomposes hydroperoxides forming

dithiophosphate, alcohol and water. The thiophosphoric acid is in turn produced by the decompositon of ZDDP by water. In essence ZDDP is decomposed by three general methods thermal, hydrolytic and oxidation. All take part and have a role to play in recycling products used in different pathways. Bancroft *et al.*[5,6] showed by x-ray absorption near edge spectrometry (XANES) that a precipitate formed on a metal surface from heating a ZDDP oil solution consisted of a long chain polyphosphate structure. These types of islands are glass like in appearance and likely to be polyphosphate aggregates that form via thermo-oxidative decomposition of ZDDP. It is thought that an oxide layer is first formed on the metal surface, 20nm thick, thereafter an inorganic polyphosphate layer approximately 40nm thick followed by an alkyl phosphate precipitate layer. Papay (1998)[7] states that ZDDP adsorbs to the metal oxide layer, the more polar the molecule and the longer the alkyl chain the greater the adsorption. Greater adsorption means a greater build up of anti-wear additive, the polyphosphate mixture of the anti-wear film is polymer like, along the lines of:

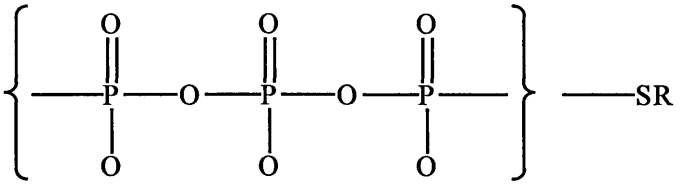

Figure 1.6 The suggested structure of a polyphosphate chain.

This is similar to a ZDDP thermal decomposition product described by Woo and Mosey (2003)[8] in a mechanism for the elimination of olefins and sulphide (seen in work carried out by Dickert and Rowe[3]). However, Woo and Mosey did not take into account the conditions within a combustion engine.

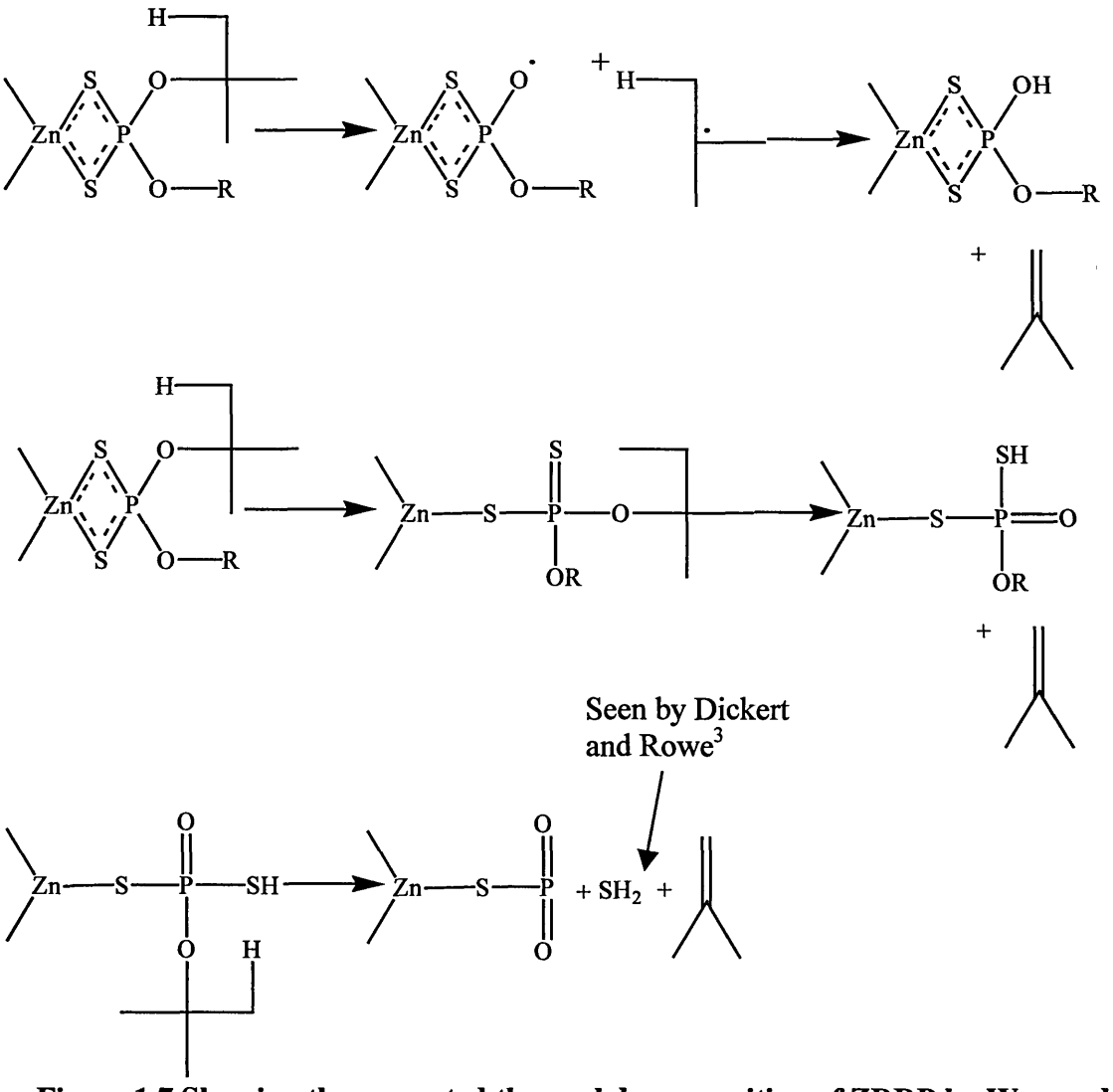

Figure 1.7 Showing the suggested thermal decomposition of ZDDP by Woo and Mosey.

ZDDP degradation was monitored by P-31 nuclear magnetic resonance spectroscopy[9]. It was determined that the major degradation products were dithiophosphates (S=P-S), thiophosphates (S=P-O and O=P-S), thiophosphoric salts (S=P-O$^-$); further oxidation of thiophosphates saw the production of phosphates (O=P-O). Unlike Roberts *et al.*[2] this study showed that, under combustion engine testing, the basic ZDDP degraded more easily than the neutral ZDDP and its anti-oxidant properties forming phosphates was very much temperature dependant.

For the production of anti-wear films it is necessary for the ZDDP to be degraded, as the active compounds for these films are phosphates, thiophosphates and thiophosphoric acids. At low temperatures a physisorbed film is formed, while at higher temperatures a more stable chemisorbed film is observed[7,10]. However at the higher temperatures oxidation of ZDDP is greater and therefore the reserve of precursor is consumed.

The presence of other additives such as metallic detergents and dispersants further complicates the reactions of ZDDP as they are known to interact within the bulk of the oil. These interactions and their results on reactions have not yet been fully established. However, Rounds[11] suggested two possible routes for the formation of thiophosphoric acid:

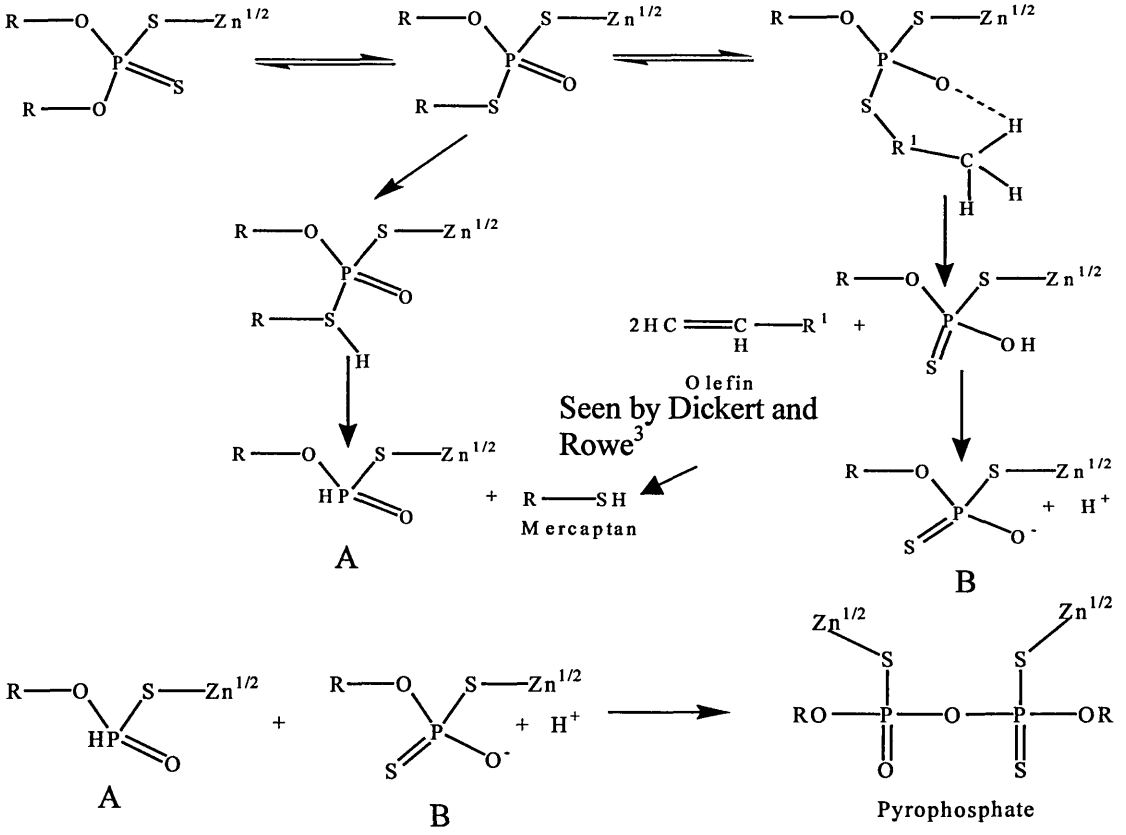

Figure 1.8 Suggested mechanism for the formation of thiophosporic acid and pyrophosphate

The formation of the pyrophosphate works in an antagonistic way for the formation of an anti wear film. Rounds says this is because of the loss of the acid phosphate; however if the formation of the layer is quicker than pyrophosphate formation, the effect is negligible. The incorporation of other additives within the lubricant package can have one or two effects on the formation of an anti-wear layer. These additives include metallic detergents and dispersants. Their interactions[11,12,13,14,15,16] complicate matters somewhat with regard to ZDDP anti-wear films as interactions occur in the bulk oil. Interactions can be antagonistic, where it is detrimental to film formation, or synergistic where film formation is improved. With use of a dispersant (amine present in the structure), the amine reacts with the pyrophosphate to form an amidophosphate and an acid phosphate (see below). Rounds[11] does iterate that the proposed reactions are no proof that they actually occur, but proposes it as a mechanism for formation of an anti-wear film by the formation of an acid phosphate decomposition product. A second explanation is molecular adsorption of ZDDP rather than additive decomposition being a critical step, with oxidation occurring *in situ*.

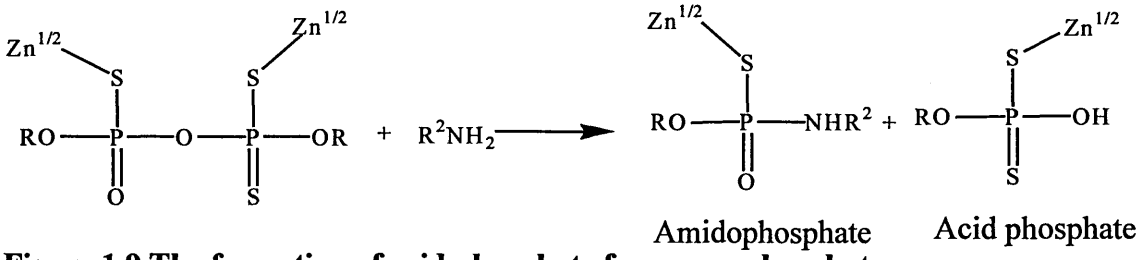

Figure 1.9 The formation of acid phosphate from pyrophosphate.

Beechi *et al.* (2001)[17], using gas chromatography mass spectrometry with electron capture and electron ionisation, showed some similarities to the decomposition products suggested by Rounds. It was demonstrated that ions are formed which correspond to the loss of an R group that is then replaced forming a hydroxyl group. Further complications are seen within diesel engines, where soot is known to interact with the ZDDP products removing it from the additive package[18,19].

Similarities are seen in work carried out in respect to the understanding of ZDDP decomposition and its ability to act as an anti-wear agent and anti-oxidant agent. However, a lot of work is required to complete the picture as very little work has taken into account the environment of the combustion engine.

1.4.3 Identification of zinc dialkyldithiophosphates

The separation and identification of ZDDPs has given problems over the years.

Killer *et al.*(1966)[20] reported the successful separation of ZDDPs by thin layer chromatography using silica plates and a solvent system consisting of n-heptane and acetic acid. The identification of the colourless complexes was carried out using fresh dithizone in chloroform (1g l^{-1}), which reacts with zinc to produce a pink product. A nickel solution (2g l^{-1}) in water was used to detemine the presence of dithiophosphate groups as yellow spots.

More recently other separation techniques have been utilised. Cardwell *et al.*(1996)[21] reported the use of normal phase liquid chromatography for the satisfactory separation of ZDDPs using two eluents, isopropylamine-acetic acid-methanol in dichloromethane 'A' and isopropylamine-acetic acid-methanol in n-heptane-dichloromethane (60:40) 'B'. The presence of the amine and the acetic acid was to prevent fronting and tailing of the peaks. Eluent 'B' provided a separation of better resolution than 'A' and sample pre-treatment was not required. Further to this work, Cardwell *et al.*(1997)[22] examined the use of reverse phase liquid chromatography and reported that this method was unsuitable for the separation of ZDDPs.

Mass spectrometry[23, 24] has been used to identify individual ligands present in mixtures of ZDDP and shows great promise for future exploratory work. Further investigations

that have been carried out into the analysis of ZDDPs include capillary supercritical fluid chromatography[25], gas chromatography[17] and a more recent use of thin layer chromatography[26]. More recently with the advent of nonaqueous capillary electrophoresis Thibon *et al.* (1999)[27] developed a capillary zone electrophoresis separation using a complex buffer consisting of methanol, tetrahydrofuran, and acetonitrile (70:15:15) with 20mM tetramethylammonium hydroxide and 10mM acetic acid as additives. The detector used a wavelength of 230nm and separation was of dialkyldithiophosphate ligands ($[(RO)_2PS_2]^-$.

1.5 Metallic Detergents

Metallic detergents encompass a family of detergents that include alkylsulphonates, alkylphenates and alkylsalicylates. They are synthesised with the metals magnesium calcium or sodium to carry out their specific roles within the lubricating oil. Metallic detergents fulfil two roles. First, they keep particulate contamination from the combustion process in suspension and prevent contaminants from adhering to the metal surfaces to form a varnish-like coating that becomes very sticky. Second, they neutralise acids from the combustion process which produces a range of acids (organic acids (RCOOH), and, mineral acids) which are prevalent in diesel and petrol fuel engines (sulphuric acid, nitric acid and hydrochloric acid). Acids attack the metal surfaces of the engine and increase the rate of wear, and 'overbased' detergents are used to reduce this problem.

Detergents generally have a large hydrocarbon tail and a polar head group. The hydrocarbon tail serves as a solubiliser in the base oil and the polar head is attracted to

the contaminants in the oil (see alkylsalicylates, what they are and how they work page 21). Detergents of this type contain metals as counter ions, the principal metals used being calcium, magnesium and sodium although others are used.

The detergents are synthesised by the neutralisation of an organic acid with a metallic base (1).

$$2RCOOH + M(OH)_2 \longrightarrow (RCOO^-)_2M^{2+} + 2H_20 \qquad (1)$$

where $M(OH)_2$ is a divalent metal hydroxide and R is the solubilising group (hydrocarbon tail)

Detergents can take three forms: neutral, basic and overbased. The structures and synthesis of the alkylsalicylates is on page 20.

Overbased detergents have an added advantage over neutral and basic detergents in that they are able to neutralise any acidic environment within a lubrication system, thus preventing corrosion. There are two main ways of producing overbased detergents, which are outlined below.

The first is an acid/base reaction which is normally used; however for overbasing an excess of inorganic base is required (2).

$$\underset{\text{Organic Acid}}{2\ RCOOH} + \underset{\text{Inorganic Base}}{nM(OH)_2} \longrightarrow \underset{\text{Overbased Detergent}}{RCOO\text{-}M\text{-}OOCR\ (n\text{-}1)M(OH)_2} + \underset{\text{Water}}{2\ H_2O} \qquad (2)$$

The more common process is the carbonation technique (3), which converts the excess inorganic base into a metal carbonate. The inorganic carbonate is stabilised by the

metallic detergent, with the excess carbonate thought to be at the micelle centre of the neutral detergent.

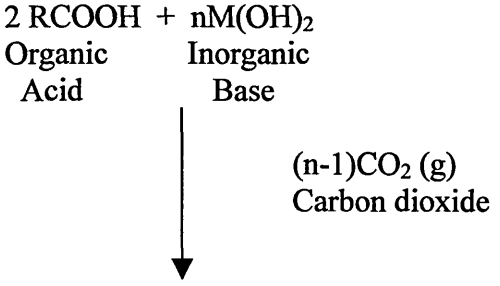

RCOO-M-OOCR (n-1)MCO_3 + (n+1) H_2O (3)

Carbonated Overbased Detergent

Water

1.5.1 Synthesis of Alkylsalicylates

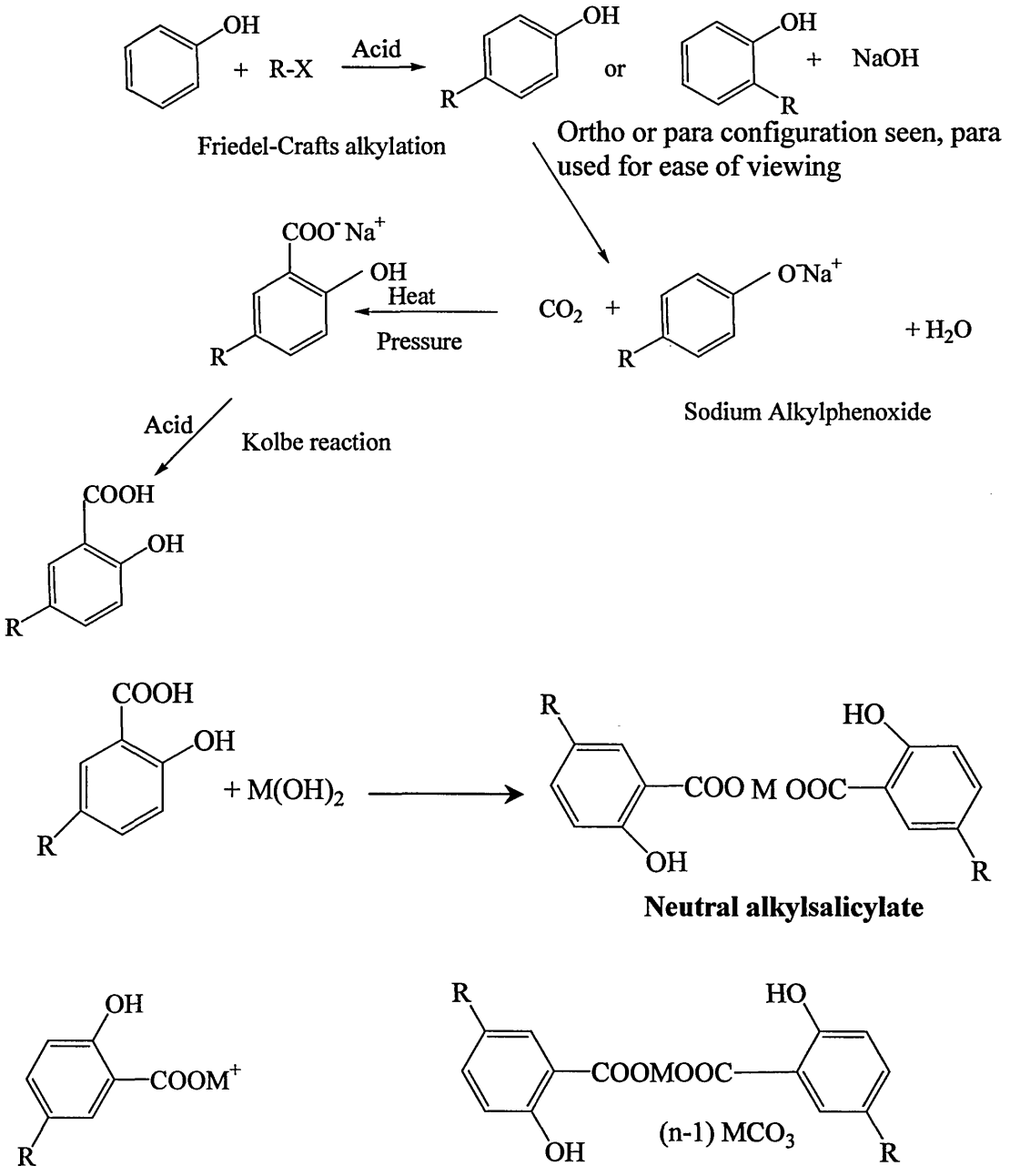

Figure 1.10 The synthesis route for alkylsalicylates.

Fialkovskii *et al.* (1983)[28] described a possible synthesis mechanism for alkylsalicylate based on dodecylphenols.

1.5.2 Alkylsalicylates - what they are and how they work

Within the hydrocarbon environment of a lubricating oil, alkylsalicylates, as all metallic detergents, can form inverse micelles. Glavati *et al.* (1989)[29] studied the structure of overbased salicylates within a lubricant oil. The structures of the micelles have been well documented and investigated by a variety of methods, including small angle neutron scattering[30,31,32,33], electron microscopy[34,35] and x-ray absorption spectroscopy[36,37]. These studies showed that the surfactant molecules surround an amorphous inorganic core. The inorganic core is composed of metallic carbonates with the possible presence of metallic hydroxide; some water may also be found at the centre. The metal present in the core is that which has been used to create the surfactant and to overbase it. Overbasing the detergents increases the total base number of the detergent and the lubricating oil. The total base number is a representation of the surfactant system's ability to neutralise the acids formed in the combustion process. It is defined as the amount of potassium hydroxide that would be required to neutralise a gram of the material (by titration) and is expressed as mgKOH/g[38]. Ruckstein (1993)[39] studied the stability of nonaqueous dispersions, describing that the surfactant alkyl chains as normally branched. Branching of the alkyl chain produces a paste of lower viscosity for the surfactant, and branching also has the effect of improving solubility within the lubricant as it allows the oil to get between the individual surfactant molecules. Robinson *et al.* (2000)[40] found that acids within the lubricant are solubilised, forming a water/oil emulsion. These then interact with the overbased detergent by acid/base interactions, neutralising the acid. Pawlak *et el.* (1991)[41] described the acid base reactions that can occur within the lubricating oil. They also state that stronger intermolecular interactions are present with alkylsalicylates than with any other metallic detergent, the stronger interaction being attributed to the presence of

two polar groups. This promotes aggregation of the surfactant in an organic solvent and the alkyl salicylates have a characteristic structure with an aggregation number of 15-30. The use of detergents to solubilise and prevent aggregation of combustion particulates has also been studied. Glavaty *et al.* (1984)[42] suggested a mechanism to prevent aggregation of soot. The micelle form stabilised the soot by adsorbing to the soot as an intact micelle without any loss of the calcium carbonate core. Once adsorbed and surrounding the soot particle, repulsion effects prevent other micelle-coated soot particles from aggregating, the stability of this structure depending on the dimensions of the micelles and the durability of fixation on the soot particle. However, this is not to say that neutral salicylates take no part in the stabilisation of soot. Neutral detergents are able to form micellar layers on the surface of the soot, preventing aggregation

Chromatographic separation techniques for identification of individual alkyl chain lengths of alkylsalicylates have not been published to my knowledge at the present time.

The work in this thesis covers a new analysis technique for the identification of lubricant additives. Nonaqueous capillary electrophoresis is a new addition to the family of capillary electrophoresis utilising organic solvents. The subsequent chapters describe the theory behind capillary electrophoresis with the addition of organic solvents at the end. The use of mass spectrometry with capillary electrophoresis is becoming more common and is of great use. Chapter 3 describes some of the theory behind mass spectrometry specifically electrospray and quadrupole analysers. Chapter 4 describes initial work to see if the instrumentation to be used is adequate for nonaqueous capillary electrophoresis and subsequently the analysis of zinc

dialkyldithiophosphates. Chapter 5 describes the analysis and identification of a metallic detergent in the form of alkylsalicylate. Chapter 6 describes the possibility of using mass spectrometry detection with nonaqueous capillary electrophoresis. This was carried out firstly by direct infusion of analytes to identify operational parameters, which were then carried across to nonaqueous capillary electrophoresis-mass spectrometry. Chapter 7 brings together the knowledge acquired during method development to the analysis of fully formulated lubricants.

Alkylsalicylates were an unknown quantity, due to their ability to form stable inverse micelles within the lubricating oil. Thus it was necessary to identify whether the separation by nonaqueous capillary electrophoresis was that of micelles or individual alkylsalicylates. Several techniques were used to determine whether the micelles were disrupted by solid phase extraction or in the presence of a polar solvent. This is dealt with in chapter 8.

References

1. Habeeb, J.J., Stover, W.H., ASLE Transactions 1987, **30**, (4), 419-426.
2. Roberts, K.J., Armstrong, D.R., Ferrari, E.S., Adams, D., Wear 1998, **217**, 276-287.
3. Dickert Jr, J.J., Rowe, C.N., Journal of the Chemistry Society Perkin III 1967, **32**, 647-653.
4. Wan, Y., Cao, L., Xue, Q., Tribology International (1998), **30**, (10), 767-772.
5. Fuller, M., Yin, Z., Kasari, M., Bancroft, M.G., Yamaguchi, E.S., Ryason, R.P., Willermet, P.A., Tan, K.H., Tribology International 1997, **30**, (4), 305-315.
6. Yin, Z., Kasari, M., Fuller, M., Bancroft, M.G., Fyfe, K., Tan, K.H., Wear 1997, **202**, 172-191.
7. Papay, A.G., Lubrication Science 1998, **10-3**, (10), 209-217.
8. Woo, T.K., Mosey, N.J., Journal of Physical Chemistry A 2003, **107**, 5058-5070.
9. Peng, P., Hong, S-Z., Lu, W-Z., Lubrication Engineering 1994, **50**, (3), 230-235.
10. So, H., Lin, Y.C., Huang, G.G.S., Chang, T.J.T., Wear 1993, **166**, 17-26.
11. Rounds, F.G., ASLE Transactions 1981, **24**, (4), 431-440.
12. Ranakumar, S.S.V., Madhusudhana, R.A, Srivastava, S.P., Wear 1992, **156**, 101-120.
13. Willermet, P.A., Dailey, D.P., Carter III, R.O., Schmitz, P.J., Zhu, W., Bell, J.C., Park, D., Tribology International 1995, **28**, (3), 167-175.

14. Kapsa, Ph., Martin, J.M., Blanc, C., Georges, J.M., Transactions of the ASME Journal of Lubrication Technology 1981, **103**, 487-496.

15. Rounds, F.G., Lubrication Engineering 1989, **45**, (12), 761-769.

16. Barcroft, F.T., Park, D., Wear 1986, **108**, 213-234.

17. Beechi, M., Perret, F., Carraze, B., Beziau, J.F., Michel, J.P., Journal of Chromatography A 2001, **905**, 207-222.

18. Gautam, M., Chitoor, K., Durbha, M., Summers, J.C., Tribology International 1999, **32**, 687-699.

19. Colacicco, P., Mazuyer, D., Tribology Transactions 1995, **38**, (4), 959-965.

20. Killer, F.C.A., Amos, R., Journal of the Institute of Petroleum 1996, **52**, 315.

21. Cardwell, T.J., Lambropoulos, N., Caridi, D., Marriott, P.J., Journal of Chromatography A 1996, **749**, 87-94.

22. Widahl, K.L., Cardwell, T.J., Journal of Chromatography A 1997, **765**, 181-186.

23. Tsuchiya, M., Kuwabara, H., Musha, K., Analytical Chemistry 1986, **58**, 695-699.

24. Cardwell, T.J., Colton, R., Lambropoulos, N., Traeger, J.C., Marriott, P.J., Analytica Chimica Acta 1993, **280**, 239-244.

25. Barnes, A.M., Bartle, K.D., Christopher, S., Heathcote, C., Journal of High Resolution Chromatography 2000, **23**, (5), 389-392.

26. Oriňák, A., Oriňáková, R., Turčániová, L., Journal of Chromatography A 1998, **825**, 189-194.

27. Thibon, V.R.A., Bartle, K.D., Abbott , D.J., McCormack, K.A., Journal of Microcolumn Separations 1999, **11**, (1), 71-80.

28. Fialkovskii, R.V., Glavati, O.L., Zhurba, A.S., Matyash, M., Skalak, P., Chemistry and Technology of Fuels and Oils 1983, **19**, (1-2), 65-68.

29. Glavati, O.L., Kurilo, S.M., Kravchuk, G.G., Gordash, Yu.T., Shilov, V.V., Tsukruk, V.V., Lokhonya, O.A., Chemistry and Technology of Fuels and Oils 1989, **25**, (5-6), 273-275.

30. Marković, I., Ottewill, R.H., Cebula, D.J., Field, I., Marsh, J.F., Colloid & Polymer Science 1984, **262**, 648-565.

31. Ottewill, R.H., Sinagra, E., MacDonald, I.P., Marsh, J.F., Heenan, R.K., Colloid & Polymer Science 1992, **270**, 602-608.

32. Marković, I., Ottewill, R.H., Colloid & Polymer Science 1986, **264**, 454-462.

33. Marković, I., Ottewill, R.H., Colloid & Polymer Science 1986, **264**, 65-76.

34. Makhlouf, R., Mansot, J.L., Hirsch, E., Wéry, J., Candau, S.J., Thomas, D., Rolland, J.P., Colloid & Polymer Science 1995, **273**, 242-251.

35. Martin, J.M., Mansot, J.L., Hallouis, M., Ultramicroscopy 1989, **30**, 321-328.

36. Mansot, J.L., Wéry, J., Lagarde, P., Colloids and Surfaces A: Physicochemical and Engineering Aspects 1994, **90**, 167-182.

37. O'Sullivan, T.P., Vickers, M.E., Heenan, R.K., Journal of Applied Crystallography 1991, **24**, 732-739.

38. Galsworthy, J., Hammond, S., Hone, D., Current opinion in Colloid Interface Science 2000, **5**, 274-279.

39. Ruckstein, E., Colloids and Surfaces 1993, **69**, 271-275.

40. Hone, D.C., Robinson, B.H., Steytler, D.C., Glyde, R.W., Galsworthy, J.R., Langmuir 2000, **16**, 340-346.

41. Fox, M.F., Pawlak, Z., Picken, D.J., Tribology International 1991, **24**, (6), 341-349.

42. Glavaty, O.L., Marchenko, A.I., Kravchook, G.G., Glavaty, O.L., Acta Chimica Hungarica 1984, **114**, (4), 367-375.Armstrong, D.R., Ferrari, E.S., Roberts, K.J., Adams, D., Wear 1997, **208**, 138-146.

Chapter 2

Capillary Electrophoresis

Theory

2.0 History

Electrophoresis has come a long way since the pioneering experiments carried out by Tiselius during the latter end of the 1930s. Tiselius[1] showed the potential of electrophoretic analysis by separating serum proteins (albumen and globulins α, β and γ). From this initial work, other electrophoresis techniques followed in the form of paper and gel electrophoresis, although open tubes were not used because of convection broadening of peaks.

In 1967 Hjertén[2] laid the groundwork for capillary electrophoretic separations which overcame the convection broadening problem of open tubes. However, the technique was not to be seen again until the late 1970s and early 80s, when Mikkers *et al.*[3] and Jorgenson and Lukacs[4] determined that capillary electrophoresis was a viable analytical technique.

Since this ground-breaking work, the use of capillary electrophoresis has exploded, and now it is used in a very wide range of analyses. This has seen capillary electrophoresis diverge into a variety of modes i.e. capillary zone electrophoresis (CZE), micellar electrokinetic capillary chromatography (MECC), capillary isoelectric focusing (CIEF), capillary isotachophoresis (CITP), capillary gel electrophoresis (CGE) and capillary electrochromatography (CEC).

2.1 Instrumentation

Instrumentation for capillary electrophoresis is simple in principle (figure 2.1, page 25)

2.1.1 Vials (inlet and outlet)

The instrument consists of two vials, a source (inlet) and destination (outlet). These contain the specific buffers for washing the capillary, for separation and for samples. The buffer composition is an important variable in electrophoretic separations and, to avoid change, the buffer is replenished periodically. Electrolysis of the buffer near the electrodes forms H^+ ions at the anode and OH^- at the cathode, changing the pH in the two vials and leading to alterations in separation and irreproducible migration times. Siphoning also alters migration times, reducing reproducibility, and to prevent this the liquid levels in the vials should be kept level.

2.1.2 Silica capillary

Between the destination and source vials is a capillary, usually silica. The capillary is the area where separations occur. The silica capillary can have internal diameters from 25 to 100μm and outer diameters of 150 to 375μm with a polyimide coating. The capillary is preconditioned prior to first use with a caustic solution to clean the interior and activate the silanol groups. The most widely used detection system is uv/vis absorbance, because silica is uv transparent and so on-column detection can be utilised. Production of the window for uv/vis detection involves the removal of a small section of polyimide coating. Other detector systems used include fluorescence, laser induced fluorescence, mass spectrometry and conductivity. Grushka *et al.*(1994)[5] described the importance of cutting the capillary straight and flat. Having a capillary edge that is not straight is detrimental to the separation as it alters the plug shape and length, the extra

length depending on the size of the angle of the slant. Cutting the capillary at an angle manifests itself in an increase in peak asymmetry and loss of efficiency and hence a straight edged capillary is necessary for high efficiencies and symmetrical peaks.

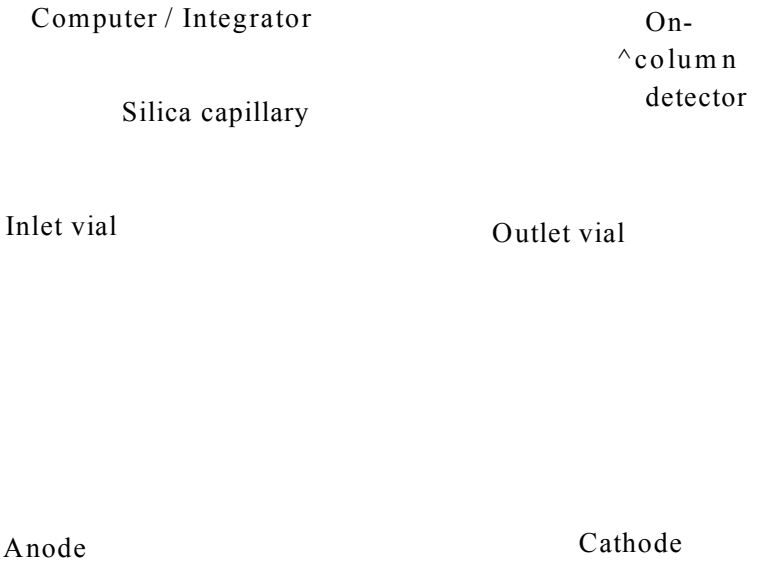

Figure 2.1 Block diagram of capillary electrophoresis instrumentation.

2.1.3 Power supply

A power supply is used to provide the electric field along the capillary. The power supply can be operated in constant voltage or constant current mode, with the ability to reverse polarity. Typically, voltages up to 30kV can be utilised and currents up to 300pA. The maximum voltage that can be used depends on several factors including the capillary inner diameter and the buffer composition (see section 2.2.4).

2.2 The process of electrophoretic separation by CE

There are three distinct stages to a separation by CE,

- Sample injection
- Separation
- Detection

A typical analysis is carried out by injecting the sample into a buffer-filled capillary. The voltage is then applied, driving the buffer and sample in the direction of the detector. The charged analytes migrate through the capillary and separate into small zones according to differences in electrophoretic mobility. The order of migration is normally cations, then neutrals, and then anions.

2.2.1 Sample injection

There are two methods for injecting samples into the capillary, hydrodynamic and electrokinetic. Samples are first prepared by dilution to the required concentration, in a small quantity of buffer or water. The ideal plug length is no more than 1% of the total capillary length.

2.2.1.1 Hydrodynamic

Hydrodynamic injections can be carried out by several methods. If pressure is applied at the source vial or a vacuum at the destination vial, then the volume of sample injected by this method can be calculated by the Poiseulle equation:

$$V_i = \Delta P r^4 \pi t / 8 \eta L \qquad (1)$$

where ΔP is the pressure applied, r is the inner diameter of the capillary, t is the time for the application of pressure, η is the viscosity and L is the total length of the capillary.

The sample may also be injected by gravity, where the source vial is elevated and siphoning is used to inject the sample. The volume injected can be calculated from equation(1), where ΔP is replaced by the gravitational equivalent (2):

$$\Delta P = \rho g \Delta H \qquad (2)$$

where ρ is the density of the buffer, g is the gravitational constant ($980 cm \cdot s^{-2}$) and ΔH is the height difference between the source and destination vial.

2.2.1.2 Electrokinetic Injection

Electrokinetic injection is carried out by applying a voltage at the source vial (containing the sample). The sample is injected as a consequence of an electroosmotic flow (section 2.2.2.1) and the sample ions electrophoretic mobility (section 2.2.2.4). The quantity injected is given by:

$$Q_{inj} = V \pi c t r^2 (\mu_{EP} + \mu_{EOF}) / L \qquad (3)$$

where V is the voltage applied, c is the sample concentration, t is the duration of the applied voltage, r is the radius of the capillary, μ_{EP} is the electrophoretic mobility and μ_{EOF} is the electroosmotic mobility.

Unlike hydrodynamic injection, electrokinetic injections suffer from sample bias, where ions that have a high mobility will be present in the capillary at higher concentrations than ions with low mobility. After repeated injections, depletion of the high mobility ions in the sample vial is seen, leading to a loss of reproducibility and errors in quantitation.

2.2.2 Separation

The application of an electric field in capillary electrophoresis leads to the buffer migrating through the capillary in a unidirectional motion. This migration is known as the electroosmotic flow (EOF); normally this migration is towards the cathode.

The most important factor in capillary zone electrophoresis (CZE) is that the solutes are charged and have electrophoretic mobilities, differences in which are the cause of the separation. The electrophoretic mobility is based on an individual ion's size to charge ratio. A negatively charged species will migrate towards the anode, while a positively charged species will migrate towards the cathode and uncharged species will not migrate in either direction. The higher the charge density (charge / solvated radius) the higher the rate of electrophoretic migration.

In capillary electrophoresis the electroosmotic flow is usually strong enough to move all charged analytes in one direction past the detector. The main downside to the CZE technique is that it is unable to separate neutral analytes, since they have no electrophoretic mobility and co-migrate at the same rate as the electroosmotic flow.

2.2.2.1 Electroosmotic flow

On the inside of the capillary wall silanol (Si-OH) groups are present that start to become ionised ($Si\text{-}O^-$) above a pH of approximately 2. This charging leads to the formation of a double layer. Double layer theory, introduced by Gouy and Chapman, considers the effect of surface ionisation and/or ion adsorption to a surface. The size of the double layer is dependent on the surface charge, which attracts ions to the surface and decays exponentially through the double layer.

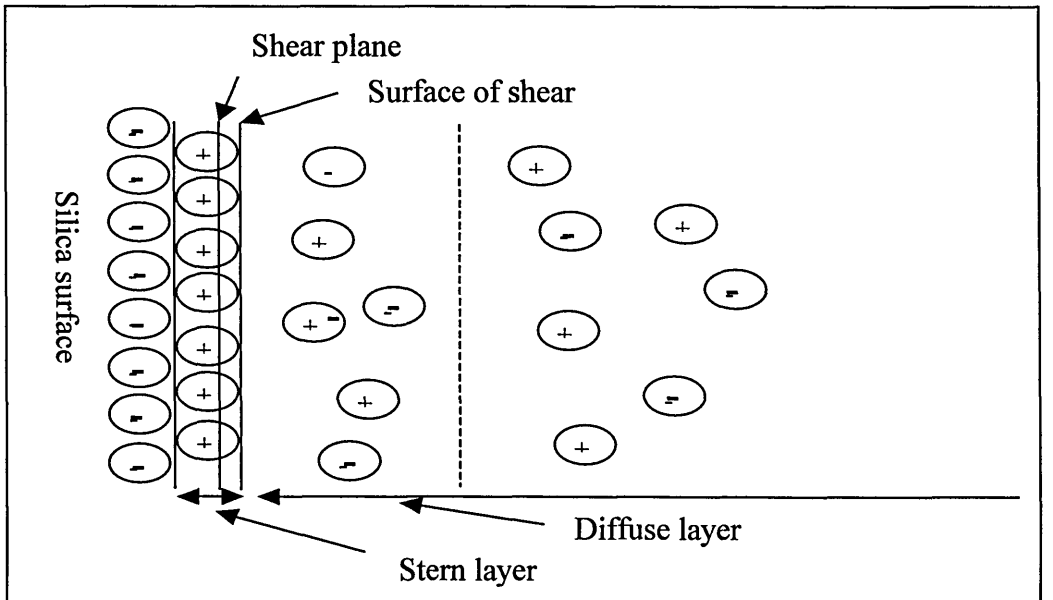

Figure 2.2 Diagrammatic representation of the double diffuse layer within a silica capillary.

The diffuse double layer theory of Stern (1924) is the accepted model for capillary electrophoresis and electroosmotic flow formation (figure 2.2). Stern proposed a model in which the double layer is divided into two parts, the Stern layer and the diffuse layer, which are separated by a plane (shear plane).

2.2.2.2 Diffuse double layer formation

Counter ions in the buffer adsorb to the inner surface of the capillary wall that has a surface potential ψ_o, forming a fixed layer. The fixed layer is made up of ions within the Stern layer and extends into the diffuse layer. The electrical potential (ψ_d) seen within the diffuse layer decays exponentially into the bulk buffer. The point where exponential decay begins is in the shear plane, where this electrical potential (charge density) is not sufficient for the ions to be fixed, and a potential plane of shear appears between the fixed and mobile ions.

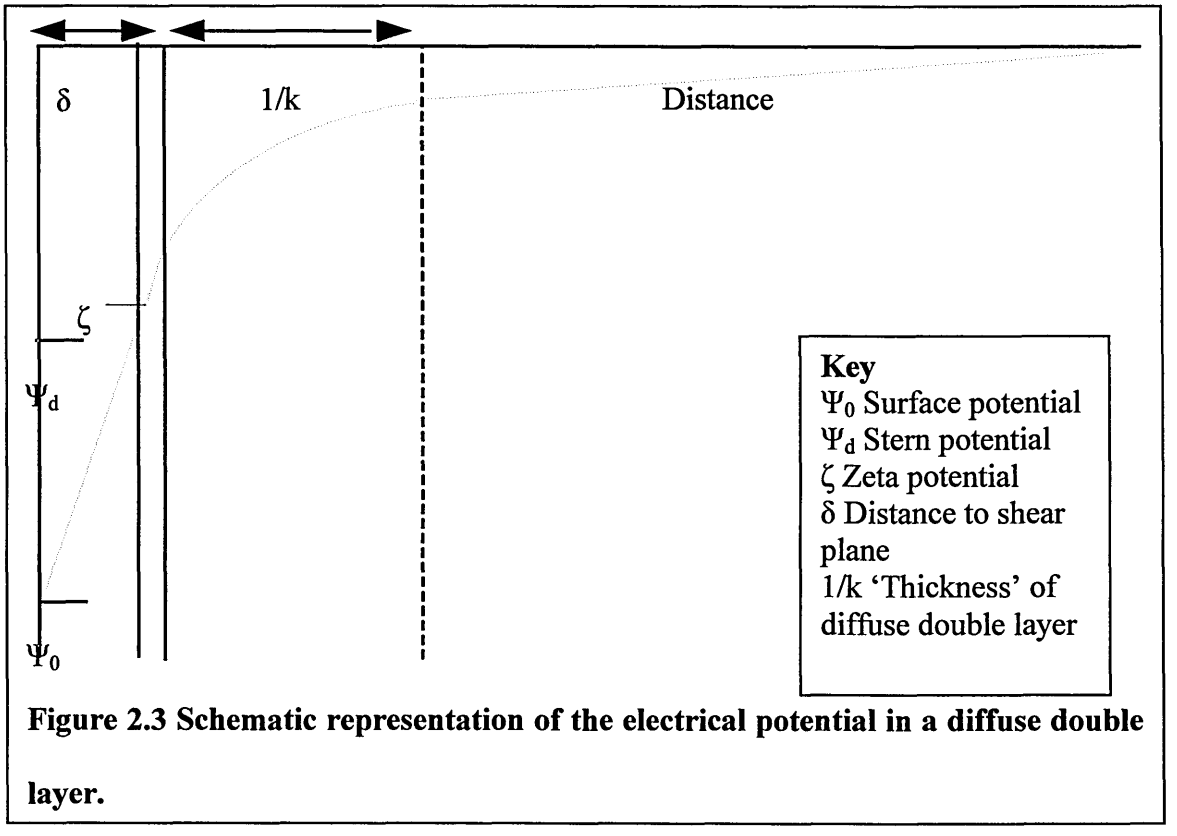

Figure 2.3 Schematic representation of the electrical potential in a diffuse double layer.

The application of an electric field causes the ions outside the plane of shear (mobile ions) to migrate towards the cathode, and because the ions are hydrated they drag the bulk buffer with them generating the electroosmotic flow (EOF).

At the plane of shear the potential difference between the fixed and mobile phases is known as the zeta potential (ζ). It has been suggested that this area is also an area of sudden viscosity change. The zeta potential is, given by:

$$\zeta = 4\pi\delta e/\varepsilon \qquad (4)$$

where δ is the thickness of the diffuse double layer, e is the charge per unit surface area (charge density), ε is the dielectric constant of the buffer.

2.2.2.3 Flow profile

Electroosmotic flow has a relatively flat profile compared to laminar or pumped flow as in HPLC. The flow next to the capillary wall is slightly slower than the rest of the capillary, due to friction, but this drag detracts very little from the overall flow profile. The flat profile ensures that analytes experience the same velocity regardless of their position across the capillary. The nature of the flow is the main reason that high efficiencies are seen in capillary electrophoresis.

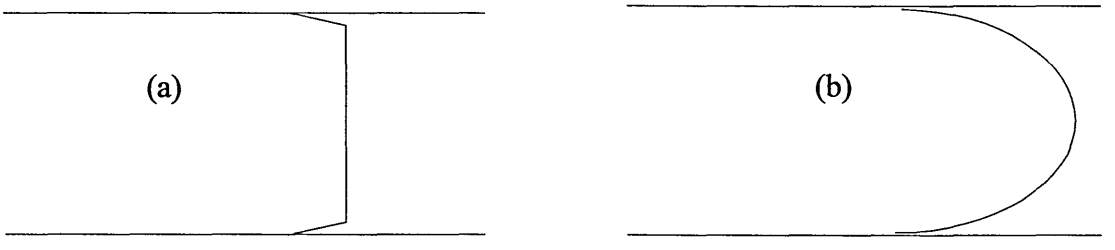

Figure 2.4 Schematic representation of flow profiles (a) electroosmotic flow, (b) laminar or pumped flow.

It is essential that the electroosmotic flow is constant, because any variations will result in variances in migration times of analytes, leading to identification and quantitation errors. The electroosmotic flow velocity can be calculated by:

$$\upsilon_{EOF} = \varepsilon\zeta E / 4\pi\eta \qquad (5)$$

where ε is the dielectric constant, ζ is the zeta potential, E is the applied electric field, and η is the viscosity of the buffer.

The electroosmotic mobility, is given by;

$$\mu_{EOF} = \varepsilon\zeta / 4\pi\eta \qquad (6)$$

The mobility of the electroosmotic flow is seen to be independent of the electric field applied.

There are several ways to measure the electroosmotic flow, but the simplest and most widely used method is the injection of a neutral marker. Neutral markers are compounds that have no ability to become charged in the buffer being used and as such do not have any inherent mobility, resulting in the marker travelling with the electroosmotic flow, allowing it to be measured. The electroosmotic flow can be calculated in two ways, as velocity (7) (cm/s) or as mobility (8) ($cm^2/V \cdot s$).

$$\upsilon_{EOF} = l / t_{nm} \qquad (7)$$

where the υ_{EOF} is the electroosmotic flow velocity, l is the length of the capillary to the detector (effective length) and t_{nm} is the migration time of the neutral marker.

$$\mu_{EOF} = \upsilon_{EOF} / E \quad (8)$$

where μ_{EOF} is the electroosmotic flow velocity, υ_{EOF} is the electroosmotic flow velocity and E is the applied electric field (V/cm).

The electroosmotic flow can be manipulated by altering experimental parameters including applied voltage, pH of the buffer, buffer concentration / ionic strength, temperature, organic solvents and modification of the capillary wall (see section 2.2.4).

2.2.2.4 Electrophoretic mobility

In CZE the most important characteristic is the electrophoretic mobility of an analyte. Electrophoretic mobility in an electric field is only attainable if the analyte is capable of attaining a charge.

The mobility of an individual charged analyte is dependent on its charge to size ratio. That is to say that a large singular charged species will have a lower mobility than a small multiply charged species (figure 2.5).

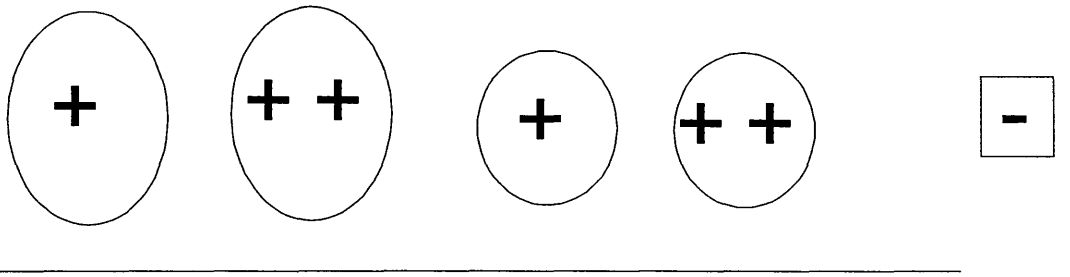

Figure 2.5 Schematic representation of electrophoretic mobility in cations, according to size to charge ratio.

Mobility may also be affected by the constituents of the buffer changing. Changes in pH may alter an analyte's charge state. Altering the size of an analyte is not so straightforward; however this can be achieved by altering the hydration sheath around it by the addition of organic solvents to the buffer.

Separation in CZE can therefore only occur with charged analytes that have differing charge-to-size ratios. If they are the same, the analytes will not be separated in this technique.

The electrophoretic velocity of a charged analyte is calculated by:

$$\upsilon_{EP} = 1/t_m - 1/t_{nm} \qquad (9)$$

and the electrophoretic mobility, is calculated by:

$$\mu_{EP} = (1/t_m - 1/t_{nm})(L/V) \qquad (10)$$

where l is the effective length, t_m is the migration time of the analyte, t_{nm} is the migration time of the neutral marker, L is the total length of the capillary (cm) and V is the applied voltage.

2.2.2.5 Efficiency

Efficiency is affected by the electroosmotic flow and electrophoretic mobility, and the faster the electroosmotic flow, the higher the efficiency is. Highest efficiency is seen when the analyte migrates with the electroosmotic flow, and the lowest efficiency is seen if the analyte migrates against the electroosmotic flow. The fast electroosmotic flow produces a lower migration time that gives less time for diffusion to occur. There are three forms of diffusion in capillary electrophoresis; longitudinal, radial and thermal (see section 2.2.2.8). Longitudinal diffusion and radial diffusion do not have a great impact on separation efficiency in general.

The effect that longitudinal diffusion has on plate height (H) for a particular separation can be calculated, by using a shortened version of van Deemter's equation (11) where:

$$H = B/u \qquad (11)$$

where B is the diffusion coefficient and u is the electroosmotic flow (flow rate).

Plate height can also be calculated by:

$$H = L/N \qquad (12)$$

where L is the length of the capillary and N is the number of plates.

The number of plates is in turn calculated by:

$$N = 5.54(t_m/w_{1/2})^2 \quad (13)$$

where t_m is the migration time of the peak and $w_{1/2}$ is the width of the peak at half height.

2.2.2.6 Resolution

Having a fast electroosmotic flow is desirable in that it decreases the analysis time and improves efficiency. However, resolution is the most important parameter in a separation. Like efficiency, resolution is affected by the electroosmotic flow. Resolution increases with time of a separation, so a slower electroosmotic flow and greater difference in electrophoretic mobility improve resolution. The resolution is better when the electroosmotic flow and electrophoretic mobility are opposite. Greatest resolution is seen when the electroosmotic flow and electrophoretic mobility is equal and opposite in direction, but realistically this will lead to a separation of infinite time! Resolution can be measured by:

$$R = 2(t_2 - t_1) / (w_1 + w_2) \quad (14)$$

where t_1 and t_2 are migration times of two peaks and w_1 and w_2 are the base widths of the two peaks.

2.2.2.7 Selectivity

Selectivity (α) is concerned with how far apart the two peaks are in a particular separation, and can be expressed as:

$$\alpha = (t_2 - t_{nm}) / (t_1 - t_{nm}) \quad (15)$$

2.2.2.8 Diffusion

The efficiency, resolution and selectivity of a separation can all be affected by diffusion. Diffusion is the nemesis of efficiency, resolution and in some aspects, sensitivity.

Diffusion spreads the analyte over a wider distance, producing a weaker, broader signal compared to if the analyte was in a narrow band, which can make detection difficult.

Thermal or convective diffusion can have a dramatic effect on efficiency as this contributes greatly to zone spreading. The application of an electric field and hence a current through the buffer generates Joule heating, and this heating warms up the buffer.

The heating of the buffer can lead to temperature gradients throughout the capillary. The gradients lead to viscosity changes within the capillary radius, with the central area being hotter than the edge. These changes in viscosity lead to analytes experiencing differing electroosmotic flow rates and electrophoretic mobilities (see figure 2.6).

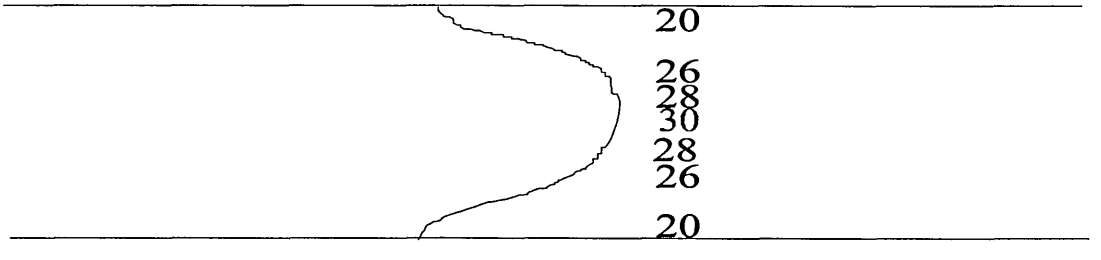

Figure 2.6 Representation of a temperature gradient inside the capillary and effect on flow profile.

For this reason heat generated has to be dissipated adequately, and one way is to use capillaries with small inner diameters. The temperature difference across the radius of a capillary can be calculated by:

$$\Delta T = (0.239Q / 4k)r^2 \qquad (16)$$

where Q is the power density in watts / m^3, k is the thermal conductivity and r is the radius of the tube. From equation 16, altering the radius will alter the temperature difference. Using a smaller inner diameter tube will lead to smaller temperature gradient. A greater surface to area ratio will lead to better heat dissipation. However it is better to prevent heating than remove the consequence, and smaller diameter tubes produce a higher resistance. The higher resistance in turn produces a lower current and as current causes Joule heating a decrease in heat generation is seen. An alternative to smaller diameter capillaries is to use a longer capillary length which also increases the resistance.

Although convective diffusion can be the most problematic cause of reduced efficiency, it is easily decreased, as described above. The total diffusion seen from a separation in capillary electrophoresis can be calculated by the total variance, (σ^2_T):

$$\sigma^2_T = \sigma^2_D + \sigma^2_{inj}\, \sigma^2_{det}\, \sigma^2_o \qquad (17)$$

where σ^2_D is the longitudinal diffusion, σ^2_{inj} is the variance of the injector system, σ^2_{det} is the variance of the detector and σ^2_o is the variance from other effects that includes thermal diffusion.

2.2.3 Detectors

A range of detectors is available for use with capillary electrophoresis, (figure 2.7). The most widely used is uv/vis absorbance, with its wide range of applicability. However, its sensitivity is very poor due to the short path lengths across the capillary, typically only 50μm. To overcome this sensitivity problem using a 50μm diameter capillary several solutions have been developed.

Detector	Approximate Detection Limits (moles)
UV/ vis absorbance	10^{-13}-10^{-16}
Fluorescence	10^{-15}-10^{-17}
Mass spectrometry	10^{-16}-10^{-17}
Conductivity	10^{-15}-10^{-16}

Figure 2.7 Some capillary electrophoresis detectors.

Tsuda *et al.*(1990)[6] used a rectangular capillary 50μm x 1000μm for the separation of some amino acids (figure 2.8). The rectangular capillary led to an increased absorbance through less light scattering and optical distortion, while the increased path length increased the sensitivity.

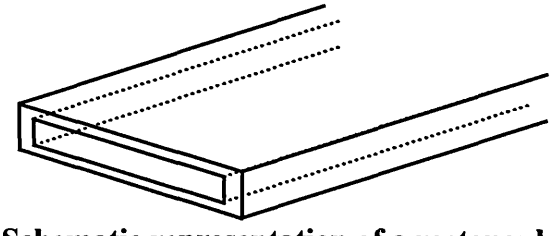

Figure 2.8 Schematic representation of a rectangular capillary.

The 'Z'cell (figure 2.9) was developed and utilised to increase the path length for the light to increase the sensitivity. Moring *et al.*(1993)[7] found this a useful method for

increasing sensitivity. The downside of this method is that two closely migrating analytes may not be seen to be separated.

Figure 2.9 A representation of a 'Z' cell and how it increases the pathlength.

An alternative to the 'Z' cell is the bubble cell. The bubble cell is designed with a short section of capillary having a greater internal diameter than the rest of the capillary (figure 2.10). Heiger *et. al.{* 1992)8 showed it was possible to get a three fold increase in sensitivity, when having a bubble three times the normal inner diameter (50 pm - 150 pm). These capillaries, however, are extremely fragile.

Figure 2.10 A bubble cell.

Sensitivity can be improved by online stacking methods, both sample stacking and field amplified sample injection. Conventionally, a sample analyte is diluted in the buffer, which when injected has the same conductivity as the rest of the buffer. In stacking

methods the sample analytes are dissolved or diluted in a solution of lower conductivity than the buffer or deionised water.

Sample stacking (figure 2.11) is carried out by hydrodynamic injection, and when the electric field is applied the sample plug has a higher resistance than the buffer and so contains a higher electric field drop. The high electric field enables the ions to migrate rapidly through the sample plug to the buffer boundary. On encountering the lower electric field of the buffer the ions become stacked in a narrow zone.

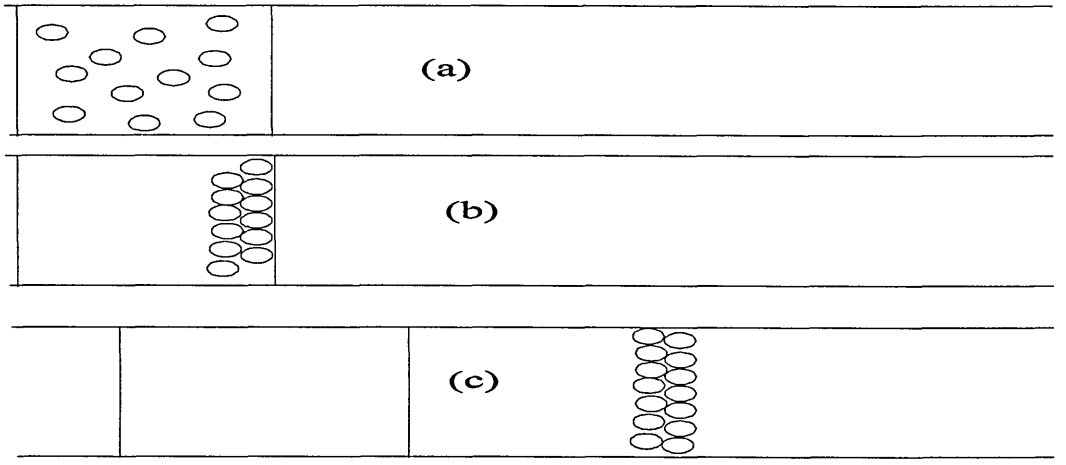

Figure 2.11 Sample stacking. (a) hydrodynamic injection of sample, (b) application of electric field, (c) time x after application of electric field.

Likewise, with field amplified injection the sample analyte is injected electrokinetically, and the sample analytes experience the same conditions as those encountered in sample stacking when the separation begins. An advantage with this method is that the separation begins as soon as the injection takes place.

With the individual analytes being stacked in a tight zone, an increase in absorbance is seen for a shorter time and separation can be seen to slightly improve.

2.2.4 Operational parameters

2.2.4.1 Applied voltage

Probably the easiest way to modify a separation in capillary electrophoresis is by varying the applied voltage. Both electroosmotic flow and electrophoretic mobility are affected by the applied voltage, through alterations in the electric field. Increasing the voltage increases the electroosmotic flow and hence reduces the analysis time. Using the highest possible voltage will produce the quickest analysis times. However, care must be taken as increasing the applied voltage/electric field can increase the current to an extent where Joule heating is detrimental to the separation. Identification of the maximum voltage can be determined by an Ohm's law plot. A second way of speeding up the analysis is to shorten the capillary. Shortening the capillary leads to an increase in current due to the decrease in resistance and is liable to the same problems as increasing the voltage.

2.2.4.2 Buffer pH

Buffer pH plays a significant role in electroosmotic flow (section 2.2.2.1) and electrophoretic mobility (section 2.2.2.4). Increasing the pH increases the charge density on the capillary wall, due to more silanol groups converting to the ionised silanoate ($Si\text{-}O^-$) form. Conversely decreasing the pH decreases the electroosmotic flow by decreasing the charge density on the capillary wall.

Altering the pH may alter the electrophoretic mobility of an analyte by altering its charge. As electrophoretic mobility is the most important factor in a separation the pH of the buffer is adjusted to provide the optimum separation.

2.2.4.3 Buffer concentration / ionic strength

In an adequately temperature-controlled environment, increasing the buffer concentration / ionic strength will decrease the electroosmotic flow because the diffuse double layer becomes more compact and the zeta potential is reduced.

However, if the environment is not adequately temperature-controlled, the increase in buffer concentration / ionic strength will increase the current. The increase in current will lead to increased Joule heating, decreasing the viscosity and leading to a faster electroosmotic flow.

Common buffers used include borate (pK_a 9.24), phosphate (pK_a 2.12, 7.21, 12.32), acetate (pK_a 4.75) and formate (pK_a 3.75).

2.2.4.4 Temperature

Separations are normally temperature-controlled. Altering the temperature for a separation may be useful in improving the separation. Increasing the temperature decreases the analysis time by increasing the electroosmotic flow via a decrease in viscosity. Careful manipulation is required as temperature gradients can form through the inner radius of the capillary and lead to zone spreading (section 2.2.2.8).

2.2.4.5 Organic solvents

The addition of organic solvents can have various effects in a buffer, altering dielectric constant, viscosity and zeta potential. For instance, it has been reported that the addition of acetonitrile to water decreases the viscosity. The use of organic solvents

can also alter the hydration/solvation sheath around individual analytes, thus altering their effective size.

2.2.4.6 Modification of the capillary wall

Modification of the capillary wall can be used to reduce, eliminate or even reverse the electroosmotic flow. The reduction and elimination of the electroosmotic flow can be brought about by blocking the charges at the wall. Reagents used for this task can be chemically bonded to the capillary wall or dissolved in the buffer to form a dynamic coating.

Dynamic coating of the capillary wall is fairly simple, where surfactants dissolved into the buffer cover the charged groups on the capillary wall. The concentration and wash times affect the amount of coating and the extent to which the electroosmotic flow is reduced or eliminated.

The analysis of anions may require reversal of the electroosmotic flow, which can lead to a decrease in analysis time. Dynamic coatings offer a simple way to produce reversed flow. Cationic surfactants such as the alkylammonium salts cetyltrimethylammonium bromide (CTAB) and tetradecyltrimethylammonium bromide (TTAB) are commonly used for this.

2.2.4.7 How dynamic coating with surfactants works

The positively charged head groups of the alkyl ammonium salts interact with the silanoate groups of the capillary wall. The hydrophobic, hydrocarbon tails of the surfactant associate with the hydrocarbon tails of free surfactants by hydrophobic

interactions, forming a bilayer where the exposed positively charged head group provides the charge at the capillary wall (figure 2.13 & 2.14).

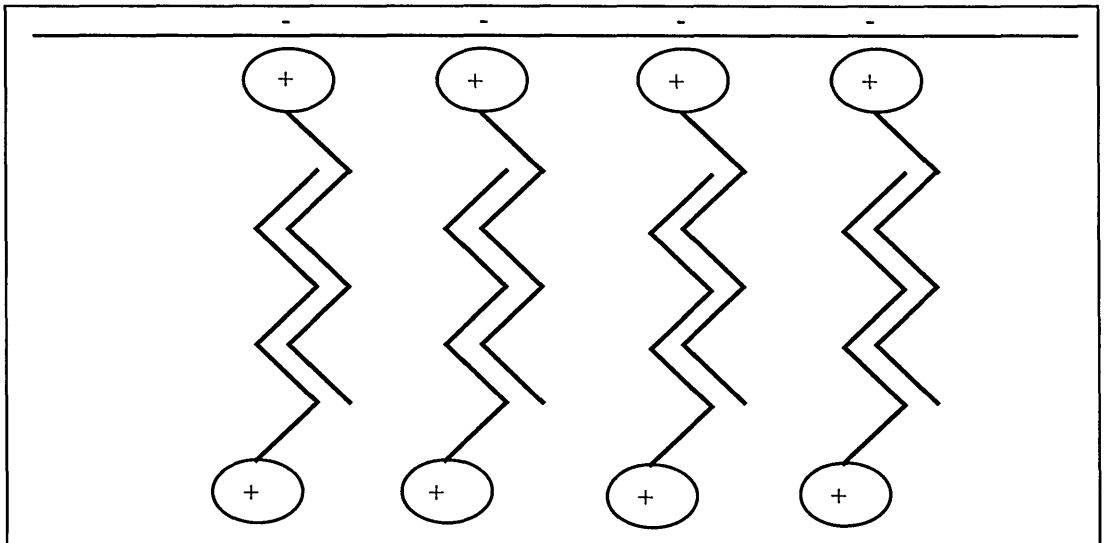

Figure 2.13 Wall coating with cationic surfactant.

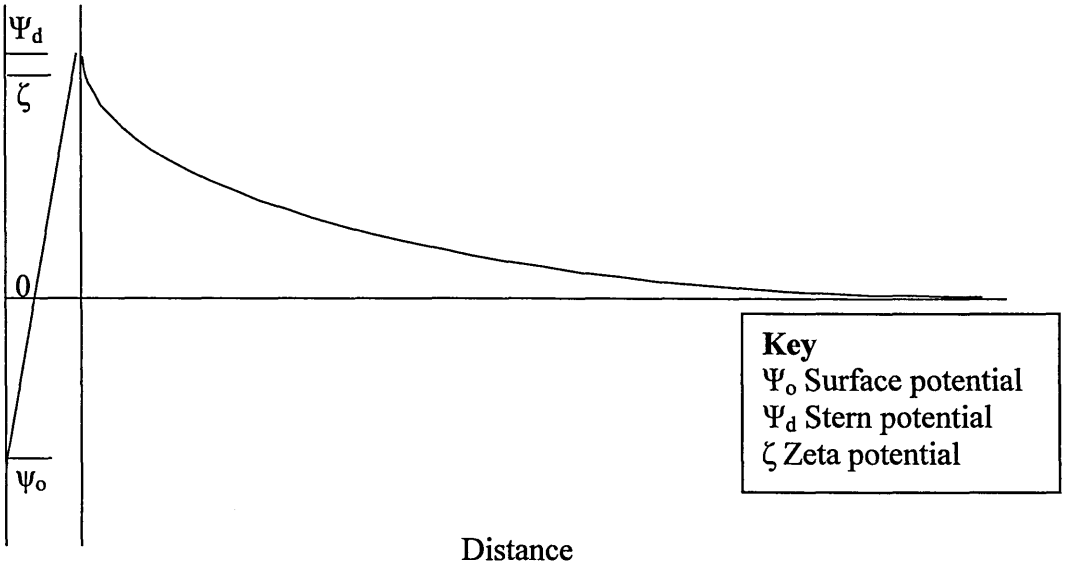

Figure 2.14 Representation of surface charge reversal due the adsorption of surfactants used in flow reversal.

2.3 Nonaqueous capillary electrophoresis

The use of pure organic buffer systems in capillary electrophoresis was reported by Walbroehl and Jorgenson in 1984[9], with a separation of five quinoline-type compounds in acetonitrile with tetraethylammonium perchlorate / hydrochloric acid. However, despite the success of this work, its potential was not taken up until the early 1990s, when nonaqueous capillary electrophoresis (NACE) was investigated as a separation technique in its own right.

Publications on nonaqueous capillary electrophoresis have gradually increased over the subsequent years. Nonaqueous capillary electrophoresis has been reported for the analysis of tamoxifen[10] and its hydrolysis products[11] and photoforin[12], a complex porphyrin mixture. Both are used in the treatment of cancer, while tamoxifen has also been prescribed as a preventative in familial cases of breast cancer. Nonaqueous capillary electrophoresis has been widely used for acidic and basic drugs, e.g. nonsteroidal anti-inflammatories[13,14], antihistamines[15] and cannabanoids[16]. The technique has also been used to analyse morphine[15] and other narcotics. Further work could see the technique not only used for providing evidence of drug abuse and trafficking but also in the world of sport to test for performance enhancing drugs. The analysis of nicotine[17] has also proved successful, which could lead to companies using tests for insurance policies in the future. The food industry also has a use for nonaqueous capillary electrophoresis as it has been shown to be a useful technique in the analysis of cholesterol[18]. It has also shown possibilities for the lubrication industry where Thibon *et al.*(1999)[19] analysed zinc dialkyldithiophosphates in a buffer consisting of methanol, acetonitrile, tetrahydrofuran with acetic acid and tetramethyl ammonium hydroxide.

As such, nonaqueous capillary electrophoresis is a very attractive method to a wide variety of industries. Organic solvents provide properties not only different to water, but also to other organic solvents. This has been used to advantage over conventional aqueous capillary electrophoresis, in which the solubility of hydrophobic analytes without the use of additives (surfactants) has extended the use of capillary electrophoresis.

2.3.1 Properties of organic solvents

The interactions between organic solvent molecules and other molecules are different from those of water.

In terms of NACE, polarity of a solvent is important in that polar solvents are able to separate moieties of opposite charge and allow similar charged moieties to come closer together. An organic solvent's polarity can be assessed in several ways, both physical and chemical. The physical aspects include cohesive pressure, dielectric constant, refractive index and dipole moment. The chemical properties include donor number and acceptor number to assess the acid-base capabilities of a solvent as well as polarity, hydrogen bond donor or acceptor potential.

These properties are important when deciding which solvent to use in NACE. For a solute to be soluble in a particular solvent, solvent-solvent intermolecular forces (cohesive pressure) and also the solute-solute intermolecular or inter-ionic forces must be disrupted. Disrupting the solvent-solvent interactions in essence creates a cavity for the solute.

Classification of molecular solvents is based on the assessment of both polarity and the acid-base properties (see table 2.15)

Low Polarity ε_r<20	High Polarity ε_r>30
Non-electrolyte	**Electrolytic**
Electron pair donor (tetrahydrofuran)	**Amphiprotic**
Polarizable (benzene)	Protogenic (sulphuric acid)
Inert (cyclohexane)	Neutral (ethanol)
	Protophilic (ammonia)
	Non-Protogenic
	Protophilic (dimethylsulphoxide)
	Protophobic (acetonitrile)
	Aprotic (sulphur dioxide)

Figure 2.15 Table identifying the classification of molecular solvents. Adapted from Chipperfield, J.R. (1999), 'Non-aqueous solvents', New York, Oxford University press inc.

For use in NACE, it is reasonable to expect that solvents of high polarity are used. High polarity solvents are suitable for the dissolution of ionic compounds to produce solutions that conduct electricity well.

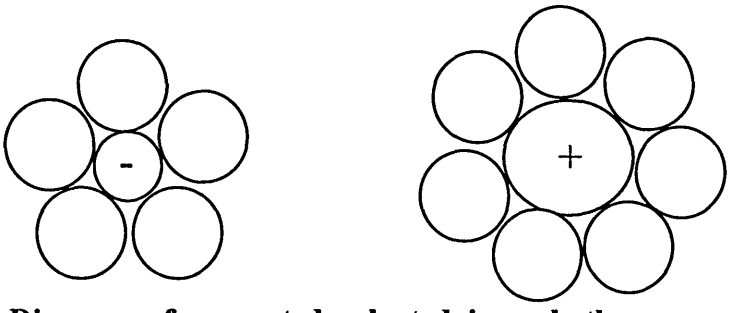

Figure 2.16 Diagram of separated solvated ions; both are responsible for conductivity.

Further classification relates essentially to the acid-base properties of a solvent i.e. if they readily give up protons (protogenic), accept protons (protophilic) or if they have the ability to both accept and donate protons (amphiprotic). Amphiprotic solvents are unique in that they are able to self-ionize or autoprotolyse resulting in a mixture of lyonium ions (cations) and lyate ions (anions).

Hydrogen bonding is also a factor to consider when assessing a solvent. Hydrogen bonding can occur intramolecularly (within a molecule) or intermolecularly (between molecules). Amphiprotic solvents can be involved in hydrogen bonding. Generally, hydrogen acceptor groups include nitrogen and oxygen (free paired electrons) and as such make good Lewis bases. The hydrogen bond acceptor groups mentioned also make good hydrogen bond donors.

There are two theories to describe acid-base reactions. The Brønsted-Lowry theory defines an acid as HA, where the proton H can be donated to a base for the formation of a conjugate acid and conjugate base, *viz.*

$$\underset{\text{Acid}}{HA} + \underset{\text{Base}}{B} \rightleftharpoons \underset{\text{Conjugate base}}{A^-} + \underset{\text{Conjugate acid}}{HB^+}$$

Likewise a Brønsted-Lowry base is a moiety that can accept a proton, the cojugate base being an anion (which can be termed as a lyate ion) and the conjugate acid being a cation (termed as a lyonium ion.)

Lewis, on the other hand, described the behavior of acids and bases differently. A Lewis acid has the ability to act as an electron-pair acceptor, whereas a Lewis base has the ability to donate an electron pair. Both of these reactants end up with the formation of an adduct, seen in figure 2.17 below.

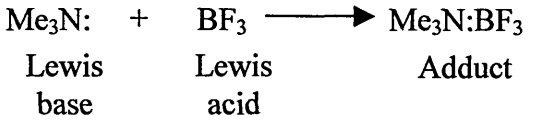

Figure 2.17 An example of a Lewis acid-base reaction.

Interactions in NACE become more complex as more compounds are added to the buffer system. The resulting solvent-analyte, solvent-additive, and analyte-additive, interactions can fall into electrostatic (ion-dipole, ion-ion, and dipole-dipole) and acid / base interactions[21].

Solvents are used to stabilise unpaired ions or dipoles, and the dielectric constant is used to determine a solvent's ability to separate solute charges and orient dipoles. The stronger the surface charge density of the ion or dipole, the higher is the required dielectric constant of the solvent.

Acid / base interactions in organic solvents are characterized by their donor and / or acceptor numbers. However it is not just the solvent's donor number (DN) that acts on

the separation but also the analytes' and additives' abilities to behave as Lewis bases in accepting free unpaired electrons. Likewise, the acceptor number (AN) (which has to account for the analytes' and additives' abilities to accept electrons acting as Lewis acids), is important in separation of analytes. Hydrogen bonding will have an effect on separations, especially for amphiprotic solvents and additives and analytes can hydrogen bond, either intra- or intermolecularly. The number of interactions possible within a nonaqueous buffer could be considerable and all will have an effect on the separation.

Solvent	Bp (°C)	pK_{auto}	ε	η (mPa s)	DN (kcal mol^{-1})
Water	100.00	14.00	78.30	0.890	18-33.00
Methanol	64.50	17.20	32.66	0.545	19-30.00
Ethanol	78.30	18.88	24.55	1.078	~32.00
Dimethylsulfoxide	189.00	33.30	46.45	1.996	29.80
N,N-Dimethylformamide	153.00	27-29	36.71	0.802	26.60
Acetonitrile	81.60	>33.30	35.90	0.341	14.10

Table 2.18 Donor number (DN), dielectric constant (ε), viscosity (η) and boiling point (Bp) for several solvents used in nonaqueous capillary electrophoresis. Adapted from Chipperfield, J.R. (1999). Non-aqueous solvents, New York, Oxford university press inc.

Most solvents used in nonaqueous capillary electrophoresis are able to act as electron donors and / or electron acceptors as are the additives and analytes. Chen *et al.*(1998)[20]

derived equations to show the interactions possible between an analyte and additive with both donor and acceptor properties.

$$D^- + A^+ \rightleftharpoons D^-A^+ \rightleftharpoons D \longrightarrow A$$

D and A are analyte electron donor and additive electron acceptor, respectively, which can progressively interact through increasing electrostatic interactions, to the transfer of an electron. The interactions can be ion-ion, ion-dipole and dipole-dipole. If the analyte or additive cannot accept or donate, electrons only the electrostatic interactions occur and vice versa.

If the solvent has donor and/or acceptor properties then their interactions with the additives and analytes have to be considered.

$$X \longrightarrow Y+S \rightleftharpoons X+Y \longleftarrow S$$

$$S+X \longrightarrow Y \rightleftharpoons S \longleftarrow X+Y$$

X electron donor
Y electron acceptor
S solvent

The solvent's acceptor and/or donor properties, hydrogen bonding and dielectric constant can affect the separation of analytes. If the solvent has very strong donor and/or acceptor properties and hydrogen bonding then the analyte may spend more time interacting with the solvent rather than the additive. This may lead to a poor resolution separation.

Altering the properties of a solvent system by introducing a second solvent can alter the interactions of the analyte and solvent, leading to an alteration in selectivity, e.g. by mixing methanol and acetonitrile. Almost all alterations in the separations reported have been ascribed primarily to the difference in electroosmotic flow caused by dielectric constant to viscosity ratio. Acetonitrile, unlike methanol, is not amphiprotic but is protophobic and nonprotogenic, (although it can be protonated in acidic conditions), so, its ability to interact with additives is mainly via stabilisation through conjugation, which alters the selectivity for a desired separation. This property was used to advantage by Khaledi *et al.* (2000)[21], who employed heteroconjugation for the separation of a variety of nitrophenols, chlorophenols and phenols.

2.4 Additives for nonaqueous capillary electrophoresis

2.4.1 Chiral separations

An invaluable aspect of CE and in particular NACE is the ability to separate isomers. This is of great use in the pharmaceutical industry and is why that industry is the predominant user of CE, where quality control of drugs, including isomeric ratios, is vital. Optical isomer separations can also be performed; chiral separations are mostly carried out by the introduction of additives into the separation buffer that act as pseudo-stationary phases, which then are able to interact with the analyte to varying degrees. The most commonly used additives are cyclodextrins where the analyte interacts with the cyclodextrin through hydrogen bonding with the hydroxyl groups present.

The use of cyclodextrins is widespread and a variety of cyclodextrins has been developed. Most commonly β- and γ- cyclodextrins are used. Riekkola *et al.* (1996)[22]

separated a variety of dansylated amino acids in N-methylformamide and compared this to a chiral separation in aqueous media. It was seen and stated that the nonaqueous media provided better results and an advantage of NACE was that the cyclodextrin had a solubility some 40x more than in aqueous media. Khaledi *et al.* (1996)[23] examined β- and γ-cyclodextrins in formamide, N-methylformamide and N,N-dimethylformamide for the separation of a variety of basic drug enantiomers.

More recently the scope of cyclodextrins has been increased by the introduction of a charged species, which is able to increase the stability of interactions between the analyte and the charged cyclodextrins. The charge also gives the cyclodextrin electrophoretic mobility against the EOF, therefore increasing migration time and resolution. Vigh *et al.*(2000)[24], Khaledi *et al.*(1999)[25] and Cai *et al.*(1999)[26] used sulphated derivatives of β-cyclodextrins for basic drugs. Khaledi *et al.*(1999)[25] found that stronger interactions occurred between the analyte and the charged cyclodextrin than with neutral cyclodextrins. Kahledi *et al.*(1998)[27] used a positively charged quaternary ammonium β-cyclodextrin to separate nonsteroidal anti-inflammatory drugs and derivatised amino acids with a reverse polarity. The use of positively charged quaternary ammonium β-cyclodextrin was also found to reverse the EOF.

Lämmerhofer *et al.*(2000)[28] used a positively charged tert-butylcarbamoylquinine as an ion pair agent for the separation of N-3,5-dinitrobenzyoylated (DNB)-protected amino acids. Using a partial filling technique they improved sensitivity. The uv absorbing ion pair agent only part filled the capillary and was not present in the separation buffer, and so was not present at the detector when the analytes were detected. The same group, used DNB-leucine as the ion pair agent[29], but coated the capillaries with

polyvinylalcohol, which stopped adsorption of analyte to the capillary wall and slowed the EOF. Pettersson *et al.*(2001)[30] used ion pairing mechanisms to separate amine isomers, and examined the effect of coating the capillary. Using an uncoated capillary they optimised the ion pair agent concentration, then coated the inner capillary wall with polyacrylamide to form a capillary wall with no charge. With partial coverage the EOF was slowed down, and total coverage of the inner wall resulted in stoppage of the EOF. This method resulted in the improvement of the separation, at best when the capillary was coated with an aminopropyl compound that produced a reversal of the EOF.

An alternative to pseudo-stationary phases is the use of a stationary phase packed within the capillary, Lindner *et al.*(2002)[31] used a silica low-molecular-weight chiral cation exchange packing for the successful separation of several amine isomers.

2.4.2 Neutral analytes

In aqueous capillary electrophoresis neutral analytes can be separated by micellar electrokinetic chromatography. A surfactant is added to the separation buffer where aggregation brings about the formation of micelles. The analytes of interest differentially partition into the micelles and, therefore, separate (figure 2.19).

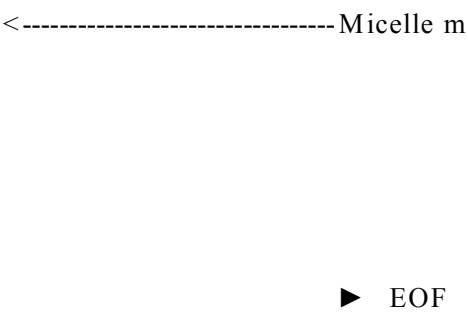

Figure 2.19 Representation of micellar electrokinetic chromatography

However if the analytes are too hydrophobic they will stay in the micelle and resolution is lost. Separation mechanisms using surfactants in organic solvents are not really understood.

Polycyclic aromatic hydrocarbons (PAH) have been analysed by NACE. Miller *et al.* (1998)32 and (1997)33 used triphenylpyrylium and tropylium cations and pyrylium salts to induce charge transfer interactions, allowing PAH to become charged and have their own mobility. Li *et al.(*1999)34 used sodium tetradecyl sulphate as surfactant for the separation of a mixture of five PAH. Unlike aqueous CE, where the separation of PAH occurs through hydrophobic interactions with micelles, in this case separation was performed through charge association of the PAH and the surfactant. Alternatively Weber *et al.(*2000)35 used lanthanide triflates to form adducts with alcohols in acetonitrile/ethylene carbonate. However, the separation was halted by the presence of water or hydroxides as the lanthanide binds to these to form adducts, and as such none of the lanthanide is available for interaction with the alcohols.

2.4.3 Electroosmotic flow

As in aqueous capillary electrophoresis, the electroosmotic flow is dependent on pH, dielectric constant to viscosity ratio and other factors. In nonaqueous capillary electrophoresis, the solvent also plays a role in the formation of the electroosmotic flow. Cassidy *et al.*(1996)[36] reported that electroosmotic flow in methanol was increased by addition of acetonitrile. This was ascribed to alterations in interactions at the capillary wall and in the bulk buffer.

Dorsey *et al.*(1997)[37] studied the behaviour of nonaqueous solvents without electrolyte in nonaqueous capillary electrophoresis. They concluded that the electroosmotic flow mobility could be correlated with the dielectric constant to viscosity ratio, and also stated that acetonitrile provided the fastest electroosmotic flow of the solvents that they studied.

2.4.3.1 Reversing electroosmotic flow

In aqueous capillary electrophoresis, reversing the electroosmotic flow is established by dynamic coatings or covalent coatings. Most widely used are dynamic coatings formed by cationic surfactants. However, in organic solvents there are little or no hydrophobic interactions and reversal of flow is not seen using the dynamic coating method.

Flow reversal has been achieved in nonaqueous capillary electrophoresis by the addition of a cationic polymer such as hexadimethrine bromide (HDB).

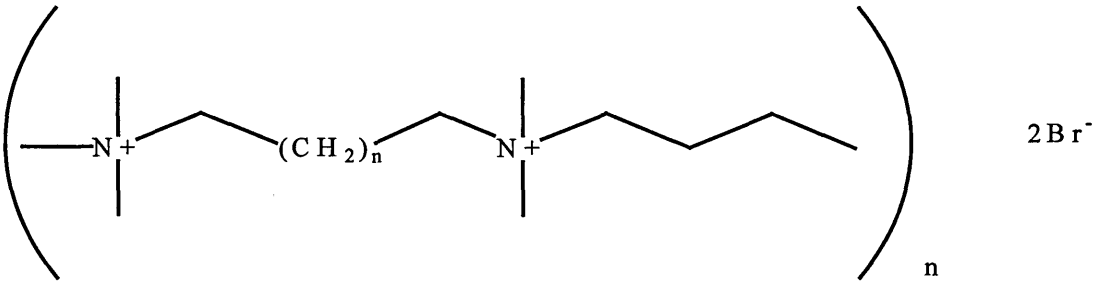

Figure 2.2. Molecular structure of HDB.

This was used by Zemann *et al.* (1997)[38] for the separation of carboxylic acids. Tjørnelund *et al.* (1998)[39] separated hydroxy- and dihydroxy-benzoic acids using HDB and an acetonitrile-methanol mix, while the separation of acetylsalicylic acid and three of its metabolites was reported by Hansen *et al.* (1998)[40] with a reversed electroosmotic flow. Covalent bonding of compounds has been used to produce a permanently fixed positive charge on the capillary wall. Gilges *et al.* (1994)[41] used poly(vinyl alcohol) as both dynamic and covalent coatings for the separation of acidic and basic proteins, while polymeric capillaries have been used by Schneider *et al.* (1998)[42] to allow separation of amino acids and peptides.

2.5 Advantages of nonaqueous capillary electrophoresis

Nonaqueous capillary electrophoresis has several advantages over aqueous capillary electrophoresis for method development:

- Wider range of analytes available for separation, especially hydrophobic compounds without the requirements for use of surfactant micelles as a pseudo-stationary phase.
- Selectivity can be easily altered by changing and mixing of solvents.
- Organic solvents run with lower currents and so can be exposed to higher electrolyte concentration and ionic strength or higher electric fields. Riekkola *et al.*(2002)[43] have applied extremely high electric field strengths to the separation of several compounds, evaluating several alcohols as solvent (methanol, ethanol, propanol and butanol) and using voltages up to 60kV. Special insulation considerations were taken into account including placing the inlet vial in oil to prevent arcing in air.
- Wider bore capillaries can be used for greater sensitivity. This derives from the lower conductivity of organic solvents. With lower conductivity wider capillary bores can be used as less joule heating is present as a result of lower current and as such less band broadening in separations is seen.

References

1 Tiselius, A., Transactions of the Faraday Society 1937, **33**, 524-531.

2 Hjertén, S., Chromatographic Reviews 1967, **9**, 122-219.

3 Mikkers, F.E.P., Everaerts, F.M., Verheggen, Th.P.E.M., Journal of Chromatography 1979, **169**, 11-20.

4 Jorgenson, J.W., Lukacs, K.D., Analytical Chemistry 1981, **53**, 1298-1302.

5 Cohen, N., Grushka, E., Journal of Chromatography A 1994, **684**, 323-328.

6 Tsuda, T., Sweelder, J.V., Zare, R.N., Analytical Chemistry 1990, **62**, 2149-2152.

7 Moring, S.E., Reel, R.T., van Soest, R.E.J., Analytical Chemistry 1993, **65**, 3454-3459.

8 Heiger, D.N., High Performance Capillary Electrophoresis: An Introduction, France; HP.Co., 1992, 101.

9 Walbroehl, Y., Jorgenson, J.W., Journal of Chromatography A 1984, **315**, 135-143.

10 Sanders, J.M., Burka, L.T., Shelby, M.D., Newbold, R.R., Cunningham, M.L., Journal of Chromatography B 1997, **695**, 181-185.

11 Li, X.F., Carter, S.J., Dovichi, N.J., Journal of Chromatography 2000, **895**, 81-85.

12 Bowser, M.T., Sternberg, E.D., Chen, D.D.Y., Analytical Biochemistry 1996, **241**, 143-150.

13 Cherkaoui, S., Veuthey, J.L., Journal of Chromatography A 2000, **874**, 121-129.

14 Fillet, M., Bechet, I., Piette, V., Crommen, J., Electrophoresis 1999, **20**, 1907-1915.

15 Leung, G.N.W., Tang, H.P.O., Tso, T.S.C., Wan, T.S.M., Journal of Chromatography A 1996, **738**, 141-154.

16 Backofen, U., Matysik, F-M., Lunte, C.E., Journal of Chromatography A 2002, **942**, 259-269.

17 Matysik, F-M., Journal of Chromatography A 1999, **853**, 27-34.

18 Xu, X-H., Li, R-K., Chen, J., Chen, P., Ling, X-Y., Rao, P-F., Journal of Chromatography B 2002, **768**, 369-373.

19 Thibon, V.R.A., Bartle, K.D., Abbott, D.J., McCormack, K.A., Journal of Microcolumn Separations 1999, **11**, (1), 71-80.

20 Bowser, M.T., Kranack, A.R., Chen, D.D.Y., Trends in Analytical Chemistry 1998, **17**, (7), 424-434.

21 Miller, J.L., Shea, D., Khaledi, M.G., Journal of Chromatography A 2000, **888**, 251-266.

22 Valkó, I.E., Sirén, H., Riekkola, M-J., Journal of Chromatography 1996, **737**, 263-272.

23 Wang, F., Khaledi, M.G., Analytical Chemistry 1996, **68**, (19), 3460-3467.

24 Zhu, W., Vigh, G., Journal of Chromatography A 2000, **892**, 499-507.

25 Wang, F., Khaledi, M.G., Journal of Chromatography B 1999, **731**, 187-197.

26 Tacker, M., Glukhovskiy, P., Cai, H., Vigh, G., Electrophoresis 1999, **20**, 2794-2798.

27 Wang, F., Khaledi, M.G., Journal of Chromatography A 1998, **817**, 121-128.

28 Lämmerhofer, M., Zarbl, E., Lindner, W., Journal of Chromatography A 2000, **892**, 509-521.

29 Zarbl, E., Lämmerhofer, M., Franco, P., Petracs, M., Lindner, W., Electrophoresis 2001, **22**, 3297-3307.

30 Carlsson, Y., Hedeland, M., Bondesson, U., Pettersson, C., Journal of Chromatography A 2001, **922**, 303-311.

31 Tobler, E., Lämmerhofer, M., Wuggenig, F., Hammerschmidt, F., Lindner, W., Electrophoresis 2002, **23**, 462-476.

32 Miller, J.L., Khaledi, M.G., Shea, D., Journal of Microcolumn Separations 1998, **10**, (8), 681-685.

33 Miller, J.L., Khaledi, M.G., Shea, D., Analytical Chemistry 1997, **69**, 1223-.

34 Li, J. Fritz, J.S., Electrophoresis 1999, **20**, 84-91.

35 Li, S., Weber, S.G., Journal of the American Chemical Society 2000, **122**, 3787-3788.

36 Salimi-Moosavi, H., Cassidy, R.M., Analytical Chemistry 1996, **68**, 293-299.

37 Wright, P.B., Lister, A.S., Dorsey, J.G., Analytical Chemistry 1997, **69**, 3251-3259.

38 Volgger, D., Zemann, A.J., Bonn, G.K., Antal Jr, M.J. Journal of Chromatography A 1997, **758**, 263-276.

39 Tjørnelund, J., Bazzanella, A., Lochmann, H., Bächmann, K., Journal of Chromatography A 1998, **811**, 211-217.

40 Hansen, S.T., Jensen, M.E., Bjørnsdottir, I., Journal of Pharmaceutical & Biomedical Analysis 1998, **17**, 1155-1160.

41 Gilges, M., Kleemiss, M.H., Schomburg, G., Analytical Chemistry 1994, **66**, 2038-2046.

42 Schneider, P.J., Engelhardt, H., Journal of Chromatography A 1998, **802**, 17-22.

43 Palonen, S., Jussila, M., Porras, S.P., Hyötyläinen, T., Riekkola, M.L., Electrophoresis 2002, **23**, 393-399.

Chapter 3

Mass spectrometry and capillary electrophoresis mass spectrometry

3.0 Introduction

Mass spectrometry plays a major role in analysis. It offers both high sensitivity (low detection limits) and qualitative information, which are of great importance to the analyst.

Mass spectrometry can be described as the separation and detection of gas phase ions from neutral compounds in a vacuum. Separation is dependent upon the differences in mass to charge ratio.

A wide variety of instrumental procedures can lead to the production of many ions, both from the parent molecule and from its fragments.

A simplistic description of a mass spectrometer consists of an ion source, mass analyser(s) and detector. The mass spectrometer is attached to a computer for control and data acquisition.

Older mass spectrometers kept the ion source, mass analyser (s) and detector all under vacuum, ensuring that the ions produced from the source did not collide with each other or other air molecules, to ensure easy interpretation of the mass spectra. Nowadays ionisation is often conducted at or near atmospheric pressure.

Ions must be created from any compound under investigation unless it is already ionised i.e. a salt. Ionisation may be by the addition or removal of an electron, producing two species of ion positive, ($M^{+\cdot}$) and negative ($M^{-\cdot}$). Ionisation may also come about by the addition or subtraction of another charged species (X^{+}) to produce

$[M + X]^+$ or $[M - X]^-$, known as quasi-molecular ions. If the compound under investigation is a salt (M^+X^-), being already ionised, it only requires the two charged species to be separated by the mass spectrometer.

Being held under a vacuum was problematic for sample introduction as the sample has to be transferred from an area at atmospheric pressure to an area under vacuum. For this reason a variety of inlets were developed including cold, hot, direct probe and gas and liquid chromatography inlets.

The area in which ionisation occurs is the ion source, of which there are a variety;

- Electron ionisation
- Chemical ionisation
- Field ionisation
- Field desorption
- Spraying and ion evaporation (see section 3.3)
- Fast atom bombardment
- Laser ionisation

Once the ions are formed in the source they are accelerated into the mass analyser by a high electrical potential (2-8kV) where they are separated by their mass to charge ratio. As with the ion source there are a variety of mass analysers, including:

- Quadrupole (see section 3.4)
- Ion trap
- Time of flight
- Magnetic and electromagnetic sectors

- Ion cyclotron

Analysers can be coupled to form tandem mass spectrometers (see section 3.5). Coupling mass analysers to chromatography opens the door to a wider use of mass spectrometry and a new variety of techniques.

Once the ions leave the mass analyser they enter the detector where electron multipliers, array detectors, or photon multipliers detect the ions. Data is then sent to a computer.

It was not until the introduction of atmospheric pressure ionisation sources that mass spectrometry could be easily used in conjunction with liquid chromatographic separation techniques such as high performance liquid chromatography and capillary electrophoresis.

3.1 Capillary electrophoresis mass spectrometry

Capillary electrophoresis has been coupled to a variety of ionisation sources, including electrospray (see section 3.3), continuous flow fast atom bombardment and inductively coupled plasma. It has also been used in offline coupling with matrix-assisted laser desorption ionisation.

Separation is initially provided by capillary electrophoresis, and the separation capillary is fed into an ionisation source. The ions move through the capillary into the ionisation source which then passes appropriate ions into the mass analyser. Separated ions escape to the detector.

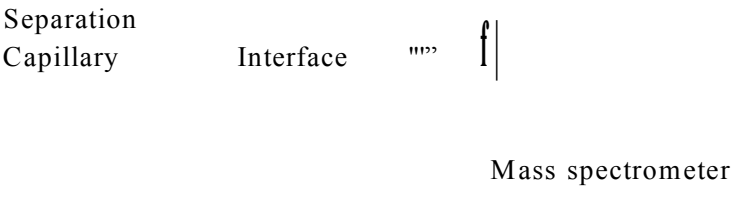

Figure 3.1 Diagram of capillary electrophoresis-mass spectrometer arrangement.

The use of capillary electrophoresis-mass spectrometry has been widespread for several years and has given rise to a variety of interfaces specifically for electrospray ionisation. The formation of continuous electrospray has been problematic, especially with the quantities of water used in CE buffers. The main problem is that the surface tension is quite high, which is detrimental for the electrospray process. Another problem seen in early development was the very low flow rates in capillary electrophoresis compared to high performance liquid chromatography. These two problems were overcome by developing the interface in two ways, firstly by the use of a nebulisation gas that assisted the electrospray formation and secondly by the use of a sheath flow which increased solvent flow into the mass spectrometer. However, the use of a sheath flow on the interface introduced a problem of reduced sensitivity by the dilution of samples with the large volumes of sheath liquid. The second type of interface used was sheathless (nanospray), where the CE eluent sprays almost directly into the mass analyser. No sheath flow is required so sample dilution is not present. The only problems seen are that with a high water content electrospray is not as stable and the capillary tip is more susceptible to blockage.

The addition of organic solvents to capillary electrophoresis separation buffers and sheath flow produces an improvement in electrospray stability, possibly by reducing the surface tension and thus improving the formation of the electrospray.

Nonaqueous capillary electrophoresis provides an ideal buffer system for use with electrospray ionisation. The development of nonaqueous capillary electrophoresis has also seen an increase in nonaqueous capillary electrophoresis mass spectrometry publications. As with nonaqueous capillary electrophoresis, most of the work published has been concerned with pharmaceutical compounds.

Naylor *et al.* (1994)[1] investigated mifetidine and its metabolites in organic solvents, particularly methanol with ammonium acetate. Tamoxifen is a drug that is readily analysed by nonaqueous capillary electrophoresis – mass spectrometry; Cole *et al.* (1996)[2] used a methanol buffer solution with sodium dodecyl sulphonate (SDS) as an additive. In his investigations he witnessed very little source fouling. Dovichi *et al.* (2001)[3] used this technique for monitoring tamoxifen and metabolites in the urine of cancer patients, specifically to investigate tamoxifen resistance in patients and identify any correlation that could be found with regard to metabolites in urine. Dovichi *et al.*(1998)[4] examined tricyclic antidepressants and amitryptyline, for which he proposed a fragmentation pathway of tricyclic antidepressants and metabolites by electrospray ionisation mass spectrometry. Raith *et al.* (1998)[5] examined phospholipids, and Veuthey *et al.* (2001)[6] examined steroidal alkaloids in plant extracts using a co-axial sheath flow interface. Veuthey *et al.* (2000)[7] also developed a method for the analysis of amphetamines in urine, again using a co-axial sheath flow, and concluded that the

use of a high drying gas flow rate reduced the sensitivity of detection. Basic and acidic drugs in general were the topic for investigation by Senior *et al.* (2000)[8].

3.2 Electrospray interfaces

The most common chromatography technique to be interfaced with mass spectrometry is high performance liquid chromatography (HPLC). The interfaces designed for this specific technique were initially replicated and modified to allow for the use of interfacing capillary electrophoresis with mass spectrometry.

The limiting factor for capillary electrophoresis mass spectrometry is the interface between the capillary electrophoresis instrumentation and the mass spectrometer. The interface performs two functions. Firstly it acts as an electrode for capillary electrophoresis and secondly is responsible for the formation of the electrospray (see section 3.3) where good electrical contact is vital.

There have been three major types of interface developed for use in capillary electrophoresis-mass spectrometry, namely sheathed flow, liquid junction and co-axial sheath flows, and sheathless nanospray. Each type of interface has been shown to be successful. Comparison between the liquid junction and co-axial sheath flow was made by Pleasance *et al.* (1992)[9], comparing the two interfaces for the analysis of some toxins and antibiotics. The co-axial sheath flow was a more robust and reproducible interface that provided greater flexibility than the liquid junction, which was prone to loss of electrophoretic performance.

The make up flows provided by the two interfaces provide an adequate volume of solvent to produce the electrospray, as the flow produced by CE is generally too low for mass spectrometry.

3.2.1 Liquid junction

Liquid junction interfaces are designed so that the make up flow is introduced at the end of the separation capillary. The mixture then travels through the electrospray needle for the electrospray process.

Figure 3.2 Adaptation of a liquid junction interface.

Henion *et al.* (1996)[10] designed a liquid junction interface with the use of a T-junction. With this type of interface a small dead volume is created between the three capillaries. This area can be problematic for electrical connection and could be the area responsible for the electrophoresis breakdown commonly seen by Pleasance *et al.* in 1992[9]. This type of interface is not as common as co-axial sheath flow.

3.2.2 Co-axial sheath flow

Co-axial sheath is the most widely used of the sheath flow interfaces. The general design consists of three concentric capillaries. The inner capillary, which is used for the separation by capillary electrophoresis, is also used for the formation of the electrospray, unlike the liquid junction design where a separate needle is used. The middle capillary is used to provide the sheath flow that mixes with the separation buffer at the end of the capillary. The outer capillary introduces the nebulizing gas, which is used to improve the formation of the spray, especially with the water content of aqueous capillary electrophoresis separations. Hau and Roberts (1999)[11] developed a successful co-axial sheath flow without the use of a nebulizing gas for vitamin B_1 solutions, but their addition of methanol to the separation may have taken away some of the requirements for a nebulization gas by the reduction of surface tension. They also pressurised the separation to reduce analysis time.

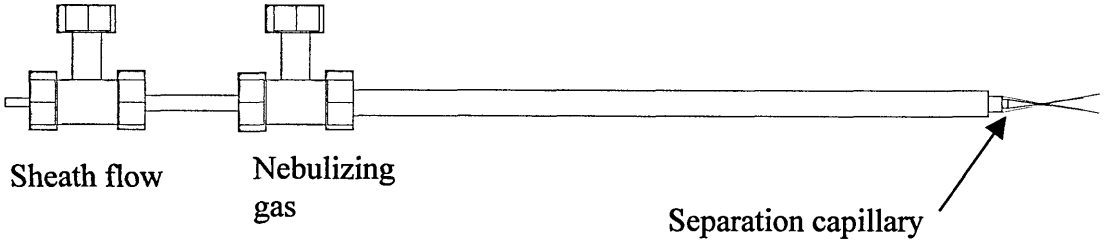

Figure 3.3 Diagrammatic representation of a co-axial sheath flow interface.

Tetler *et al.* (1995)[12] examined the effect of relative capillary dimensions on the performance of a capillary electrophoresis-mass spectrometry interface. They concluded that an optimum ratio of inner and outer capillary diameters aided the formation of a stable electrospray. Kirkby *et al.* (1996)[13] went on to shape the tip of capillaries to improve electrospray performance. Creating a smaller inner diameter

increased the velocity of flow out of the capillary, while shaping the outside improved the electrical contact to provide a more stable electrospray.

3.2.3 Sheathless flow

More recent work has specifically investigated the use of sheathless interfaces (nanospray). This work would not be possible if it were not for improvements in mass spectrometer performance. Initial work used the separation capillary as the electrospray needle. Cook *et al.* (1995)[14] investigated cone shaped tips that were coated in gold to provide a durable interface. Petersson *et al.* (1999)[15] produced a successful separation and detection of four fatty acids and six prostaglandins using a sheathless flow. In this case, the separation capillary was pulled through a stainless steel tube liner to provide the required electrical connection.

More recently Chang and Her (2000)[16] used a separation capillary that was carbon-coated at the end to provide electrical connection. Mioni (2001)[17] developed a split flow technique by drilling a hole near the tip of the capillary. The whole was covered by metal where the voltage could be applied for the electrospray, this area allows for a better electrical connection. The new design gave the sensitivity of a sheathless interface in conjunction with the simplicity of a sheath flow. Bergquist *et al.* (2002)[18] utilised a conductive polymer composed of polypropylene / graphite mix, either as a housing for the separation capillary tip or as a coating that was melted onto the capillary. Both were reported to provide desirable nanospray features with long term stability and low cost of manufacture.

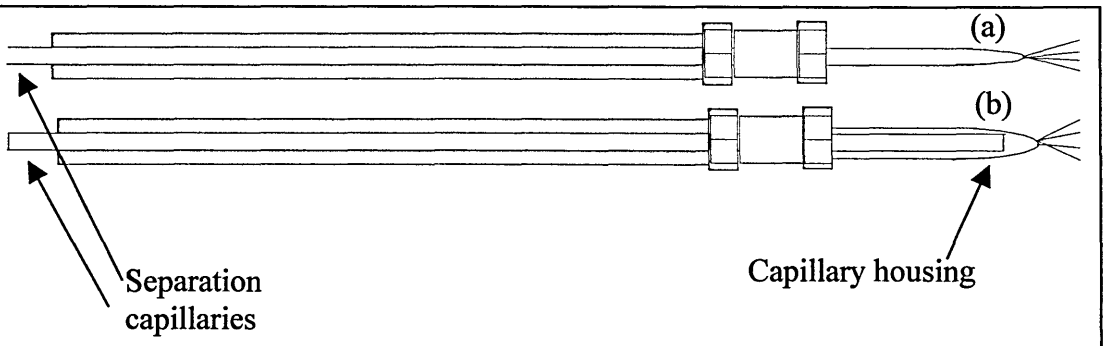

Figure 3.4 (a) Sheathless interface using the separation capillary for electrospray formation. (b) Sheathless interface with a capillary housing for electrospray formation.

In nanospray there is no dilution and so sensitivity is greater.

3.3 Electrospray ionisation

Electrospray ionisation can be described as the generation of a fine mist of charged droplets from a solution, by using coulombic repulsion to break up the liquid into smaller droplets.

Electrospray ionisation can be split up into several points:

- Nebulisation of sample into a fine mist of charged droplets
- Production of ions from droplets and movement into the mass analyser

Electrospray ionisation is a soft ionisation technique. There is generally no fragmentation of analytes and only the molecular ion or quasi-molecular ions are seen. However, it is possible to obtain multiple charging of macromolecules if they have many protonation / deprotonation sites. This is advantageous with macromolecules that

are too large to be measured on specific analysers since multiple charging extends the effective mass range of analysers by increasing the charge in the mass to charge ratio.

The formation of an electrospray depends on the solvent used, which dictates the electrical potential required to form the electrospray. A potential difference is applied between the capillary and the counter electrode. The optimal potential difference leads to the formation of a 'Taylor cone' where the surface tension of the solvent is broken and droplets are formed.

Figure 3.5 Representation of a 'Taylor cone' and droplet formation.

The droplets formed are highly charged, either positive or negative. As the charged droplets migrate across the ionisation source the solvent is evaporated. This evaporation process is carried out by a curtain gas such as nitrogen which removes the solvent from the droplet. The droplets shrink to a point where the collective repulsion from coloumbic forces is such that it exceeds the surface tension of the droplet. Once the surface tension is broken the droplet effectively explodes, releasing smaller droplets. This desolvation cascade continues until the droplets are small enough that ions desorb for analysis.

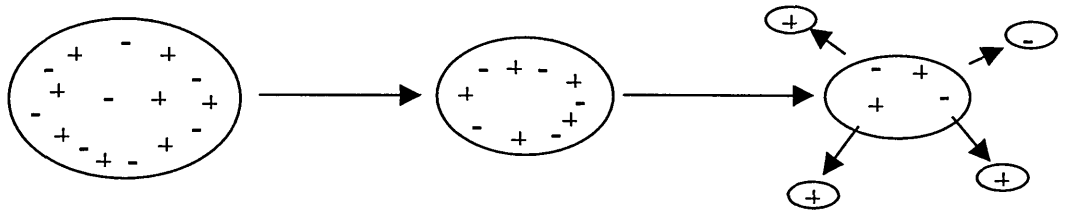

Figure 3.6 Representation of proposed solvent evaporation and ion ejection.

A second atmospheric pressure ionisation source (apart from electrospray) is atmospheric pressure chemical ionisation (APCI). In APCI the effluent from the chromatographic technique is sprayed into the ionisation source via a pneumatic nebuliser, and this spray is then converted into a thin fog by nitrogen gas. The solvents present from the chromatography are evaporated by passage through a desolvation/vaporisation chamber from whence it flows into the ionisation area. In the ionisation area the gas flows past a corona discharge needle or a β-particle emitter, where chemical ionisation leads to primary ion formation and then reaction with the vaporised water or solvent molecules to produce secondary reactant gas ions. These go on to react with the analytes of interest to form molecular ions through proton transfer or adduction of the reactant gas for positive ions and proton abstraction or adduct formation for negative ions. As the molecular ions pass into the vacuum region the solvent or gaseous water molecules are stripped away to allow analysis. The flow rates for this technique are 0.2 to 2ml min^{-1}, however, the flow rates from CE are too low for this ionisation technique and as such it is only suitable for HPLC.

3.4 Mass analysers

As with ion sources there are many types of mass analyser, in all of which the ions created in the ion source are separated according to their mass to charge ratio (m/z)

Mass analysers used today include quadrupole, ion trap, magnetic sector, cyclotron and time of flight systems, of which the most widely used for capillary electrophoresis-mass spectrometry is the quadrupole.

3.4.1 Quadrupole mass analyser

Quadrupoles are cheap and robust compared to other analysers. They are designed such that there are four parallel rods, arranged in the manner as shown in figure 3.7. The rods are connected to a direct current voltage (U) with a superimposed radiofrequency (RF) potential ($V\cos(\omega t)$). V is the max amplitude, ω is the angular frequency of the RF voltage and t is the time. The distance between a pair of opposite and electrically connected rods is $2r_o$.

Ions created by the ion source are ejected into the quadrupole analyser by a voltage of 5v which provides acceleration for the ions. When inside the analyser the ions follow an oscillating trajectory governed by the effects of the electric fields from the rods. The acceleration is a necessity for the ions to transverse the quadrupole, figure 3.8 shows the electrical field variations from the rods. There is no applied field along the Z axis, so without the acceleration ions would merely oscillate within the rod set up of the quadrupole.

Figure 3.7 Representation of quadrupole set up for voltage supplies.

The motion of the ions can be related to a form of the Mathieu equation.

Figure 3.8 Representation of electrical fields in respect of a,, and qu along the quadrupole.

As long as the motion in the x y plane remains less than r_0 the ions will traverse the quadrupoles and be detected. The ions will not be detected if motion in x and/or y is greater or equal to r_0, here the ions strike the rods and are discharged.

$$a_u = \frac{8zeU}{(m\omega^2 r_o^2)} \qquad \text{Where } U = a_u \frac{m}{z}\frac{\omega^2 r_o^2}{8e}$$

$$q_u = \frac{4zeV}{(m\omega^2 r_o^2)} \qquad \text{Where } V = q_u \frac{m}{z}\frac{\omega^2 r_o^2}{4e}$$

a_u and q_u determine if the ions of mass m are found to be in the stable region or not (see figure 3.9).

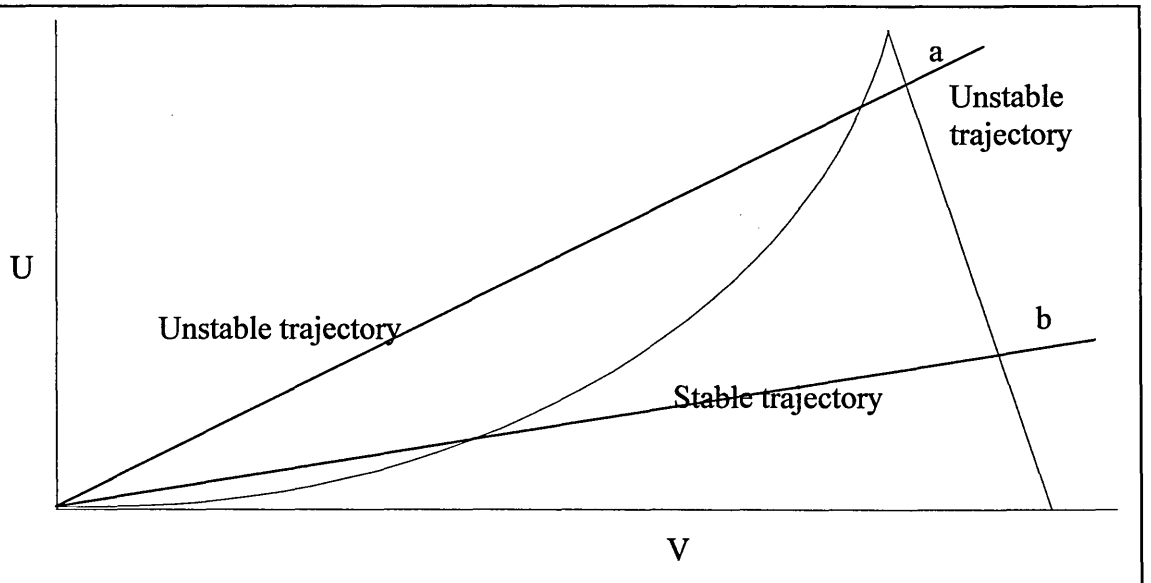

Figure 3.9 Diagram showing a stability region for an ion of a particular mass.

Figure 3.9 shows the relationship between direct current voltage (U) and radio frequency voltage (V). The two lines that cross the stable trajectory represent the relationship between U and V; the slope represents the different ratios of alterations to

U and V. The shallower slope covers a wide range of masses within the stable trajectory region and thus allows a wide range of masses through the mass analyser. The steeper slope covers a narrower area of the stable trajectory area and thus allows fewer ion masses through the analyzer. To this end, to allow one ion of a particular mass through the analyser, U and V must give a slope that crosses the stable trajectory area that covers one mass unit.

However, when looking at several different masses of interest using a low slope is inadequate, as many masses will travel across the mass analyser, this has the effect of decreasing resolution for the peaks of interest. Figure 3.10 shows the stability regions for three ion masses, and by altering the ratio of U and V, a slope that intercepts all three stability regions can be obtained. This allows only the masses of interest through by selective ion monitoring, increasing the resolution between the particular peaks.

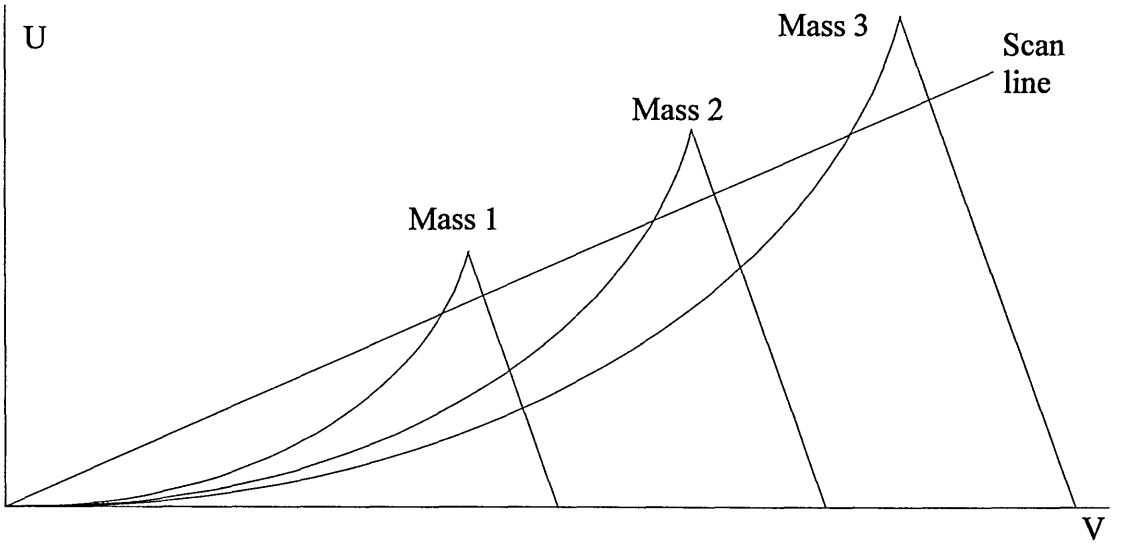

Figure 3.10 Showing the stability regions of ions of three masses.

3.5 Tandem mass spectrometry

Deliberately increasing the internal energy of an ion, and moving the ion to an excited energy state, can be used to identify the structure of a compound. The increased internal energy causes the ion to fragment, and in tandem mass spectrometry (MS/MS) the fragment or product ions are then separated and identified.

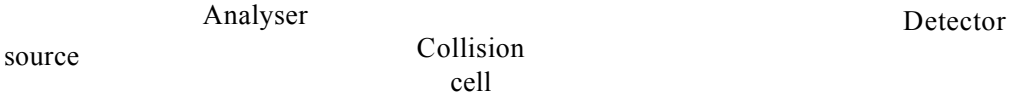

Figure 3.11 Arrangement for tandem mass spectrometry.

Tandem mass spectrometry can be achieved in space by coupling two instruments or in time by carrying out sequential steps in an ion storage device.

With triple quadrupole mass analysers, the first (Q1) and third (Q3) quadrupole analysers are used to scan and / or select specific ions of interest whilst the second (Q2) is used as a collision cell.

Figure 3.12 Representation of a quadrupole tandem mass spectrometer.

The ions enter the first mass analyser and scanning or ion selection is performed. The ions then enter the collision cell where a collision gas increases the internal energy of the ions. The ions fragment and then enter the final mass analyser where the product ions are again selected or scanned.

Within the collision cell two processes occur. The first is the collision of the ion with a gas where the energy from the gas is passed onto the ion and converted into internal energy to yield an ion in an excited state. Only a fraction of the energy is converted into internal energy.

This is then followed by decomposition of the ion, collision induced decomposition or dissociation (CID).

Two types of CID are found; high energy (keV) and low energy collision (eV). High energy is used in electromagnetic or hybrid instruments, where a high energy gas such as helium is used as the collision gas.

Low energy collision (1-100eV) is used in triple quadrupole and hybrid instruments, where the collision cell is a quadrupole analyser operated in the RF mode only, to focus the ions after collisions have taken place. Heavy gases such as argon are used where low energy transfer occurs. Using a quadrupole for the collision cell allows multiple collisions to occur along the length of the cell and high yields are seen.

There are a variety of scan modes possible with such instruments; product ion, precursor ion, neutral loss and selected reaction monitoring.

In product ion scans, a precursor ion is selected in Q1 and then the product ions after collision induced decomposition are scanned in Q3.

Precursor scan is carried out by selecting a product ion in Q3 , scanning the precursor ions in Q1.

In neutral loss, a neutral fragment is selected and fragmentations from the loss of the neutral fragment are identified. Q1 and Q3 are scanned synchronously with a constant mass offset between them.

In selected reaction monitoring, both Q1 and Q3 are used in selected ion mode. Ions are only detected when both Q1 and Q3 are set for the correct masses.

Several reports,[19-21] describe the use of tandem mass spectrometry with online capillary electrophoresis.

References

1. Tomlinson, A.J., Benson, L.M., Gorrod, J.W., Naylor, S., Journal of Chromatography B 1994, **657**, 373-381.
2. Lu, W., Poon, G.K., Carmichael, P.L., Cole, R.B., Analytical Chemistry 1996, **68**, 668-674.
3. Carter, S.J., Li, X-F., Mackey, J.R., Modi, S., Hanson, J., Dovichi, N.J., Electrophoresis 2001, **22**, 2730-2736.
4. Liu, C-S., Li, X-F., Pinto, D., Hansen Jr., E.B., Cerniglia, C.E., Dovichi, N.J., Electrophoresis 1998, **19**, 3183-3189.
5. Raith, K., Wolf, R., Wagner, J., Neubert, R.H.H., Journal of Chromatography A 1998, **802**, 185-188.
6. Cherkaoui, S., Rudaz, S., Veuthey, J-L., Electrophoresis 2001, **22**, 491-496.
7. Geiser, L., Cherkaoui, S., Veuthey, J-L., Journal of Chromatography A 2000, 111-121.
8. Senior, J., Rolland, D., Tolson, D., Chantzis, S., De Biasi, V., Journal of Pharmaceutical and Biomedical Analysis 2000, **22**, 413-421.
9. Pleasance, S., Thibault, P., Kelly, J., Journal of Chromatography 1992, **591**, 325-339.
10. Wachs, T., Sheppard, R.L., Henion, J., Journal of Chromatography B 1996, **685**, 335-342.
11. Hau, J., Roberts, M., Analytical Chemistry 1999, **71**, 3977-3984.
12. Tetler, L.W., Cooper, P.A., Bowell, B., Journal of Chromatography A 1995, **700**, 21-26.
13. Kirkby, D.P., Thorne, J.M., Götzinger, W.K., Karger, B.L., Analytica Chemistry 1996, **68**, 4451-4457.

14. Kriger, S., Cook, K.D., Ramsey, R.S., Analytical Chemistry 1995, **67**, 385-389.

15. Petersson, M.A., Hulthe, G., Fogelqvist, E., Journal of Chromatography A 1999, **854**, 141-154.

16. Chang, Y.Z., Her, G.R., Analytical Chemistry 2000, **72**, 626-630.

17. Moini, M., Analytical Chemistry 2001,**73,** 3497-3501.

18. Wetterhall, M., Nilsson, S., Markides, K.E., Bergquist, J., Analytical Chemistry 2002, **74**, 239-245.

19. Thibault, P., Kelly, J.F., Ramaley, L., Analytical Chemistry 1997, **69**, 51-60.

20. Yates III, J.R., Tong, W., Link, A., Eng, J.K., Analytical Chemistry 1999, **71**, 2270-2278.

21. Peter-Katalinic, J., Zamfir, A., Electrophoresis 2001, **22**, 2448-2457.

Chapter 4

The analysis of

Zinc dialkyldithiophosphates by nonaqueous capillary electrophoresis

with ultraviolet absorbance detection

Experimental details

4a Chemicals and Reagents

All chemicals and reagents were of HPLC grade.

Methanol (99.99%, Fisher, UK).

Acetonitrile (99.99%, Fisher, UK).

Dimethyl sufoxide (99.5%, Sigma, UK).

Acetic acid (100%, BDH, UK).

2-Butanone (99.5%, Aldrich, UK).

Diethyl ether (99.8%, Aldrich, UK).

n-Hexane (95%, Fisher, UK).

Cyclohexane (99.5%, BDH, UK).

Ammonium acetate (BDH, UK).

Hexadimethrine bromide (Sigma, UK).

Tetramethyl ammonium hydroxide (25% in methanol, Aldrich, UK)

Methyl formamide (Aldrich, UK)

Benzalkonium chloride (Sigma, UK)

Salicylic acid (99%, Aldrich, UK)

Deuterated chloroform (99.96%, Aldrich, UK)

NMR Tubes (Aldrich, UK)

All ZDDPs were contained within a base oil, with an unknown concentration of ZDDP and base oil blend.

All Alkylsalicylates used were of an unknown concentration contained within an unknown base oil blend.

Formulated oil samples both new and used contained unknown concentrations of additive package in an unknown base oil blend.

Syringe filters Acrodisc® PTFE filters with 0.2pm pore size, 13 or 25mm filters used depending on the size of sample.

Supelclean LC-Si solid phase extraction cartridges with lOg of packing, diameter 40-45pm with pore size of 60A in polypropylene tubes (Supelco, UK)

4b Instruments and accessories

Figure 4b.l: CE system used for NACE with uv absorbance detection.

Capillary electrophoresis (Crystal CE system, Prince Technologies, Netherlands) instrumentation with uv/vis detector (Prince Technologies, Netherlands).

DaX 6.1 software used for data acquisition and analysis.

Figure 4b.2 Instrumental arrangement for CE-MS experiments,

Capillary electrophoresis (Crystal CE system, Prince Technologies, Netherlands) instrumentation interfaced with mass spectrometer (VG Quattro series 1, Micromass, UK), and infusion driver (Harvard II, US) on top.

Ultrasonic bath (Branson ultrasonics corporation, USA).

Silica capillary internal diameter 50 & 75pm, external diameter 365pm (Composite Metal Services Ltd, UK).

pH meter (Fisherbrand Hydrus 300, USA).

Fourier transform infra red spectrometer (Genesis ATI Mattson USA).

Nuclear magnetic resonance spectrometer (AC 250 Bruker, UK).

Inductively coupled plasma-optical emission spectrometer (Spectro analytical instruments, Germany).

4c Initial capillary electrophoresis procedures

Buffer preparation was carried out by weighing the correct amount of ammonium acetate and hexadimethrine bromide into a beaker (where required) to this some HPLC grade methanol was added. The mixture was then thoroughly mixed in a sonicator until all the ammonium acetate was dissolved. After thorough mixing this was placed into a volumetric flask, and made up to the mark with methanol. The buffer was then thoroughly mixed and degassed in the sonicator. Approximately 20ml of buffer was removed into a beaker and the pH* adjusted using tetramethyl ammonium hydroxide in methanol. The buffer was then filtered slowly through a PTFE acrodisc filter prior to use in capillary electrophoresis.

Lubricant additives were contained within a blended base oil, so sample preparation was carried out where possible with larger sample sizes to remove this base oil. The removal of base oil was carried out by solid phase extraction, with a Supelclean LC-Si solid phase extraction cartridge containing 10g of packing. 3g of the additive was weighed out into a beaker and dissolved in 50ml of hexane and the following procedure carried out:

1. Silica packing was prewetted with 50ml hexane.
2. Sample was introduced and the eluate waste was collected for disposal
3. Washed with 50ml hexane, eluate waste collected for disposal.
4. Washed with 50ml of a 1:1 mixture of hexane and diethyl ether, eluate waste collected for disposal.
5. Washed with 25ml 2-butanone the eluate was collected only for ZDDP analysis otherwise, collected for disposal.
6. Washed with 50ml methanol all eluate was collected into a pre-weighed beaker for both ZDDP and alkylsalicylate analysis.

7. For ZDDP analysis the 2-butanone and methanol eluates were mixed.
8. Sample containing solvents were then left, until all the solvent had evaporated.
9. Beaker containing additive was then re-weighed to obtain the weight of sample and hence the concentration of the stock solution to be made.

Sample preparation was carried out in a similar manner, the beaker containing the sample was washed with the appropriate solvent (for ZDDP initially dichloromethane and alkylsalicylate with hexane) to re-suspend the additive and poured into a volumetric flask, to ensure all the sample was removed and poured into a volumetric flask, then sonicated to ensure thorough mixing of additive and solvent. The stock additive solution was the filtered slowly through the PTFE acrodisc filter prior to dilution for use with capillary electrophoresis.

The additive sample was diluted by removal of a known aliquot and placing into a capillary electrophoresis vial, at this point thiourea or salicylic was added. A known volume of buffer or methanol was added to reach the separation concentration.

Fresh silica capillary preparation		
Electrophoresis stages	**Pressure / Voltage**	**Time**
NaOH in methanol (1mol L^{-1})	2000 mbar	5 minutes
Pre buffer wash where required (HDB not in saparation buffer)	2000 mbar	5 minutes
Separation buffer wash	2000 mbar	5 minutes
Sample injection (Optimised)	20 mbar	0.2 minutes
Electrophoresis	-30kV	Upto 20 minutes

Table 4.1a Fresh capillary preparation and operational parameters for NACE.

Silica capillary preparation between separations		
Electrophoresis stages	**Pressure / Voltage**	**Time**
Pre buffer wash where required (HDB not in separation buffer)	2000 mbar	2 minutes
Separation buffer wash	2000 mbar	2 minutes
Sample injection (Optimised)	20 mbar	0.2 minutes
Electrophoresis	-30kV	Up to 20 minutes

Table 4.1b Capillary preparation and operational parameters for NACE.

The EOF was measured using thiourea at a concentration of 50 μg/ml in methanol. ZDDP concentrations were 10,000 μg/ml as weighed for stock in dichloromethane, diluted to 1000 μg/ml separation concentration in buffer.

Alkylsalicylate stock concentrations were weighed at 10,000 μg/ml within hexane and diluted to required concentrations for separation.

A stock solution of salicylic acid was made up to a concentration of 10,000μg/ml then added to the sample to create an analysis concentration of 200μg/ml.

4.0 Chemicals and reagents

See section 4a

4.1 Instrumentation

See section 4b

4.2 Procedures

See section 4c

4.3 Results and discussion

4.3.1 Electroosmotic flow reproducibility

Initial experiments were carried out to assess the viability of using nonaqueous solvents with the instrument to be used. The reproducibility of the EOF in two solvents, acetonitrile and methanol, was assessed.

Weeks	Average migration time (minutes) n=6	Standard deviation	RSD (%)
1	4.63	0.1530	3.31
2	4.72	0.0148	0.31
3	4.53	0.3582	7.92
4	4.34	0.0520	1.20
5	4.36	0.0475	1.09
6	3.89	0.2055	5.28
7	3.54	0.1241	3.51
Week to Week	**4.29**	**0.4258**	**9.93**

Table 4.2a Run to run variation in migration time for thiourea in methanol.

Weeks	Average migration time (minutes) n=6	Standard deviation	RSD (%)
1	1.73	0.0264	1.53
2	1.41	0.0444	3.15
3	1.84	0.0753	4.09
4	1.94	0.0109	0.56
5	1.60	0.1239	7.75
6	1.78	0.0110	0.62
7	1.52	0.0084	0.55
Week to Week	**1.69**	**0.1732**	**10.25**

Table 4.2b Run to run variation in migration time for thiourea in acetonitrile.

Table 4.2a shows that the thiourea migration time in methanol had 0.31 to 7.92 RSD (%) run to run, and a week to week RSD of 9.93%. In contrast acetonitrile (figure 4.2b) showed an RSD of 0.55 to 7.75% for run to run and 10.25% week to week. There was no significant difference between the reproducibilities of the EOF in either solvent. However, acetonitrile had a much stronger EOF than methanol (migration times 2 and 4 minutes respectively). This agrees with previous work stating that the properties of acetonitrile (viscosity and dielectric constant) give it the fastest EOF of all solvents including water.

As there was little difference in the migration time reproducibility of the solvents, methanol was chosen as the starting solvent for the analysis of the zinc dialkyl dithiophosphates (ZDDP).

Previous in-house work had affirmed that methanol was the appropriate solvent for this study, using a 50mM ammonium acetate as buffer and with reverse polarity. This set up led the analytes to migrate against the EOF; the amount of acetate utilised was designed to slow the EOF adequately to allow the analytes to migrate at a reasonable rate.

A novel method to look at these analytes would be to use a flow modifier to reverse the EOF, leading to reduced migration and analysis times. This would also lead to greater efficiency than the analytes migrating against the EOF, and be more suitable for interfacing with mass spectrometry at a future date.

The flow modifier hexadimethrine bromide, a polycation, has been previously used for flow reversal in NACE (see section 2.4.3.1). A concentration of 0.025mM was used in the separation buffer.

The capillary was conditioned by washing with the buffer. Injection of analyte was carried out using a pressure of 25mbar for 0.2minutes and separation was carried out at -30kV.

Several ZDDPs were analysed utilising this particular buffer, three of which were ligands of C_8/C_8; C_4/C_4, C_4/C_8, C_8/C_8 and C_3/C_3, C_3/C_4, C_4/C_4, C_3/C_8, C_4/C_8 and C_8/C_8.

The detected peaks were presumed to be the ligands minus the zinc metal, and the number of peaks give some justification to this presumption. Work carried out by Cardwell *et al.* (1997)[1] using reverse phase HPLC suggested that the complexes break up in aqueous buffers, however it could simply be that they break up under polar conditions.

The results from the electropherograms indicate that separation was achievable in a very short time. However, the electropherogram for the $C_3/C_4/C_8$ mixture of ligands was not well resolved. The main lack of resolution is in peak four, which corresponds to C_3/C_8 and C_4/C_8 respectively as the ligands are considered to be singly charged they migrate in correspondence to their masses with the smallest first. As this standard provided the worst separation, it was chosen for further studies.

One way to develop the method was to reduce the EOF, providing a longer time for the separation to occur. Electrolyte concentration, pH*, sample solvent and applied voltage were varied in this study.

4.3.2 Ammonium acetate concentration study

The effect of increasing the electrolyte concentration is to compact the double diffuse layer at the capillary wall, in turn reducing the zeta potential and the EOF. The viscosity of the buffer also increases, reducing the flow.

Migration of ZDDP (C3/C4/C8) in three ammonium acetate concentrations

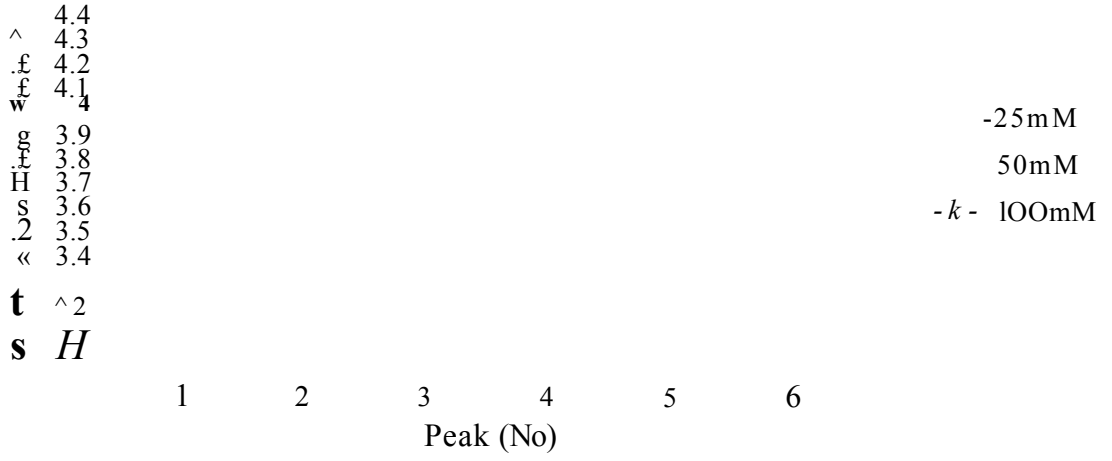

Figure 4.3 The effect of ammonium acetate on the migration of ZDDP ligands **(C3/C4/C8).** Conditions: buffer methanol, ZDDP concentration of lOOOpg/ml, injection 20mbar for 0.2min, pH 7.2*, Capillary length 65/50cm; detection wavelength 230nm separation voltage -30kV.

The results (figure 4.3), show that the increase in ammonium acetate concentration had no real effect on the separation. The increase in ammonium ion concentration did not increase any interactions with the analytes, even though the migration times increased as expected. What was not expected was that a decrease in ammonium acetate concentration did bring about a slight improvement in the separation, although this was very slight, indicating that any interactions occurring with the ammonium counter ions are weak.

4.3.3 The effect of pH* on the separation

The pH* of the buffer was altered by the addition of tetramethylammonium hydroxide in methanol. This was used as it does not introduce much water to the buffer, so as not

to alter any possible interactions. Any improvements in the separation should thus be due only to change in pH*.

Altering the pH* of the buffer can have varying effects, and can alter the separation of the analytes. Changing pH* can alter the EOF by altering the charge state of the fused silica wall of the capillary. Increasing the pH* increases the charge density at the capillary wall, which in turn increases the EOF. Changing pH* can also alter the charge state of the analytes.

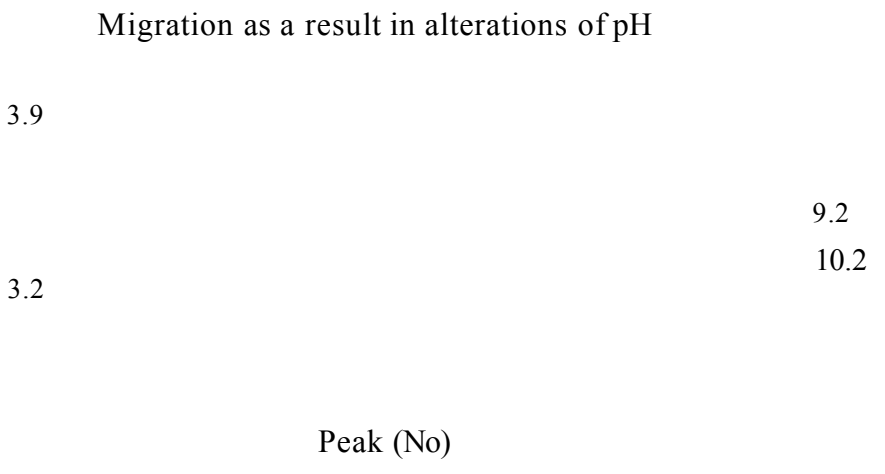

Figure 4.4 The effect of pH* on the separation of ZDDP ligands ($C_3/C_4/C_8$). Conditions: buffer methanol with 25mM ammonium acetate, Capillary length 65/50cm; detection wavelength 230nm; inj. 20mbar 0.2min with a total ZDDP concentration of lOOOpg/ml, injection 20mbar for 0.2min, separation voltage -30kV.

The results shown in figure 4.4 are slightly confusing, since increasing the pH* led to a decrease in migration time in line with the ionisation of the silanol groups. However, the use of the flow modifier to coat the capillary wall should cover the silanol groups. At pH 13.2* migration time increased. This increase in the migration time could be caused by a decrease in the interactions between the capillary wall and the flow

modifier, thus slowing the EOF. If enough of the flow modifier is removed the EOF will not be reversed. However, the pH* did not have the desired effect on the separation, since any effect the pH* has on one particular ligand an equal effect on the other ligands is seen (the ligands are essentially the same and only slightly differ in mass, so if the ligands are totally dissociated the pH* should not really have an effect on the separation as the pKa`s of the analytes should be essentially the same).

4.3.4 Voltage

The separation was carried out at two voltages (-20kV and –30kV) to see if voltage had any significant effect on the separation.

Decreasing the voltage did not yield sufficient improvement in resolution to warrant further investigation. A decrease in the applied voltage decreased migration time, as expected due to a decrease in the electrophoretic mobility of the ions.

4.3.5 Organic solvents

Various solvents were added to the methanol to try and improve the separation, these were acetonitrile, dimethyl sulfoxide and methyl formamide. Addition of the solvents had no effect on the separation. Acetonitrile decreased the migration time without altering the resolution and hence caused no alteration in the analytes' interactions with the buffer. The addition of the other solvents only led to loss of sensitivity and eventual loss of the analyte signal due to solvent absorbance at the wavelength used for the identification of ZDDPs.

4.3.6 Additives

Cationic surfactants have been used in aqueous CE to provide a pseudostationary phase, giving micellar electrokinetic electrochromatography. The analytes interact with the micelles to varying degrees and hence alter the separation. In nonaqueous solvents the lack of solvophobic interactions stops the formation of micelles, the surfactants being left as charged monomers and able to interact with the analyte.

The concentration of cationic surfactant, in this case benzalkonium chloride, to bring about an adequate improvement in the separation was a minimum of 50mM, which was placed in the separation buffer. The flow modifier was removed from the buffer and used as an additional wash prior to washing with the buffer. The improvement in the separation as seen in electropherogram 4.7 (page 106) is due to the addition of the surfactant, which allowed the analytes to interact with it. As the additive is moving against the EOF, it had the effect of increasing the capillary length by decreasing the electrophoretic mobility of the analyte. Even if the interactions were weak, if enough additive is present lots of weak interactions can have the same effect as a few strong interactions.

Possible interactions could be:

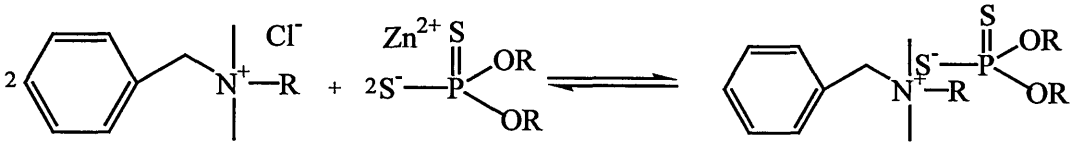

+ $ZnCl_2$

Although this method improved the separation to an adequate level, for future use in conjunction with mass spectrometry it would be ideal to remove the surfactant to prevent possible ion source fouling.

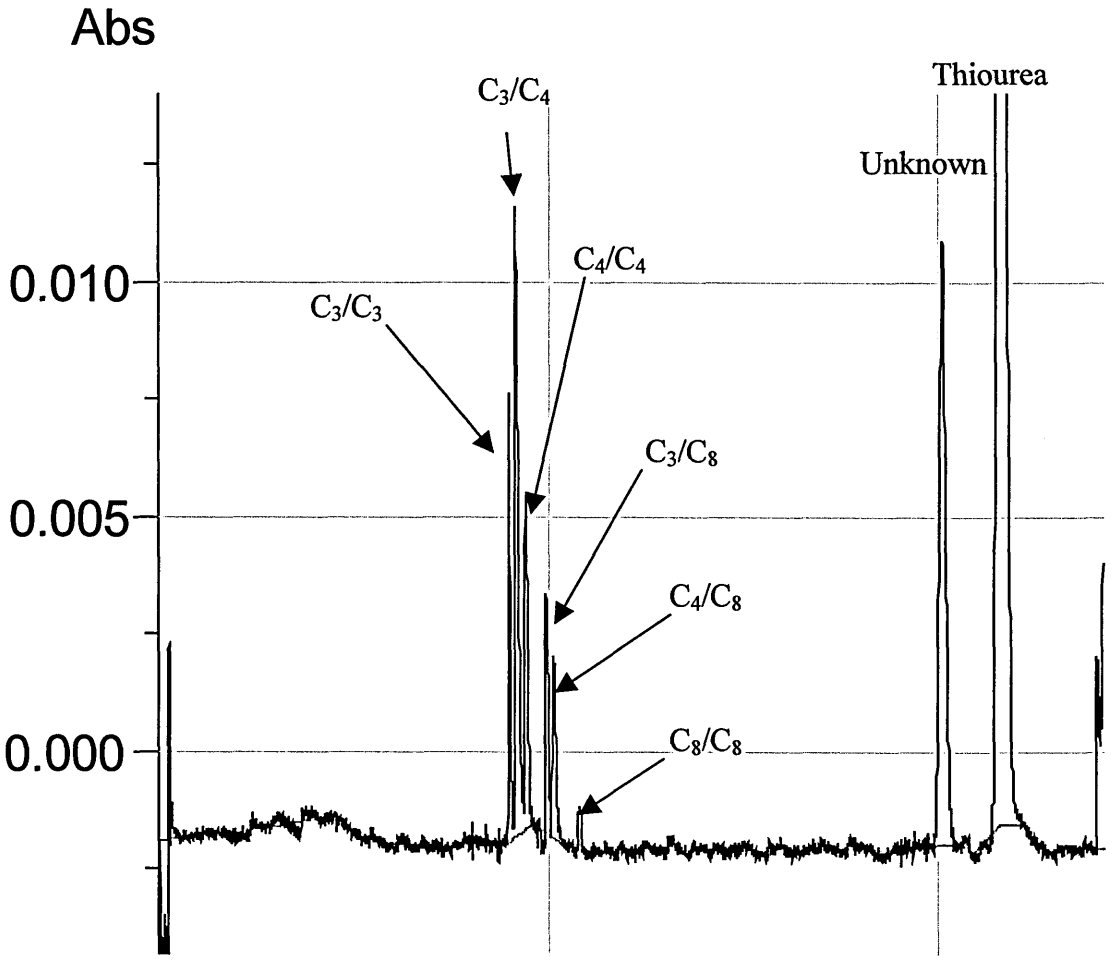

Figure 4.7 Electropherogram of ZDDP $C_3/C_4/C_8$ with 50mM benzalkonium chloride added to the separation buffer of 25mM ammonium acetate in methanol pH 9.01* adjusted using tetramethylammonium hydroxide. HDB 0.025mM was added to methanol as a pre-separation wash. Capillary length 65/50cm; detection wavelength 230nm; inj. 20mbar 0.2min with a total ZDDP concentration of 1000 µg/ml contained within a base oil and separation voltage of –30kV.

4.3.7 Removal of the Surfactant

From the work carried out on HDB (see sections 2.4.3.1 and 5.4.4), reducing the HDB concentration to 0.0025mM with the 80cm capillary slowed down the flow and improved the separation. Use of hexane to prepare the stock solution instead of dichloromethane (DCM) might improve the separation, hexane providing an environment similar to the base oil in which the ZDDP work.

As a result of these alterations the separation was now equivalent to the separation with the surfactant added although the separation time was longer (see figure 4.8).

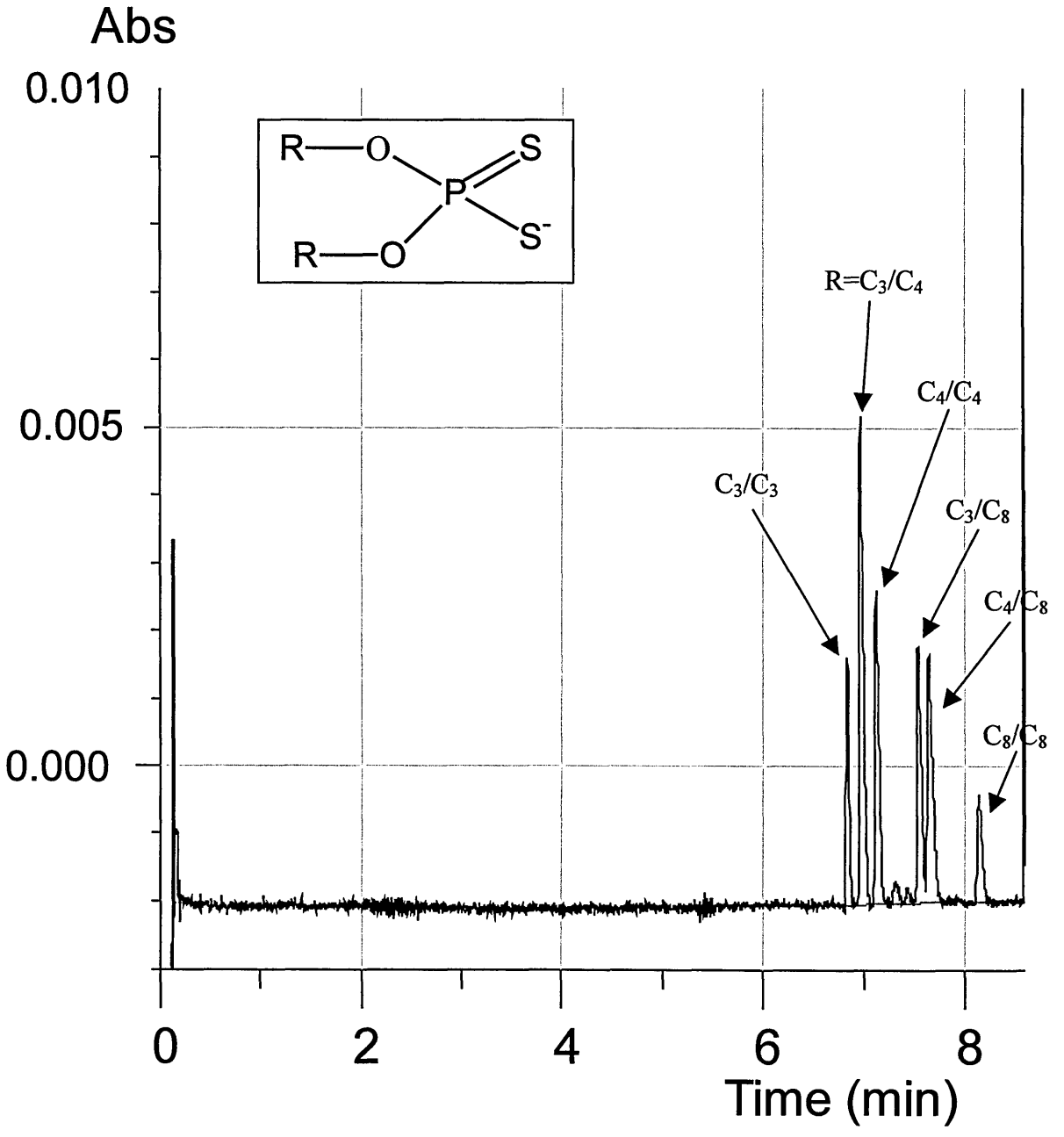

Figure 4.8 Electropherogram of ZDDP $C_3/C_4/C_8$ after removal of benzalkonium chloride from the separation buffer. Separation buffer of 25mM ammonium acetate, 0.0025mM HDB in methanol, pH 9.02* adjusted with tetramethylammonium chloride. Capillary length 80/65cm; detection wavelength 230nm; inj. 20mbar 0.2min with a total concentration of ZDDP and base oil of 1000 µg/ml inclusive in methanol and separation voltage of –30kV.

4.3.8 Different sample injection methods

It was felt that further improvements to the separation might arise from the use of sample stacking and field-amplified injection techniques, which could improve the sensitivity and efficiency and, through these, the resolution. Sample stacking and field amplified injections are methods encountered in aqueous CE, the sample being dissolved in deionised water or $1/10^{th}$ concentration buffer. Its use in NACE is not as common; Kim and Chong (2002)[1] carried out large volume stacking using a methanol run buffer, dissolving their analytes in deionised water. They made comparisons of aqueous CE and NACE for the separation of ten organic compounds, mostly acids. Large volume sample stacking used hydrodynamic pressure injection. Electrokinetic injection of analytes was then studied, and enhanced concentration sensitivities of 300 to 430 fold were reported. Shihabi (2002)[2] used transient isotachophoresis, dissolving the analytes in methanol or water. The terminating buffer in this case was aqueous triethanolamine 200mM, compared with using mixtures of methanol/water (80:20) and 100% methanol for the terminating buffer still obtained the same increase in sensitivity. As well as providing highly efficient peaks, the actual analysis time was reduced. However, there are more steps to carry out than in the normal analysis so the overall analysis time may not be reduced.

The analyte of interest was diluted to a separation concentration of 1000 µg/ml in methanol instead of buffer for both sample stacking and field amplified injection methods. For sample stacking the injection pressure and time were previously optimised at 20mbar for 0.2min. However this has not been done for electrokinetic injections.

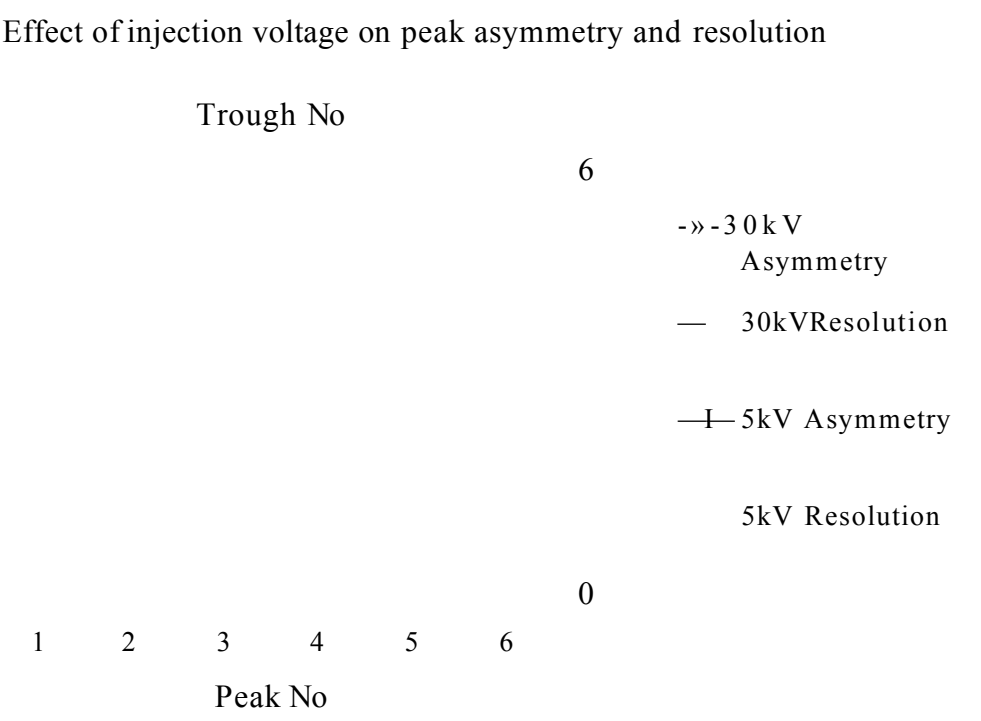

Figure 4.9. Optimisation of field amplified injection in response to asymmetry and resolution. Separation buffer of 25mM ammonium acetate, 0.0025mM HDB in methanol, pH 9.03* adjusted by the use of tetramethylammonium chloride. Capillary length 80/65cm; detection wavelength 230nm; inj. Electrokinetic for 0.2min with a total concentration of ZDDP and base oil of 1000 pg/ml in methanol and separation voltage of -30kV.

Figure 4.9 illustrates the effect that injection voltage applied for 0.2mins has on peak asymmetry and resolution. Asymmetry increased with the injection voltage, and likewise the resolution from peak to peak deteriorated with the increase in voltage. The optimised injection voltage for field amplified injection was -5kV in reverse polarity for best resolution and asymmetry.

From the work carried out here and previously, both field amplified injection and sample stacking seem applicable for the separation of these analytes. However sample stacking is the preferred choice.

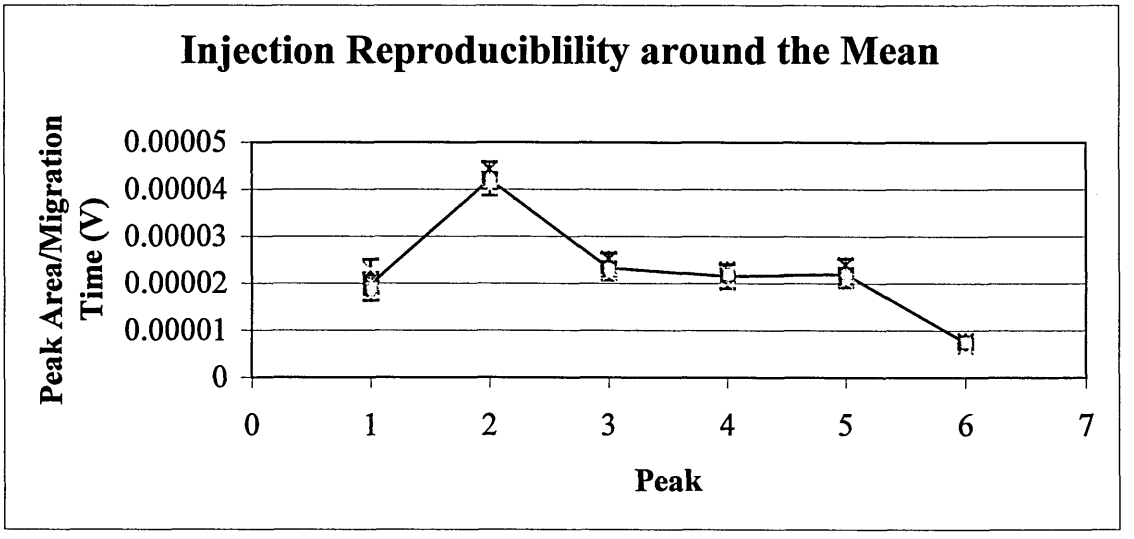

Figure 4.10 Injection reproducibility of ZDDP $C_3/C_4/C_8$ through sample stacking. Separation buffer of 25mM ammonium acetate, 0.0025mM HDB in methanol, pH 9.03* adjusted by the use of tetramethylammonium chloride. Capillary length 80/65cm; detection wavelength 230nm; inj. Electrokinetic for 0.2min with a total concentration of ZDDP and base oil of 1000 µg/ml in methanol and separation voltage of –30kV.

The quantitative reproducibility (n=6) for the analytes of interest was analysed by dividing peak area by migration time. The RSD maximum was 10%. However, the use of an internal standard should improve the reproducibility of the injection technique.

4.3.9 Reproducibility

As seen in section 5.4.7, migration time reproducibility was poor in this work, with the low concentration of HDB. Rinsing the capillary between experimental runs saw a

decrease in migration times run to run. Increased concentrations of HDB on the capillary inner wall could be responsible for this trend. Build up will continue until the inner capillary wall is coated. When no wash was carried out with HDB between runs the mobility of the analyte ions decreased gradually over repeated runs. It seemed that HDB interactions with the capillary wall in organic solvent was such that HDB required replacing after runs. It would be better to incorporate the HDB into the separation buffer and increase capillary length, with increased HDB concentration (0.025mM) to remove this variability and produce more reproducible migration times.

4.3.10 Analyte concentration effects

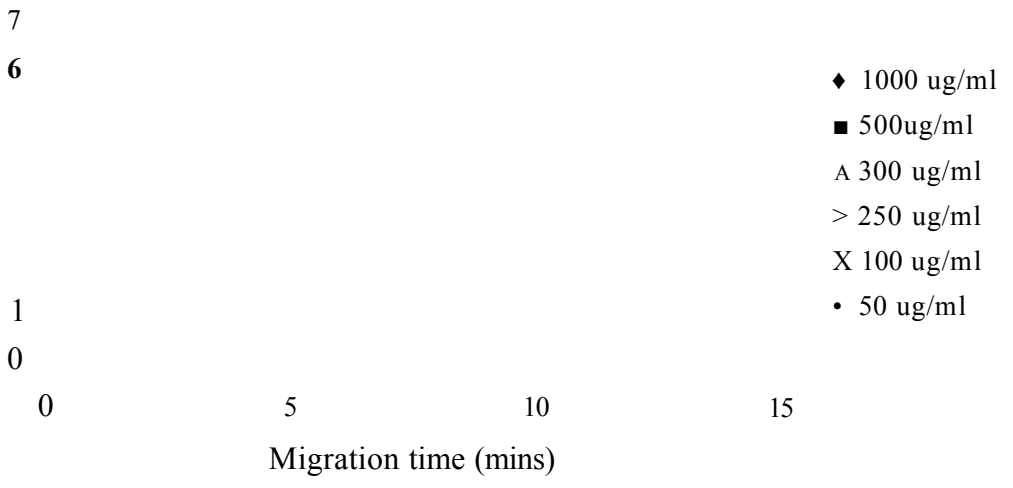

Figure 4.11 The effect that high concentration has on peak asymmetry (each point is a peak). Separation buffer of 25mM ammonium acetate, 0.025mM HDB in methanol, pH 9.05* adjusted by the use of tetramethylammonium chloride. Capillary length 90/75cm; detection wavelength 230nm; inj. 20mbar for 0.2min with a total concentration of ZDDP and base oil of 1000 pg/ml in methanol and separation voltage of -30kV.

Figure 4.11 and 4.12 show the effect sample concentration had on the overall separation. Varying concentrations resulted in a wide range of peak asymmetry, that follows a general trend (figure 4.11). As the concentrations decreased from 300 pg/ml, asymmetry was improved with the decrease in sample concentration, until 100 pg/ml, from where only slight differences were seen. Figure 4.12 shows that resolution was increased in line with decrease in concentrations. The migration times do not seem to be responsible for the improvements in resolution. The results indicate an agreement with the peak asymmetry results, such that improvements in resolution may be down to improvements in asymmetry and reduced peak tailing.

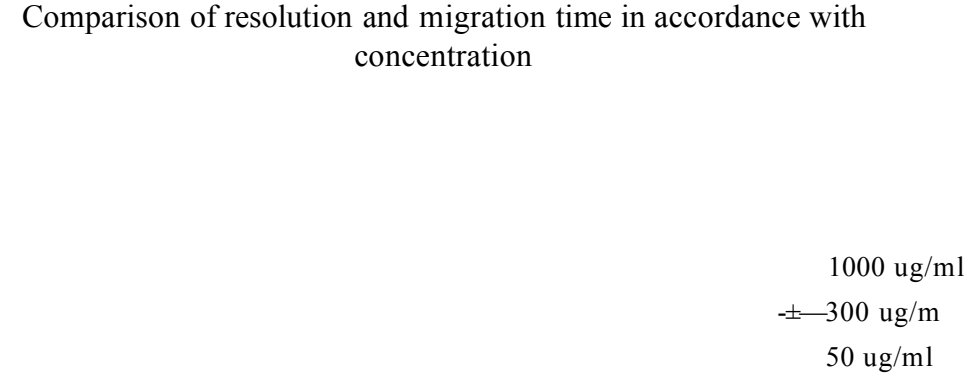

Figure 4.12 The effect of concentration has on resolution and migration time. Separation buffer of 25mM ammonium acetate, 0.025mM HDB in methanol, pH 9.01* adjusted by the use of tetramethylammonium chloride. Capillary length 90/75cm; detection wavelength 230nm; inj. 20mbar for 0.2min with a total concentration of ZDDP and base oil of 1000 pg/ml in methanol and separation voltage of -30kV.

4.3.11 Assessment of final buffer and conditions

The final buffer of 25mM ammonium acetate in methanol, pH* adjusted to 9, was assessed for peak reproducibility. With alkylsalicylates (see section 5.4.7), salicylic acid was added as an internal standard for quantitation and improvements in reproducibility, and also as a reference point for identification of ZDDP compounds by selectivity, resolution or relative migration times.

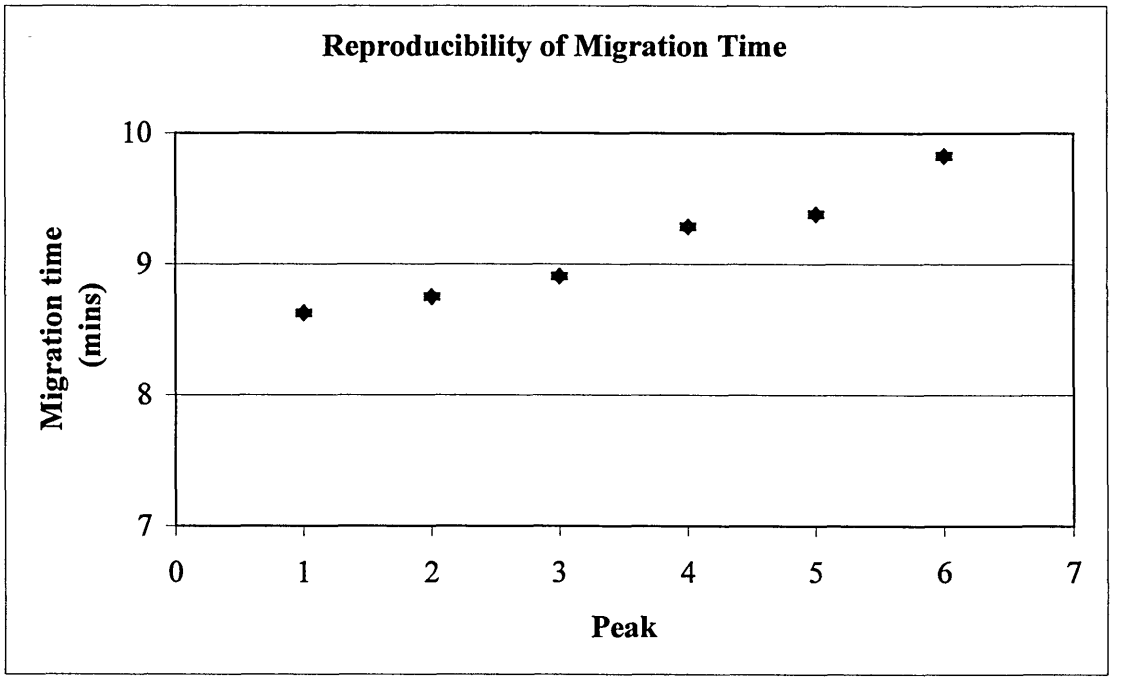

Figure 4.13 Reproducibility of final buffer separation. Separation buffer of 25mM ammonium acetate, 0.025mM HDB in methanol, pH 9.03* adjusted by the use of tetramethylammonium chloride. Capillary length 90/75cm; detection wavelength 230nm; inj. 20mbar for 0.2min with a total concentration of ZDDP and base oil of 1000 µg/ml in methanol and separation voltage of –30kV.

The reproducibility of the migration times for individual ligands (figure 4.3) was very good with a run-to-run RSD of under 0.5%. This showed that the lengthening of the capillary and increased HDB concentration controlled the EOF very reproducibly. However, environmental factors can have a significant factor on migration times. With

the air cooled Crystal instrument, temperature can not be adequately controlled and this can have a large effect on the migration times, especially in summer and winter.

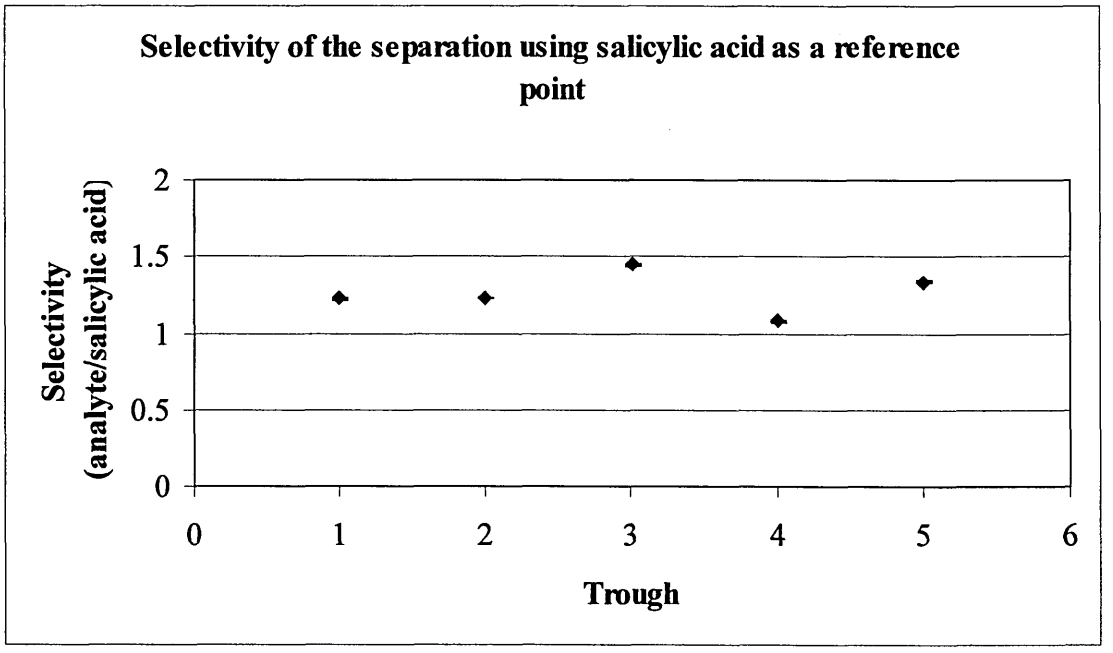

Figure 4.14 Assessment of selectivity as an identification process. Separation buffer of 25mM ammonium acetate, 0.025mM HDB in methanol, pH 9.03* adjusted by the use of tetramethylammonium chloride. Capillary length 90/75cm; detection wavelength 230nm; inj. 20mbar for 0.2min with a total concentration of ZDDP and base oil of 1000 µg/ml in methanol and separation voltage of –30kV.

Figures 4.14 and 4.15 show the possibilities of using selectivity and relative migration times as possible methods for identification of ZDDP ligands. Both methods are reproducible. Selectivity was reproducible to 1% RSD, whereas relative migration times were slightly better with a reproducibility between 0.039 and 0.2% RSD, respectively. However, as all ZDDPs are essentially synthesised in the same way using primary and /or secondary alcohols, different products synthesised using the same ligands should produce the same migration ratios and selectivity. It does not, however,

lead to the same quantitative ratios of ligands since that depends on the ratios of alcohols used in the synthesis.

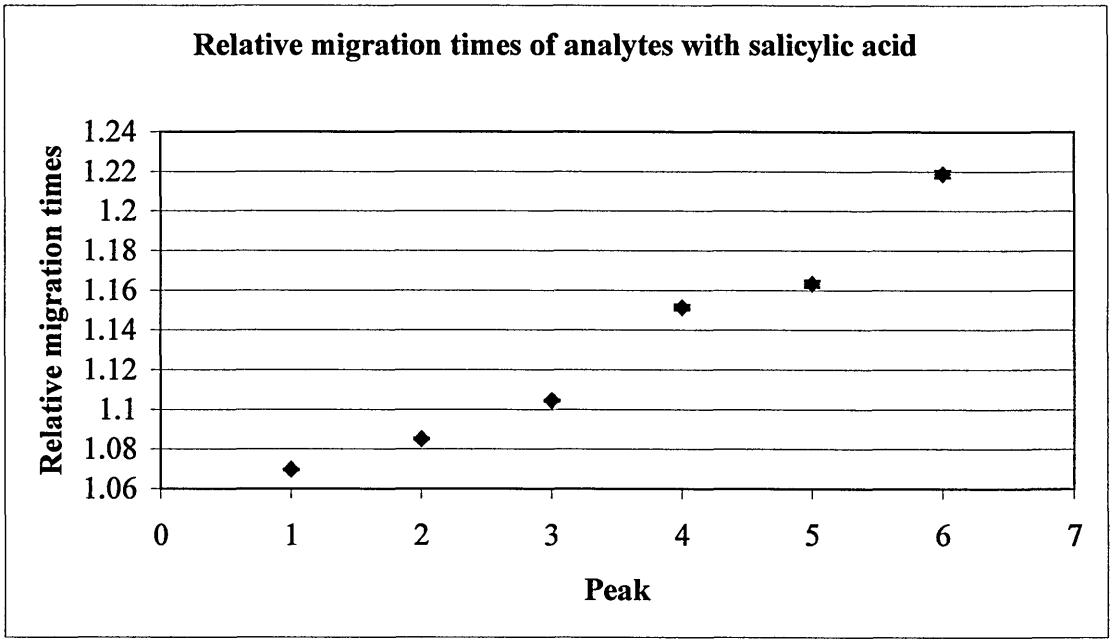

Figure 4.15 Relative migration times of analytes with reference to salicylic acid for possible identification process. Separation buffer of 25mM ammonium acetate, 0.025mM HDB in methanol, pH 9.03* adjusted by the use of tetramethylammonium chloride. Capillary length 80/65cm; detection wavelength 230nm; inj. 20mbar for 0.2min with a total concentration of ZDDP and base oil of 1000 µg/ml in methanol and separation voltage of –30kV.

	C_3/C_3	C_3/C_4	C_4/C_4	C_3/C_8	C_4/C_8	C_8/C_8
$C_3/C_4/C_8$ (n=5)	1.06964	1.08514	1.10446	1.15144	1.16339	1.21868
SD (±)	0.00045	0.00042	0.00044	0.00209	0.00282	0.00296

	C_3/C_3	C_3/C_4	C_4/C_4	C_3/C_8	C_4/C_8	C_8/C_8
$C_3/C_4/C_8$ (n=5)	1.08917	1.10467	1.12873	1.18378	1.19767	1.26753
SD (±)	0.00121	0.00146	0.00168	0.00235	0.00231	0.00328

Table 4.16 Showing possible relative migration times for individual ligands of ZDDP. Top Hitec 1656 and bottom ADX 308.

Hitec 1656, containing $C_3/C_4/C_8$ ligands, was used throughout the development of the separation buffer. ADX 308 is another $C_3/C_4/C_8$ mixture of ligands, for which the reproducibility showed good agreement with selectivity/relative migration times (0.14% to 0.23% and 0.11% to 0.26%RSD). However, using relative migration times as an identification process, it is seen that although very reproducible, the times were different and not ideal to identify the same ligands. The problem may be that the selectivity and resolution are so close. If the separation could be improved, the difference in relative migration times may be greater. The increase would allow for greater error with less chance for overlapping of different ligands relative migration times and so identification may be more reliable.

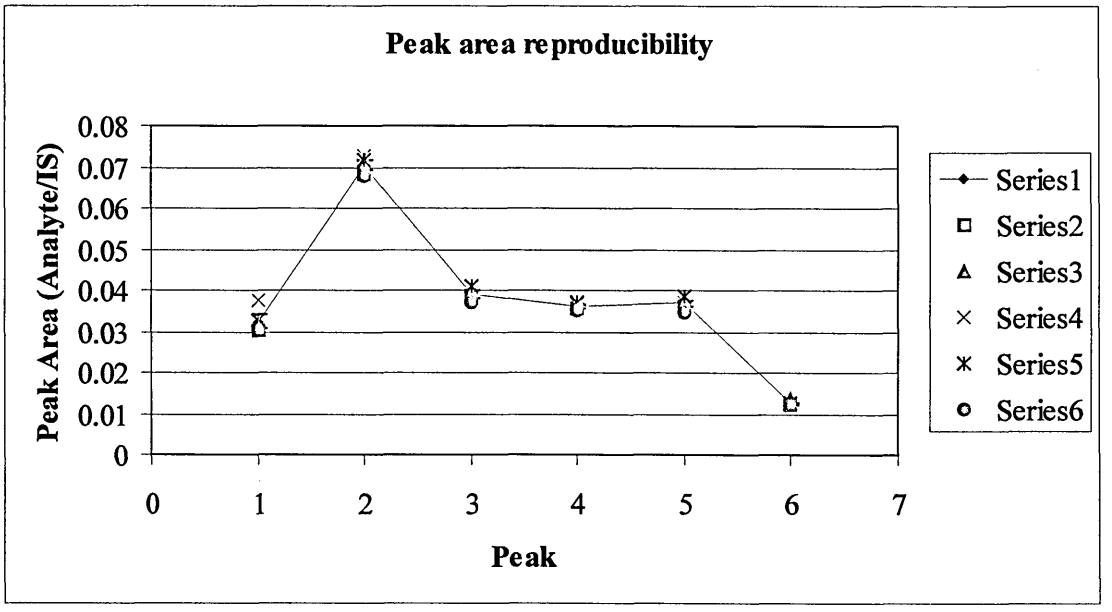

Figure 4.17 Peak area reproducibility with an analyte concentration of 500 µg/ml. Separation buffer of 25mM ammonium acetate, 0.025mM HDB in methanol, pH 9.03* adjusted by the use of tetramethylammonium chloride. Capillary length 90/75cm; detection wavelength 230nm; inj. 20mbar for 0.2min with a total concentration of ZDDP and base oil of 500 µg/ml in methanol and separation voltage of –30kV.

The majority have an RSD of less than 5%; however, one of the ligands has an RSD of 9.7% (series 1 is the average of all areas). In figure 4.17, for one injection, a single peak area stands alone as a rogue area. It is this area that decreases the reproducibility. If the peak area is not taken into account, the reproducibility improves in line with the other ligands at 3.8%.

4.3.12 Peak patterns

Peak patterns can be used to identify the number of alcohols used for synthesis and the percentage of each ligand. What is not taken into account is the ratio of isomers as they are not identified in this separation; the alcohols used to synthesise the $C_3/C_4/C_8$ are primary and secondary and each will have slightly different properties in their abilities to form antiwear layers. It may be that each will have dominance in different layers as dictated by steric hindrance. Results of two different $C_3/C_4/C_8$ mixtures can be seen in figure 4.18.

	C_3/C_3 (%)	C_3/C_4 (%)	C_4/C_4 (%)	C_3/C_8 (%)	C_4/C_8 (%)	C_8/C_8 (%)
ADX 308	11.2	29.6	18.9	14.3	19.6	6.5
Hitec 1656	13.7	30.6	17.5	15.4	17.1	5.7

Table 4.18 Comparisons of peak area percentages for each additive mixture.

From the descriptions given it is not clear whether each alcohol is a mixture of primary and secondary or if each alcohol is solely either primary or secondary. However, the results showed the mixture of alcohols to be similar for the two products tested, suggesting that the original sources for the alcohols may be the same. In this case the

individual products cannot be identified by their percentage peak area ratios but the number of alcohols used for ZDDP synthesis can.

Other ZDDPs

Several ZDDPs (figs 4.19 to 4.22) have been analysed to look at how well the method worked. The separations were successful, and all the individual ligands could be seen. The use of relative migration times does not seem to be suitable for the individual ZDDPs, although reproducibility for each ZDDP was good at less than 1%.

Errors could occur when using relative migration times. For instance two ligands with a total number of eight carbons had a relative migration time of 1.148, whereas two ligands with a total carbon number of 12 had a relative migration time of 1.144. The ligand with the greater number of carbons should have the greater relative migration time.

What can be seen is that the peak patterns for individual ZDDPs atre very different and as such the peak patterns could be used for individual identification of ZDDPs.

The patterns seen are due to the different alcohols used at different concentrations during ZDDP synthesis. The alcohols are mixed prior to synthesis and are not used individually to synthesise the ZDDP. Individual manufacturers may use different concentrations of alcohols and peak patterns along with relative migration may be a way of identifying not only ZDDPs but also their manufacturers

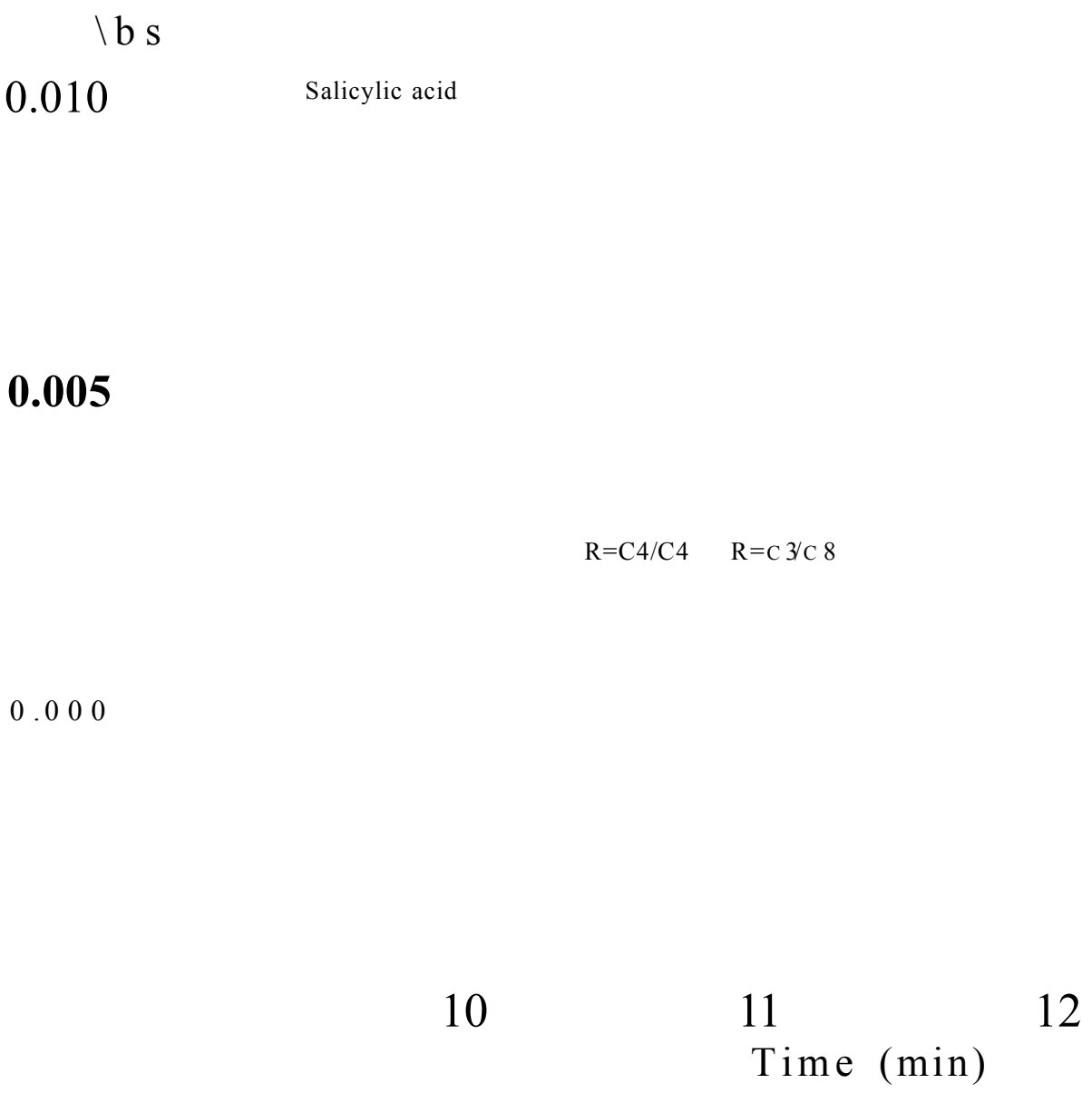

Figure 4.19 The electropherogram of ZDDP $C_3/C_4/C_8$. Separation buffer of 25mM ammonium acetate 0.025mM HDB in methanol pH 9.02* adjusted using tetramethylammonium acetate. Capillary length 90/75cm; 230nm; inj. 20mbar 0.2min with a total concentration of ZDDP and base oil of 500 pg/ml and separation voltage of-30kV. The large peak at 9.317min is salicylic acid 200pg/ml.

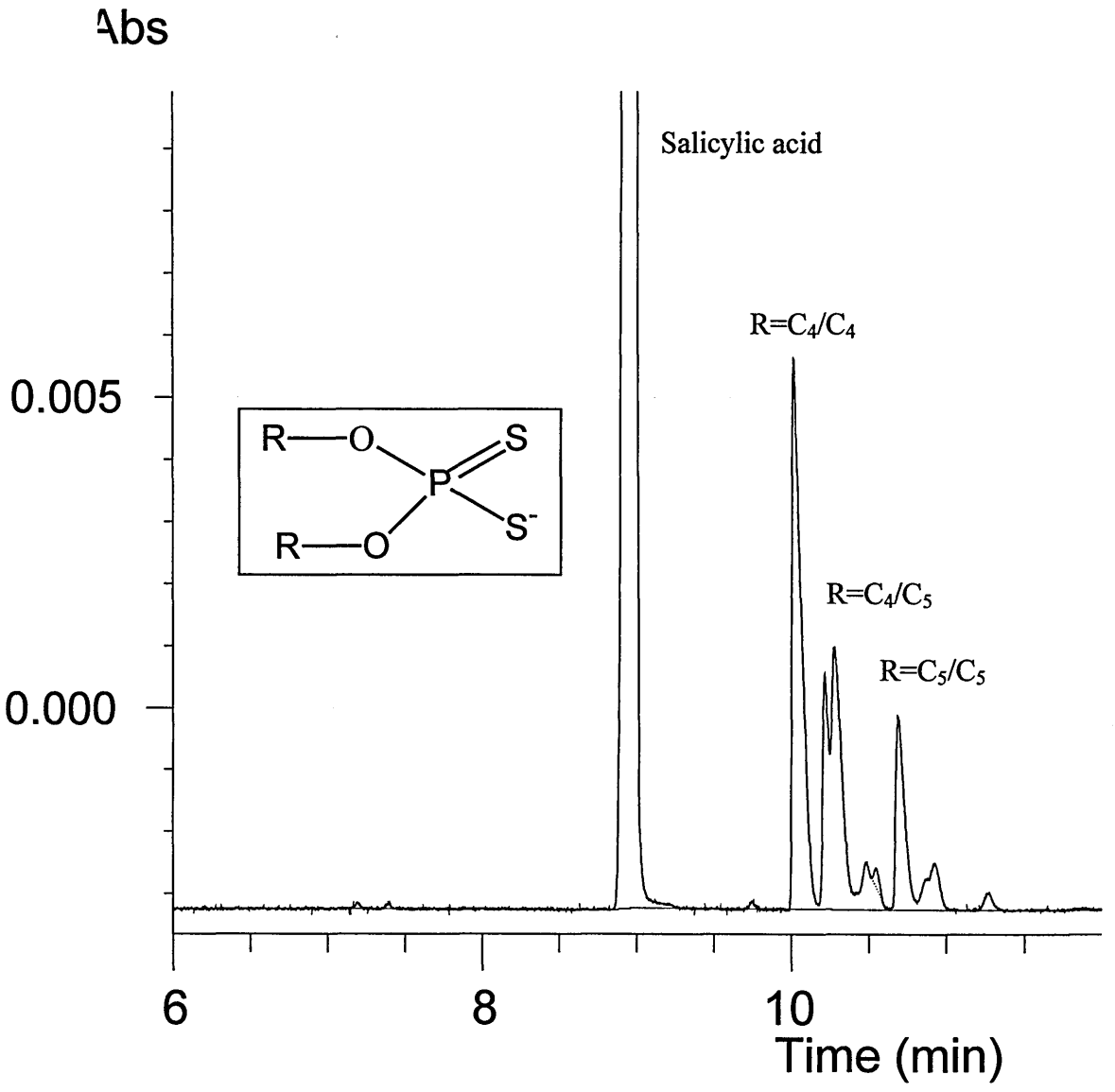

Figure 4.20 The electropherogram of ZDDP C_4/C_5. Separation buffer of 25mM Ammonium acetate, 0.025mM HDB in methanol, pH 9.02* adjusted using tetarmethylammonium hydroxide. Capillary length 90/75cm; 230nm; inj. 20mbar 0.2min with a total concentration of ZDDP and base oil of 500 µg/ml and separation voltage of –30kV. The large peak at 8.956 is salicylic acid 200 µg/ml.

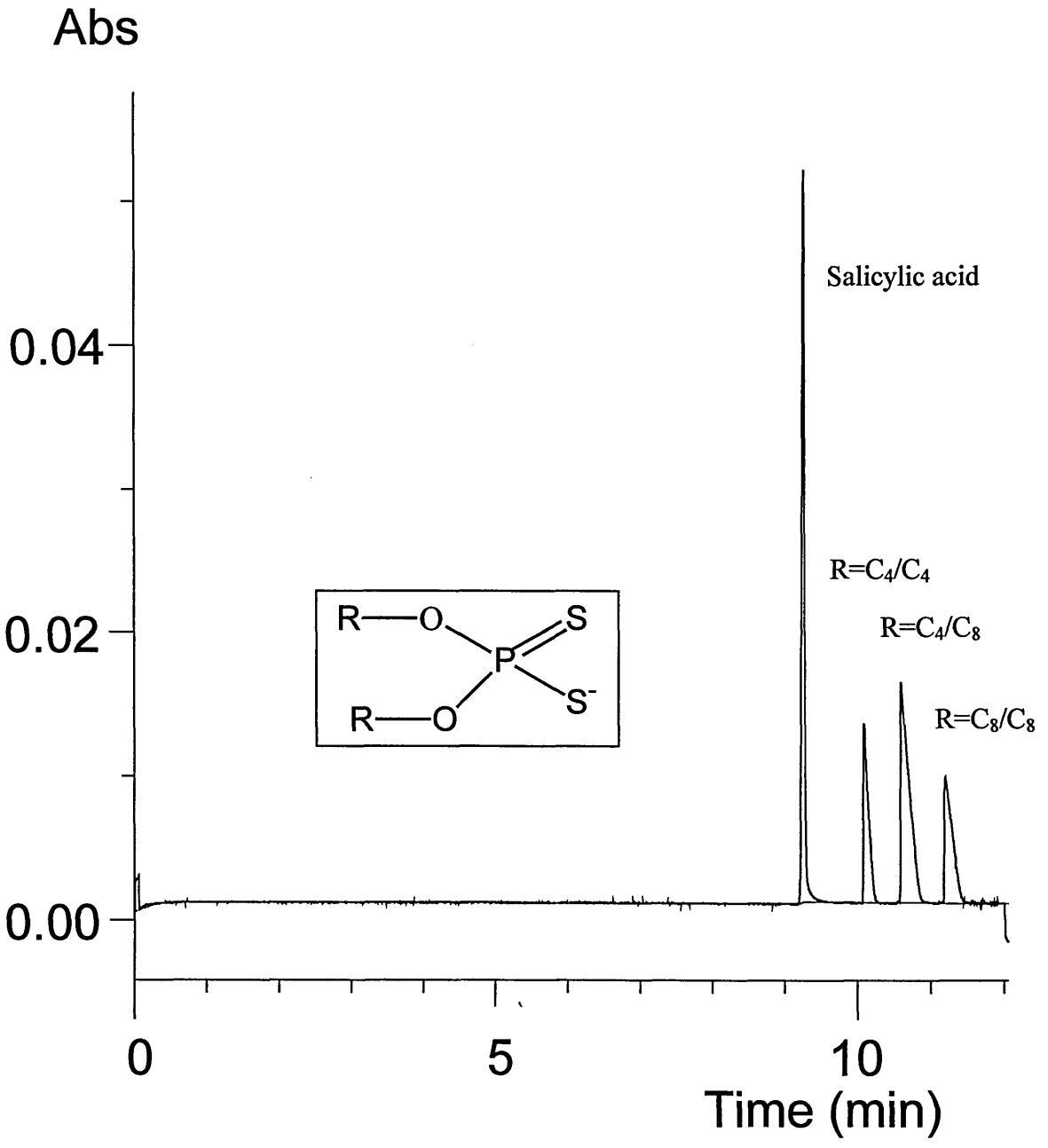

Figure 4.21 The electropherogram of ZDDP C_4/C_8. Separation buffer of 25mM ammonium acetate and 0.025mM HDB in methanol pH9.02* adjusted using tetramethylammonium hydroxide. Capillary length 90/75cm; 230nm; inj. 20mbar 0.2min with a total concentration ZDDP and base oil of 500 µg/ml and separation voltage of –30kV. The large peak at 9.263min is salicylic acid 200 µg/ml.

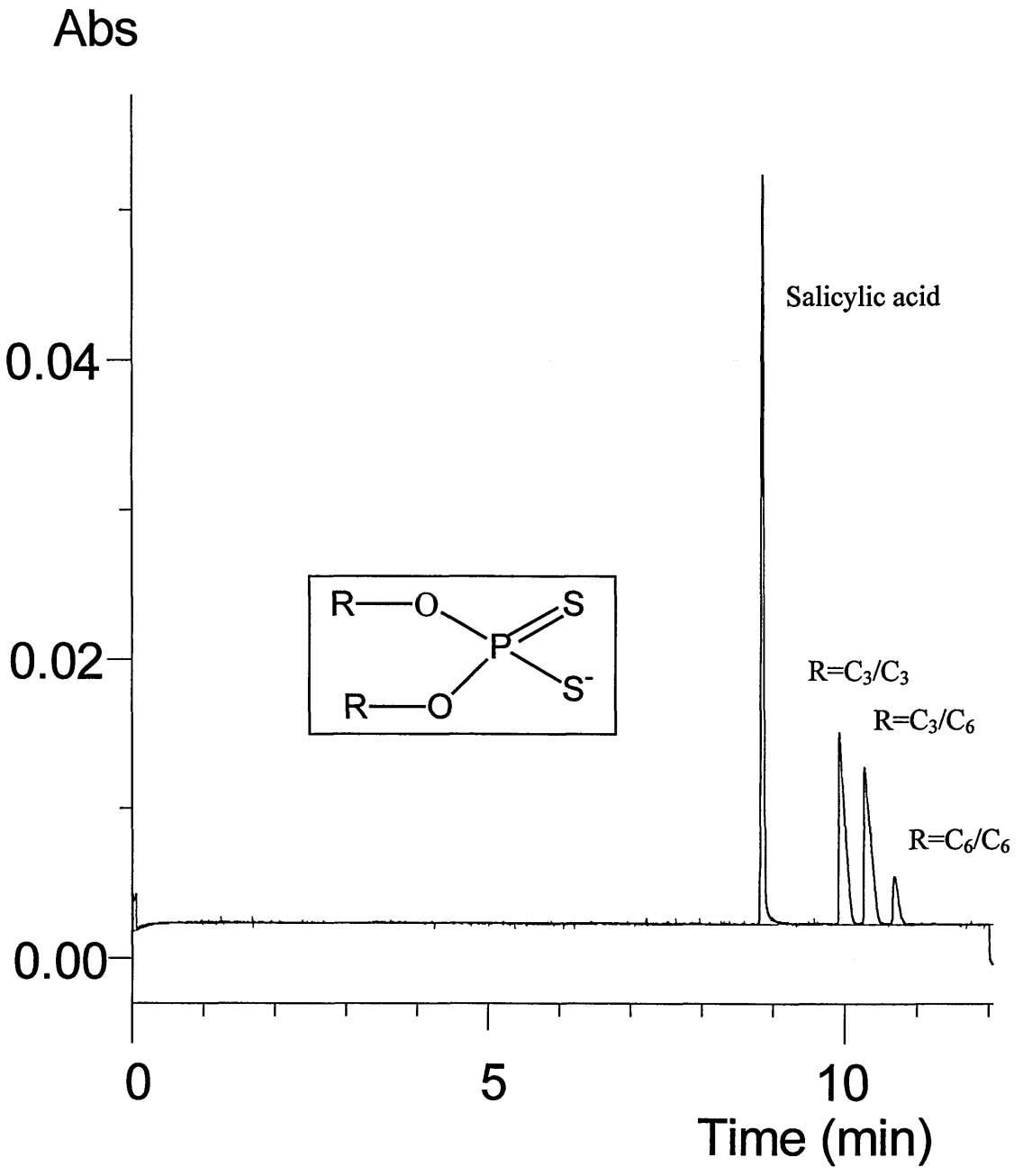

Figure 4.22 The electropherogram of ZDDP C_3/C_6. Separation buffer of 25mM ammonium acetate and 0.025mM HDB in methanol pH 9.02* adjusted using tetramethylammonium hydroxide. Capillary length 90/75cm; 230nm; inj. 20mbar 0.2min with a total concentration of ZDDP and base oil of 500 µg/ml and separation voltage of –30kV. The large peak at 8.862min is salicylic acid 200 µg/ml.

4.4 Conclusion

Initial work used a 65cm/50cm (effective length) capillary coated with 0.025mM HDB. From the effect of ammonium acetate it was concluded that any ionic interactions were very weak. If significant interactions were occurring with the ammonium ions then increased ammonium concentration would yield an increase in interactions and an improvement in the separation. However, this was not the case.

Increasing the pH* decreased the migration time for analysis. The increase in migration rate was attributed to the total dissociation of the metal salt, and not to the ionisation of the capillary wall because the increase in migration was not large and the silanol groups were covered by HDB, preventing ionisation. Decreasing the voltage applied had the desirable effect of slowing down the migration rate, however the separation was not improved.

The inclusion of an additive to increase analyte interactions was tried, benzalkonium chloride being added to the separation buffer at a concentration of 50mM. The results showed that the addition of this surfactant brought about analyte additive interaction that was capable of providing a separation equivalent to that of Thibon *et al.*(1999)[3] but in a shorter analysis time. However, the separation was to be eventually coupled to a mass spectrometer and so added surfactant was undesirable.

Work carried out on alkylsalicylates led to improvements in the separation by changing the standard storage solvent from DCM to hexane, and this was also observed for ZDDP's. However, the biggest improvement was seen by the use of sample stacking, which improved efficiency, sensitivity and resolution. Further improvements were seen

by alterations in HDB concentration and then increasing the capillary length and returning to the original HDB concentration to improve reproducibility. The use of salicylic acid as an internal standard led to more accuracy and better methodology for identification, however, as the analytes migrated close together there was little difference in selectivity. Particular ligands could be identified by patterns, although when this method is transferred to mass spectrometric detection, ligand identification will be unequivocal.

In all, with the possibility of mass spectrometry detection and the results obtines so far, I believe that the method developed is an improvement to that of Thibon *et. al.*[3]

References

1. Chung, D.S., Kim, B., Electrophoresis 2002, **23**, 49-55.

2. Shihabi, Z.K., Electrophoresis 2002, **23**, 1628-1632.

3. Thibon, V.R.A., Bartle, K.D., Abbott, D.J., McCormack, K.A., Journal of Microcolumn Separations 1999, **11**, (1), 71-80.

Chapter 5

The analysis of alkylsalicylates by capillary electrophoresis with ultraviolet absorption detection

5.0 Introduction

Initially, separation of alkylsalicylates was attempted by the method used for ZDDPs, 25mM ammonium acetate, 50mM benzalkonium chloride in methanol. The result was that no analyte was detected, suggesting that the analytes had strong interactions with the benzalkonium chloride and migrated into the inlet vial. Development of the method then centred around the basic parameters of separation i.e. variation in pH*, buffer concentration, organic solvent and surfactant (HDB) concentration study.

5.1 Chemicals and Reagents

See section 4a.

5.2 Instrumentation

See section 4b

5.3 Procedures

See section 4c

5.4 Results and Discussion

5.4.1 Effect of pH*

Ionisation of the analytes was examined by varying the pH* through the range 3-12. The electrophoretic mobility of individual species was assessed at different pH* values. Separation should not occur due solely to ionisation, as the alkylsalicylates are essentially the same and differ only in alkyl chain lengths and hence should have the same ionisation constant.

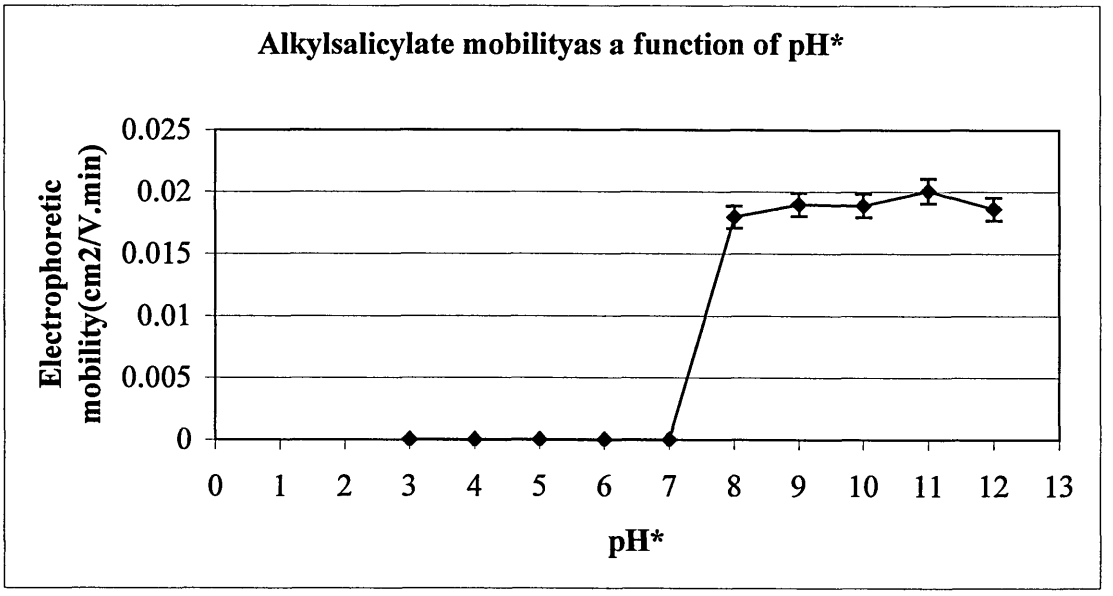

Figure 5.1. Effect of pH* on the mobility of alkylsalicylates. Conditions: buffer methanol, tetramethylammonium hydroxide or acetic acid were used as pH* adjusters. HDB was coated onto the inner capillary wall in a pre-separation wash at a concentration of 0.025mM. Capillary length 65/50cm (total length/effective length), 210nm, inj. 20mbar 0.2min Neutral marker thiourea 50µg/ml, separation voltage –30kV.

The results in figure 5.1 show that upto pH 7* the alkylsalicylates (from this point referred to as the analytes) have no electrophoretic mobility, which indicates that they are not ionised. The analytes co-migrated with the neutral marker, which was used to calculate the analyte electrophoretic mobility. Above pH 7* a sudden increase in mobility of the analyte was observed and by pH 8*, the analyte seemed to be fully ionised as no further increase in mobility was observed.

No separation was observed, probably because the EOF was too fast and the analytes were not interacting well enough with the buffer components to be separated. While electrophoresis was occurring (evidenced by the EOF) it was noted that very little current was flowing (0.1 to 1.0µA). To show that pH* has no effect on the EOF due to

the dynamic coating of the inner capillary wall, the EOF mobility was calculated from the electropherograms.

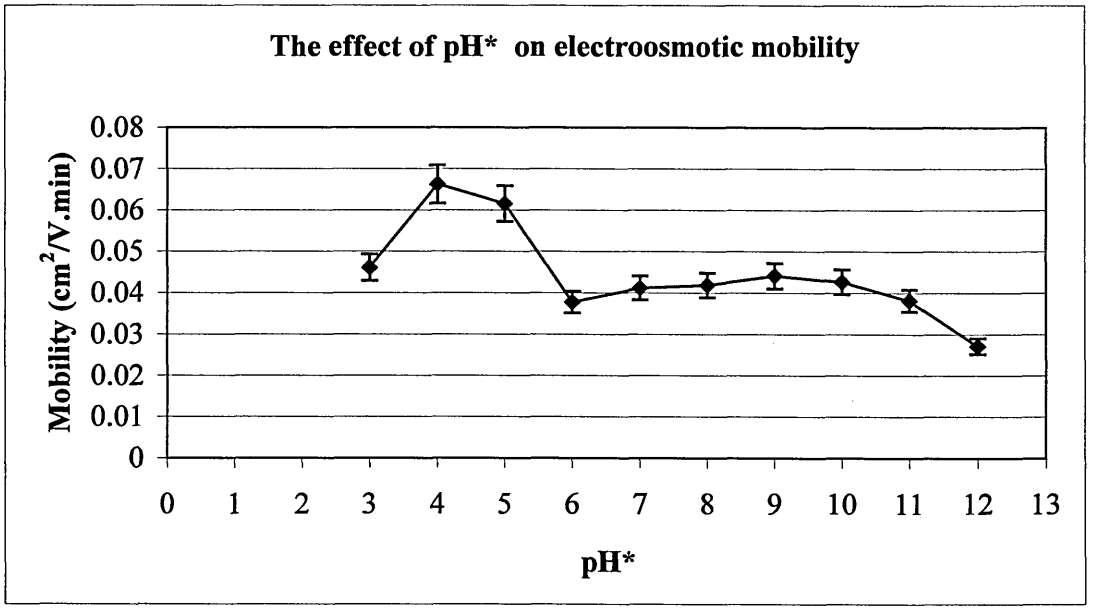

Figure 5.2. Electroosmotic mobility as a function of pH*. Conditions: buffer methanol, tetramethylammonium hydroxide acetic acid as pH* adjusters. HDB was coated onto the inner capillary wall in a pre-separation wash at a concentration of 0.025mM. Capillary length 65/50cm, 210nm, inj. 20mbar 0.2min Neutral marker thiourea (50 µg/ml), separation voltage -30kV.

Figure 5.2 shows an overall slight reduction in the electroosmotic mobility with increasing pH*, the mobility seeming to increase slightly then decrease. If no coating were present then the EOF would be expected to increase as silanol groups deprotonate above pH 3*, and then increase further with pH until all the silanol groups are deprotonated.

5.4.2 Ammonium acetate concentration study

The addition of ammonium acetate to the buffer will effect the separation in several ways. It will slow down the EOF, provide further ammonium ions for the analytes to interact with, and increase the ionic strength and hence current. Slowing of the EOF will be due to increase in viscosity of the buffer and the lower zeta potential due to the compacting of the diffuse double layer.

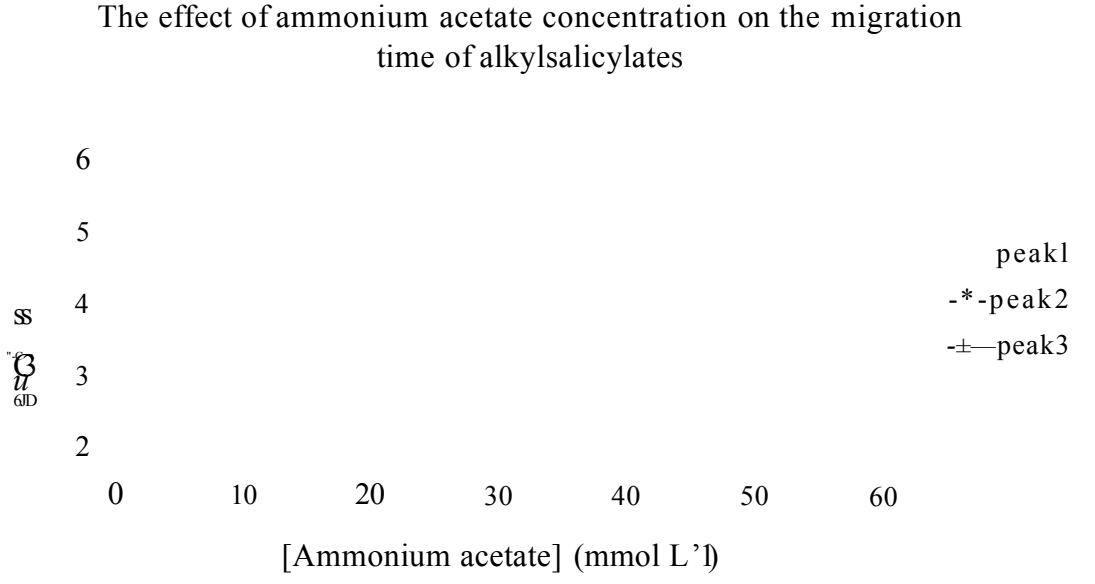

Figure 5.3. The effect of ammonium acetate on the separation of alkylsalicylate. Conditions: buffer methanol, pH 9.01* using tetramethylammonium hydroxide. HDB was coated onto the inner capillary wall in a pre-separation wash at a concentration of 0.025mM. Capillary length 65/50cm, 210nm, inj. 20mbar 0.2min with a total alkylsalicylate and base oil concentration Of 2000pg/ml and a separation voltage -30kV.

The addition of ammonium acetate did produce an improvement in the separation of individual analytes (figure 5.3). As the ammonium acetate concentration was increased

to 40mM, resolution increased so that separate peaks were seen. This improvement may be due to the increased migration time of the analytes, as a result of a slower EOF and/or to increased interaction between the ammonium ions and the analytes. Higher concentrations of ammonium acetate led to currents in excess of 150μA, and breakdown of electrophoresis. For this reason 50mM ammonium acetate (130μA) was deemed the most appropriate concentration to use. However, several problems were encountered by the introduction of ammonium acetate at this concentration, mostly due to the immiscibility of the high salt phase with the hexane solution of the analytes. High analyte concentrations (2000 μg/ml) were required to obtain any result and only one run could be carried out before the sample required re-mixing with the buffer. Clearly the separation system was not ideal.

5.4.3 Organic solvents

Mixtures of organic solvents have been widely used in NACE, mostly mixtures of methanol and acetonitrile. Acetonitrile has weaker interactions with the analyte than methanol; it is a solvent that is difficult to protonate and is non-protogenic. It was thought that introducing acetonitrile to the buffer system might yield an increase in analyte and ammonium interactions that could improve selectivity. However, a net improvement would only be seen if improvements as a result of increased interactions were greater than the detrimental effect acetonitrile has on the EOF, since the addition of acetonitrile will increase the velocity of the EOF. The increase in the EOF velocity will increase the migration rate and as a result improve efficiency and reduce resolution.

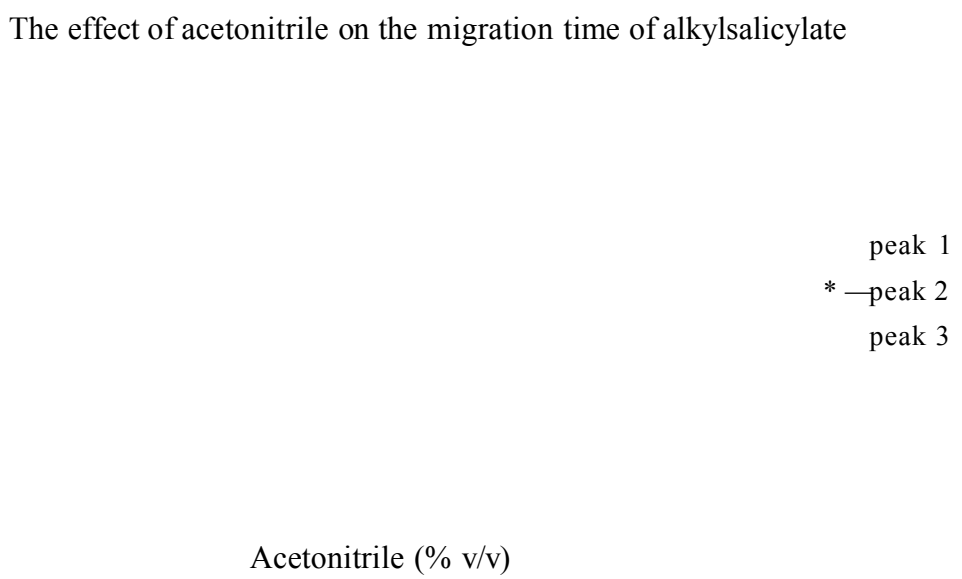

Figure 5.4. The effect of addition of acetonitrile on analyte migration. Conditions: buffer methanol: acetonitrile, 50mM ammonium acetate, pH 9.03* using tetramethylammonium hydroxide. HDB was coated onto the inner capillary wall in a pre-separation wash at a concentration of 0.025mM. Capillary length 65/50cm, 210nm, inj. 20mbar 0.2min with a total alkylsalicylate and base oil concentration of 2000pg/ml and separation voltage -30kV.

Figure 5.4 shows that the addition of acetonitrile increased the migration rate of the individual analytes with a slight deterioration in selectivity, possibly because the EOF was too strong to allow the ammonium ions to travel against the EOF. In this case the analytes interacting with the ammonium ions are simply forced in the direction of the detector, and thus the low migration time does not allow enough interactions to occur or the mass differences to improve the separation. Additionally, the sensitivity of the separation decreased and the miscibility problem was not improved.

Another solvent that could be utilised in low concentrations is hexane, bearing in mind the immiscibility of the high salt phase and the hexane solution of the analyte. Increase in miscibility will improve sensitivity and allow multiple injections without the need to remix prior to each injection of sample.

Addition of hexane to the separation buffer could improve the miscibility of the analytes with the 50mM ammonium acetate buffer, and also improve the separation by reducing the EOF. Cyclohexane rather than n-hexane might further improve the separation. Any improvement seen may due to cyclohexane bulkiness as a ring structure interfering with the migration of the analytes. Although not strictly appropriate for NACE, being non-electrolytic and of low polarity, when present in small amounts electrophoresis could still occur.

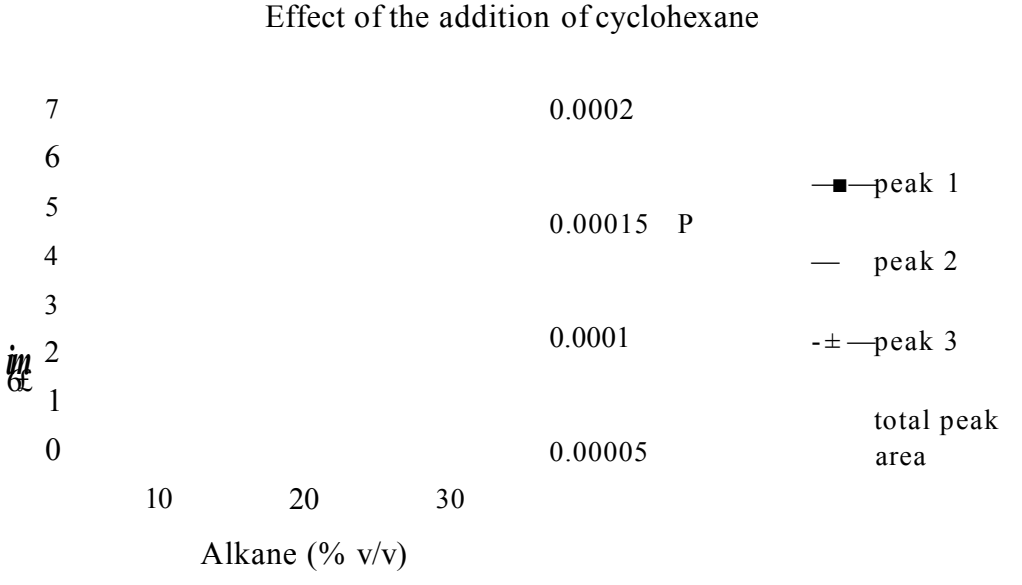

Figure 5.5. The effect of introducing cyclohexane to the separation buffer. Conditions: buffer methanol, 50mM ammonium acetate, pH 9.06* using tetramethylammonium hydroxide. HDB was coated onto the inner capillary wall in a pre-separation wash at a concentration of 0.025mM. Capillary length 65/50cm, 210nm, inj. 20mbar 0.2min with a total alkylsalicylate and base oil concentration of 2000pg/ml and separation voltage -30kV.

Figure 5.5 shows that the addition of cyclohexane to the separation buffer did alter the migration time of the analytes. As the proportion of hydrocarbon in the buffer was increased, the migration time increased. However, the total peak area was maximal at 20% v/v cyclohexane. The total peak area has been divided by the migration time to take into account the effect of differing EOF as would be done for external standardization. The addition of cyclohexane did improve the sensitivity, although at 30% v/v cyclohexane content, a decrease in peak area was seen. The increase in sensitivity observed may be due to improved miscibility of sample with buffer. Runs could be repeated without the problem of mixing the samples prior to every injection.

5.4.4 Altering the EOF mobility

In order to improve resolution during the separation of cations in aqueous CE, a low pH is used, which has the effect of reducing the number of ionised silanol groups and thereby slowing the EOF. This was not used in this case because a higher pH* was required to ensure that the analytes were ionised. Other ways to improve migration time so that resolution is improved are to firstly increase the capillary length and secondly to decrease the concentration of the flow modifier.

Lengthening of the capillary from 65 to 75cm showed an improvement in the separation. On average the migration times increased by three minutes and resolution improved from 0.33 and 0.42 to 0.90 and 0.88 respectively. The greatest improvements occurred through the reduction of the flow modifier concentration. The effect on EOF is shown in figure 5.6.

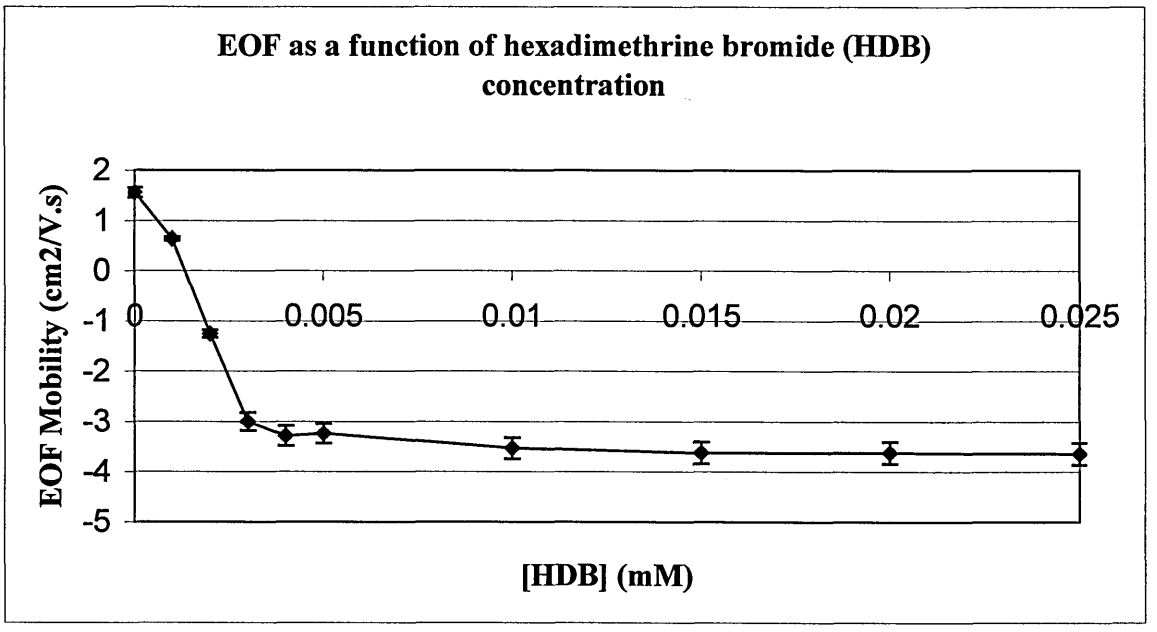

Figure 5.6. EOF mobility in relation to HDB concentration. Conditions: buffer methanol, 50mM ammonium acetate, pH 9.00* using tetramethylammonium hydroxide. HDB was coated onto the inner capillary wall in a pre-separation wash at varying concentrations, using fresh capillary after each separation. Capillary length 65/50cm, 210nm, neutral marker thiourea 50µg/ml, inj. 20mbar 0.2min with separation voltage –30kV.

Figure 5.6, as expected, shows that low concentrations of the flow modifier HDB had a dramatic effect on the EOF. A concentration of 0.025mM was previously used; however, figure 5.6 shows that concentrations as low as 0.01mM gave almost identical mobility. This result suggests that a concentration of 0.01mM is sufficient to cover the entire internal diameter of the silica capillary after a 2 minute wash.

A concentration of 0.0025mM will provide a reversed flow at approximately half the rate of the original flow. As fewer silanol groups will be covered, pH* will start to exert an effect on the EOF mobility. The concentration of HDB at pH 9* that resulted in no net EOF was approximately 0.00135mM. The results of the use of a

concentration of 0.0025mM as compared to 0.025mM can be seen in figures 5.7 and 5.8 (pages 137 and 138). It is important to note that the migration time increased by over a minute, which allowed the separation to improve slightly. This may be due to the extra time for the migration, where slight differences in the size to charge ratios, and increased interactions of the analyte within the buffer environment, have more time to exert a greater difference in the separation.

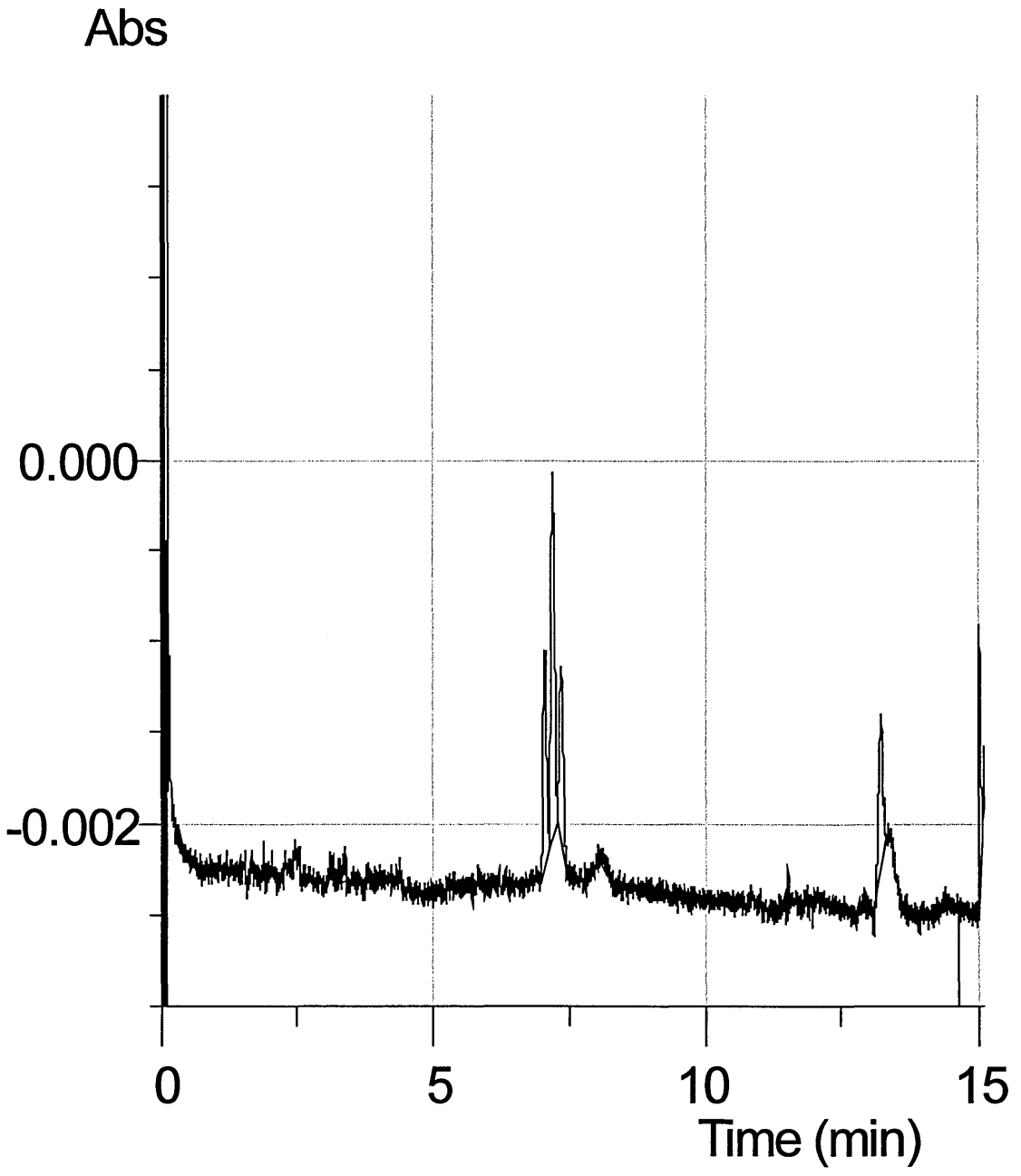

Figure 5.7 The electropherogram of alkylsalicylate, prior to the removal of base oil by solid phase extraction: Separation buffer of 50mM ammonium acetate and 20% v/v cyclohexane in methanol pH 9.01*. HDB was coated onto the inner capillary wall in a pre-separation wash at a concentration of 0.025mM. Capillary length 65/50cm; 210nm; inj. 20mbar 0.2min with a total alkysalicylate and base oil concentration of 2000 µg/ml and separation voltage of –30kV.

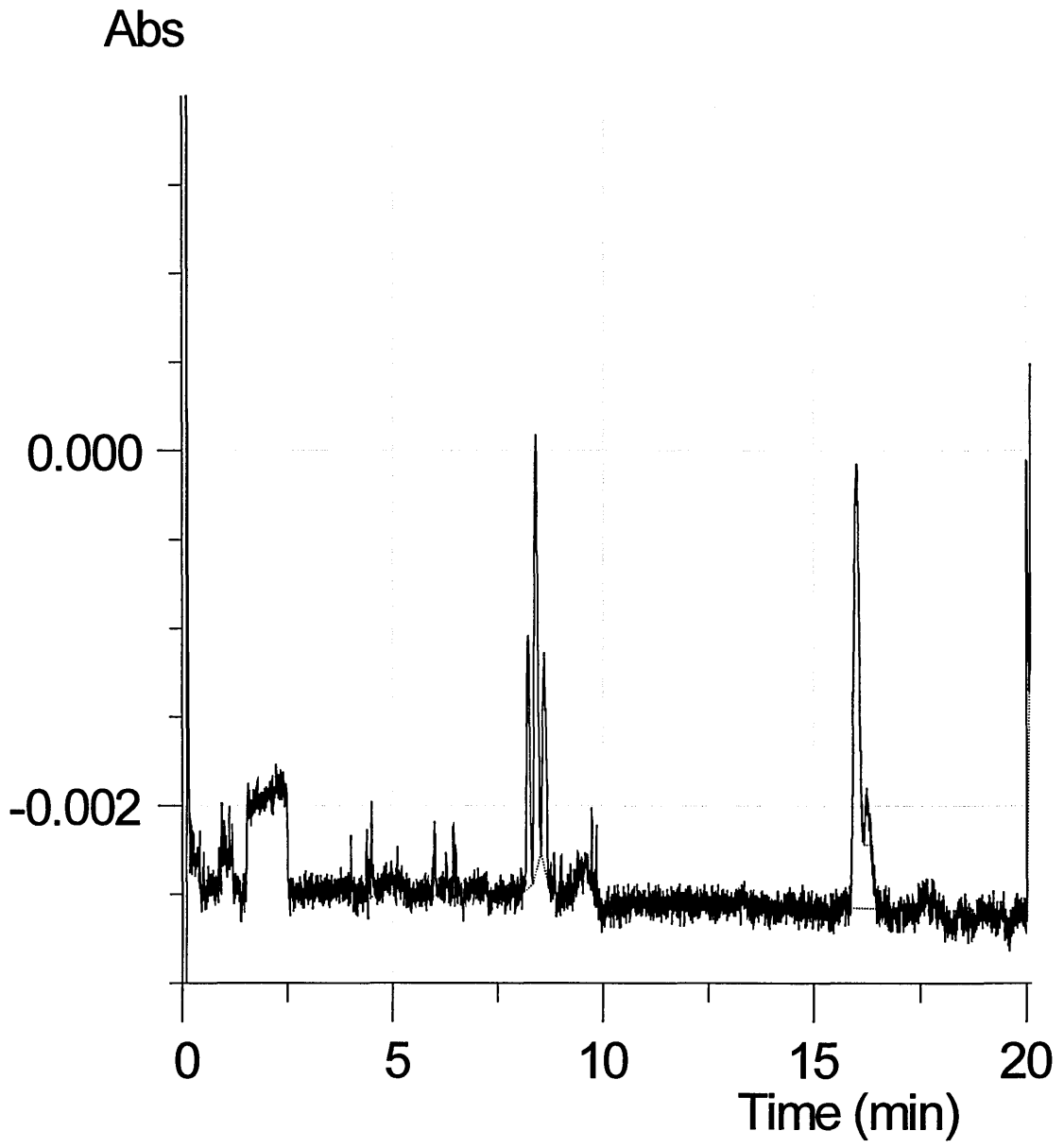

Figure 5.8 The electropherogram of alkylsalicylate, prior to the removal of base oil by solid phase extraction: Separation buffer of 50mM ammonium acetate and 20% v/v cyclohexane in methanol pH 9.01*. HDB was coated onto the inner capillary wall in a pre-separation wash at a concentration of 0.0025mM. Capillary length 75/60cm; 210nm, inj. 20mbar 0.2min with a total alkylsalicylate and base oil concentration of 2000 µg/ml and separation voltage of –30kV.

5.4.5 Solid phase extraction

The preceding work was carried out with the analyte in base oil due to the small amounts of alkylsalicylate available at that time. The arrival of more samples allowed the use of solid phase extraction to remove the base oil. The main sample used for further development was a magnesium alkylsalicylate believed to be the same as that previously analysed. In all subsequent figures, the analyte concentration was 1000 μg/ml unless otherwise stated.

The effect of sample pre-treatment by solid phase extraction is obvious in the electropherogram in figure 5.9 on page 141. The sensitivity increased considerably, with some detriment to the separation.

5.4.6 Different sample injection methods

In the previous work, the analyte was diluted with the separation buffer prior to injection. Improvements in separation in aqueous CE can be achieved by the use of sample stacking and field amplified injection, involving the use of dilute buffer or deionised water in the sample loading plug. Sample dilution with methanol was carried out to see whether a similar effect would be observed in NACE.

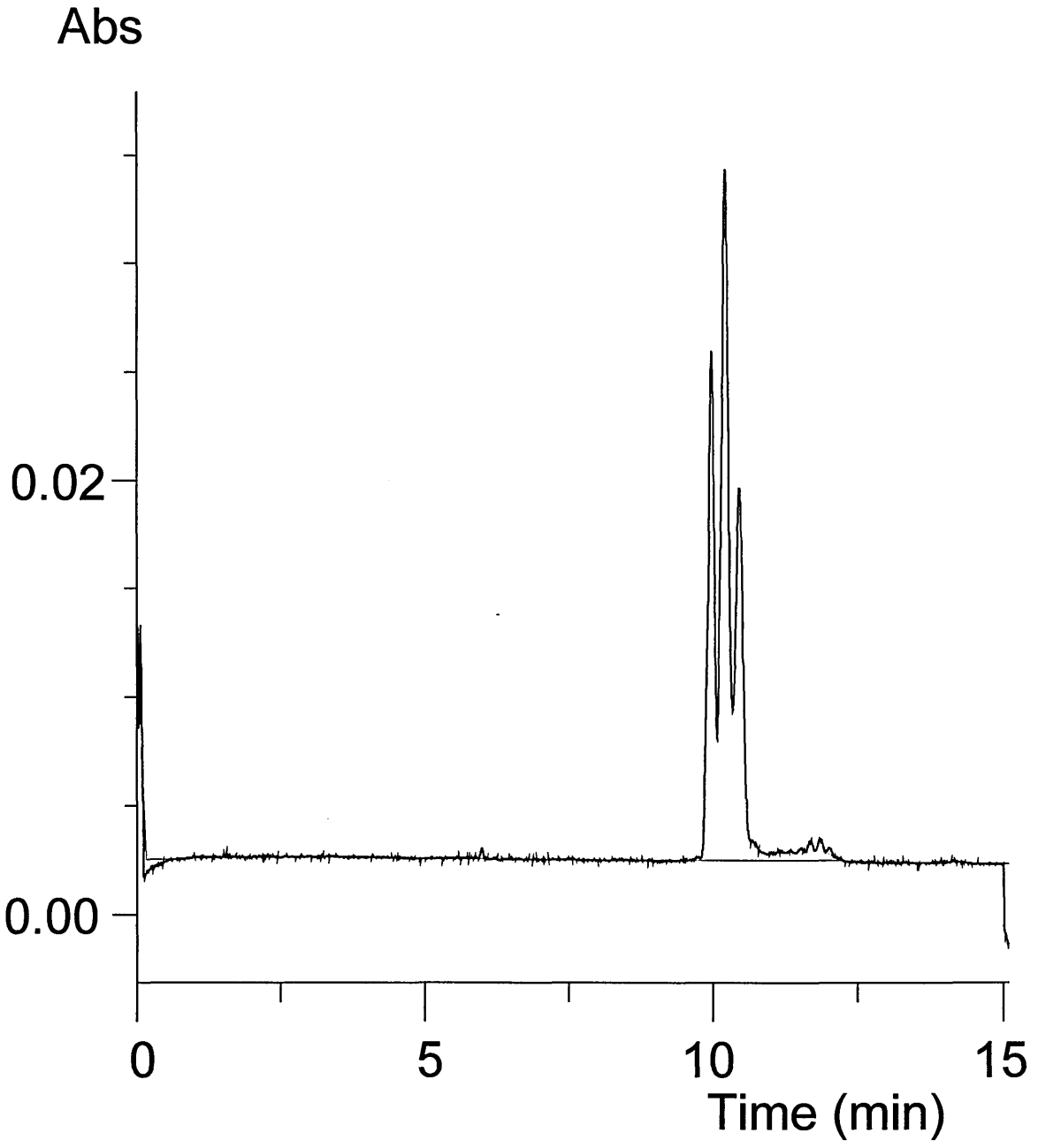

Figure 5.9 The electropherogram of alkylsalicylate, after the removal of base oil by solid phase extraction: Separation buffer of 50mM ammonium acetate and 20% v/v cyclohexane in methanol pH 9.02*. HDB was coated onto the inner capillary wall in a pre-separation wash at a concentration of 0.0025mM. Capillary length 75/60cm; 210nm; inj. 20mbar 0.2min, uv wavelength 210nm with an alkylsalicylate concentration of 1000 µg/ml and separation voltage of –30kV.

The analytes were injected as 1000 pg/ml solutions in methanol, and the resulting asymmetry, peak intensity, and efficiency were measured. Peak asymmetry is related to the shape of the peak, ideally Gaussian shaped and denoted by 1. Asymmetry will produce numbers greater than 1 for peak fronting or less than 1 for peak tailing if the peak is non Gaussian. Peak intensity is the height of the peak, the greater the intensity the greater the sensitivity for an analyte. Peak efficiency is related to plate height; the lower the theoretical plate height (or the greater the plate number) the better the efficiency. Peak efficiency was assessed in terms of theoretical plate numbers.

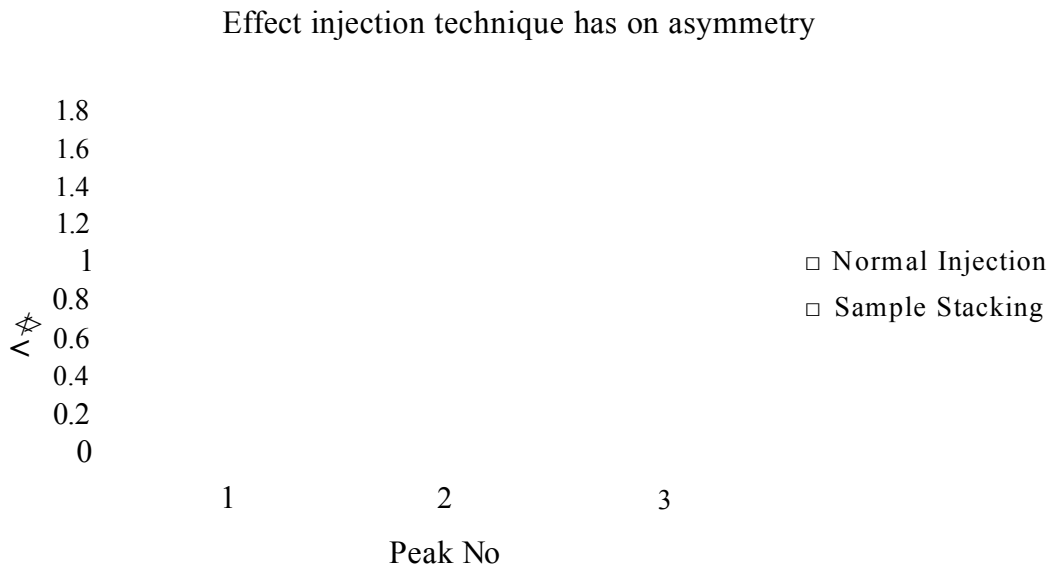

Figure 5.10. The effect of injection technique on peak asymmetry. Conditions: separation buffer 50mM ammonium acetate, 20% v/v cyclohexane in methanol, pH 9.02* adjusted using tetramethylammonium hydroxide. HDB coverage of wall carried out by a pre-separation wash of 0.0025mM HDB in methanol. Normal injection alkylsalicylate diluted to 1000 pg/ml in buffer, sample stacking alkylsalicylate diluted to 1000 pg/ml in methanol. Injected at 20mbar for 0.2mins, uv wavelength 210nm. Separation voltage -30kV.

Figure 5.10 shows the effect of sample stacking on peak asymmetry; sample stacking altered peak asymmetry somewhat, with greater fronting, but the alteration in asymmetry was small when compared to the improvements in selectivity and sensitivity (figure 5.13 page 146).

Sample stacking improved the sensitivity of separation 10-fold, as shown in figure 5.11. The low conductivity within the sample stacking injection plug led to a considerable increase in sensitivity, and a slight increase in peak fronting, whereas when the analyte was diluted in buffer the electrical conductivity was matched and the peaks were more symmetrical. If increased sensitivity is seen with similar peak areas then the efficiency is greater and if migration times are similar then an improvement in resolution is present. Efficiency was improved by stacking, as shown in figure 5.12, and any detrimental effect of asymmetry was overcome by the increased efficiency of the separation, as can be seen by comparison of figure 5.09 with figure 5.13. The effect of sample stacking also enabled the use of lower concentrations of analytes (in this case 500 μg/ml).

The effect of injection technique on sensitivity

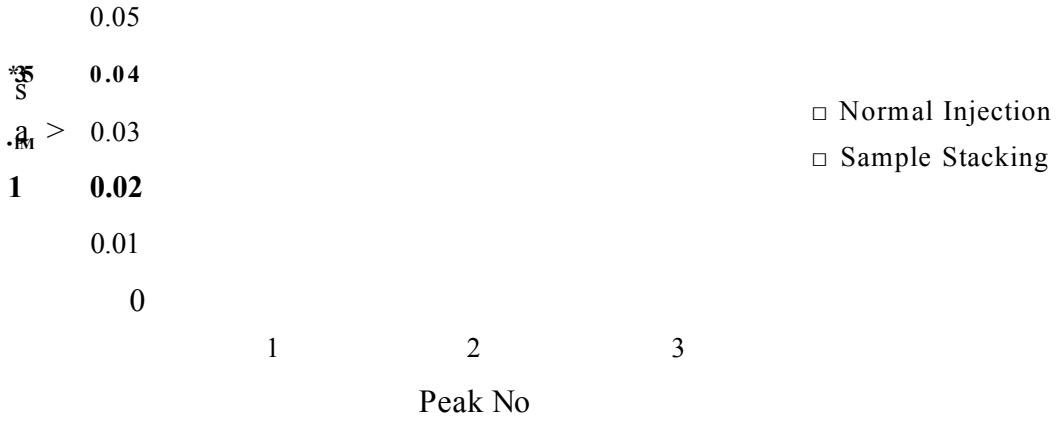

Figure 5.11. The effect of injection technique on sensitivity. Conditions: separation buffer 50mM ammonium acetate, 20% v/v cyclohexane in methanol, pH 9.02* adjusted using tetramethylammonium hydroxide. HDB coverage of wall carried out by a pre-separation wash of 0.0025mM HDB in methanol. Normal injection alkylsalicylate diluted to 1000 pg/ml in buffer, sample stacking alkylsalicylate diluted to 1000 pg/ml in methanol. Injected at 20mbar for 0.2mins, uv wavelength 210nm. Separation voltage -30kV.

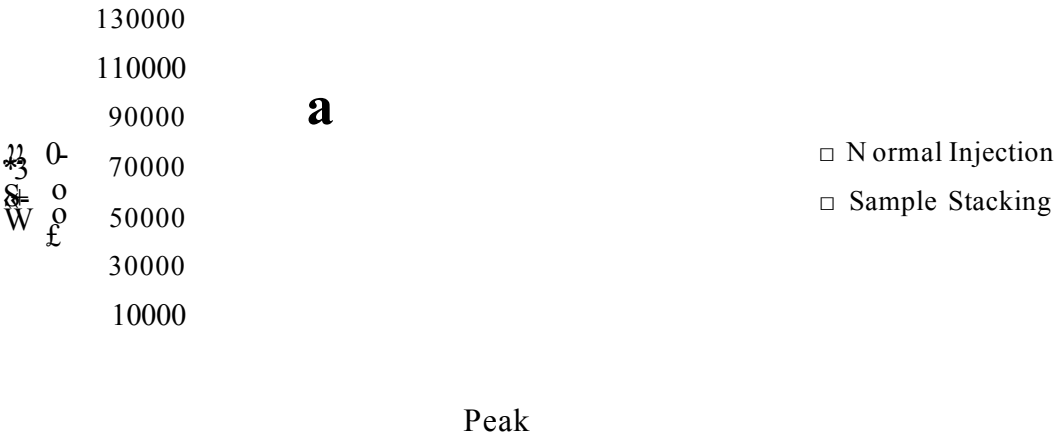

Figure 5.12. The effect of injection methods on peak efficiency. Conditions: separation buffer 50mM ammonium acetate, 20% v/v cyclohexane in methanol, pH 9.02* adjusted using tetramethylammonium hydroxide. HDB coverage of wall carried out by a pre-separation wash of 0.0025mM HDB in methanol. Normal injection alkylsalicylate diluted to 1000 pg/ml in buffer, sample stacking alkylsalicylate diluted to 1000 pg/ml in methanol. Injected at 20mbar for 0.2mins, uv wavelength 210nm. Separation voltage -30kV.

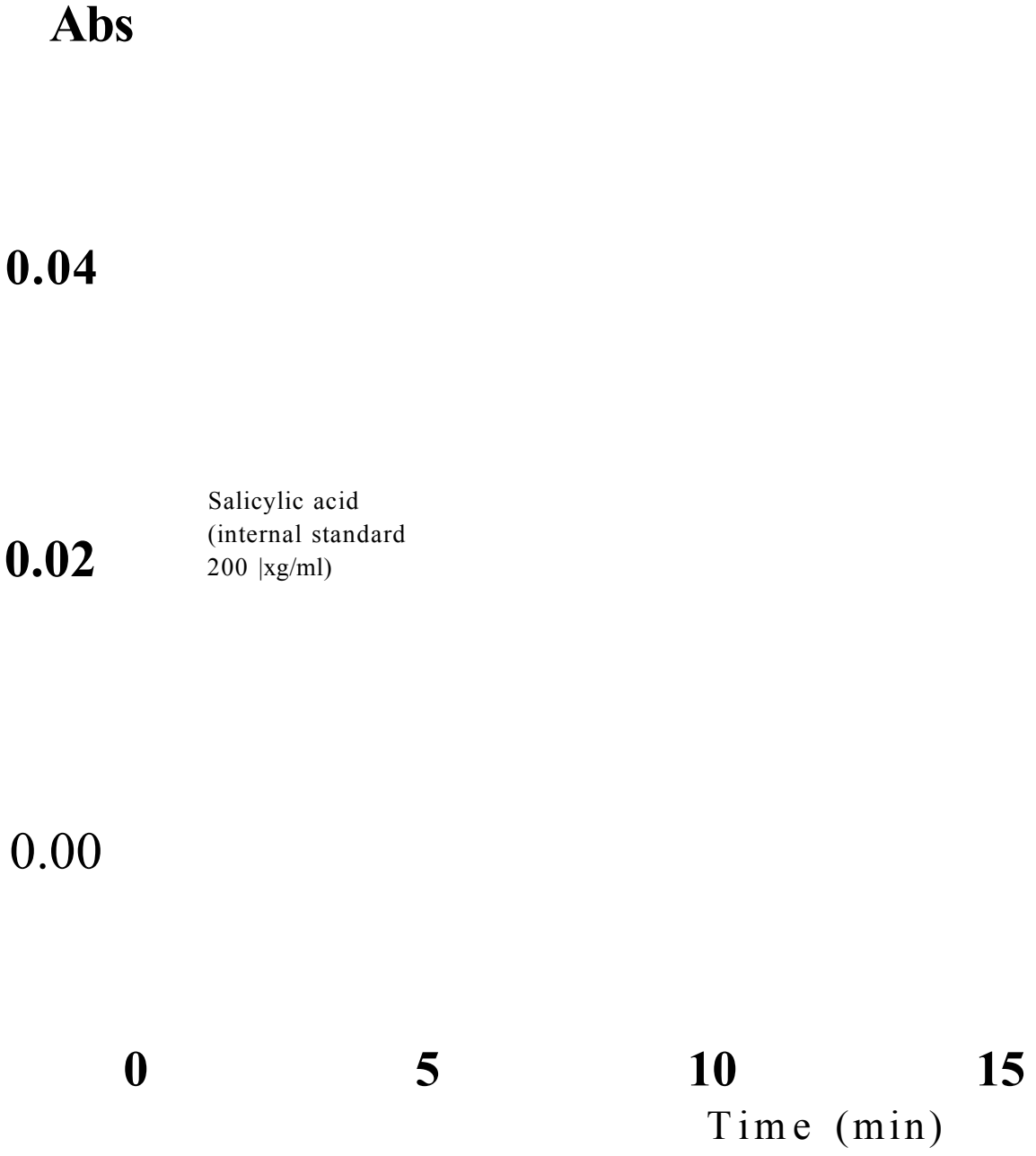

Figure 5.13. The electropherogram of alkylsalicylate using sample stacking, with sample diluted in methanol. Separation buffer: 50mM ammonium acetate, 20% v/v cyclohexane in methanol pH 9.02* adjusted using tetramethylammonium hydroxide. HDB coated the capillary wall in a capillary wash at a concentration of 0.0025mM. Capillary length 75/60cm; uv wavelength 210nm, injection 20mbar 0.2min with an alkylsalicylate concentration of 1000 pg/ml and separation voltage of -30kV.

5.4.7 Reproducibility

Although the separation had been developed to a suitable stage, problems were occurring with reproducibility. The low concentration of HDB led to decrease in reproducibility of run times, probably because the wash between runs caused a build up of HDB on the capillary wall with consequent reduction of migration times. If washing was not performed between runs, the migration rate began to decrease. The use of an internal standard (in this case salicylic acid at 200 μg/ml) helped to resolve the issue, allowing comparison of migration rates and compensation for changes. A more effective way to resolve this problem and increase reproducibility was to increase the concentration of HDB and lengthen the capillary to obtain similar migration times. The capillary length with HDB at 0.025mM was 95cm which, after a five minute wash to ensure complete capillary coverage, gave increased reproducibility.

5.4.8 Final Buffer

With the analyte now diluted in methanol and not the separation buffer, the need for cyclohexane in the separation buffer was re-examined. With the high concentration of HDB, both conductivity and reproducibility were not consistent, which led to the differences in migration. These problems could be due to the presence of cyclohexane in the buffer, if it was not thoroughly mixed.

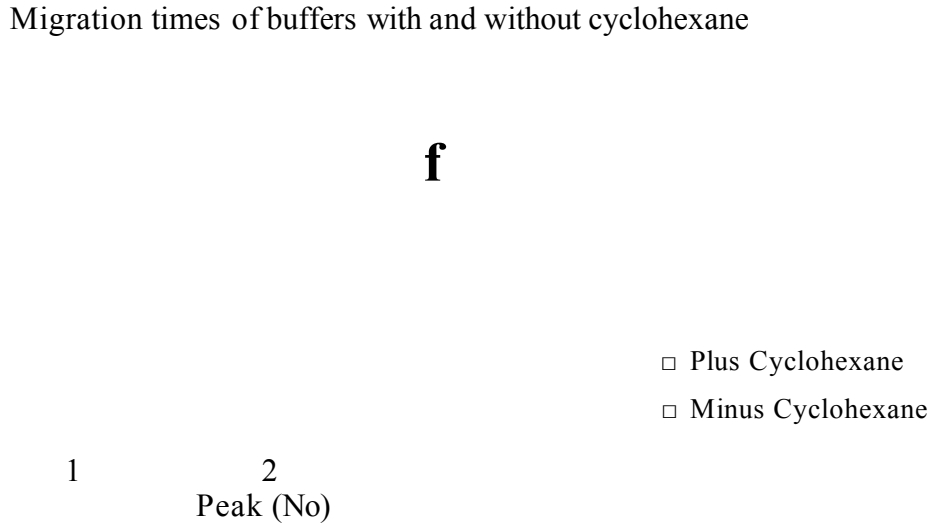

Figure 5.14. The effect of removing 20%cyclohexane on the separation.
Conditions: separation buffer 50mM ammonium acetate, +/-20% v/v cyclohexane in methanol, pH 9.04* adjusted using tetramethylammonium hydroxide. HDB coverage of wall carried out by a pre-separation wash of 0.025mM HDB in methanol. Capillary length 95/80cm; uv wavelength 210nm, injection 20mbar 0.2min. Sample stacking alkylsalicylate diluted to 1000 pg/ml in methanol. Separation voltage -30kV.

Figure 5.14 shows that removing the cyclohexane from the buffer reduced migration times. Reproducibility was also slightly better, reduced from 0.6% to 0.3% RSD. The

faster migration time was not detrimental to the overall separation. Asymmetry was slightly improved (figure 5.15) although the efficiency of the separation was not greatly improved by the removal of the cyclohexane.

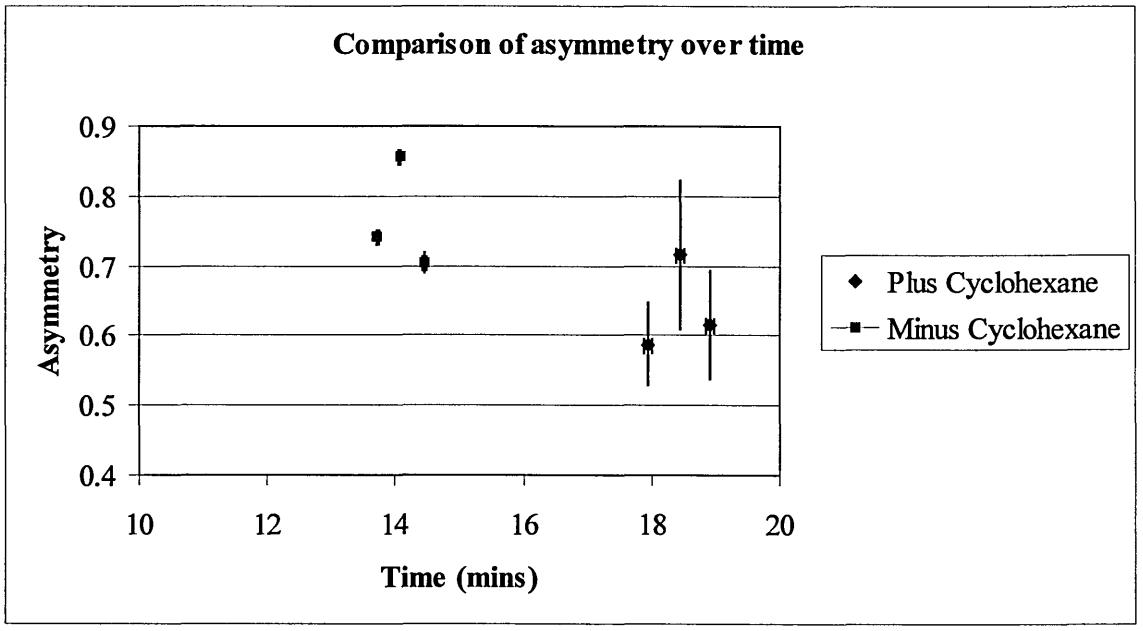

Figure 5.15. Effect of removing 20%cyclohexane on separation time and peak asymmetry.

Conditions: separation buffer 50mM ammonium acetate, +/-20% v/v cyclohexane in methanol, pH 9.04* adjusted using tetramethylammonium hydroxide. HDB coverage of wall carried out by a pre-separation wash of 0.025mM HDB in methanol. Capillary length 95/80cm; uv wavelength 210nm, injection 20mbar 0.2min, Sample stacking alkylsalicylate diluted to 1000 µg/ml in methanol. Separation voltage –30kV.

Figures 5.16 and 5.17 show that peak area ratios and migration ratios of analyte to salicylic acid were altered, and that reproducibility was much improved (as indicated by the error bars corresponding to standard deviation n=6). Electropherograms give a better perspective of this reproducibility from run to run analysis (figure 5.18). It was

concluded that the separation buffer no longer required cyclohexane for the separation of analytes.

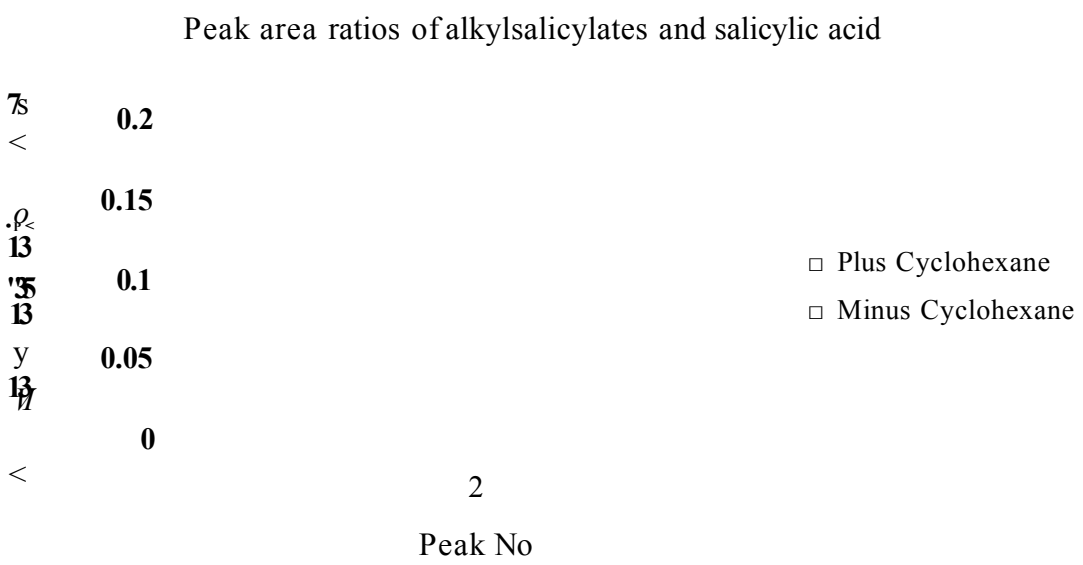

Figure 5.16. The effect of removal of 20% cyclohexane on the peak area ratios of alkylsalicylate.

Conditions: separation buffer 50mM ammonium acetate, +/-20% v/v cyclohexane in methanol, pH 9.04* adjusted using tetramethylammonium hydroxide. HDB coverage of wall carried out by a pre-separation wash of 0.025mM HDB in methanol. Capillary length 95/80cm; uv wavelength 210nm, injection 20mbar 0.2min. Sample stacking alkylsalicylate diluted to 1000 pg/ml in methanol. Separation voltage -30kV.

Comparison of alkylsalicylate migration with salicylic acid migration

Figure 5.17. The effect of the removal of 20% cyclohexane on migration ratio reproducibility.

Conditions: separation buffer 50mM ammonium acetate, +/-20% v/v cyclohexane in methanol, pH 9.04* adjusted using tetramethylammonium hydroxide. HDB coverage of wall carried out by a pre-separation wash of 0.025mM HDB in methanol. Capillary length 95/80cm; uv wavelength 210nm, injection 20mbar 0.2min. Sample stacking alkylsalicylate diluted to 1000 pg/ml in methanol. Separation voltage -30kV.

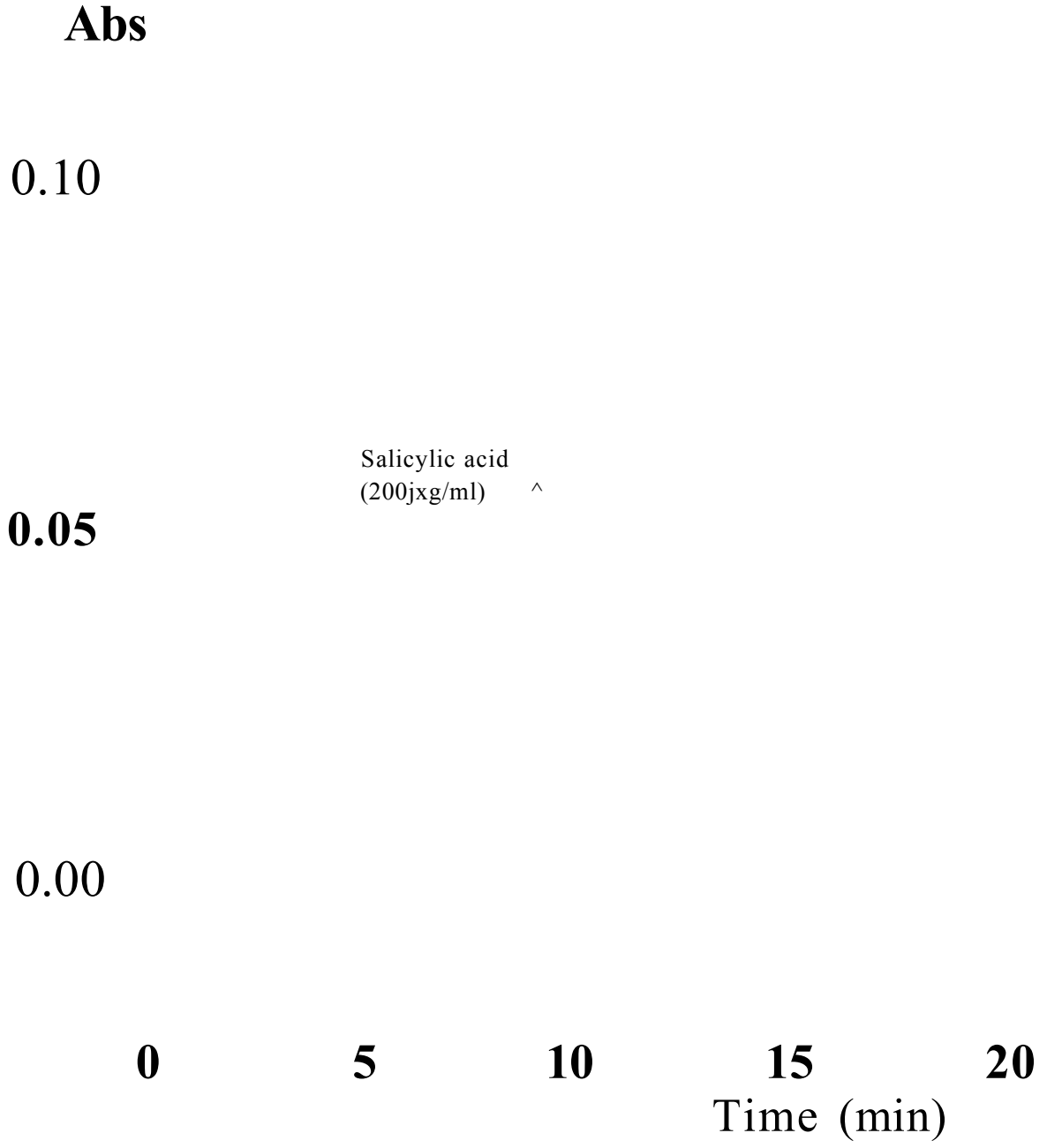

Figure 5.18. Multiple overlaid electropherograms showing reproducibility of the separation of an alkylsalicylate, base oil removed by solid phase extraction. Separation buffer of 50mM ammonium acetate in methanol pH 9.02*, adjusted using tetramethylammonium hydroxide. HDB coverage of wall carried out by a pre-separation wash of 0.025mM HDB in methanol. Capillary length 95/80cm; uv wavelength 210nm, injection 20mbar 0.2min, alkylsalicylate concentration of 500 pg/ml and separation voltage of-30kV.

5.4.9 Identification Methods

There are several possibilities for analyte identification resolution, selectivity, relative migration time with respect to salicylic acid, and peak patterns. Any of the techniques or combinations can be used as the differences between the analytes and the internal standard stay constant.

5.4.10 Other Alkylsalicylates

Alkylsalicylates come in different formulations with variations in the metal used and the amount of overbasing used. Three types of overbased products were examined, and it was concluded that the amount of overbasing had no effect on the separation. This was not surprising as alternative analysis techniques (see section 8) showed that the metal carbonate used for the overbasing is removed in the first stages of the clean up process. The metal used within the alkylsalicylate also had no effect on the separation, which shows that when the alkylsalicylate becomes charged at neutral or basic pH* the metal dissociates from the alkylsalicylate. If the metal was not removed from the analytes then the size to charge ratio would change on the alkylsalicylates and differences would be seen in the separation. From the electropherograms (figure 5.13 and figure 5.20) it seems that the alkylsalicylates examined were manufactured using the same method and ingredients, even though the metals (magnesium or calcium) are different, confirming that the metal dissociates from the alkylsalicylate. Figures 5.19 to 5.24 show the separation of several alkylsalicylates using identification methods suggested previously, (section 5.4.9) and several conclusions can be drawn from the results. Samples SR 404, (figure 5.20) and SR1027 (figure 5.21), have been synthesised with the same starting materials, with unknown chain lengths. Samples SR 1024, SR 1023, SR 1025 (figures 5.19, 5.23 and 5.24) show alkylsalicylates that have been synthesised by a manufacturer with different starting materials as compared to

5.20 and 5.21. The differences between the two products are obvious from the peak patterns. The relative migration times of SR 1023-1025 suggest that the alkyl chain lengths are larger than in SR 404 and 1027. As previously suggested the use of mass spectrometry will identify the differences and size of the individual chain lengths. Identification of individual manufacturers alkylsalicylates is possible by the use of NACE.

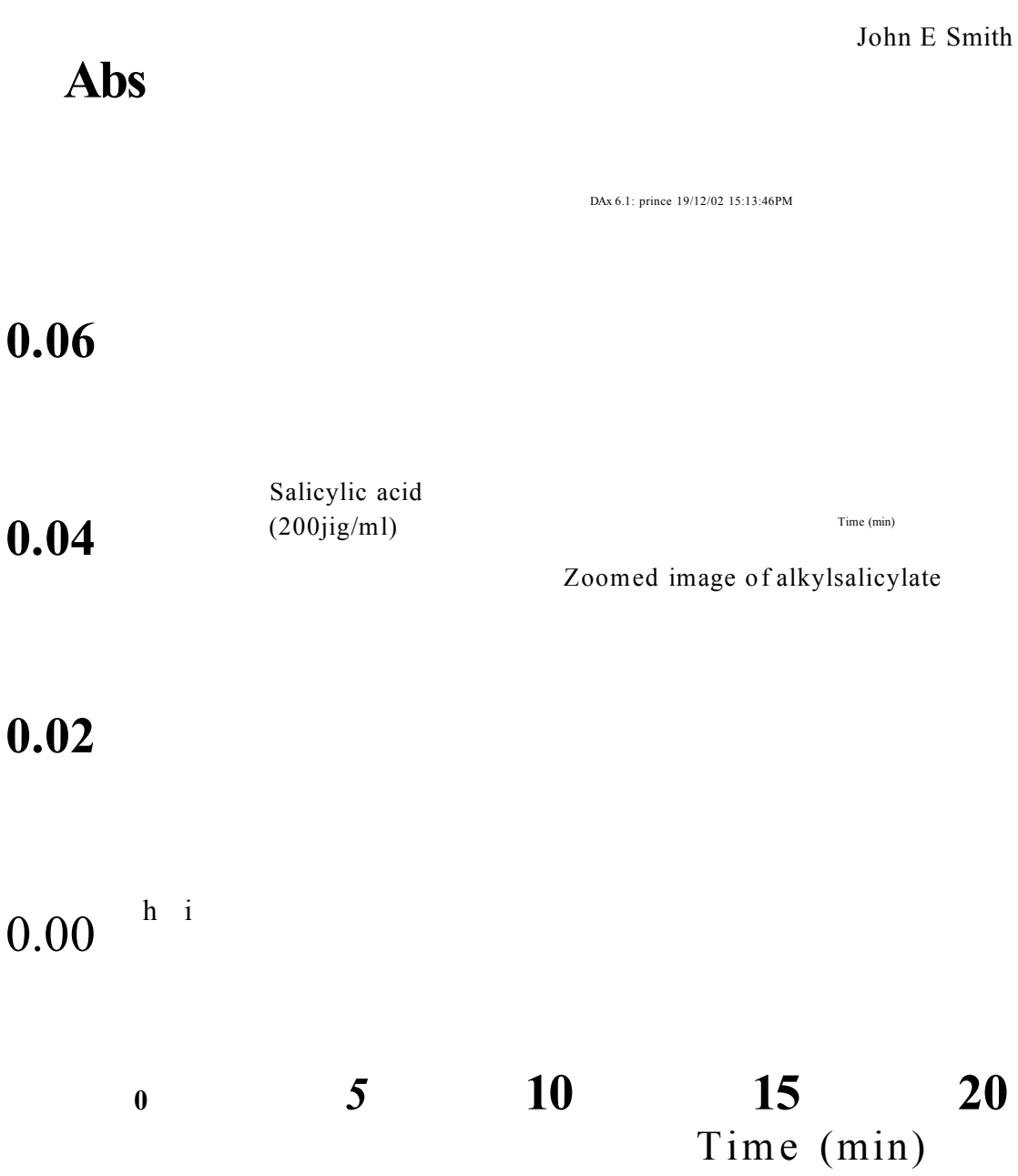

Figure 5.19. The electropherogram of SR 1024, base oil removed by solid phase extraction. Separation buffer of 50mM ammonium acetate with 0.025mM HDB in methanol pH 9.02*, adjusted using tetramethylammonium hydroxide. Capillary length 95/80cm; uv wavelength 210nm, injection 20mbar 0.2min, alkylsalicylate concentration of 500 pg/ml and separation voltage of-30kV.

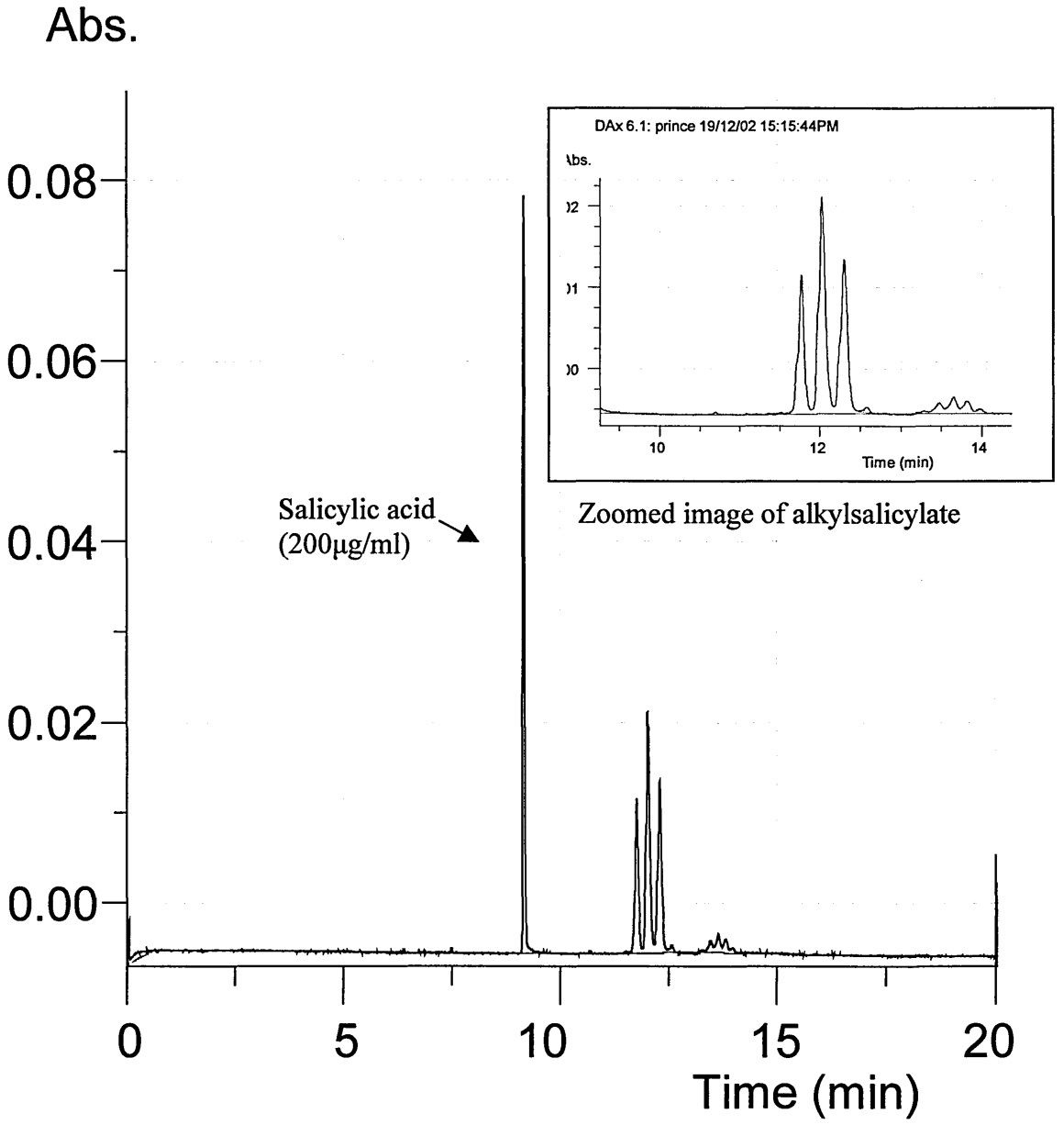

Figure 5.20. The electropherogram of SR 404, base oil removed by solid phase extraction. Separation buffer of 50mM ammonium acetate with 0.025mM HDB in methanol pH 9.02*, adjusted using tetramethylammonium hydroxide. Capillary length 95/80cm; uv wavelength 210nm, injection 20mbar 0.2min, alkylsalicylate concentration of 500 µg/ml and separation voltage of –30kV.

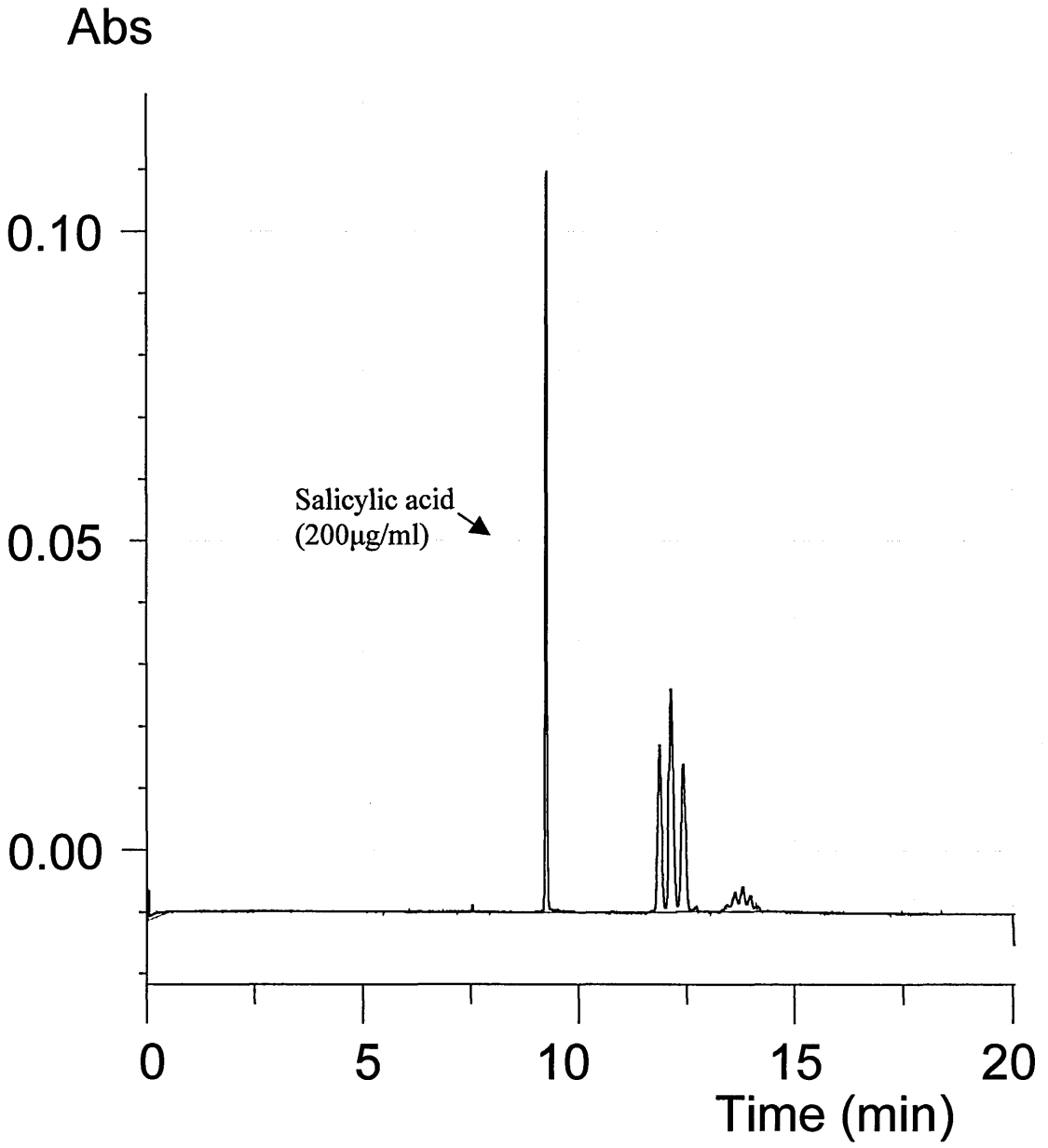

Figure 5.21. The electropherogram of SR 1027, base oil removed by solid phase extraction. Separation buffer of 50mM ammonium acetate with 0.025mM HDB in methanol pH 9.02*, adjusted using tetramethylammonium hydroxide. Capillary length 95/80cm; uv wavelength 210nm, injection 20mbar 0.2min, alkylsalicylate concentration of 500 µg/ml and separation voltage of –30kV.

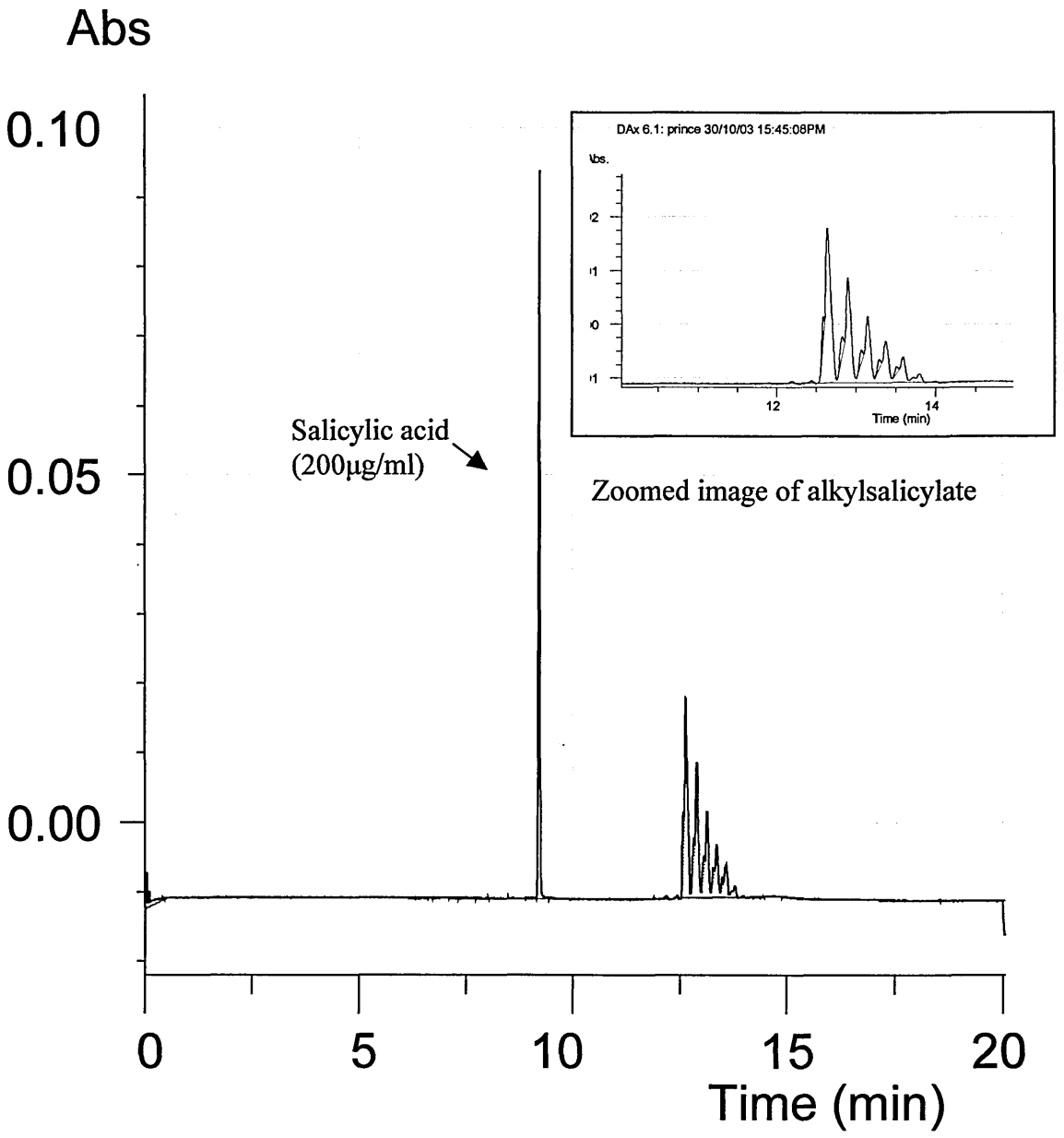

Figure 5.22. The electropherogram of SR 1023, base oil removed by solid phase extraction. Separation buffer of 50mM ammonium acetate with 0.025mM HDB in methanol pH 9.02*, adjusted using tetramethylammonium hydroxide. Capillary length 95/80cm; uv wavelength 210nm, injection 20mbar 0.2min, alkylsalicylate concentration of 500 µg/ml and separation voltage of –30kV.

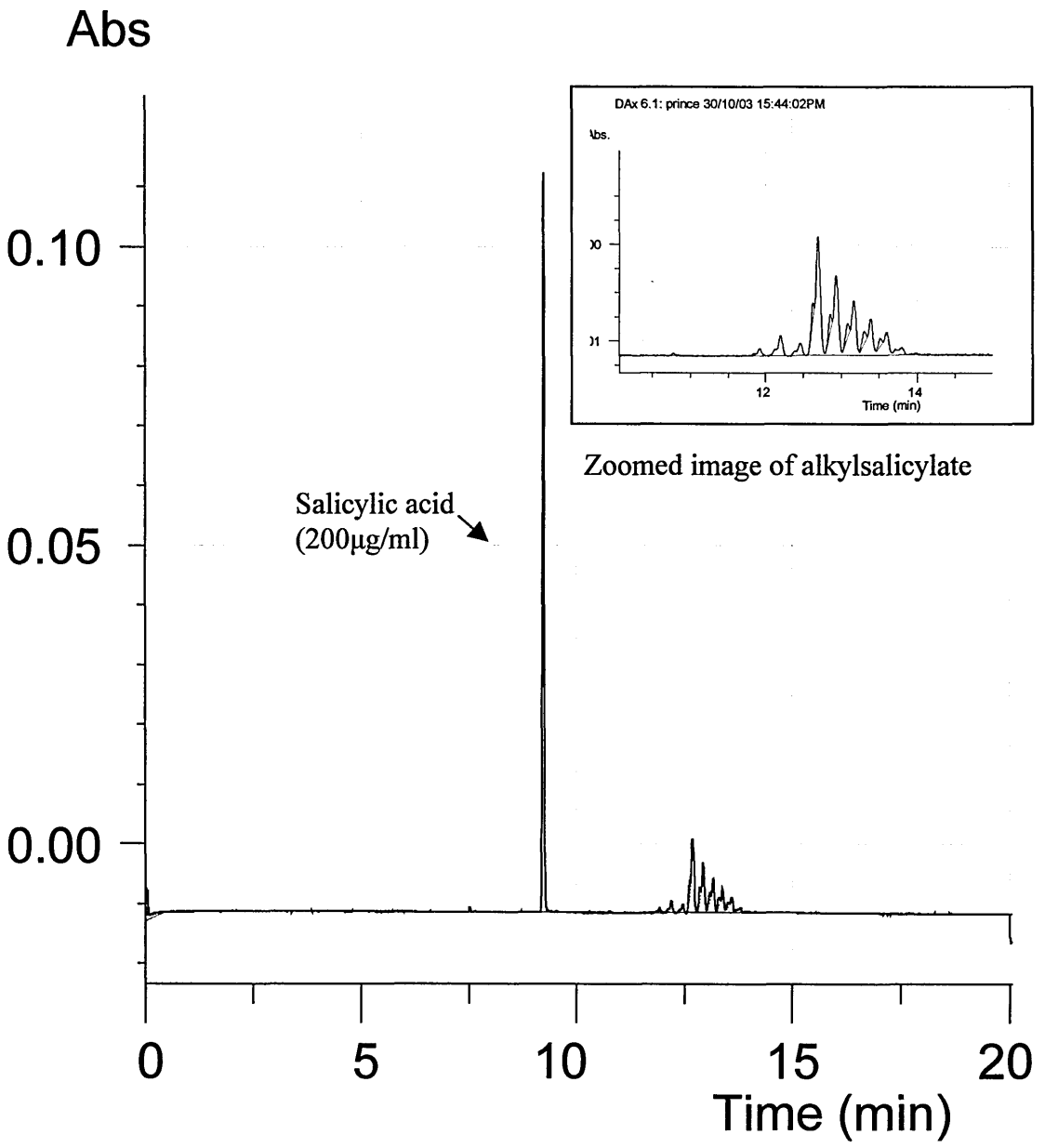

Figure 5.23. The electropherogram of SR 1025, base oil removed by solid phase extraction. Separation buffer of 50mM ammonium acetate with 0.025mM HDB in methanol pH 9.02*, adjusted using tetramethylammonium hydroxide. Capillary length 95/80cm; uv wavelength 210nm, injection 20mbar 0.2min, alkylsalicylate concentration of 500 µg/ml and separation voltage of –30kV.

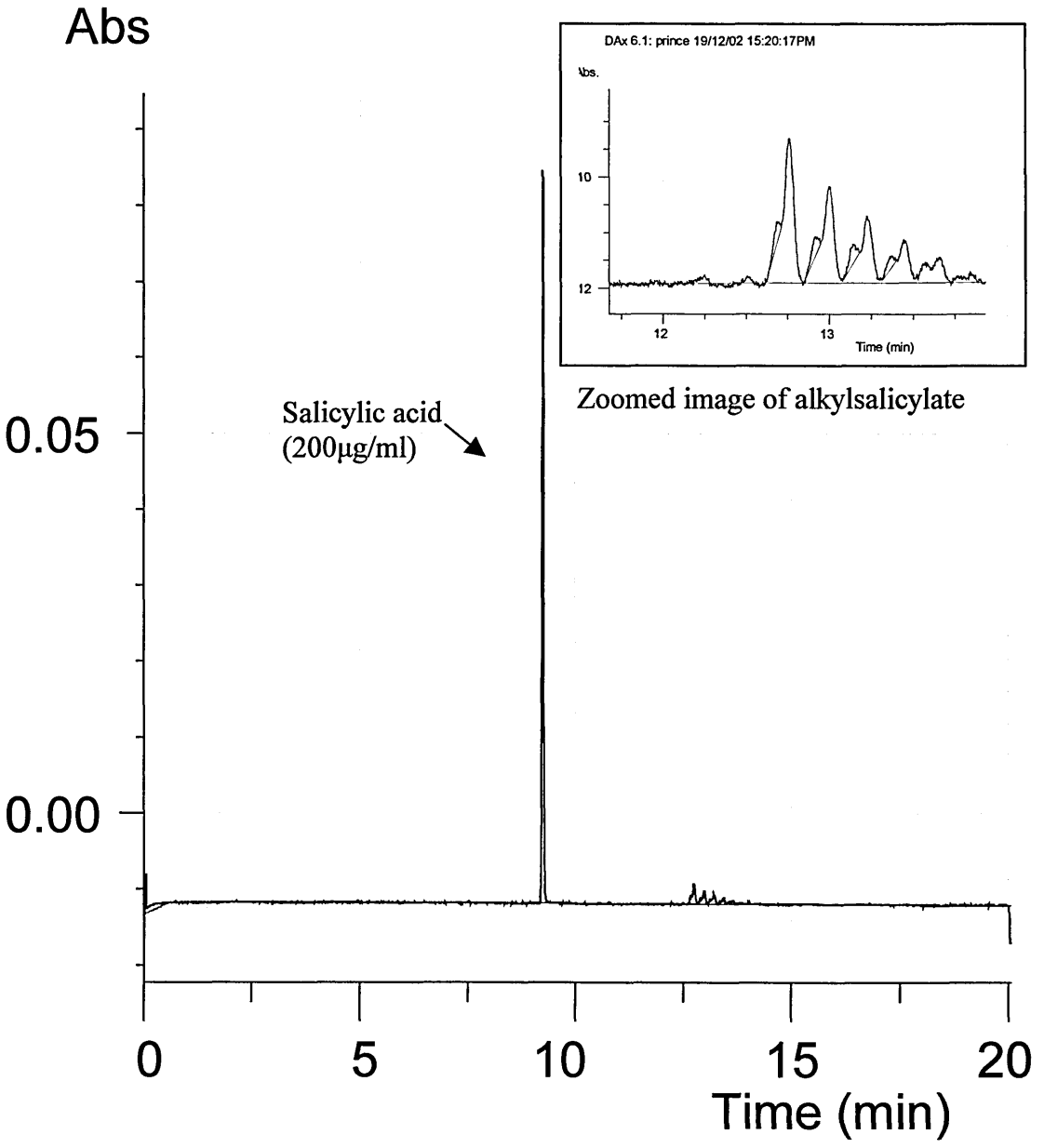

Figure 5.24. The electropherogram of SR 1233, base oil removed by solid phase extraction. Separation buffer of 50mM ammonium acetate with 0.025mM HDB in methanol pH 9.02*, adjusted using tetramethylammonium hydroxide. Capillary length 95/80cm; uv wavelength 210nm, injection 20mbar 0.2min, alkylsalicylate concentration of 500µg/ml and separation voltage of –30kV.

5.5 Conclusion

The work carried out on the analysis of alkylsalicylates has scratched the surface of the possibilities for the use of NACE within the lubrication industry.

- A simple buffer has been used for the successful separation of alkylsalicylates.
- HDB has been utilised to control the EOF.
- Run to run reproducibility was under 1%.
- Sample stacking was shown to improve the overall separation.
- Different formulations could be identified.
- The use of ammonium acetate with no other additives ensured compatibility for mass spectrometry.

Chapter 6

Analysis of zinc dialkyldithiophosphates and alkylsalicylates by mass spectrometry and nonaqueous capillary electrophoresis-mass spectrometry

6.1 Chemicals and reagents

See section 4a

6.2 Instrumentation and procedures

See section 4b and 4c

6.3 Direct infusion

When using mass spectrometry detection, it is easiest to set up the instrument parameters while directly infusing a solution of the analyte into the mass spectrometer. The nebulising gas was set at 40 l $hour^{-1}$ and drying gas at 200 l $hour^{-1}$.

Initial work centred on adjustment of capillary voltage and cone voltage for the formation of a continuous ion spray. In each case the analytes intended for examination were used to identify the effects seen on the total ion current.

6.4 Alkylsalicylate

6.4.1 Capillary voltage and cone voltage

The cone voltage was set at -30V for examination of the effects of capillary voltage and the nebulising gas and drying gas were set as above. The mass spectrometer was operated in MCA scanning between 60 and 1000 mass units, and each spectrum was obtained after four minutes of continuous acquisition.

Figure 6.1 shows that the most abundant negative ions were seen with the capillary voltage set to -3.0kV; ion current decreased at greater negative voltages. Increasing the voltage of the capillary resulted in the total ion current decreasing, and hence further work was carried out with the capillary voltage set at -3.0kV.

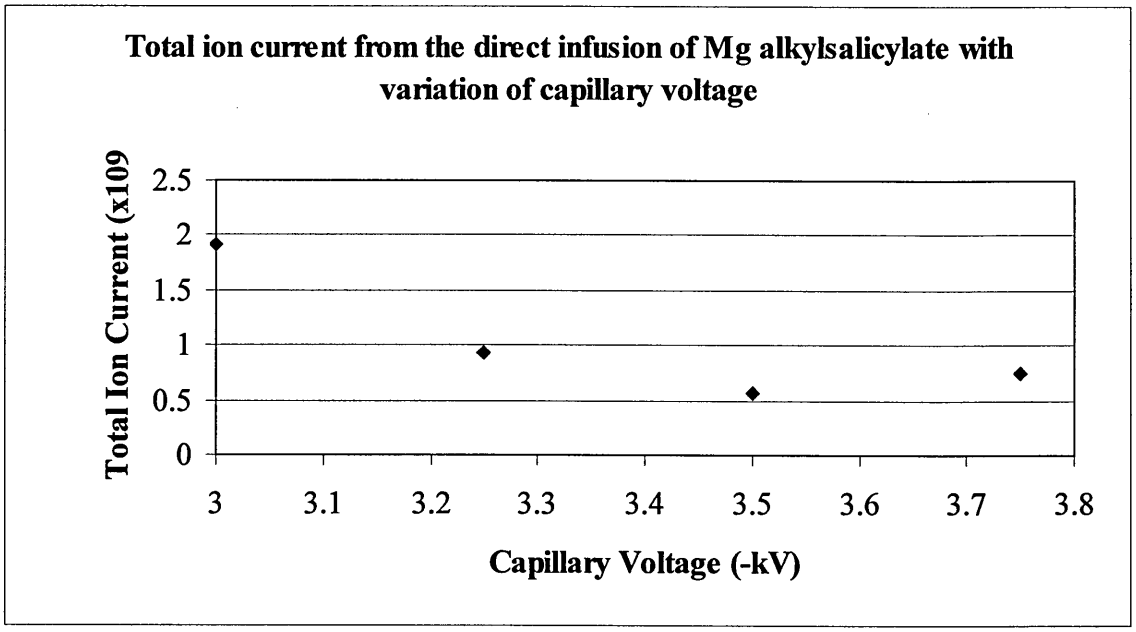

Figure 6.1 The effect of capillary voltage on the direct infusion of Mg alkylsalicylate. Conditions: Alkylsalicylate at a concentration of 1000µg/ml contained within a buffer of 50mM ammonium acetate in methanol. Nebulising gas was set to 40 l hour^{-1} whilst the drying gas was set to 200 l hour^{-1}. Cone voltage was maintained at -30 V while varying the capillary voltage. MCA was used scanning between 60 and 1000 mass units for a total time of 4 minutes.

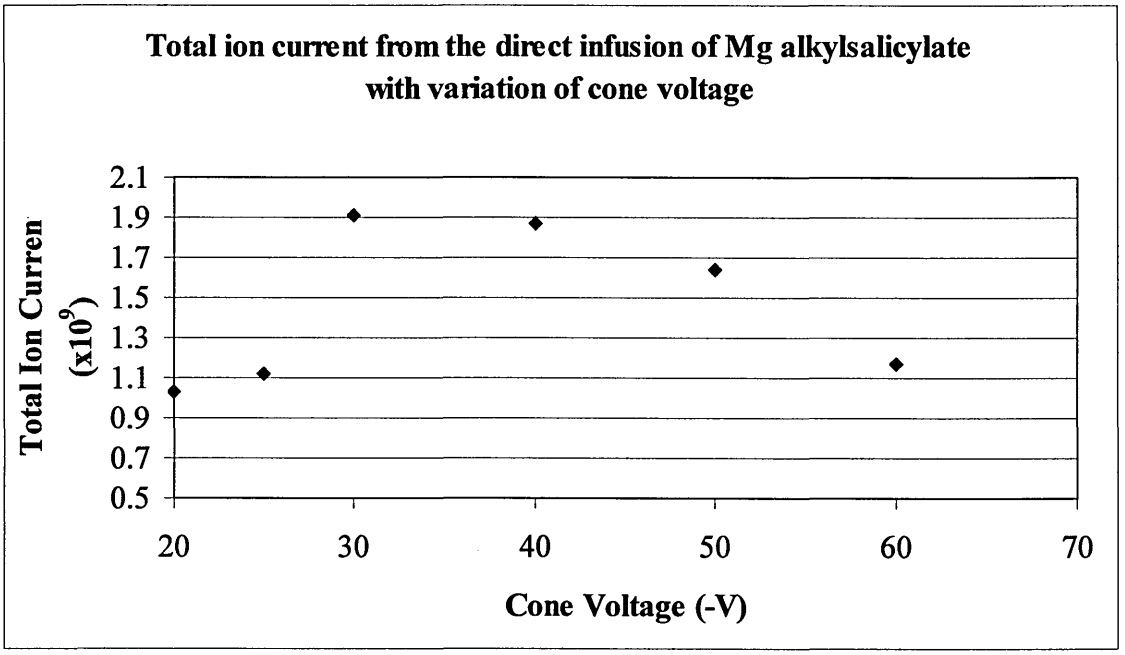

Figure 6.2 The effect of altering cone voltage on the direct infusion of Mg alkylsalicylate. Conditions: Alkylsalicylate at a concentration of 1000µg/ml contained within a buffer of 50mM ammonium acetate in methanol. Nebulising gas was set to 40 l hour^{-1} whilst the drying gas was set to 200 l hour^{-1}. Capillary voltage was maintained at -3.0 kV while varying the cone voltage. MCA was used scanning between 60 and 1000 mass units for a total time of 4 minutes.

At a cone voltage of less than -20V, negative ions were not seen (figure 6.2), Increasing the cone voltage gave an increase in the total ion formation up to -30V, after which the total ion current reduced and smaller peaks were seen in the mass spectra.

In both cases the mass spectra obtained showed patterns that were seen from the NACE separation. Figure 6.3 is a mass spectrum obtained from this work showing three masses of interest at 333, 361 and 389, which correspond to alkyl chain lengths of C_{14} to C_{18}. Isotopic ratios could be used to identify whether the alkyl chain is from a synthetic process or from natural sources such as crude oil extracts. It is not possible to

identify the isotopic ratios at this moment with the resolution available on this instrument.

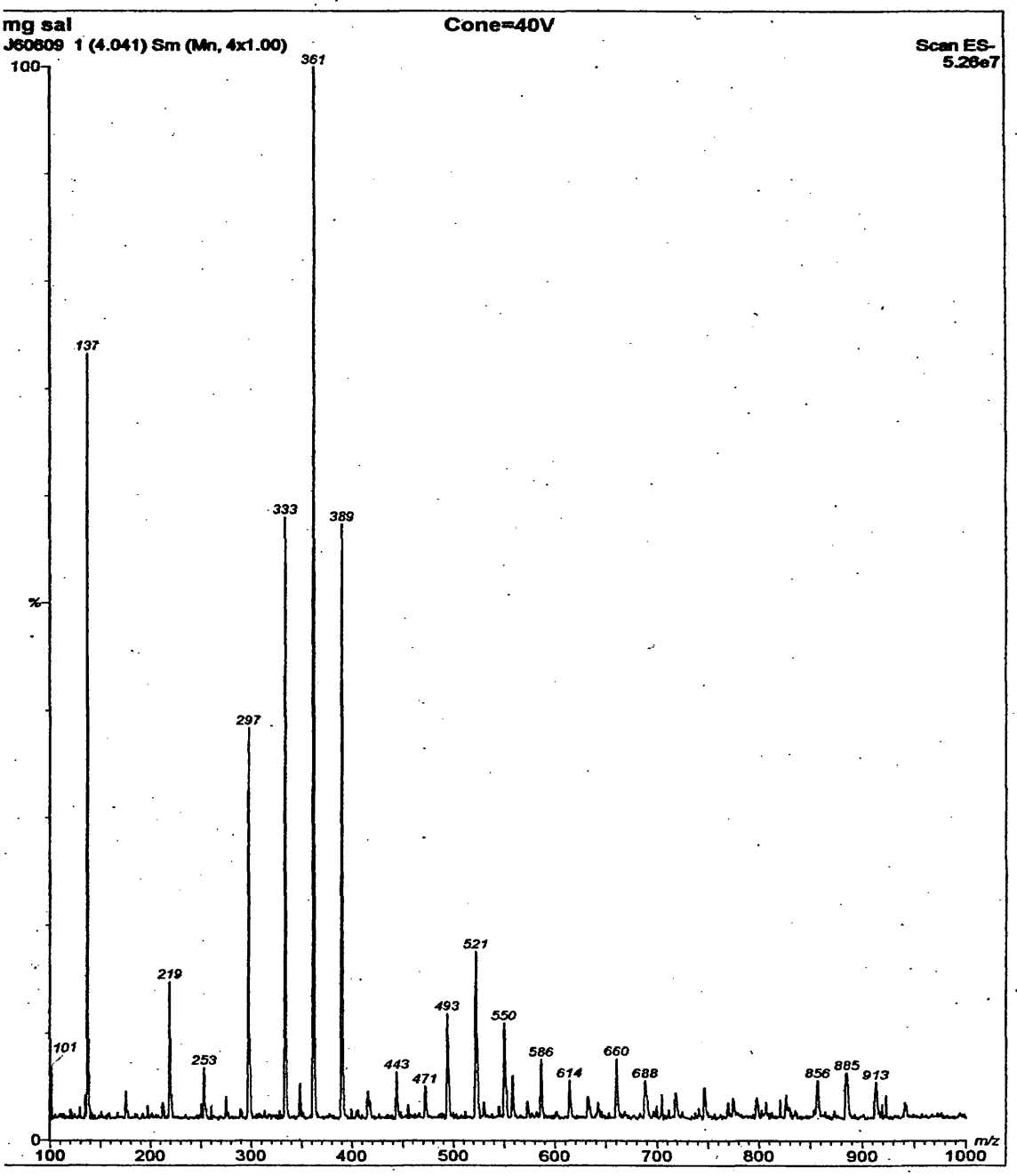

Figure 6.3 Conditions: Mg alkylsalicylate at a concentration of 1000µg/ml contained within a buffer of 50mM ammonium acetate in methanol. Nebulising gas was set to 40 l hour^{-1} whilst the drying gas was set to 200 l hour^{-1}. Cone voltage was maintained at -30 V while the capillary voltage was set at -3.0kV. MCA was used scanning between 60 and 1000 mass units for a total time of 4 minutes.

6.5 Zinc dialklyldithiophosphate

6.5.1 Capillary voltage and cone voltage

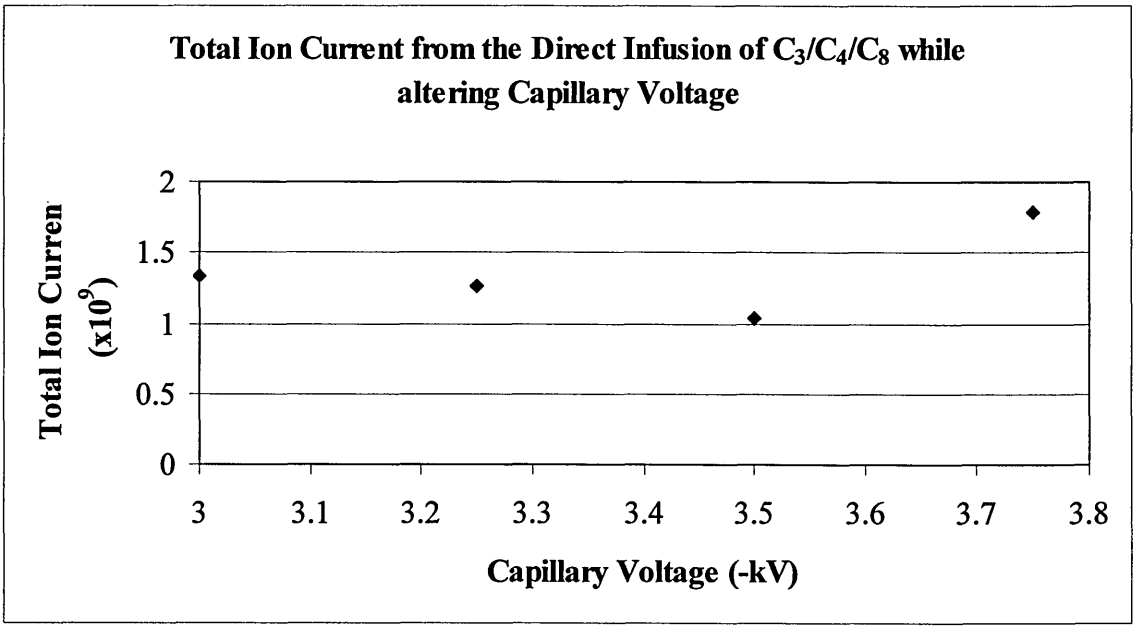

Figure 6.4 The effect of altering the capillary voltage on the total ion current from a $C_3/C_4/C_8$ ZDDP sample. Conditions: ZDDP ($C_3/C_4/C_8$) at a concentration of 1000µg/ml contained within a buffer of 50mM ammonium acetate in methanol. Nebulising gas was set to 40 l hour^{-1} whilst the drying gas was set to 200 l hour^{-1}. Cone voltage was maintained at -30 V while varying the capillary voltage. MCA was used scanning between 60 and 1000 mass units for a total time of 4 minutes.

The results in figure 6.4 show the capillary voltage did not have the same effect on total ion current with ZDDP infusion as it did with the magnesium alkylsalicylate. This suggests that the capillary voltage did not affect the ion formation in this particular case. As the sample was in the same buffer as that of the NACE separation, it is possible that the ions are pre-formed before the introduction into the ionisation source.

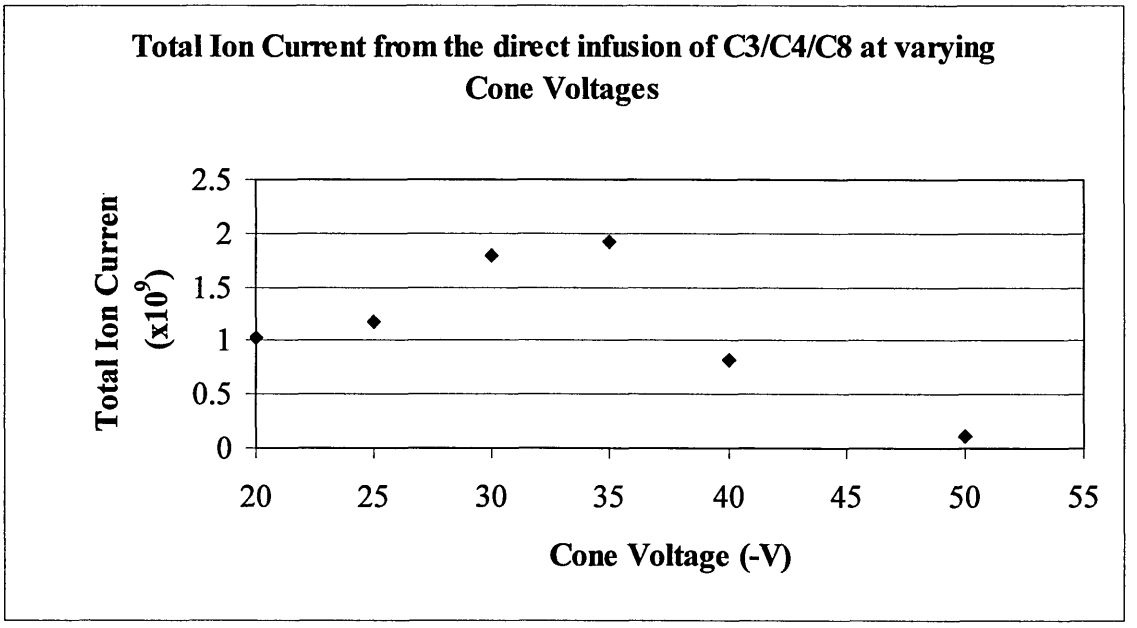

Figure 6.5 The effect of altering the cone voltage on the total ion current from a $C_3/C_4/C_8$ ZDDP sample. Conditions: ZDDP ($C_3/C_4/C_8$) at a concentration of 1000µg/ml contained within a buffer of 50mM ammonium acetate in methanol. Nebulising gas was set to 40 l hour^{-1} whilst the drying gas was set to 200 l hour^{-1}. Capillary voltage was maintained at -3.0 kV while varying the cone voltage. MCA was used scanning between 60 and 1000 mass units for a total time of 4 minutes.

Unlike the effect of capillary voltage, the cone voltage (figure 6.5) did effect the total ion current. The total ion current was seen to increase up to -35V and decrease greatly hereafter.

The masses of interest identified in the spectra are 213, 227, 241, 283, 297 and 353 respectively. These masses correspond to the expected molecular ions for the ligands C_3/C_3, C_3/C_4, C_4/C_4, C_3/C_8, C_4/C_8 and C_8/C_8 respectively; quasi-molecular ions were not seen. However, there are possibilities for errors especially if the ligand patterns are very similar. For example, with C_3/C_3 the nominal chain length tallies to C_6 and so the ligands may be C_2/C_4 or C_5/C_1 and the other possible ligands have to be accounted for

to discount them i.e. look for C_2/C_2 and C_4/C_4. In the case of C_4/C_4, C_2/C_4 these cannot be discounted; however no mass response is seen for C_2/C_2 and hence C_2/C_4 can be removed from consideration.

Figures 6.6 and 6.7 show mass spectra obtained from $C_3/C_4/C_8$ and C_4/C_5 ZDDP mixtures. The results correspond with those obtained from NACE.

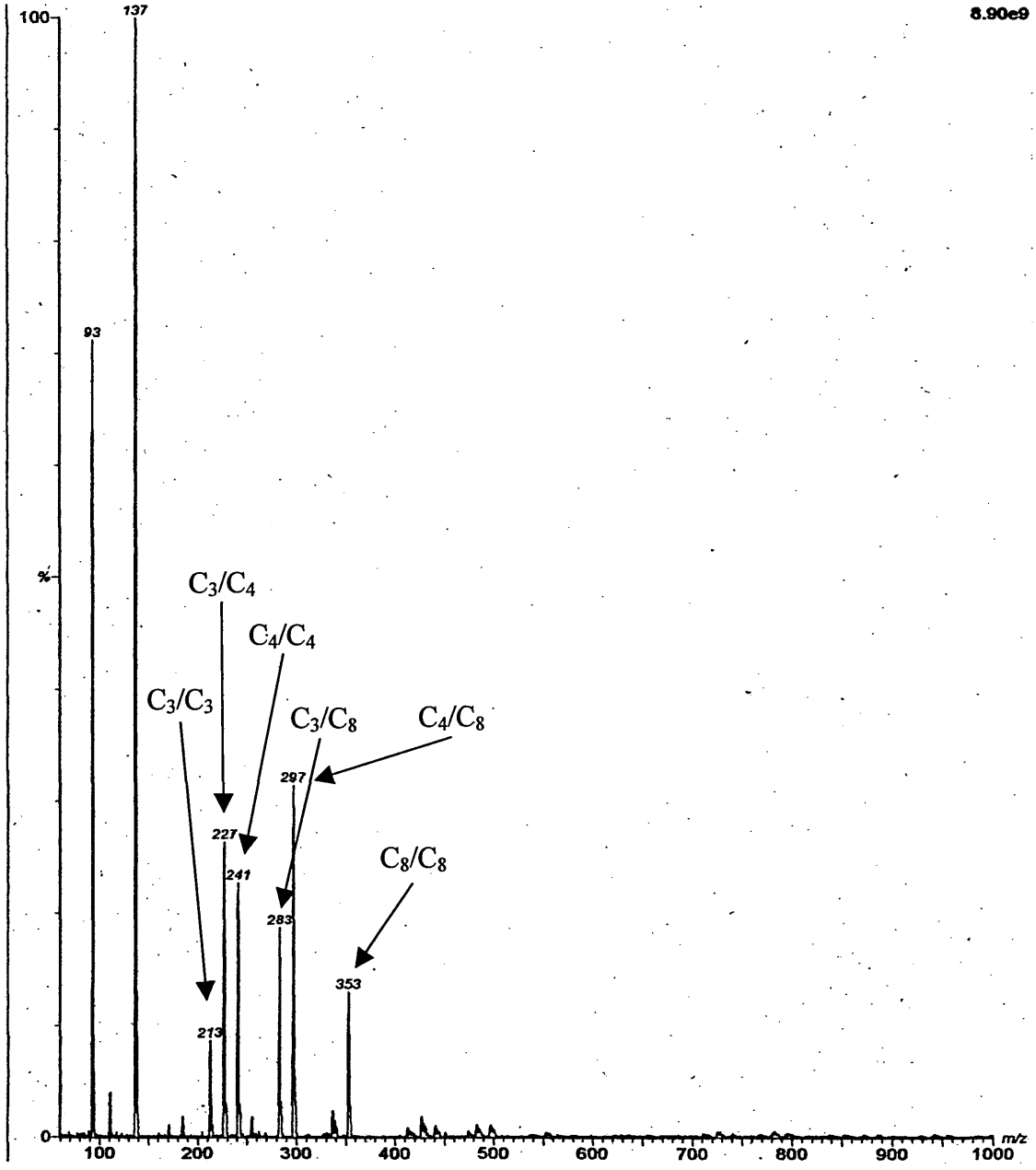

Figure 6.6 Analyte: ZDDP $C_3/C_4/C_8$ with salicylic acid (137). Conditions: ZDDP ($C_3/C_4/C_8$) at a concentration of 1000µg/ml contained within a buffer of 50mM ammonium acetate in methanol. Nebulising gas was set to 40 l hour^{-1} whilst the drying gas was set to 200 l hour^{-1}. Cone voltage was maintained at -30 V while capillary voltage was maintained at -3.0 kV. MCA was used scanning between 60 and 1000 mass units for a total time of 4 minutes.

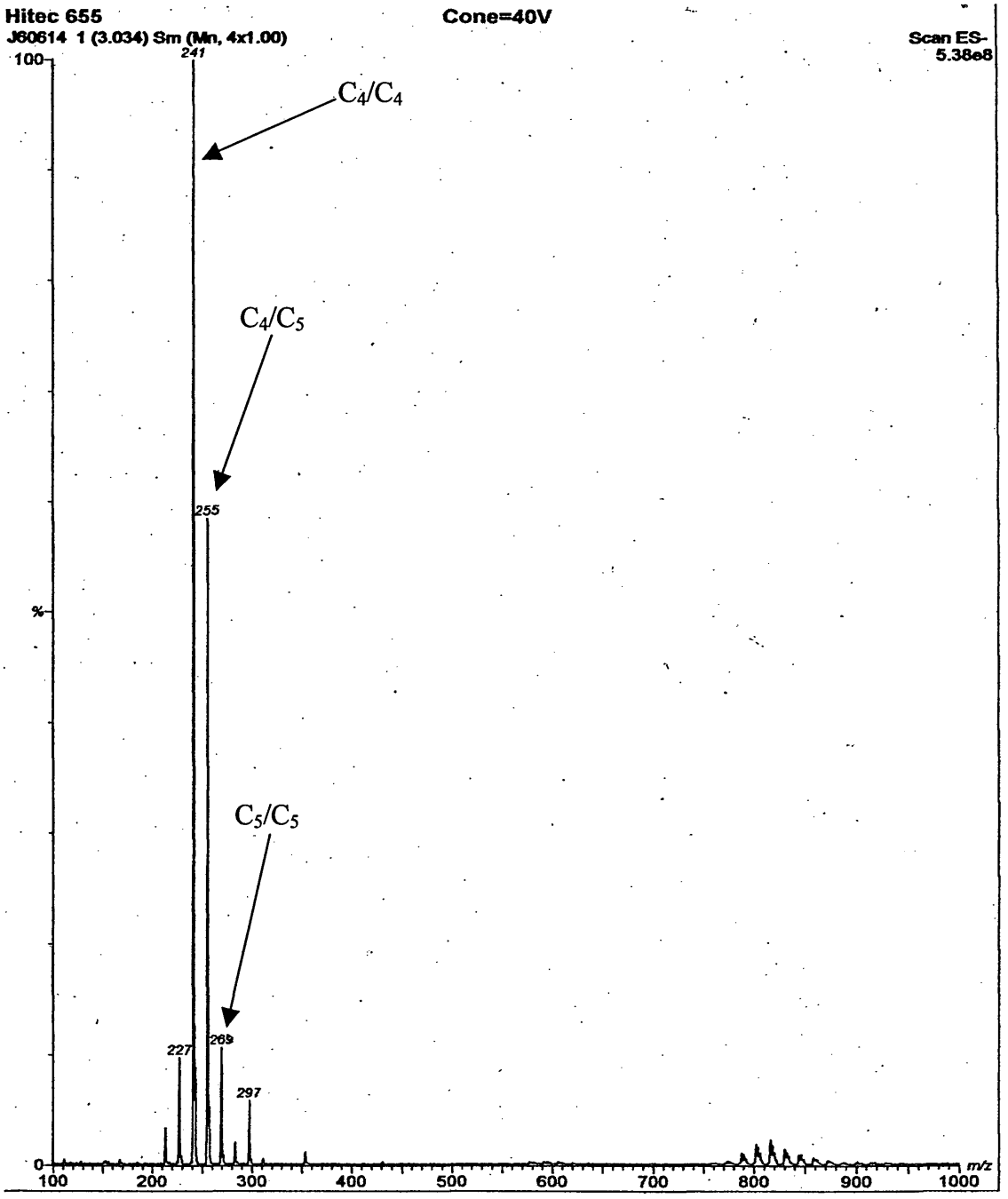

Figure 6.7 Analyte: ZDDP C_4/C_5. Conditions: ZDDP (C_4/C_5) at a concentration of 1000µg/ml contained within a buffer of 50mM ammonium acetate in methanol. Nebulising gas was set to 40 l hour^{-1} whilst the drying gas was set to 200 l hour^{-1}. Cone voltage was maintained at -30 V while capillary voltage was maintained at -3.0kV. MCA was used scanning between 60 and 1000 mass units for a total time of 4 minutes.

6.6 Nonaqueous capillary electrophoresis-mass spectrometry

The interfacing of mass spectrometry and capillary electrophoresis is in its infancy as a technique and is not straightforward. Many problems are faced, especially with obtaining a stable electrospray while maintaining an electric field for the capillary electrophoresis separation.

Initial work centred on the use of a methanol sheath flow with a co-axial flow interface. The major problem encountered was that current in the capillary electrophoresis section could not be maintained. Various problem sources were identified. First was the source temperature; it was thought that, with the sheath flow and separation buffer mobility so low, the buffer was evaporating at the capillary tip. On examination of the separation capillary, bubbles were seen at the capillary tip. The source temperature was decreased from 60°C to 50°C, which increased the stability of the separation current.

Most CE separations when interfaced with mass spectrometry use the separation capillary protruding outside the probe tip, and pressure applied to the NACE separation ensures that flow is continuous so the electrical connection is maintained. However, in this work the samples migrate so close together that separation will not occur because the pressure will cause the peaks to co-migrate. Having the capillary tip protrude from the interface tip could therefore be problematic for electrical connection in NACE separation. It would make sense therefore that, for the separation to occur, the capillary is withdrawn inside the interface to ensure electrical connection.

6.6.1 Capillary Withdrawal

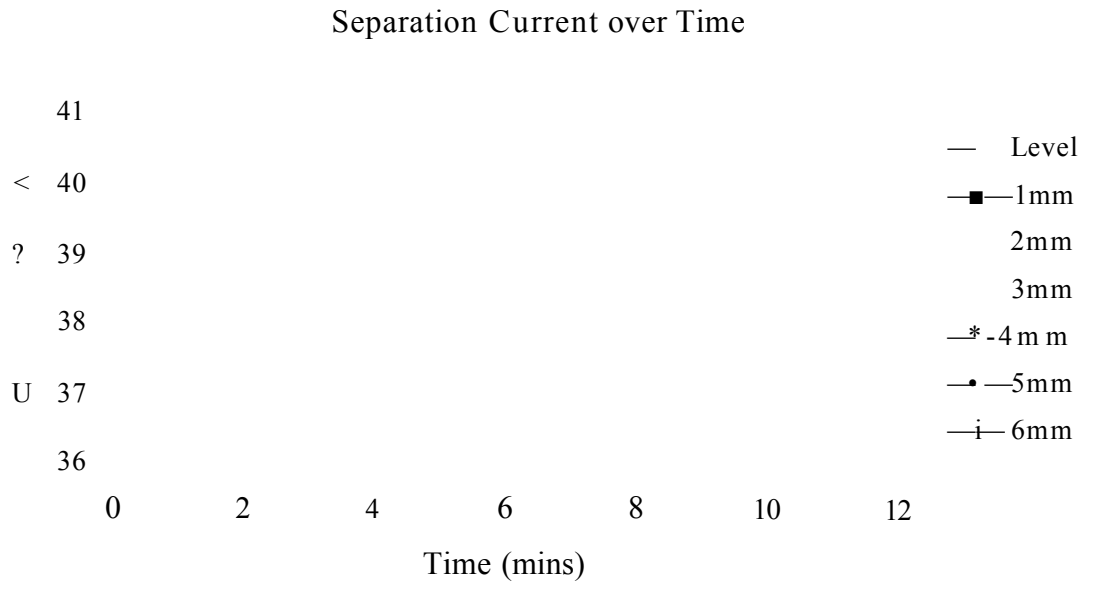

Figure 6.8 The effect of withdrawing the silica capillary tip inside the interface probe on the current in NACE separation (pressurised flow). Conditions: Infusion of a buffer of 50mM ammonium acetate in methanol using electrophoresis at -30kV. Sheath flow methanol. Nebulising gas was set to 40 l hour'1whilst the drying gas was set to 200 l hour'1. Cone voltage was maintained at -30 V while the capillary voltage was maintained at -3.0kV, Source temperature was 50°C. MCA was used scanning between 50 and 70 mass units whilst monitoring the current on the CE for a total time of 10 minutes.

As stated previously, the use of pressure ensures that the electrical connection is maintained by a continuous flow of buffer which allows the separation to occur by NACE (see figure 6.8). However, the separation was ruined by the use of pressure, and, as soon as the pressure was removed, the electrical current in the NACE separation was lost almost immediately. Figure 6.9 shows that pressure could be removed and

electrical current still maintained. Removal of pressure with the separation capillary withdrawn by 6mm gave a current lower than with the use of pressure. The sheath flow consisted of methanol, and the pH* was not adjusted as it did not seem to be important in negative ion formation. Using the buffer used for the separation as the sheath flow, the electrical current was maintained at the level seen with a pressure assisted separation. The increase in current was expected because a sheath flow consisting of methanol could be constantly diluting the separation buffer electrolytes, resulting in a loss of current. Using the buffer as the sheath flow overcame this problem.

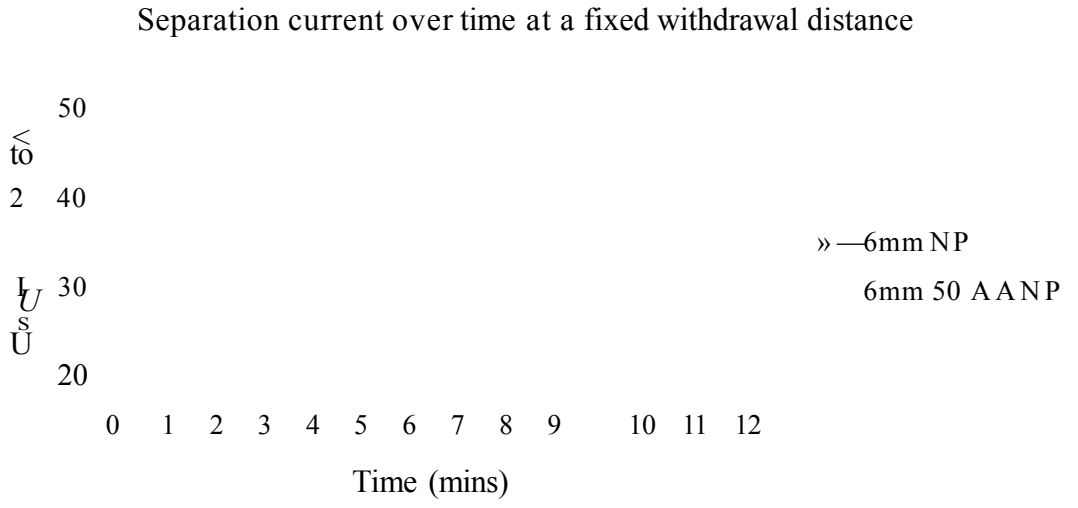

Figure 6.9 The effect of removing the separation pressure (NP no pressure, AA ammonium acetate) and changing the sheath flow constituents on current in NACE separation. Conditions: Infusion of a buffer of 50mM ammonium acetate in methanol by electrophoresis at -30kV. Sheath flow methanol +/- ammonium acetate. Nebulising gas was set to 40 1hour'1whilst the drying gas was set to 200 I hour'1. Cone voltage was maintained at -30 V while the capillary voltage was maintained at -3.0kV, Source temperature was 50°C. MCA was used scanning between 50 and 70 mass units whilst monitoring the current on the CE for a total time of 10 minutes.

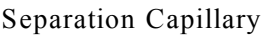

Figure 6.10 Diagrammatic representations to compare the original position of the separation capillary to the improved repositioning, showing the improved electrical connection potential and mixing of the sheath and separation buffers.

6.6.2 Alkylsalicylate

With the separation current being as stable as possible at this time, a separation by NACE was carried out with mass spectrometry detection. However, the analytes of interest were not identified by the mass spectrometer at lOOOpg/ml. Increasing the plug length and concentration did not improve the sensitivity. Keeping the plug length at that for the separation by NACE, a sample was injected and then pushed through the capillary to see if the analytes could be seen on the tuning page. Increasing the pH* using tetramethylammonium hydroxide in the sheath flow did not improve the identification. Reports have suggested that the use of acid within the sheath flow can increase the number of negative ions obtained; the mechanism is not fully understood, but it is thought that alterations in the acid-base equilibrium play a part.

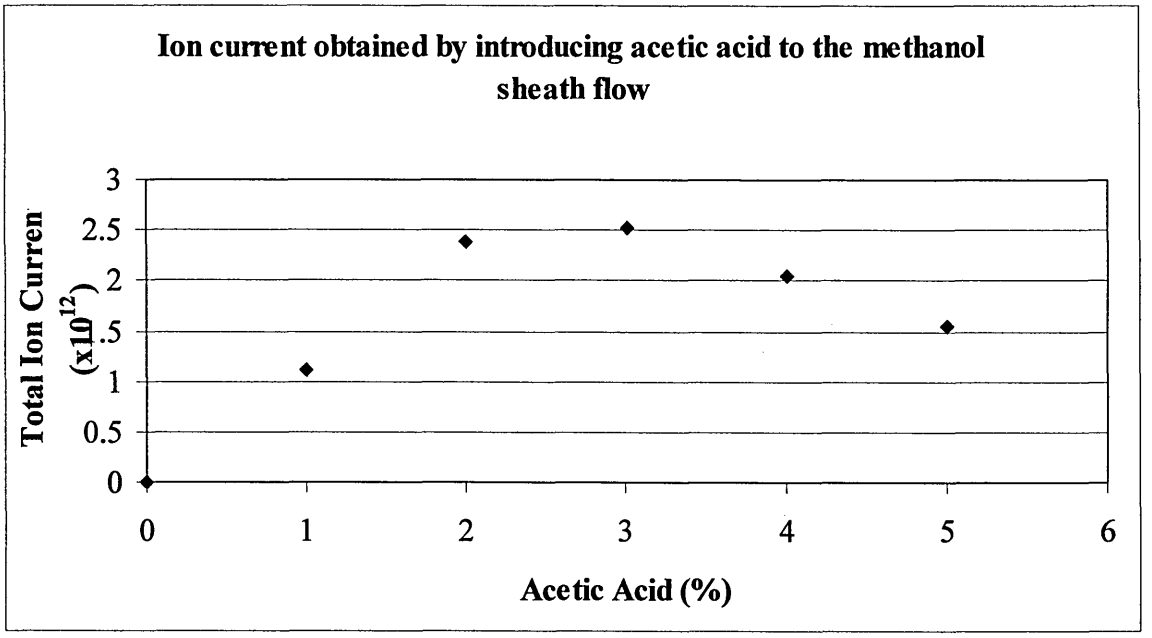

Figure 6.11 The effect of adding acetic acid to the sheath flow on the production of alkylsalicylate negative ions. Conditions: Infusion of a buffer of 50mM ammonium acetate in methanol. Sheath flow 50mM ammonium acetate methanol varied acetic acid (% v/v). Alkylsalicylate injected –5kV for 0.1min at a concentration of 1000µg/ml. Nebulising gas was set to 40 l hour^{-1} whilst the drying gas was set to 200 l hour^{-1}. Cone voltage was maintained at -30 V while the capillary voltage was maintained at -3.0kV, Source temperature was 50°C. Selected ion monitoring set at 333, 361 and 389 mass units.

The addition of acetic acid to the sheath flow and removal of tetramethylammonium hydroxide did drastically improve the formation of alkylsalicylate negative ions (see figure 6.11), so the sheath flow was made up of 50mM ammonium acetate, with 2% acetic acid in methanol. However, analysis still proved unsuccessful when injecting the analyte with pressure in methanol. The only way the separation could be carried out with sample detection was by injecting the 1000µg/ml concentrated sample using a field-amplified injection of –5kV for 0.1min.

The first separation carried out showed no real resolution of the analytes. The CE was then raised in comparison to the mass spectrometer inlet, The effect of this was to speed up the migration rate and reduce the resolution of the separation. The CE was then lowered so the inlet vial buffer was level with the tip of the electrospray probe. This slowed down the separation and some resolution was obtained. The result of the improvements made can be seen in figure 6.12. However, the analyser used in this instrument does have its limitations. The analytes migrate so close together that the only reliable way to detect the analytes is by the use of selected ion monitoring. The use of the scanning mode on the quadrupole analyser was not successful in this case, because in full scan mode the mass of interest is only detected for a small amount of time, and the analyser spends most of its time outside the mass range of interest. This leads to decrease in sensitivity. This can be problematic when analysing formulated oil as the analyte in question will be present in very small quantities. The use of selected ion monitoring will allow detection of the analytes and the possible identification of the manufacturer. Figure 6.12 shows the successful separartion by NACE-MS of Mg alkylsalicylate all three peaks have been identified at 333, 361 and 389 which, correspond to C_{14}, C_{16} and C_{18}. Salicylic acid was identified at 137 mass units.

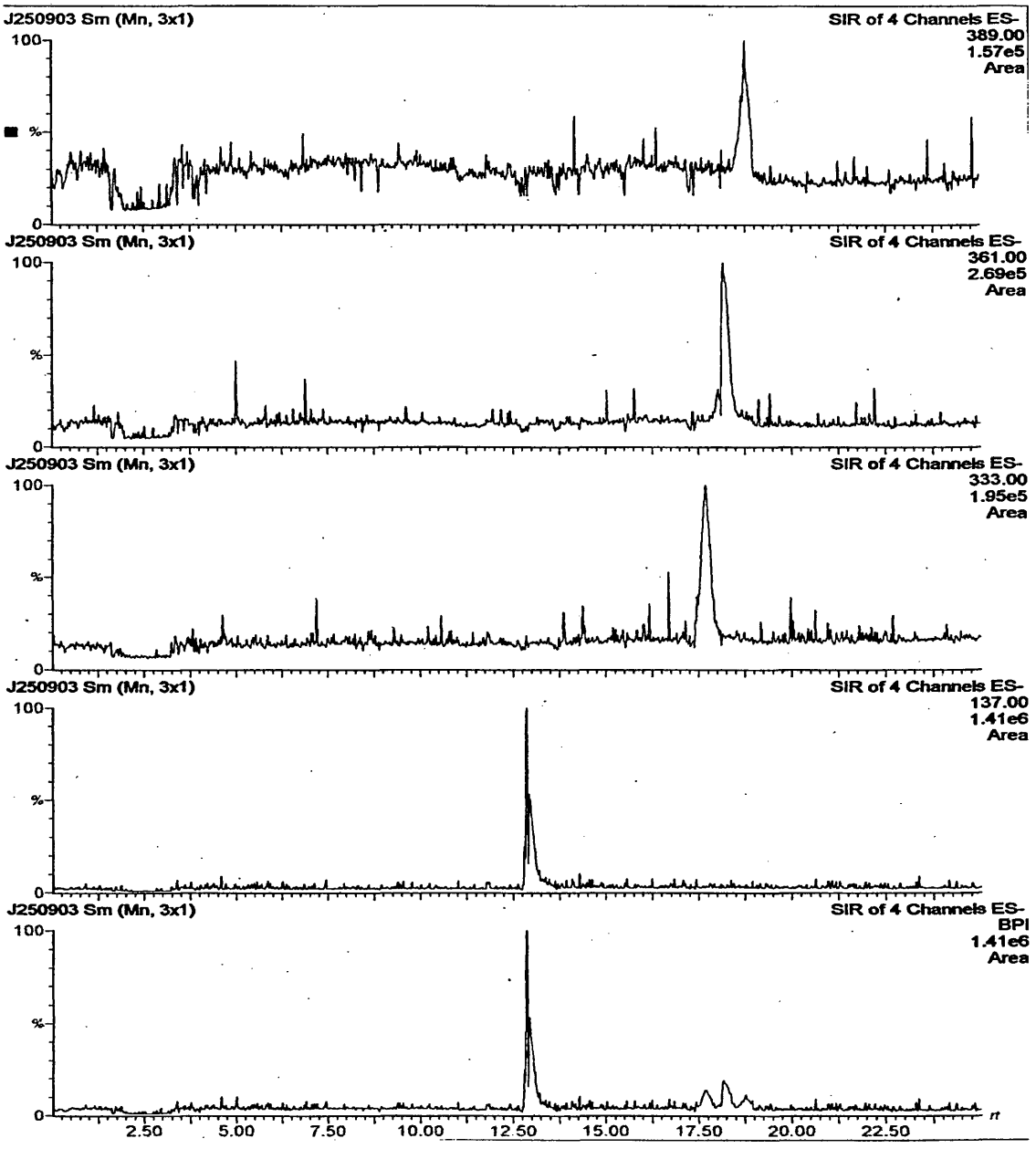

Figure 6.12 NACE-MS selected ion monitoring of Mg alkylsalicylate at m/z 333, 361 and 389. Conditions: NACE buffer 50mM ammonium acetate, methanol pH 9.01* adjusted using tetramethyl ammonium hydroxide. Alkylsalicylate at a concentration of 1000µg/ml in methanol injected at –5.0kV for 0.1 min, separation voltage of –30kV. MS sheath flow 50mM ammonium acetate, methanol 2% acetic acid nebulising gas 40 l hour^{-1}, drying gas 200 l hour^{-1} cone voltage -30v capillary voltage -3.0kV, source temp 50°C Separation capillary withdrawn 6.0mm.

6.6.3 Zinc dialkyldithiophosphate

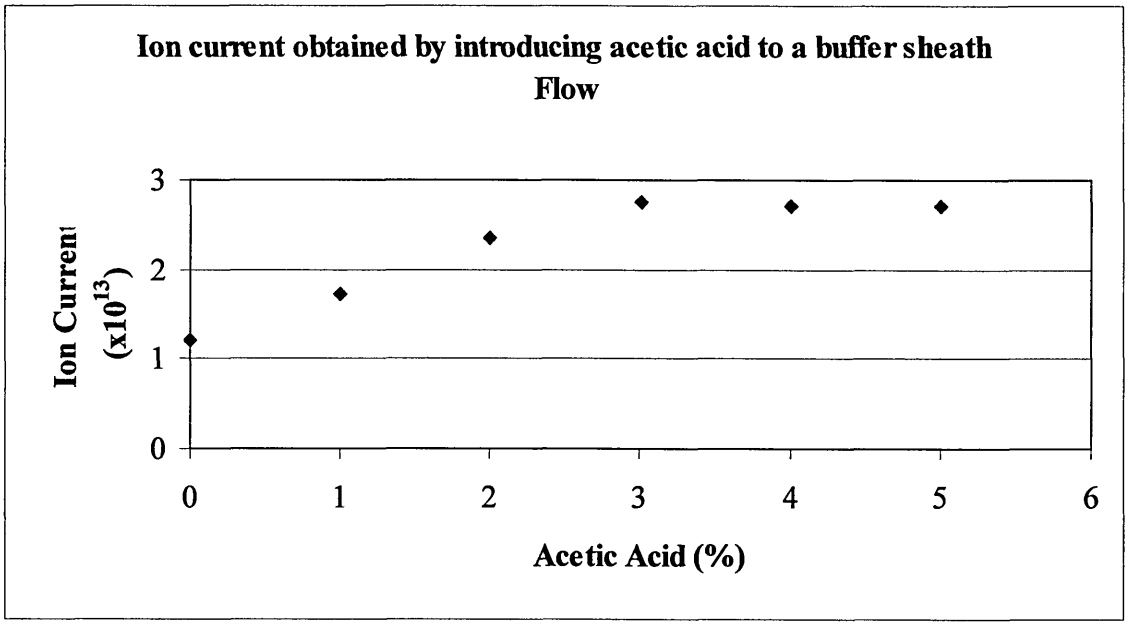

Figure 6.13 The effect of acetic acid on the ion current when used in buffer sheath flow. Conditions: Infusion of a buffer of 25mM ammonium acetate in methanol pH 9.02* adjusted using tetramethylammonium hydroxide. Sheath flow 25mM ammonium acetate methanol varied using acetic acid (% v/v). ZDDP (C_4/C_5) in methanol injected at –5kV for 0.1min at a concentration of 1000µg/ml. Nebulising gas was set to 40 l hour^{-1} whilst the drying gas was set to 200 l hour^{-1}. Cone voltage was maintained at 30 V while the capillary voltage was maintained at 3.0kV, Source temperature was 50°C. Selected ion monitoring was set at 241, 255, 269 mass units.

The detection of ZDDP analytes, as with alkylsalicylates, was not possible without the addition of acetic acid to the sheath flow. The maximum ion current was seen at 3%, and above. However, 2% acetic acid was used, since this would allow the identification of both ZDDPs and alkylsalicylates in one single run for future analysis of formulated lubricants.

The experimental conditions developed for alkylsalicylates were used for identification of ZDDP. The inlet buffer was level with the electrospray probe, field amplified injections were used (-5kV for 0.1min), and the sheath flow was 25mM ammonium acetate and 2% acetic acid in methanol. Separation was carried out in a 25mM ammonium acetate in methanol with pH* adjusted to 9. The standard used for this analysis was a C_4/C_5 mixture, which had proved just as difficult to separate as the $C_3/C_4/C_8$ mixture. Figure 6.14 shows the results of the successful separation with mass detection. Mass units were identified at 241, 255 and 269 which correspond to C_4/C_4, C_4/C_5 and C_5/C_5 respectively. The separation was not as good as with uv detection, which was also the case for the alkylsalicylates. The presence of the sheath flow also reduced sensitivity as it diluted the analyte and may have caused zone broadening, with reduction in the separation. However, each component could be distinguished by a combination of retention time and selected ion monitoring.

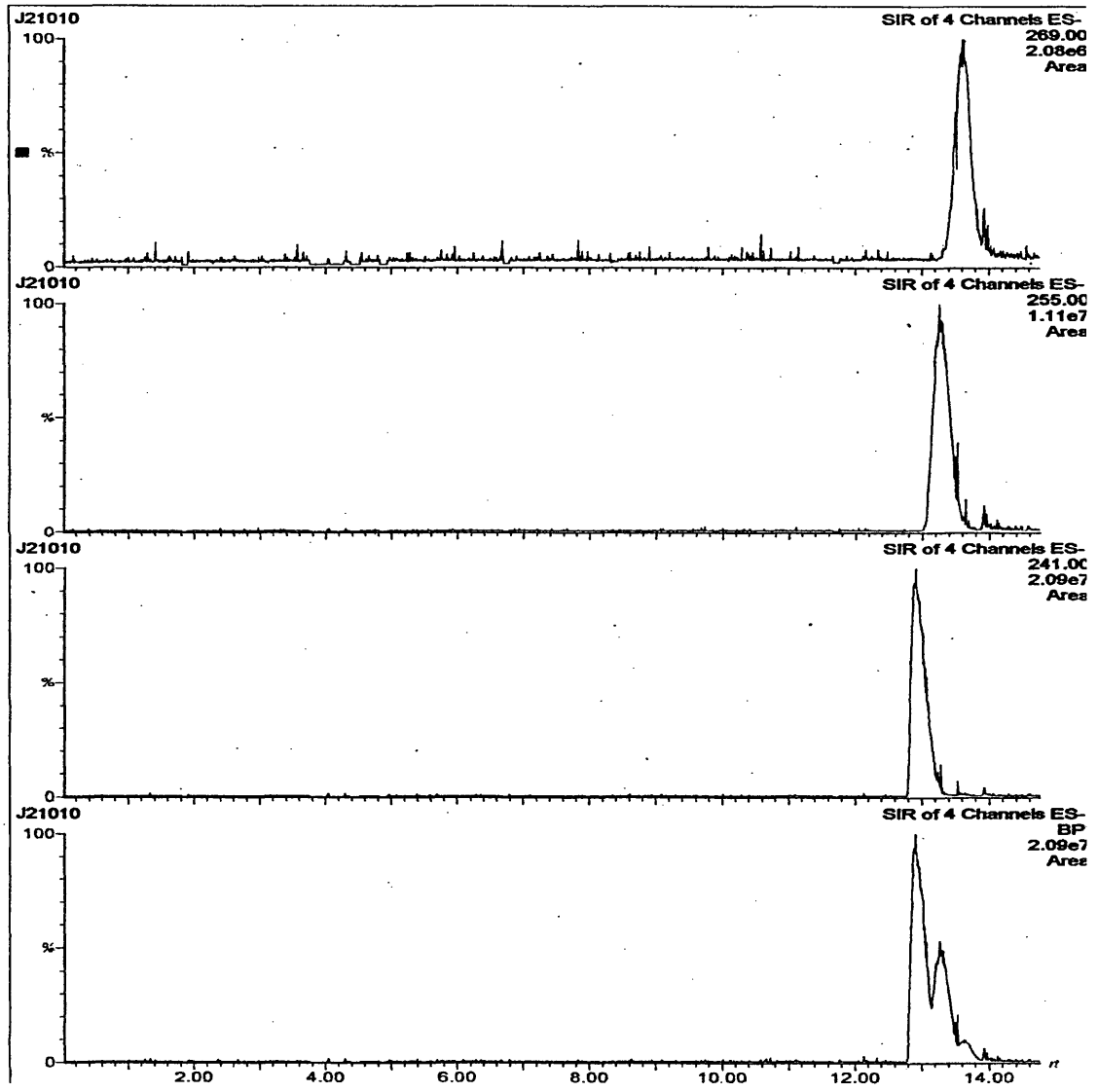

Figure 6.14 NACE-MS selected ion monitoring of a ZDDP at m/z 241, 255 and 269. Conditions: NACE buffer 50mM ammonium acetate, methanol pH 9.01* adjusted using tetramethyl ammonium hydroxide. ZDDP (C_4/C_5) at a concentration of 1000µg/ml in methanol injected at –5.0kV for 0.1 min, separation voltage of –30kV. MS sheath flow 50mM ammonium acetate, methanol 2% acetic acid nebulising gas 40 l hour^{-1}, drying gas 200 l hour^{-1} cone voltage -30v capillary voltage -3.0kV, source temp 50°C Separation capillary withdrawn 6.0mm.

6.7 Conclusion

Direct infusion was used to identify masses present in the additive under analysis for NACE-MS. Direct infusion was seen to be a very successful way of identifying additives, the use of ion scan allowing a mass range to be used that could effectively analyse formulated oils quickly and efficiently. Unlike work carried out by Cardwell *et. al.*[1] the method developed here required no addition of dithiophosphate ions or dimethylsulphoxide to produce the molecular ion.

Most work to date for CE-MS and NACE-MS has reported that the separation capillary should protrude from or be level with the electrospray needle tip. In this work, the separation capillary needed to be withdrawn from the electrospray tip for several reasons: it improved the electrical connection for the separation, it allowed the removal of supplementary pressure which stopped any separation, and it reduced further the chance of bubble formation at the end of the separation capillary tip by continual submersion in buffer.

MS sensitivity was limited, and full ion scan mode for mass detection was only possible with direct infusion of the analytes. NACE-MS was only possible in selected ion mode.

Although Beechi *et. al.*[2] determined the structure of ZDDP by gas chromatography-mass spectrometry (GC-MS) and achieved identification of ZDDP. No molecular ions were seen-only fragments from the electron ionisation process. The use of gas chromatography required derivatization of ZDDPs to render them volatile enough for separation by gas chromatography, a complex and potentially unreliable process.

The separation seen by NACE-MS is adequate and does not require any derivatization. Separation times were quicker and the molecular ions for individual ligands were always seen, so NACE-MS clearly offers advantages over GC-MS for analysis of oil additives.

References

1. Cardwell, T.J., Colton, R., Lambropoulos, N., Traeger, J.C., Marriott, P.J., Analytica Chimica Acta 1993, **280**, 239-244.

2. Beechi, M., Perret, F., Carraze, B., Beziau, J.F., Michel, J.P., Journal of Chromatography A 2001, **905**, 207-222.

7.1 Introduction

The combustion of air and fuel mixtures within internal combustion engines leads to the production of waste products. These products are a direct result of oxidation. The combustion cycles of diesel and petrol driven engines are slightly different. In a petrol engine the fuel and air mix is ignited by sparks from a spark plug, while diesel engines work by introducing air into the combustion chamber compressing it, with increase in temperature, then injecting the fuel with spontaneous combustion.

The combustion cylinders are coated in lubricant oil to ensure smooth running of the pistons and piston rings prevent lubricant getting into the combustion area. However after time the rings wear and combustion of oil occurs. The products can then run into the sump where the oil, with contaminants, is recycled and further contamination occurs.

In both cases the by-products are similar- water, carbon monoxide, carbon dioxide, hydrogen, nitrogen oxides, volatile organic compounds, mineral and organic acids.

Sulphur trioxide and nitrogen oxides in the presence of water produce sulphuric and nitric acids, which increase engine wear.

Formulated oil products are a mixture of base oil and an additive package. The additive package is a mixture of compounds that improve the working capabilities and extend the life expectancy of the oil.

During analysis a solid phase extraction (SPE) clean up process was used to remove the base oil. However, individual additives eluted from the solid phase extraction cartridge at all stages. Thus when evaluating the oil, the additives analysed were the ones that eluted at individual stages, not the whole additive package. As well as this, several additives may elute within a single phase of the clean up process, leading to the presence of unidentifiable peaks. In addition, due to the low quantities of each individual additive, some may not have been detected. Interactions between additives in formulated oil might also have complicated the identification process.

In order to analyse formulated oils, slight modifications were required in the clean up process. The amount of formulated oil used in sample preparation and clean up was increased to 40g. As the concentrations of analytes within the oils were unknown and also as the amount of various additives was unknown, high initial amounts were utilised.

7.2 Reagents and Chemical

See section 4a, five samples were analysed: three new oils and two used oils.

A0573A/001A/02 and A0573A/002A/02 are new formulated oils designed for use with petrol driven engines. A0573A/007A/02 is a used formulated oil, its usage has been 1000 hours running time.

T45767/00 a fully formulated oil designed for use within a diesel engine. Likewise T45523/01 is a used fully formulated oil designed for diesel engines with approximately 1000 hours running time.

7.3. Instrumentation

See section 4b

7.4. Procedures

See section 4c

7.5 Results and Discussion

7.5.1 Nonaqueous capillary electrophoresis-ultraviolet absorbance detection

The solid phase extraction method was carried out as previously stated, though with 40g samples of formulated oil instead of the 3g sample used for the known samples. One important note is that the analytes were collected from the 2-butanone and methanol fractions. The 2-butanone was collected as some of the ZDDP analytes were known to elute in this media.

The 'blind' analysis of several formulated oils showed uv spectra with multiple peaks. The peak patterns and migration ratios were used to identify the relevant analytes that the methods had been developed for. Only one method was used for the detection of both types of analyte (50mM ammonium acetate buffer) as it is able to separate both ZDDP and alkylsalicylates. The 25mM ammonium acetate buffer was not capable of separating the alkylsalicylates and was not used.

7.5.1.1. Unused Formulated Oil

In figures 7.1 and 7.2, both electropherograms show similar trends. Initially the sample was injected at a concentration of 1000μg/ml. However, it was not possible to ensure that all analytes were being detected due to individual concentrations being unknown and since patterns and migration ratios are used for identification, the analysis was

carried out with initial concentrations of 2000μg/ml. The separation was slightly worse but all analytes were detected.

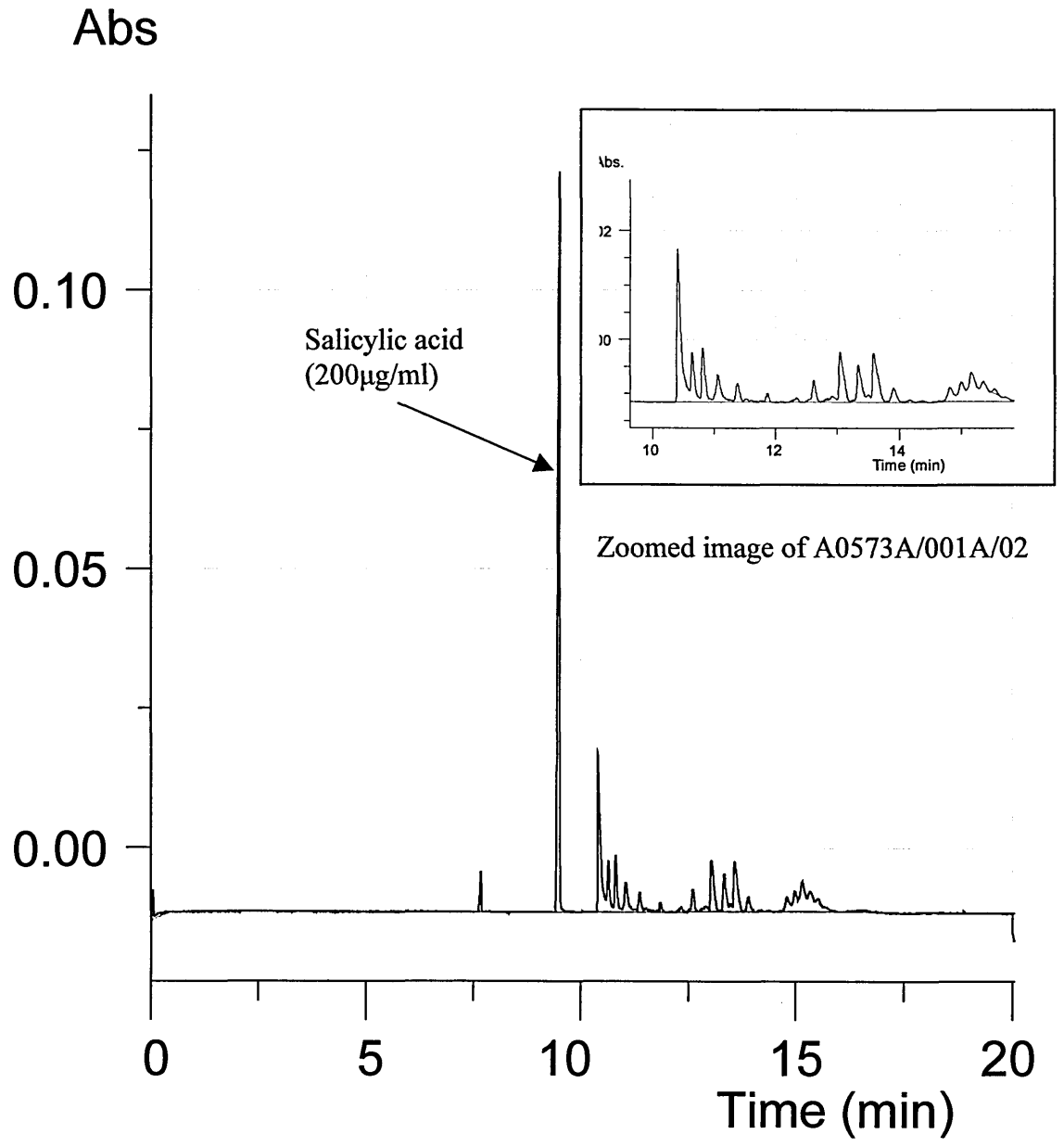

Figure 7.1. The analysis of A0573A/001A/02 by NACE with uv absorbance detection of 210nm. Base oil was removed by solid phase extraction. Separation buffer was 50mM ammonium acetate with 0.025mM HDB in methanol pH 9.03*, adjusted using tetramethylammonium hydroxide. Capillary length 95/80cm; injection 20mbar 0.2min, sample concentration of 2000µg/ml in methanol and separation voltage of –30kV.

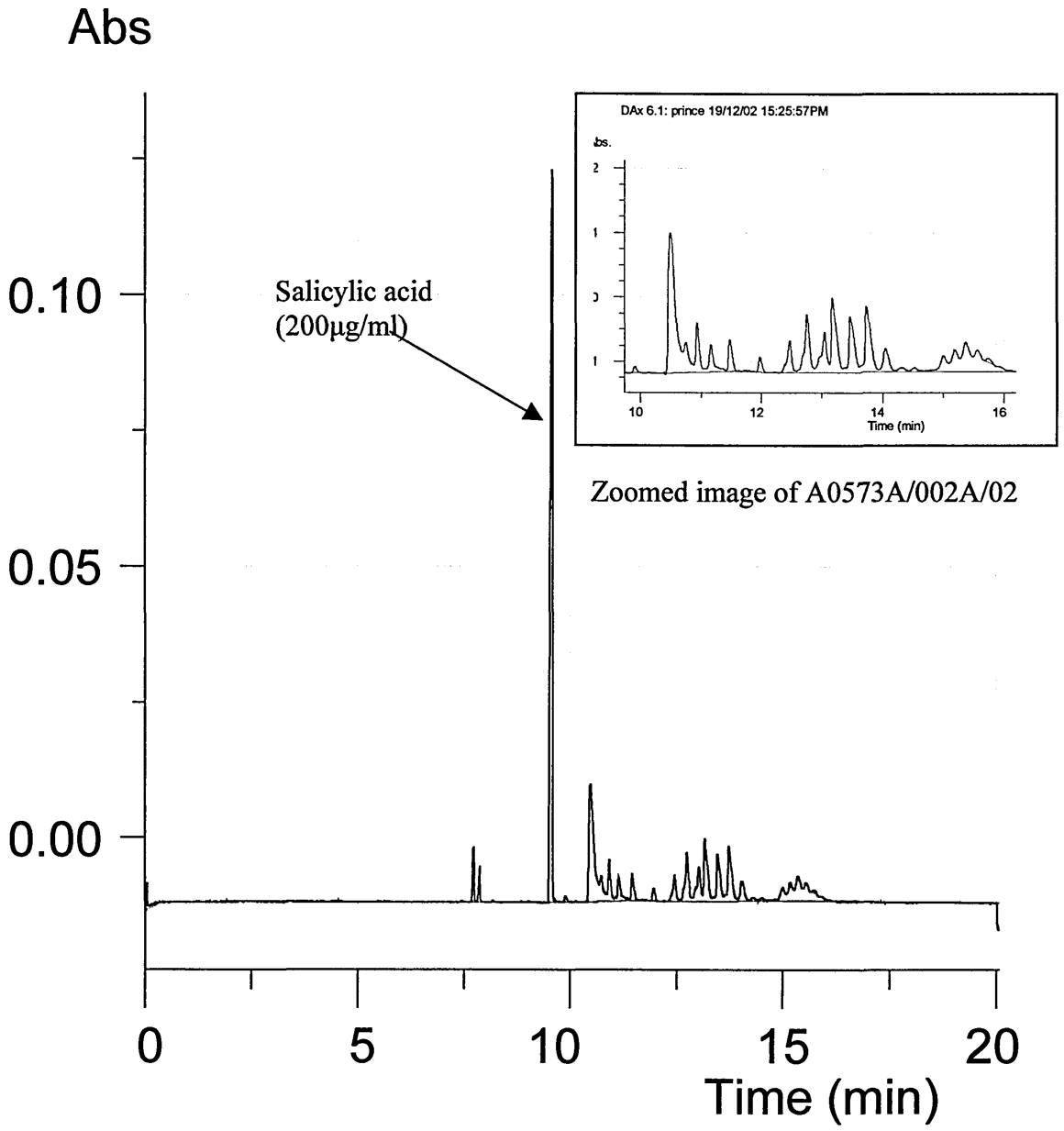

Figure 7.2. The analysis of A0573A/002A/02, by NACE with uv absorbance detection of 210nm. Base oil was removed by solid phase extraction. Separation buffer was 50mM ammonium acetate with 0.025mM HDB in methanol pH 9.03*, adjusted using tetramethylammonium hydroxide. Capillary length 95/80cm; injection 20mbar 0.2min, sample concentration of 2000µg/ml in methanol and separation voltage of –30kV.

Both electropherograms can be roughly split into three windows and are depicted in the tables below.

Peak Time (mins)	Migration Ratio (±0.01)	Possible Identification
10.485	1.09	C_3/C_3
10.742	1.12	C_4/C_4
10.928	1.14	C_3/C_6
11.158	1.16	C_4/C_7
11.468	1.20	C_6/C_6
11.973	1.25	C_7/C_7

Table 7.3 Showing possible identification of ZDDP in accordance with migration ratios in sample A0573A/001A/02.

Peak Time	Migration Ratio (±0.01)	Possible Identification
12.467	1.30	C_{14}
12.755	1.33	C_{16}
13.040	1.36	C_{18}
13.173	1.38	C_{20}
13.472	1.41	C_{22}
13.732	1.43	C_{24}
14.048	1.47	C_{26}

Table 7.4 Showing possible identification of alkylsalicylate in accordance with migration ratios in sample A0573A/001A/02.

Peak Time	Migration Ratio (±0.01)	Possible Identification
15.005	1.57	
15.185	1.59	
15.373	1.61	
15.545	1.62	
15.738	1.64	

Table 7.5 Showing unknown analytes in sample A0573A/001A/02.

Peak Time (mins)	Migration Ratio (±0.01)	Possible Identification
10.405	1.09	C_3/C_3
10.642	1.12	C_4/C_4
10.815	1.14	C_3/C_6
11.055	1.16	C_4/C_7
11.373	1.20	C_6/C_6
11.867	1.25	C_7/C_7

Table 7.6 Showing possible identification of ZDDP in accordance with migration ratios in sample A0573A/002A/02.

Peak Time	Migration Ratio (±0.01)	Possible Identification
12.345	1.30	C_{14}
12.613	1.33	C_{16}
12.905	1.36	C_{18}
13.045	1.37	C_{20}
13.342	1.40	C_{22}
13.587	1.43	C_{24}
13.905	1.46	C_{26}

Table 7.7 Showing possible identification of alkylsalicylate in accordance with migration ratios in sample A0573A/002A/02.

Peak Time	Migration Ratio (±0.01)	Possible Identification
14.813	1.57	
14.995	1.58	
15.162	1.60	
15.350	1.62	
15.530	1.64	

Table 7.8 Showing unknown analytes in sample A0573A/002A/02.

The analysis of A0573A/001A/02 (Figure 7.1) and A0573A/002A/02 (Figure 7.2), by NACE with uv absorption detection showed that their formulations may contain the same ingredients, although the components may differ in concentration. The identifications were carried out by using the migration ratio of the peaks to that of salicylic acid (tables 7.3-7.8). It seems that two mixtures of ZDDP are present, C_3/C_6 and C_4/C_7. The migration ratios were similar for individual ZDDPs although there could be other analytes present with similar migration ratios, but mass spectrometry can be used to resolve the issue. The salicylates present seemed to be similar to several standards, SR 404, 1231, 1027 and 862. However, other additives such as alkylphenates could migrate in the same window. This peak pattern is seen clearly in figure 7.2, with probable alkylsalicylate peaks at 12.467, 12.755 and 13.040mins. However, the peak patterns following these had not been seen previously, so mass spectrometry was needed to provide information about their identities.

Further analysis, specifically for ZDDPs, required alteration of the detection wavelength to 230nm, at which the presence of ZDDP should show by an increase in peak intensity. However, the peaks in this case did not show any such increase, but

instead a decrease in intensity was seen. Again the use of mass spectrometry might provide conclusive evidence, but this was complicated by not knowing exactly what additives were present in the oils.

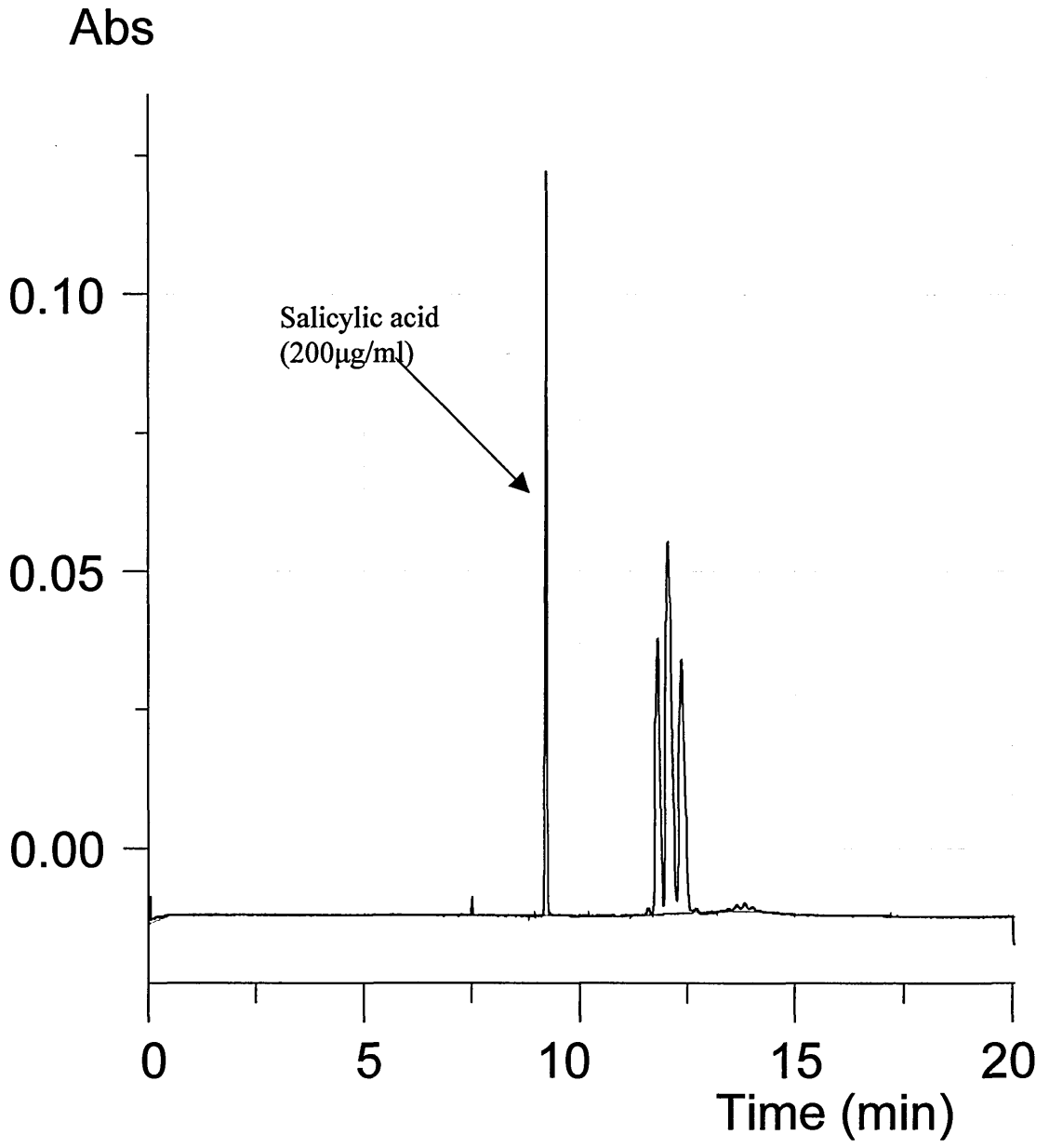

Figure 7.9. The analysis of T45767/00 by NACE with uv absorbance detection at 210nm. Base oil was removed by solid phase extraction. Separation buffer was 50mM ammonium acetate with 0.025mM HDB in methanol pH 9.03*, adjusted using tetramethylammonium hydroxide. Capillary length 95/80cm; injection 20mbar 0.2min, sample concentration of 500µg/ml in methanol and separation voltage of –30kV.

Peak Time	Migration Ratio (±0.01)	Possible Identification
12.173	1.29	C_{14}
12.450	1.32	C_{16}
12.762	1.35	C_{18}

Table 7.10 Showing unknown analytes in sample T45767/00.

The analysis of T45767/00 at a total concentration of 500 µg/ml is shown in figure 7.10, in which three peaks are identified. These were also seen in the previous two formulations analysed, although in smaller concentrations. The peaks are tentatively attributed to alkylsalicylates from the migration times and the peak pattern, with ligands of C_{14} to C_{18}.

7.5.1.2 Used Formulated Oil

The used formulated oil A0573A/007A/02, shows a very altered pattern (Figure 7.13). The peaks seem to be smeared together in a large group, also several peaks that are not present in the unused oils have appeared next to the salicylic acid peak. The peak that appears before the salicylic acid peak in all traces has increased in area, although this is yet to be identified. Some discrimination is required to determine which are real peaks and which are noise. The table below shows the attempts at identification.

Peak Time	**Migration Ratio (±0.01)**	**Possible Identification**
9.738	1.01	
9.883	1.03	
10.007	1.04	
11.243	1.17	
11.622	1.21	
12.113	1.26	
12.452	1.30	C_{14}
12.720	1.33	C_{16}
13.127	1.37	C_{20}
13.312	1.39	C_{22}
13.573	1.42	C_{24}
13.900	1.45	C_{26}
14.238	1.48	C_{28}
15.453	1.61	

Table 7.11 Showing possible peak identification of A0573A/007A/02 using migration ratio with reference to salicylic acid.

Identification is not easy, as most of the peak pattern similarities in the electropherogram of the fresh oil are not seen in that of the used oil. The ZDDP compounds seem to have disappeared. A large volume of oil product remained in the beaker after the extraction and clean up process, which may have caused loss in

sensitivity and more interference. Unidentifiable peaks would be expected to be present, and some of the analytes or their degradation products may have remained in the oil phase after SPE.

Peak Time	**Migration Ratio (±0.01)**	**Possible Identification**
12.173	1.29	C_{14}
12.450	1.32	C_{16}
12.762	1.35	C_{18}

Table 7.12 Showing unknown analytes in sample T45523/01.

Figure 7.14 shows the electropherogram obtained from sample T45523/01 at 500µg/ml, the pattern seen being identical to that of the unused oil (T45767/00). However, the peaks are smaller in area and intensity. Although the method is not quantitative this suggests that the additive is being exhausted through the use of the lubricant

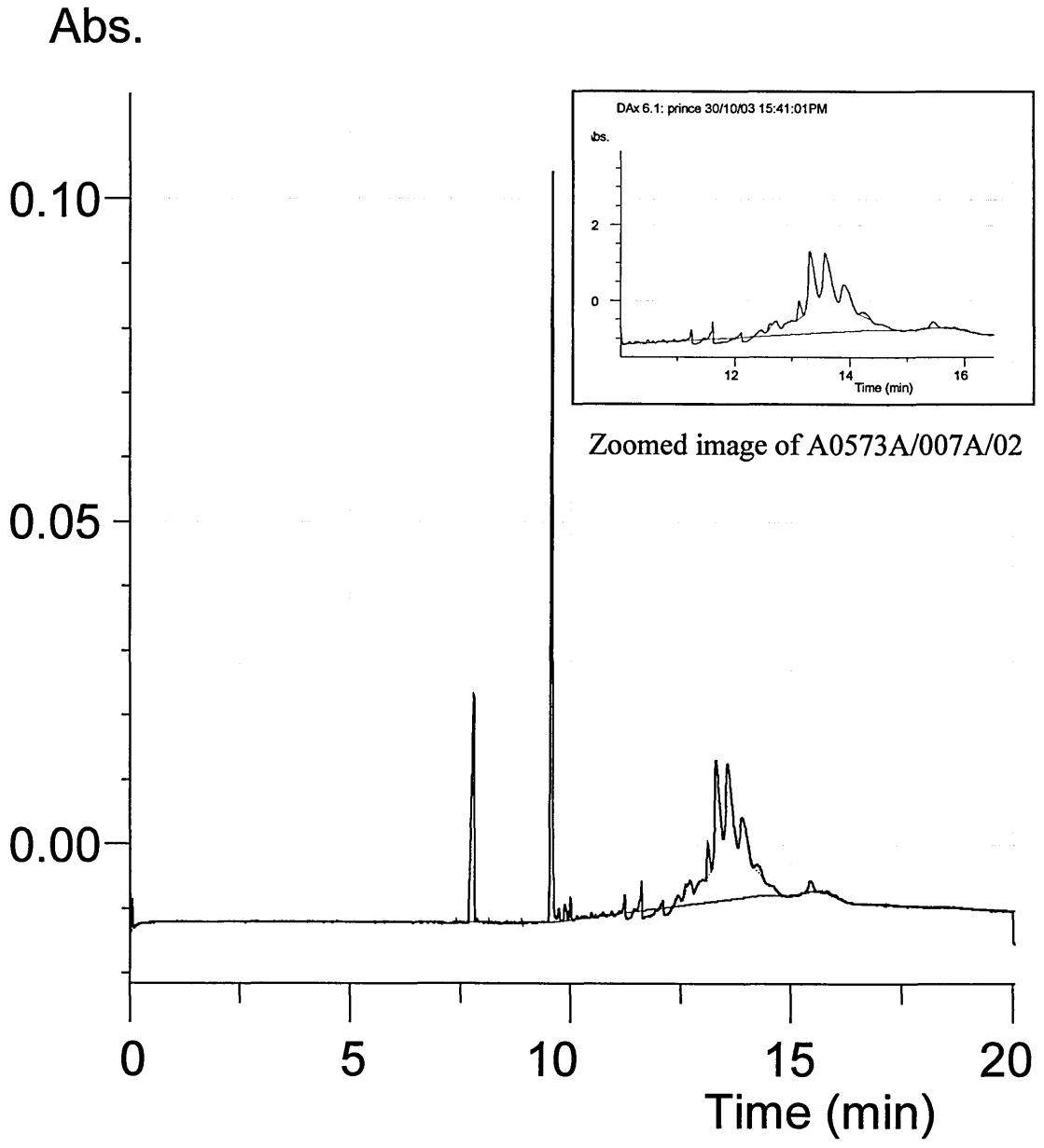

Figure 7.13. The analysis of A0573A/007A/02 by NACE with uv absorbance detection at 210nm. Base oil was removed by solid phase extraction. Separation buffer was 50mM ammonium acetate with 0.025mM HDB in methanol pH 9.03*, adjusted using tetramethylammonium hydroxide. Capillary length 95/80cm; injection 20mbar 0.2min, sample concentration of 2000µg/ml in methanol and separation voltage of –30kV.

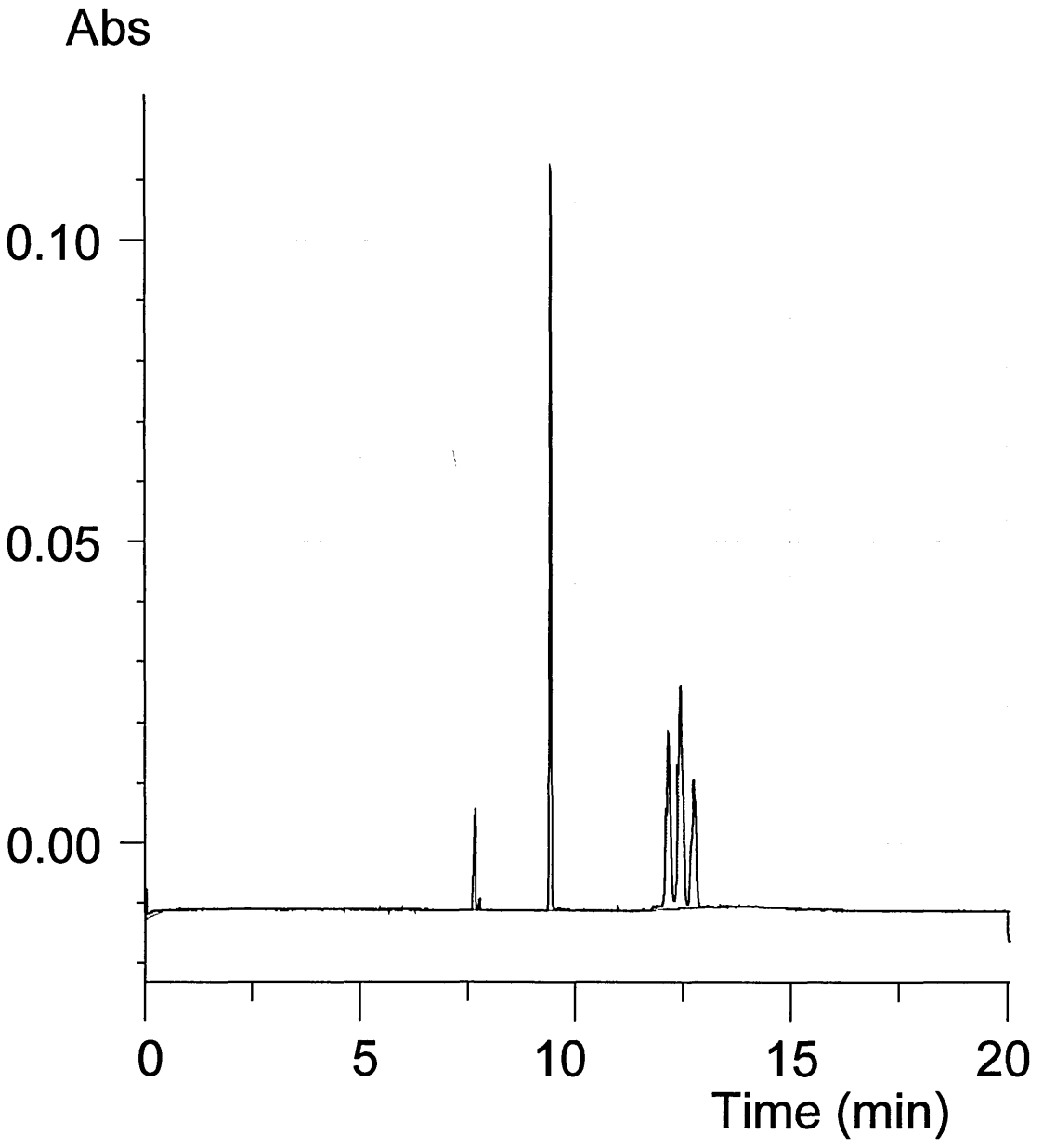

Figure 7.14. The analysis of T45523/01 by NACE with uv absorbance detection at 210nm. Base oil removed by solid phase extraction. Separation buffer of 50mM ammonium acetate with 0.025mM HDB in methanol pH 9.03*, adjusted using tetramethylammonium hydroxide. Capillary length 95/80cm; injection 20mbar 0.2min, sample concentration of 500µg/ml in methanol and separation voltage of –30kV.

7.5.2 Direct Infusion mass spectrometry

7.5.2.1 Unused formulated oil

Mass spectrometry led to slightly different conclusions than NACE-uv for the samples A0573A/001A/02 and A0573A/002A/02 (Figures 7.16 and 7.17). There is some agreement in that ions from a ZDDP is indicated by mass, probably a C_3/C_6 mixture with masses corresponding to 213 (C_3/C_3), 255 (C_3/C_6) and 297 (C_6/C_6). There are some differences in their individual concentrations as an increase in ion abundance is apparent in A0573A/001A/02 compared to A0573A/002A/02.

Other peaks are seen at masses 197 (C_3/C_3), 239 (C_3/C_6) and 281 (C_6/C_6); these peaks have been identified as possible products of ZDDP oxidation. The mass differences between the original peaks and these new peaks is 16 mass units, suggesting replacement of sulphur by oxygen to form thiophosphates (Figure 7.15)[1,2,3,4]. As the lubricant is unused these results could suggest that oxidation has occurred whilst in storage.

Original Compound	Degradation Compound
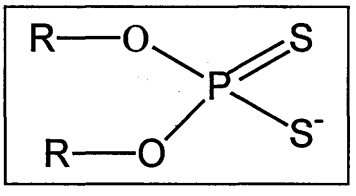	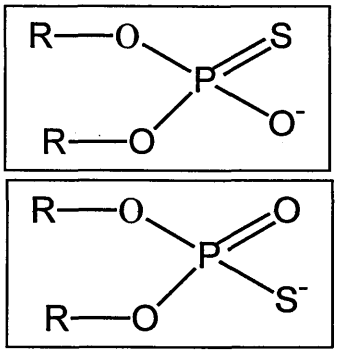

Figure 7.15 Possible structures for the unknown peaks (R= alkyl chains C_3/C_6)

The mass spectrum does not identify alkylsalicylates in negative ion mode for samples A0573A/001A/02 and A0573A/002A/02.

Analysis of T45767/00 (Figure 7.18) using mass spectrometry, as expected from the uv electropherogram, shows the presence of alkylsalicylates with alkyl chains corresponding to C_{14}, C_{16} and C_{18}. No other masses of relevance were detected in this formulated oil.

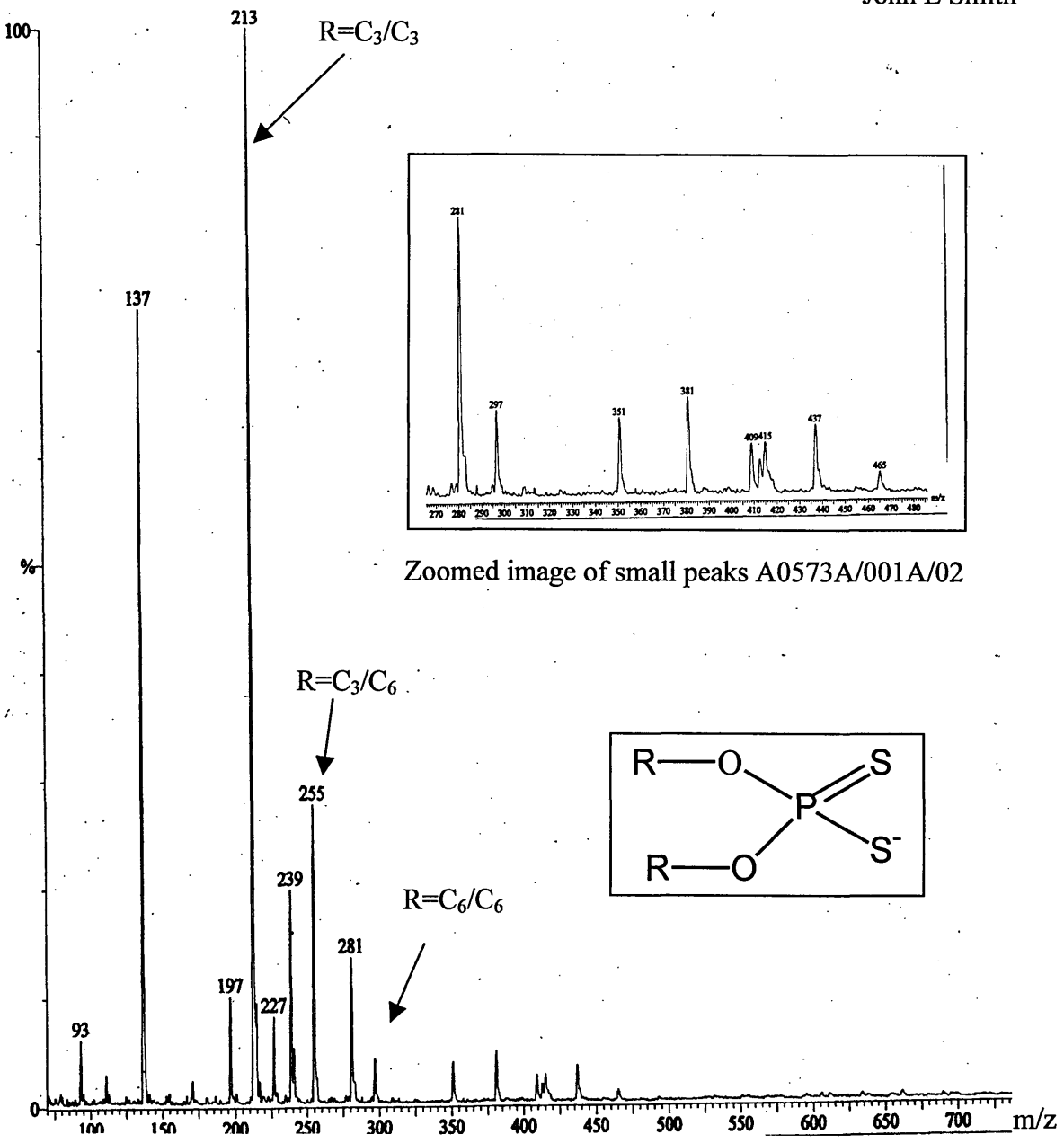

Figure 7.16 Mass spectrum of sample A0573A/001A/02 by direct infusion in negative ion mode. Base oil was removed by solid phase extraction. Sample concentration of 2000µg/ml contained within a buffer of 50mM ammonium acetate in methanol. Nebulising gas was set to 40 l hour^{-1} whilst the drying gas was set to 200 l hour^{-1}. Cone voltage was maintained at -30 V while capillary voltage was maintained at -3.0kV. MCA was used scanning between 60 and 1000 mass units for a total time of 4 minutes.

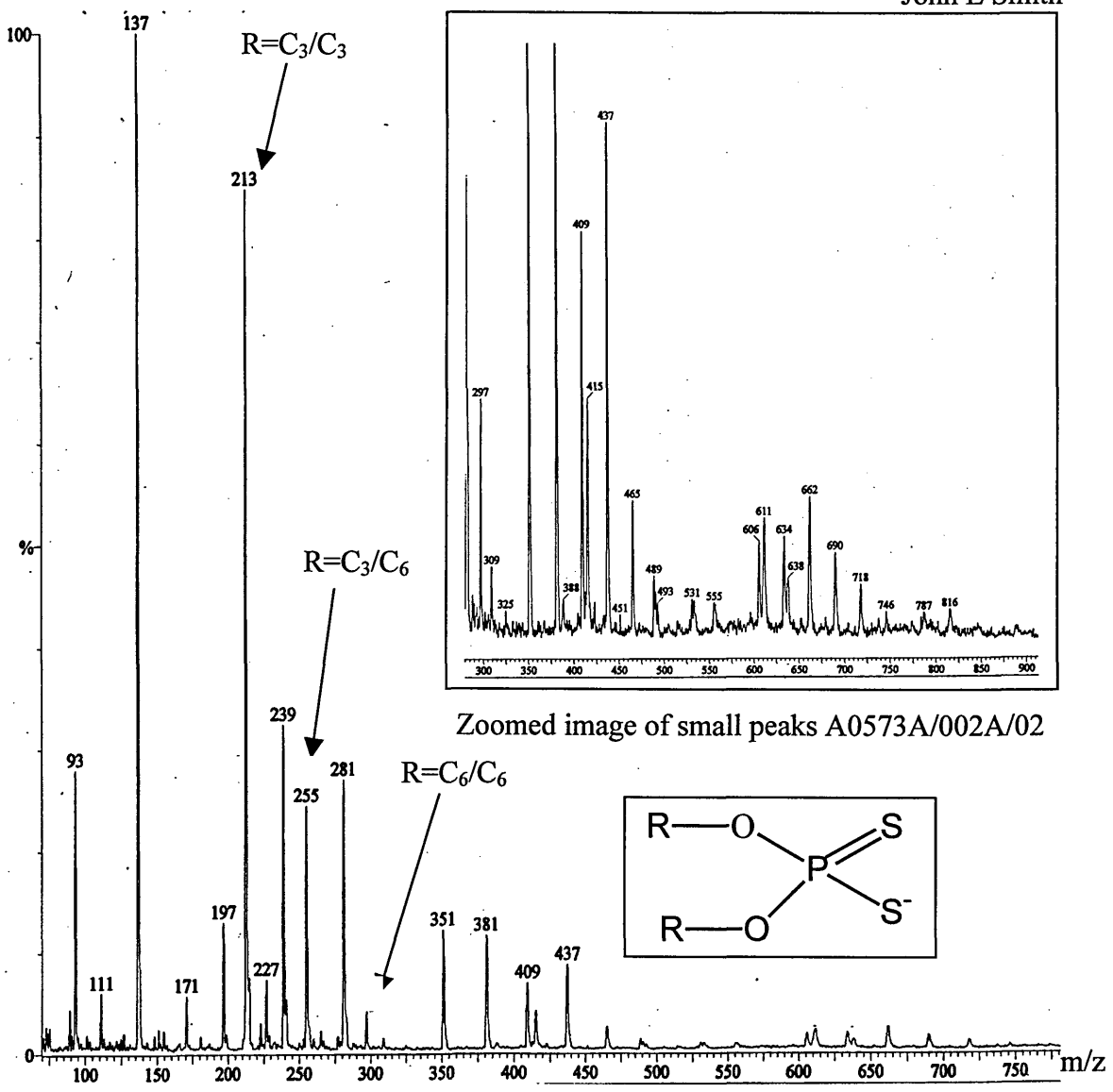

Figure 7.17 Mass spectrum of sample A0573A/002A/02 by direct infusion in negative ion mode. Base oil was removed by solid phase extraction. Sample concentration of 2000µg/ml contained within a buffer of 50mM ammonium acetate in methanol. Nebulising gas was set to 40 l hour^{-1} whilst the drying gas was set to 200 l hour^{-1}. Cone voltage was maintained at -30 V while capillary voltage was maintained at -3.0kV. MCA was used scanning between 60 and 1000 mass units for a total time of 4 minutes.

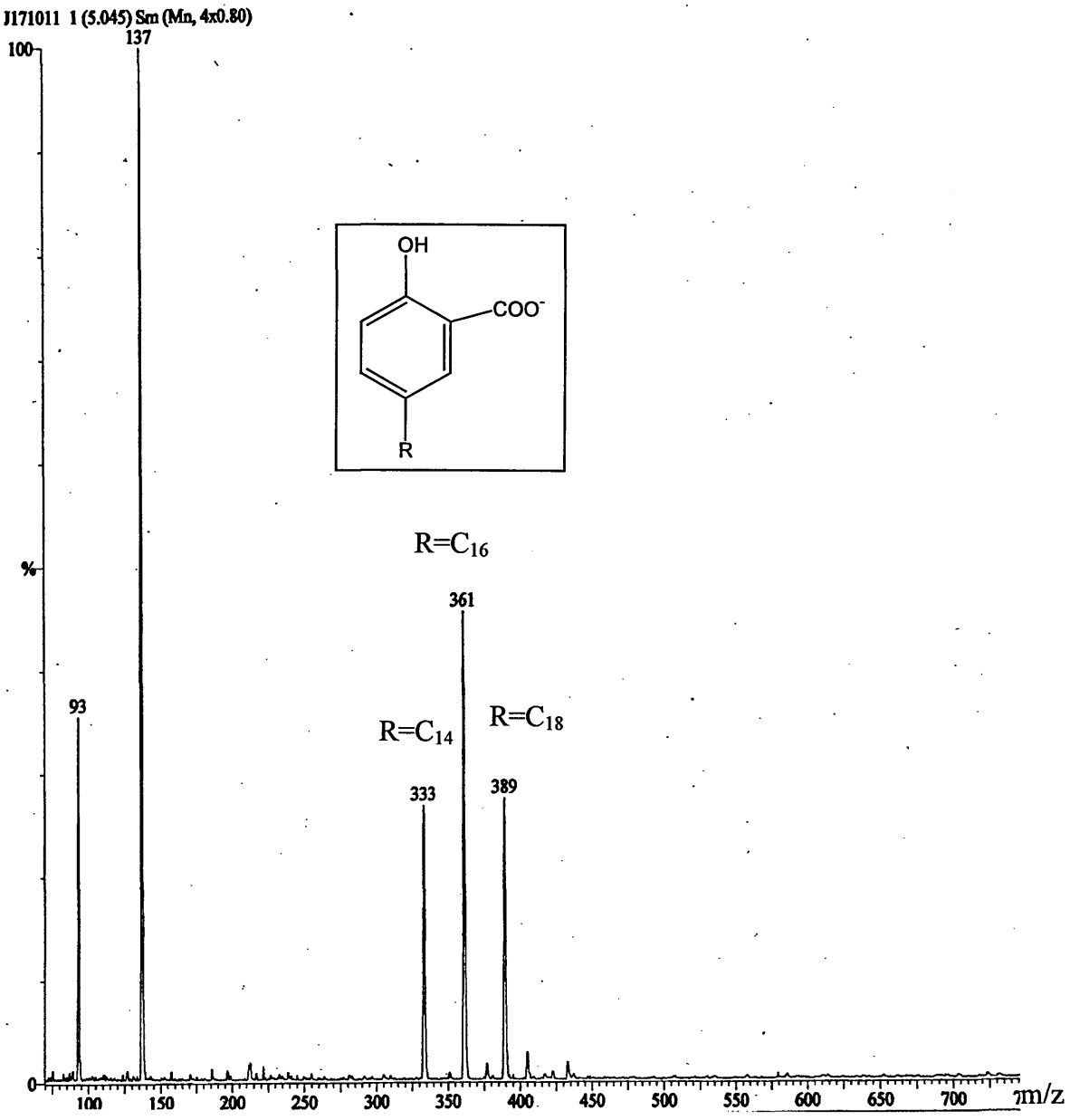

Figure 7.18 Mass spectrum of sample T45767/00 by direct infusion in negative ion mode. Base oil was removed by solid phase extraction. Sample concentration of 500µg/ml contained within a buffer of 50mM ammonium acetate in methanol. Nebulising gas was set to 40 l hour^{-1} whilst the drying gas was set to 200 l hour^{-1}. Cone voltage was maintained at -30 V while capillary voltage was maintained at -3.0kV. MCA was used scanning between 60 and 1000 mass units for a total time of 4 minutes.

7.5.2.2 Used formulated oil

Identification of individual analytes by mass alone is difficult, but differences in the spectra are present and easy to spot. Figure 7.22 (A0573A.007A/02) shows the appearance and disappearance of masses through possible degradation.

New Masses or Increased Intensity	Masses Disappeared or Decreased Intensity
181	213
223	239
265	255
451	281
465	297
493	351
535	381
	606
	611
	634
	662
	690
	718

Table 7.19 Showing the differences in mass spectra for new and used formulated oil.

Figure 7.19 shows the differences in spectra for A0573A/007A/02 and A0573A/001A/02. However, if they are products of depletion and degradation, then it could suggest that in this used oil sample the additive resources have been almost fully depleted. The peaks present originally at m/z 213 (C_3/C_3), 255 (C_3/C_6) and 297 (C_6/C_6) for ZDDP C_3/C_6 are not seen (Figure 7.19) in this used oil sample.

The masses of the peaks of interest are 181 (C_3/C_3) 223 (C_3/C_6) and 265 (C_6/C_6); these are some 32 mass units smaller than the original ZDDPs and a further 16 mass units smaller than the 2nd set of peaks seen in the new lubricants. This suggests further oxidation and the exchange of all sulphur atoms for oxygen atoms resulting in the formation of phosphates (Figure 7.20), which are important for the formation of the

anti-wear layer on metal surfaces. However these results do not correspond to the suggested degradation pathways given by Woo and Mosey[5] and Rounds[6]. Rounds suggested that the zinc remains attached to the degradation product, whilst Woo and Mosey suggested that the alkyl chains are also removed during degradation.

Original Compound	Degradation Compound
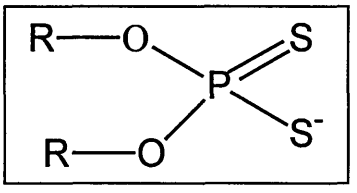	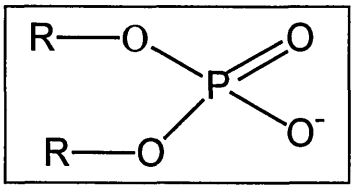

Figure 7.20 Possible structure for the unknown peaks (R= alkyl chains C_3/C_6) at m/z 181, 223, 265.

Analysis of T45523/01 (Figure 7.23) showed very little alteration to the mass spectra from the fresh oil (T45767/00), in agreement with the uv spectra from the NACE analysis. However, several peaks were more prominent. The results suggest that changes to the initial alkylsalicylate have occurred, as the detergents do have some alkalinity, allowing them to partly control the acidity of a working oil. The presence of sulphuric acid and nitric acid from reactions within combustion engines and blow-by gases could result in nitration of the benzene ring with sulphuric acid working as a catalyst.

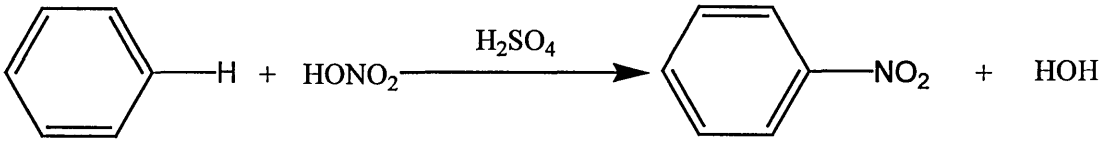

Nitric acid is removed from the system, however, sulphuric acid remains and more water is incorporated into the oil. This process will lead to greater concentrations of

acids whilst the alkylsalicylate is used up. This would continue to be the case until all the alkalinity from the alkylsalicylates is depleted. This effect would still be seen with overbased detergents, but over a longer time period.

If this nitration is occurring within the lubricant then the alkylsalicylate mass would increase by 45. Peaks are seen in figure 7.23 at 378, 406 and 434, which, do in fact correspond to such a mechanism.

Original alkylsalicylate structure	Degradation product of alkylsalicylate
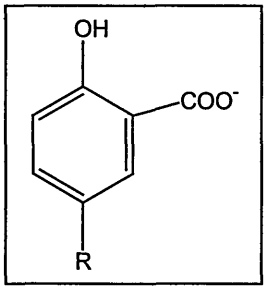 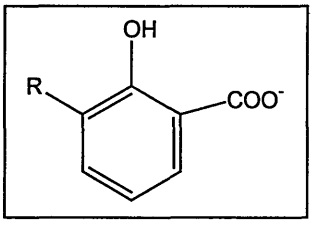	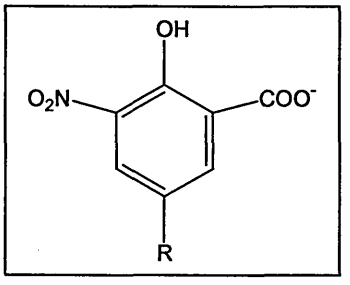 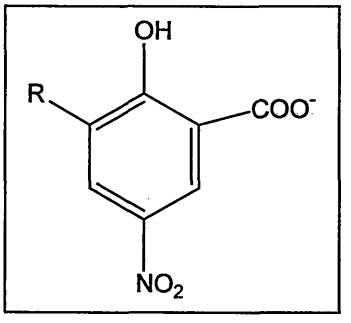

Figure 7.21 Structure of the original alkylsalicylates (o-, p-) and their possible nitro derivatives.

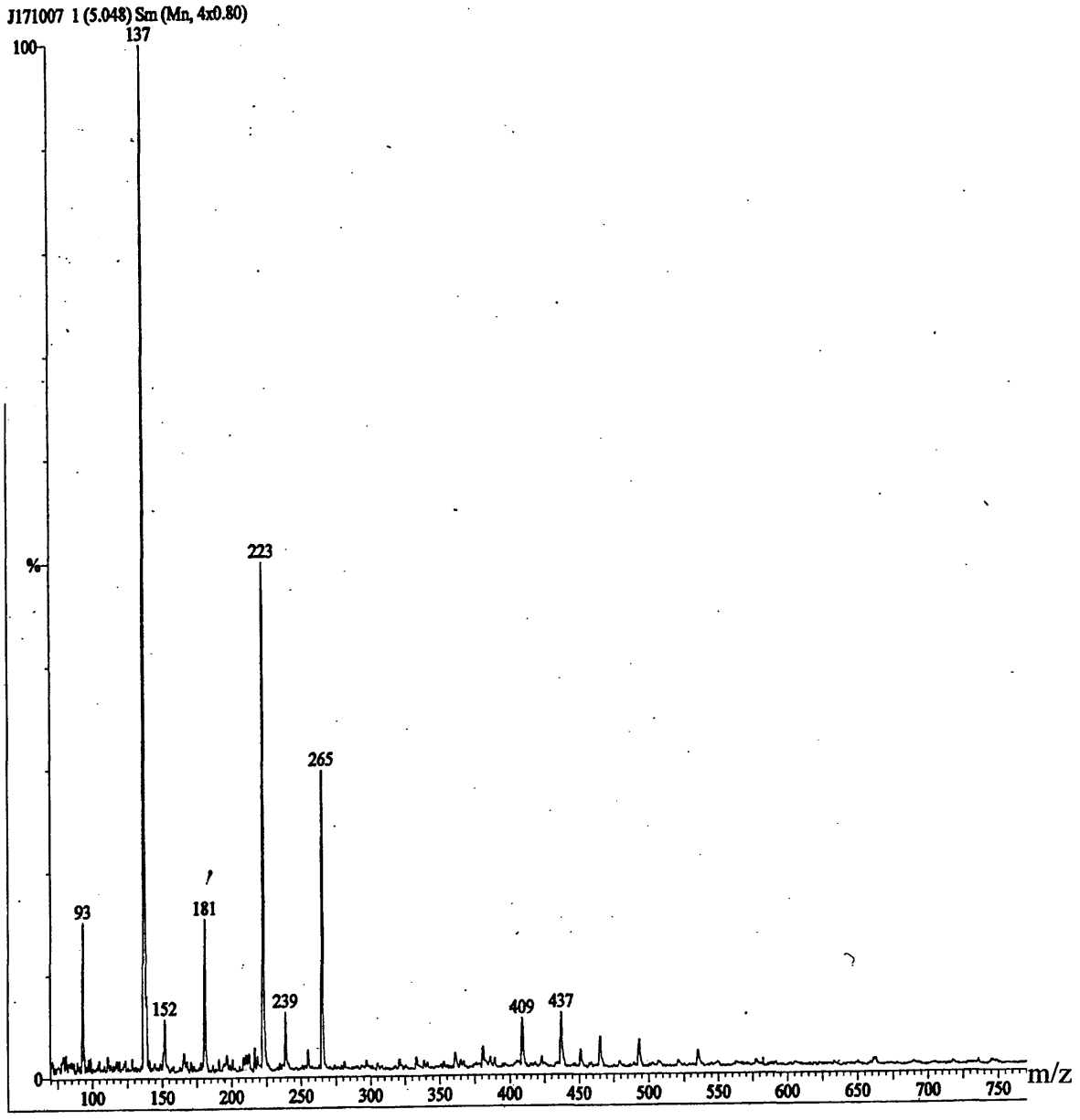

Figure 7.22 Mass spectrum of sample A0573A/007A/02 by direct infusion, negative ion mode. Base oil was removed by solid phase extraction. Sample concentration of 2000µg/ml contained within a buffer of 50mM ammonium acetate in methanol. Nebulising gas was set to 40 l hour^{-1} whilst the drying gas was set to 200 l hour^{-1}. Cone voltage was maintained at -30 V while capillary voltage was maintained at -3.0kV. MCA was used scanning between 60 and 1000 mass units for a total time of 4 minutes.

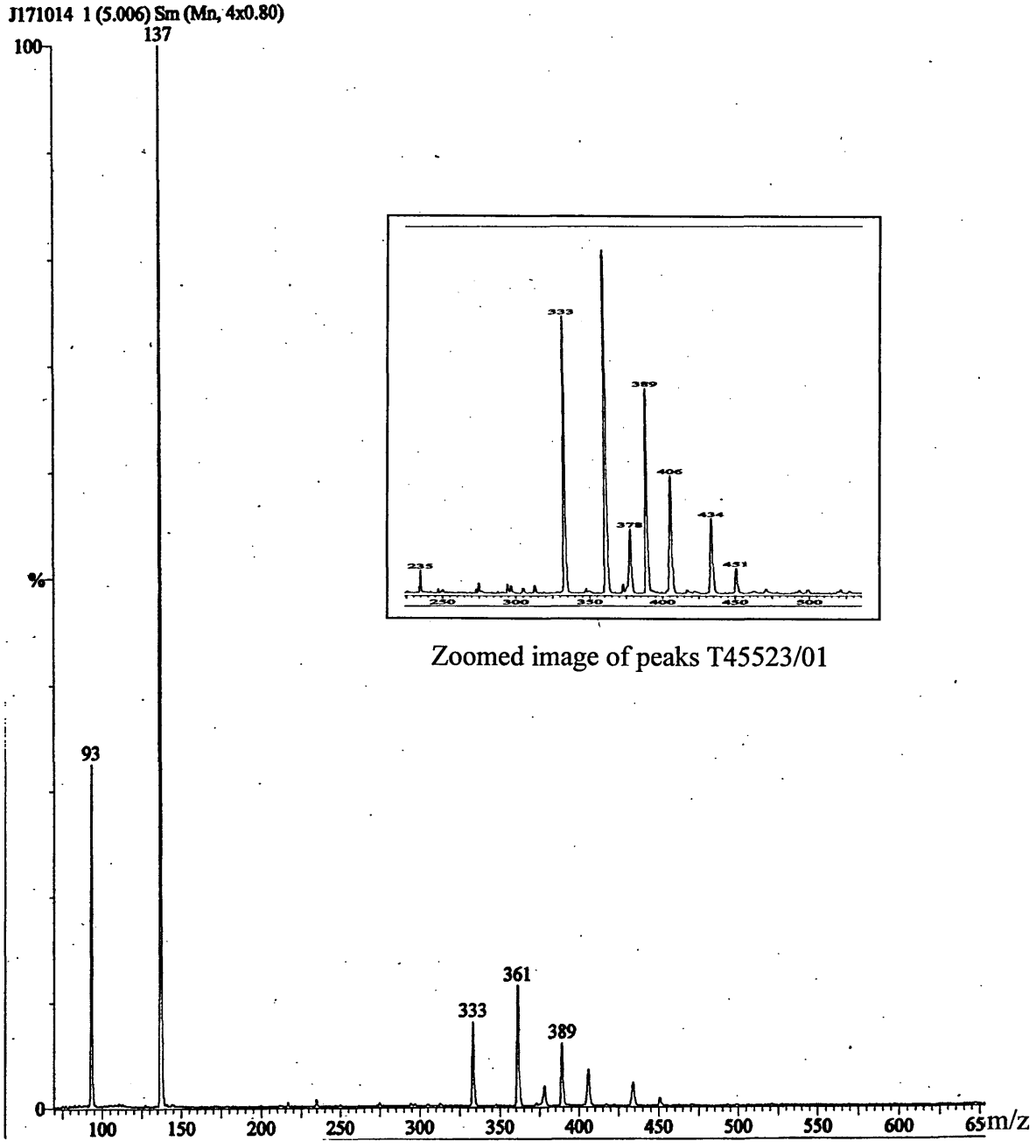

Zoomed image of peaks T45523/01

Figure 7.23 Mass spectrum of sample T45523/01 by direct infusion, negative ion mode. Base oil removed by solid phase extraction. Sample concentration of 500µg/ml contained within a buffer of 50mM ammonium acetate in methanol. Nebulising gas was set to 40 l hour^{-1} whilst the drying gas was set to 200 l hour^{-1}. Cone voltage was maintained at -30 V while capillary voltage was maintained at -3.0kV. MCA was used scanning between 60 and 1000 mass units for a total time of 4 minutes.

7.5.3 Nonaqueous capillary electrophoresis-mass spectrometry

As already stated, mass spectrometry in scanning mode is not possible for these analytes unless in high concentrations. Selected ion monitoring was used in the examples here.

Samples A0573/001A/02 (Figure 7.24), A0573A/002A/02 (Figure 7.25) and A0573A/007A/02 (Figure 7.26) were analysed at a concentration of 30,000μg/ml. With selected ion monitoring, only few analytes were identified, of the original ZDDP only m/z 213 (C_3/C_3) is identified. But even so some of the initial degradation products were seen at m/z 239 and 281. The technique was able to detect the probable ZDDP breakdown products at masses 181, 223 and 265 seen in figure 7.26. The use of a sheath flow led to dilution of the analytes. However, post clean-up, there seemed to be a lot of sample left after blowing down to concentrate the sample. The effectiveness of the clean up process is therefore in doubt, not only for the used oil but for unused oils as well.

Analysis of T47567/00 (Figure 7.27) showed the three peaks seen in direct infusion; some separation was observed and the peak for salicylic acid was seen within the scan. Again the separation was not as good as the one seen in NACE-UV. Figure 7.28 shows the analysis of the used oil T45523/01, and again peaks are identified for the original analytes, mass values 333, 361 and 389 that correspond to the C_{14}-C_{18} ligands. However, of the peaks detected as possible combustion by-products of lubricant use, only one new peak is identified (m/z 406).

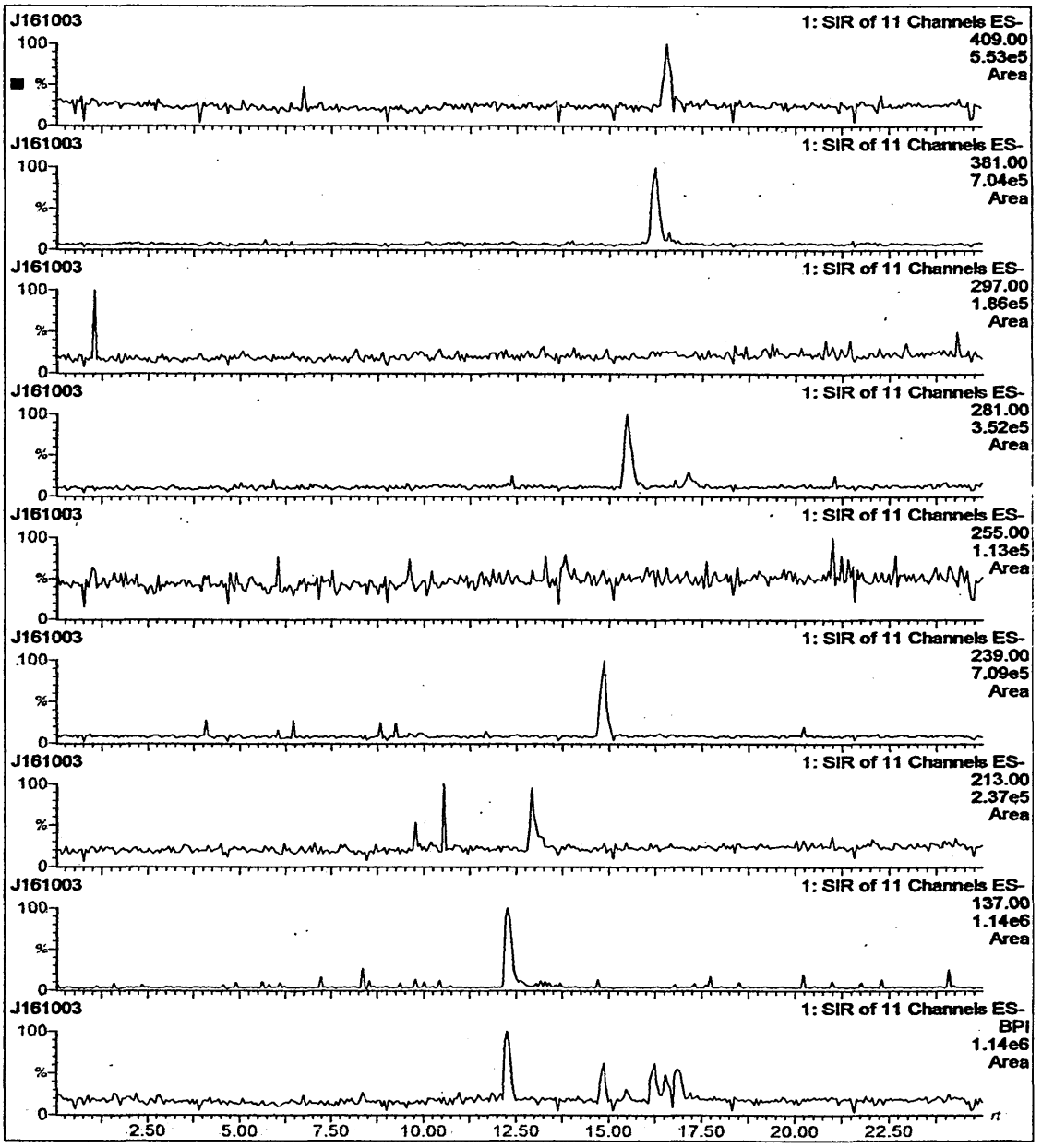

Figure 7.24 NACE-MS selected ion monitoring of A0573/001A/02. Base oil was removed by solid phase extraction. Conditions: NACE buffer 50mM ammonium acetate, methanol pH 9.01* adjusted using tetramethylammonium hydroxide. Sample at a concentration of 30,000µg/ml in methanol injected at –5.0kV for 0.1 min, separation voltage of –30kV. MS sheath flow 50mM ammonium acetate, methanol 2% acetic acid nebulising gas 40 l hour^{-1}, drying gas 200 l hour^{-1} cone voltage -30v capillary voltage -3.0kV, source temp 50°C Separation capillary withdrawn 6.0mm.

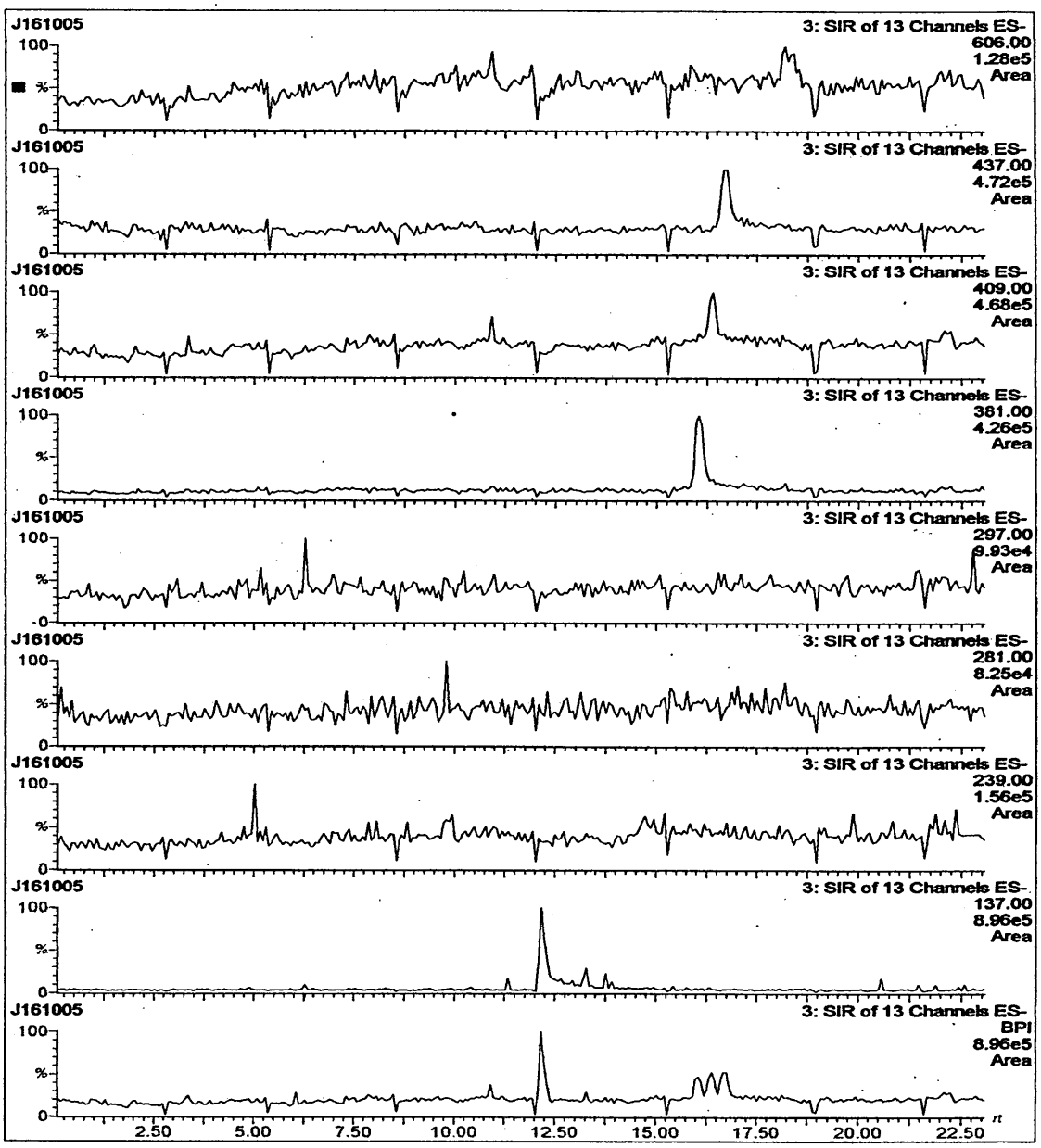

Figure 7.25 NACE-MS selected ion monitoring of A0573/002A/02. Base oil was removed by solid phase extraction. Conditions: NACE buffer 50mM ammonium acetate, methanol pH 9.01* adjusted using tetramethylammonium hydroxide. Sample at a concentration of 30,000µg/ml in methanol injected at –5.0kV for 0.1 min, separation voltage of –30kV. MS sheath flow 50mM ammonium acetate, methanol 2% acetic acid nebulising gas 40 l hour^{-1}, drying gas 200 l hour^{-1} cone voltage -30v capillary voltage -3.0kV, source temp 50°C Separation capillary Withdrawn 6.0mm.

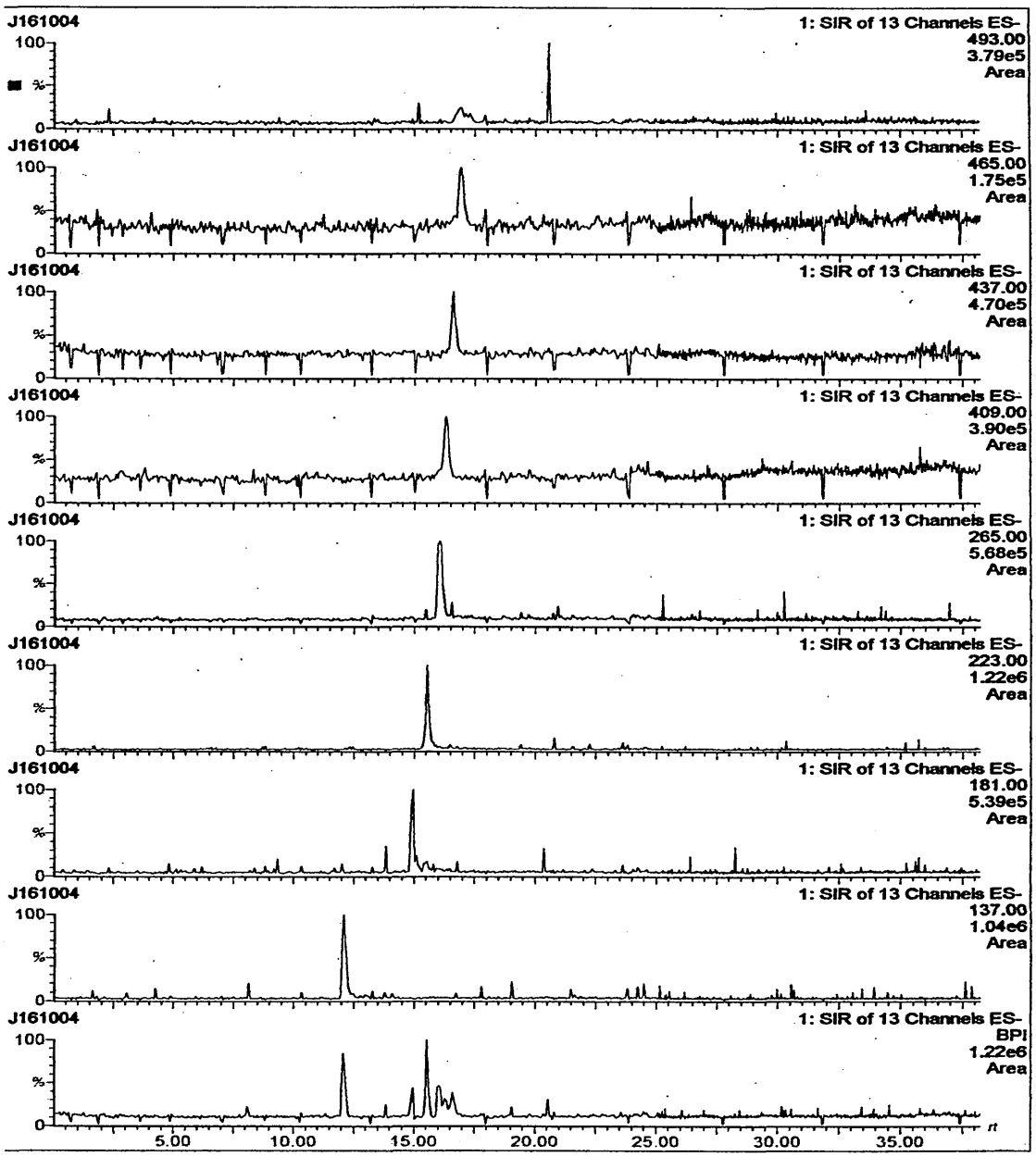

Figure 7.26 NACE-MS selected ion monitoring of A0573/007A/02. Base oil was removed by solid phase extraction. Conditions: NACE buffer 50mM ammonium acetate, methanol pH 9.01* adjusted using tetramethylammonium hydroxide. Sample at a concentration of 30,000µg/ml in methanol injected at –5.0kV for 0.1 min, separation voltage of –30kV. MS sheath flow 50mM ammonium acetate, methanol 2% acetic acid nebulising gas 40 l hour^{-1}, drying gas 200 l hour^{-1} cone voltage -30v capillary voltage -3.0kV, source temp 50°C Separation capillary withdrawn 6.0mm.

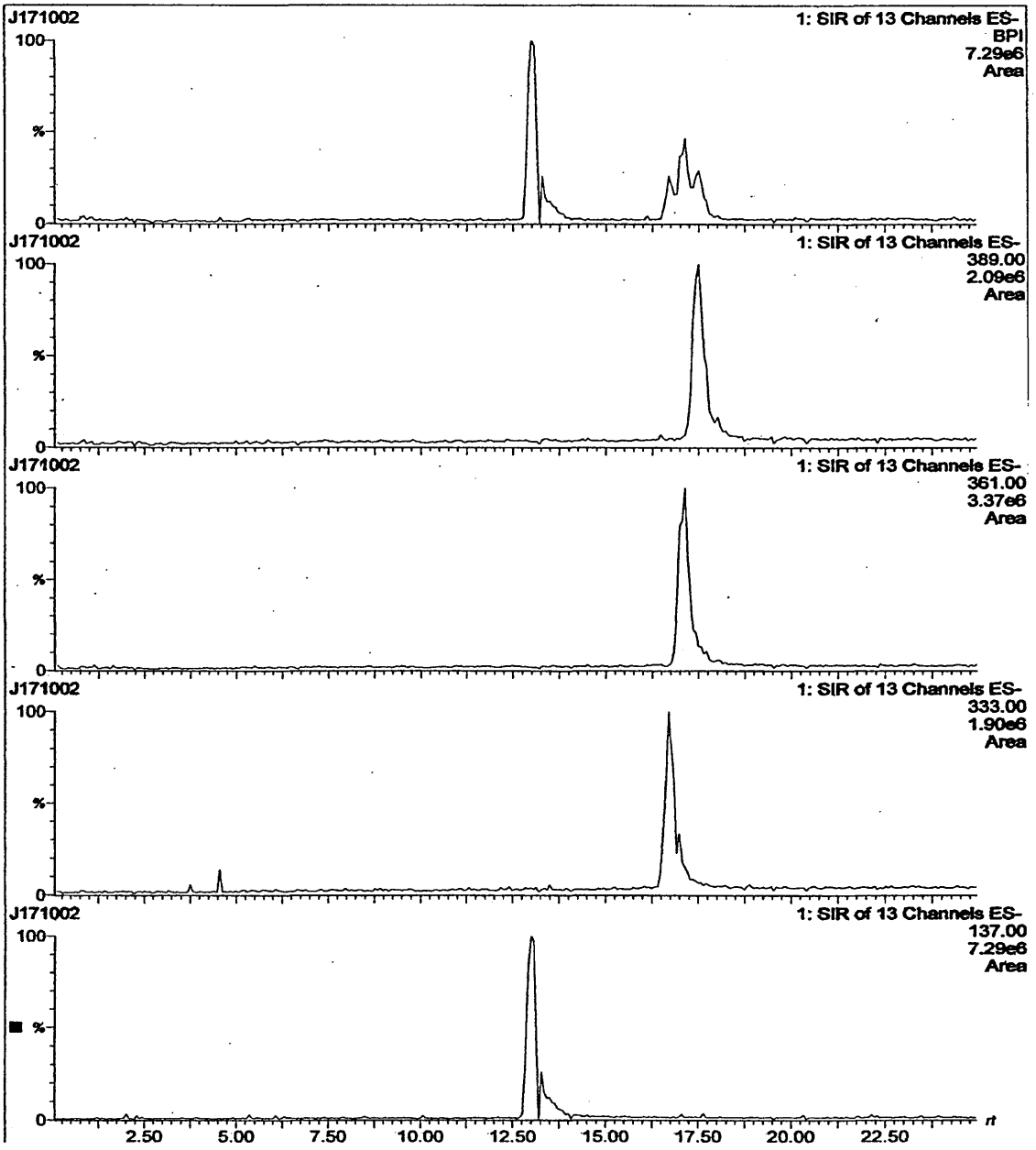

Figure 7.27 NACE-MS selected ion monitoring of T47567/00. Base oil was removed by solid phase extraction. Conditions: NACE buffer 50mM ammonium acetate, methanol pH 9.01* adjusted using tetramethylammonium hydroxide. Sample at a concentration of 10,000µg/ml in methanol injected at –5.0kV for 0.1 min, separation voltage of –30kV. MS sheath flow 50mM ammonium acetate, methanol 2% acetic acid nebulising gas 40 l hour^{-1}, drying gas 200 l hour^{-1} cone voltage -30v capillary voltage -3.0kV, source temp 50°C Separation capillary withdrawn 6.0mm.

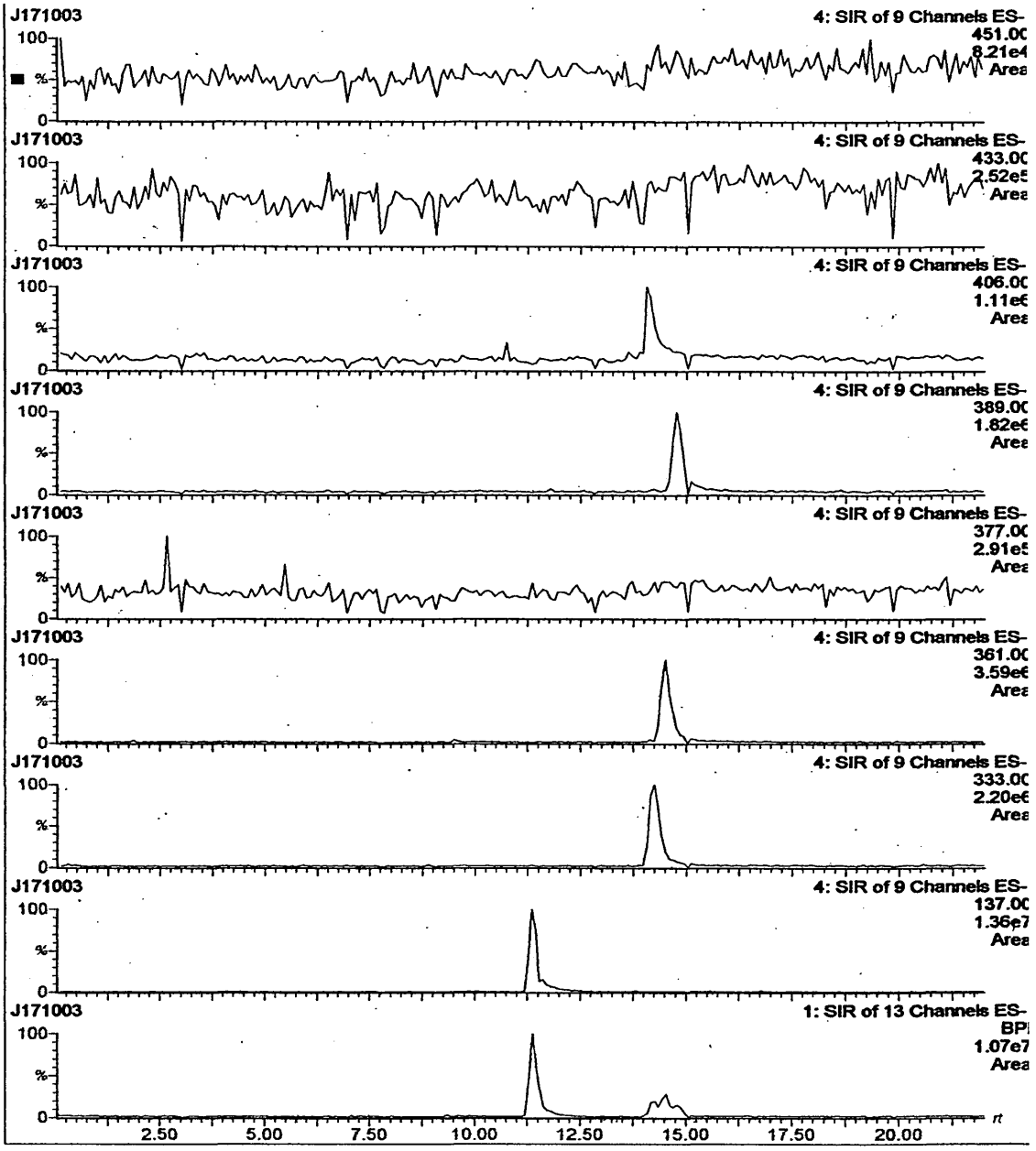

Figure 7.28 NACE-MS selected ion monitoring of T45523/01. Base oil was removed by solid phase extraction. Conditions: NACE buffer 50mM ammonium acetate, methanol pH 9.01* adjusted using tetramethylammonium hydroxide. Sample at a concentration of 10,000µg/ml in methanol injected at –5.0kV for 0.1 min, separation voltage of –30kV. MS sheath flow 50mM ammonium acetate, methanol 2% acetic acid nebulising gas 40 l hour^{-1}, drying gas 200 l hour^{-1} cone voltage -30v capillary voltage -3.0kV, source temp 50°C Separation capillary withdrawn 6.0mm.

7.6 Conclusion

A method for the analysis of formulated oil has been developed, but it has identified several points that have to be addressed in the future. The use of NACE with uv detection showed a very good separation of additives in formulated oil, and some of the components were tentatively identified through the use of migration ratios with salicylic acid. However, as many components are possibly present within the cleaned up oil, mass spectrometry detection would be useful to provide mass information as further evidence. Migration ratios predicted the presence of ZDDP and alkylsalicylates within the new and used oil products. However, in altering the wavelength for ZDDP identification, no increase in signal was seen as would be expected.

In samples A0573A/001A/02 and A0573A/002A/02, the use of NACE-UV detection suggested that two ZDDP products were present. However, the use of direct infusion mass spectrometry showed that only one ZDDP product was present. The used version of the oils, A0573A/007A/02, showed the presence of new masses and the depletion of other masses, indicating that the oil had undergone chemical changes.

Analysis of T45523/01 and T45767/00 showed agreements between NACE-uv and direct infusion mass spectrometry. The used oil showed decrease in concentration of the alkylsalicylates and an increase in a degradant. NACE-UV seemed an adequate technique for the analysis of lubricant additives and deserves further examination for its usefulness.

Direct infusion of extracts from the formulated oil has been very successful for the identification of ZDDPs and possible oxidative degradation products. These oxidation products were seen in fresh oil, but at more abundance in the used oil.

NACE-MS alone was unsuccessful as it was not sensitive enough for formulated oils with the instrumentation used here. Analysis of additive standards was possible using NACE-MS, some progress was made in identifying phosphate and thiophosphate degradation products of ZDDP, and nitrated alkylsalicylates.

NACE-MS could be ideal for monitoring the depletion of additives over time if better instrumentation was used.

Formulated Oil	Additive present	Identified / Not identified
A0573A/001A/02,	Sulphonate	Not Identified
	Phenate	Not Identified
	ZDDP (C_3/C_6)	Identified
A0573A/002A/02	Sulphonate	Not Identified
	Phenate	Not Identified
	ZDDP (C_3/C_6)	Identified
A0573A/007A/02 (used oil)	Sulphonate	Not Identified
	Phenate	Not Identified
	ZDDP (C_3/C_6)	Not Identified
T47567/00	Ca Salicylate	Identified
T45523/01 (used oil)	Ca Salicylate	Identified

Figure 7.29 Actual contents of the analysed formulated oil.

Figure 7.29 shows the actual content of the formulated oils. This shows that the analysis of formulated oils was successful, even though alkylsalicylate was found in only one product.

Improvements to the sample clean up procedure may help to overcome the problems encountered in this work.

References

1. Peng, P., Hong, S-Z., Lu, W-Z., Lubrication Engineering 1994, **50**, (3), 230-235.

2. Papay, A.G., Lubrication Science 1998, **10-3**, (10), 209-217.

3. So, H., Lin, Y.C., Huang, G.G.S., Chang, T.J.T., Wear 1993, **166**, 17-26.

4. Roberts, K.J., Armstrong, D.R., Ferrari, E.S., Adams, D., Wear 1998, **217**, 276-287.

5. Woo, T.K., Mosey, N.J., Journal of Physical Chemistry A 2003, **107**, 5058-5070.

6. Rounds, F.G., ASLE Transactions 1981, **24**, (4), 431-440.

Chapter 8

Fourier transform infrared, nuclear magnetic resonance and inductively coupled plasma optical emission spectrometry analysis of Alklysalicylates

8.1.Introduction

Three different alkyl salicylates had been separated by nonaqueous capillary electrophoresis. However, whether they had been separated as monomers by differences in chain lengths or as salts in micelles was uncertain. The use of solid phase extraction to remove the base oil from the standard and to pre-concentrate the samples suggested that the micelles were disrupted, but more definitive evidence was required. Various analysis techniques were therefore used to establish exactly what was being separated.

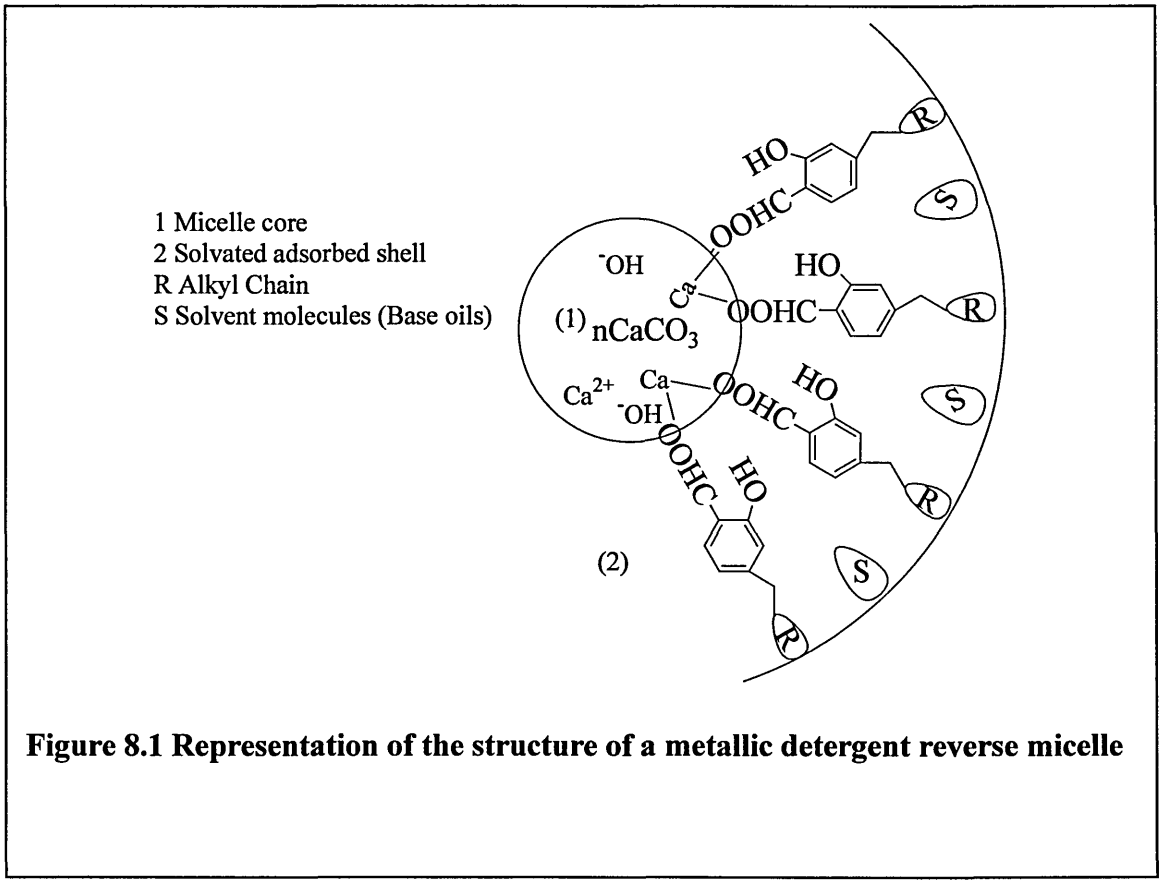

Figure 8.1 Representation of the structure of a metallic detergent reverse micelle

The micelle consists of an organic outer shell made up of the alkylsalicylate, which stabilises the inorganic core. The latter is mostly made up of inorganic carbonate (usually calcium or magnesium) with some metal hydroxides. The carbonates and

hydroxides provide most of the basicity for neutralising the acids (nitric, sulphuric) that are by-products of combustion.

Fractions from the various stages of solid phase extraction were analysed to see where the alkylsalicylate eluted, whether it was found in one or more eluting solvent, and whether the carbonate eluted with the alkylsalicylate. Infrared spectroscopy (IR), nuclear magnetic resonance spectrometry (NMR), and inductively coupled plasma optical emission spectrometry (ICP-OES) were used in these experiments.

The synthesis of overbased alkylsalicylates (section 1.5 1.5.1. page 17 and 20) indicates a correlation between the amount of carbonate present and the amount of metal. The greater the overbasing (noted by the total base number (TBN)) of the detergent, the more carbonate will be present, and as the carbonate is present as a metal salt an increase in the quantity of metal will be seen. Identifying the fate of the metal will thus indicate where the carbonate is in the fractions and hence the amount of overbasing.

A similar set of experiments was carried out by Griffiths *et al.* (1995)[1] to study the structure and properties of alkyl phenates, which are used as detergents in much the same way as the alkylsalicylates.

The work reported here examines alkylsalicylates with differing TBN and two different metals, calcium and magnesium. The calcium alkylsalicylates were overbased to 64TBN, 168TBN and 280TBN. The amount of magnesium overbasing was unknown. All alkylsalicylates were contained in a base oil at unknown concentrations.

8.1.1. Fourier Transform Infrared Spectroscopy

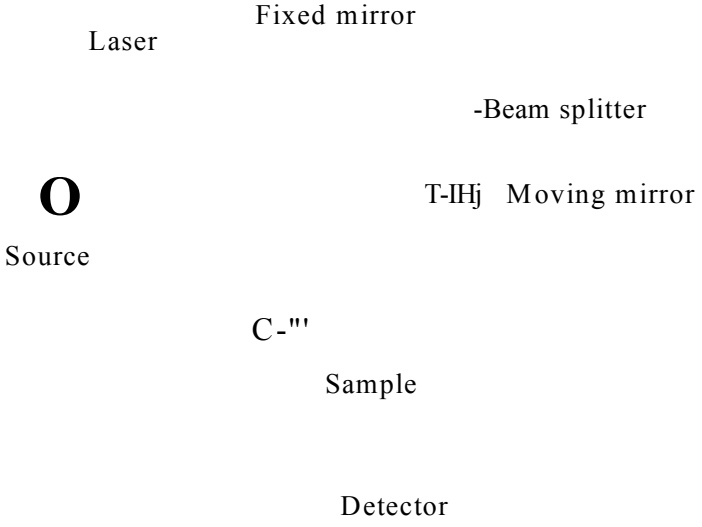

Figure 8.2. Diagram of an FTIR instrument based on the Michelson interferometer

The diagram in figure 8.2 shows the layout of an FTIR spectrometer based on the Michelson interferometer. Radiation from the source strikes the beam splitter, which for the mid-infrared region is made from a potassium bromide support coated with a germanium film, allowing half the radiation through to strike the moving mirror and reflecting half to the stationary mirror. Both beams are then reflected back onto the beam splitter and half of each are combined and directed to the sample. As the radiation beams travel different distances they oscillate in and out of phase with each other when they reach the detector due to differences in the retardation, 5. This results in a sinusoidal variation in intensity at the detector for each frequency present. The radiation striking the sample will be absorbed by the sample at characteristic wavelengths, corresponding to the vibrational frequencies of stretching and bending of bonds in the sample molecules. The position of the moving mirror is determined from a separate interferogram of a visible laser.

Unlike double beam spectrometers these single beam instruments require a background reading to be taken. A transmission spectrum is obtained by dividing the sample spectrum by the background spectrum.

The analysis of lubricants and lubricant additives by infrared spectroscopy is well established. Dong *et al.* (2000)[2] produced a quantitative method for the determination of the contribution carboxylic acids had on the total acid number of lubricating oils due to oil oxidation. Infrared spectroscopy is readily used to identify and quantify individual functional groups through their absorption at specific wavelengths, and has been used to monitor the increase over time of carboxylic acids in oils.

Stellman *et al.* (1999)[3] monitored the degradation of synthetic lubricant oil with usage by looking at functional group changes over time.

Baladincz *et al.*(1998)[4] utilised Fourier transform infrared spectroscopy to study the interactions of several lubricant oil additives, characterising the changes in chemical structures of additives due to their interactions.

Kutova *et al.*(1988)[5] studied the depletion of lubricant additives over time, concentrating on the conversion of additive salts into their constitutive acids. An increase in total acid number and a decrease in total base number were seen and after 987 hours of operation, zinc dialkyldithiophosphates, calcium salicylates and the calcium sulphonates concentrations had decreased by 35% to 40%.

8.1.2. Nuclear magnetic resonance spectroscopy (NMR)

NMR can be utilised in structural and quantitative analysis by looking at a variety of nuclei including ^{1}H, ^{1T}C, ^{1Q}F and ^{Ol}P. There are two types of NMR spectrometer continuous wave and pulse (Fourier transform), the latter being the more commonly used.

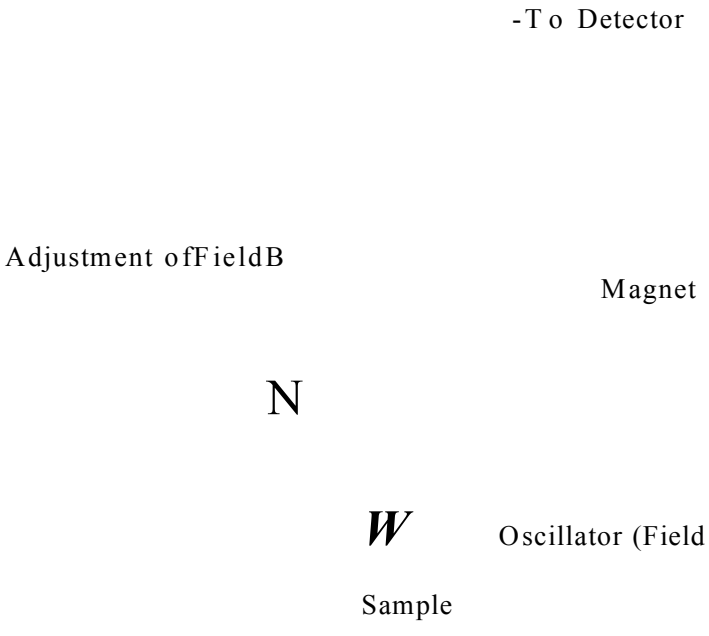

Figure 8.3. Diagram showing the position of the sample within the sample probe for NMR

Because nuclei have charge and spin they also have a magnetic moment (p) associated with them. Outside a magnetic field the magnetic moment has no preferred orientation. However, when a nucleus with a spin number of *H* is placed in a magnetic field, its magnetic moment will align itself with or against the external field, as shown in figure 8.4 page 228, giving two possible energy levels. The nuclei aligned with the magnetic field are in the lower energy state (p = +1/2). The spin of the aligned nucleus induces precession about the axis of the magnetic field. Exposing the nucleus to a pulse of electromagnetic radiation (from an oscillator coil) at 90° to the fixed magnetic field

flips the angle of precession. If the energy absorbed by the nucleus is the same as the energy required to take the nucleus into the higher energy state, the magnetic moment in essence flips and aligns against the fixed magnetic field. When the electromagnetic radiation emission ceases the nuclei that were flipped lose the energy gained and return to their lower energy state.

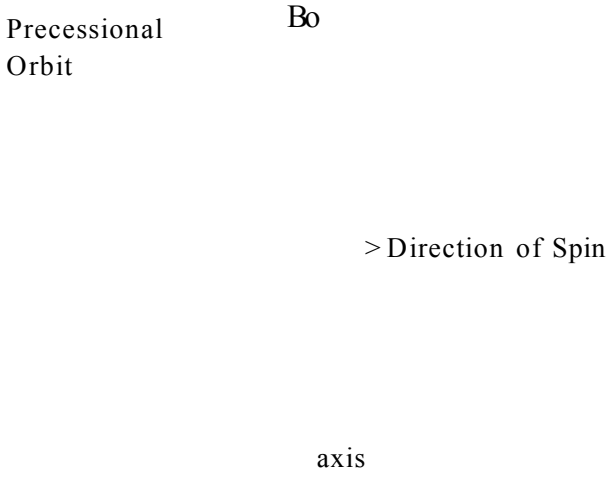

Figure 8.4. Showing the two possible orientations of spin of 'H nucleus.

NMR has been used for the monitoring of lubricants and lubricant additives and their interactions. Inoue *et al.* (1982)7 studied calcium dodecylsalicylate micelles in chloroform, recording 13C spectra. This was found to be problematic, which was ascribed to the structure of the micelle with its very rigid inner calcium core preventing adequate relaxation. Sarnia *et al.* (1998)8 characterised various lubricants and lubricant additives, including metallic detergents, dispersants and an anti-wear additive, through the study of ’H, IjC and 31P. Harrison *et al.* (1992)9 and Kapur *et al.* (1999)6 studied the interactions of succinimide- type lubricating oil dispersants with zinc diiso-butyl dithiophosphate, and also the interactions between various mixtures of ZDDP, overbased sulphonate and dispersant, by examining differences in chemical shifts due to the interactions. From these studies it was found that interactions involving ZDDP

were reversible. Additive-additive interactions in the bulk lubricants were a result of weak complexes, with no stable transformed product.

In the study reported here ^{1}H NMR only was used. The aim was to identify the fraction in which the alkyl salicylate was eluted.

8.1.3. Inductively coupled plasma optical emission spectrometry

Inductively coupled plasma optical emission spectrometry (ICP-OES) is a convenient method for monitoring trace metals in lubrication oils. Figure 8.5 (page 230) shows a diagram of a plasma torch, in which the plasma is created from a flow of ionised argon and the temperature can reach up to 8,000 kelvin.

The liquid sample is nebulised by an inert carrier gas (argon) prior to introduction to the plasma torch. The ICP consists of two concentric quartz tubes; the inner tube is used to introduce the ionised argon and the sample while the outer tube carries argon to keep the inner tube cool and also to keep the plasma away from the outer quartz tube. Around the outer tube is a water cooled conducting coil, connected to a radio-frequency generator that typically works at 27MHz. The ions and the electrons from the ionised argon interact with the magnetic field and flow in an annular path. Heating is a consequence of the ions and electrons resistance to this movement. The sample enters the plasma at the base, and is heated so that the temperature of the plasma is sufficient to excite nearly all elements, allowing measurement to be made from the wavelength and amount of radiation emitted as the ions relax.

Figure 8.5. An outline of an inductively coupled plasma torch

ICP-OES can be used for routine analysis in the lubricating industry due to its ease of use and speed of analysis. Sample preparation is the limiting factor when it comes to sample turnover.

Generally ICP is set up for the analysis of aqueous samples and the introduction of extremely high organic content samples can be detrimental to the plasma. The result of introducing organic samples (such as oil) into the plasma is the formation of carbonaceous by-products such as soot, which can cause electrical short circuits on the induction coil and subsequently the destruction of the plasma. For this reason high organic content samples should be prepared specially for analysis by ICP.

Samples can undergo various methods of preparation, including wet digestion or dilution with xylene. Turunen *et al.* (1995)[10] used wet digestion with a mixture of nitric acid and sulphuric acid, and also carried out dilutions with xylene in a ratio 1:10, for the analysis of oil. Al-Swaidan (1996)[11] mixed an aliquot of oil sample with tetralin

which acts as a co-solvent, 0.5ml of Triton X , 5ml of 40% (v/v) nitric acid solution and 0.5ml of 100ppm indium solution. This was used for the analysis of lead, nickel and vanadium with high recovery. Escobar *et al.*(1996)[12] used dilution with xylene for the determination of aluminium, magnesium, iron and yttrium in lubricant oil.

8.2. Experimental

8.2.1. Chemicals and reagents

See section 4a

8.2.2. Instrumentation

See section 4b

8.2.3. Solid phase extraction (SPE) procedure

The following procedure was used:

1. Pre wet cartridge with hexane
2. Weigh 4g of standard and disperse in 50g of hexane. Pour onto column, and collect eluate.
3. Wash with 50ml of hexane and collect eluate
4. Wash with hexane:diethylether (50:50) 50ml and collect eluate
5. Wash with 2-butanone 25ml and collect eluate
6. Wash with methanol 50ml and collect eluate.

The collected samples were blown down as dry as possible using nitrogen. Aliquots were taken for analysis by infrared spectrometry, nuclear magnetic resonance spectrometry and inductively coupled plasma optical emission spectrometry.

8.2.3.1. Recoveries From SPE

Calcium Salicylate (64 TBN)	Recovery Weight (g)	Sample Weight (g)
Sample Loading Phase	4.277	**4.565**
Hexane wash	0.1041	
Hexane : Diethyl ether wash	0.204	
2-Butanone wash	0.0511	
Methanol wash	0.023	**Recovery (%)**
Sum of Recovery	**4.659**	**102**

Table 8.6a Showing sample recovery calcium salicylate (64TBN).

Calcium Salicylate (168 TBN)	Recovery Weight (g)	Sample Weight (g)
Sample Loading Phase	3.387	**4.854**
Hexane wash	0.228	
Hexane : Diethyl ether wash	0.613	
2-Butanone wash	0.52	
Methanol wash	0.103	**Recovery (%)**
Sum of Recovery	**4.851**	**99.94**

Table 8.6b Showing sample recovery calcium salicylate (168 TBN).

Calcium Salicylate (280 TBN)	Recovery Weight (g)	Sample Weight (g)
Sample Loading Phase	3.963	**4.016**
Hexane wash	0.092	
Hexane : Diethyl ether wash	0.138	
2-Butanone wash	0.014	
Methanol wash	0.045	**Recovery (%)**
Sum of Recovery	**4.252**	**105.89**

Table 8.6c Showing sample recovery calcium salicylate (280 TBN).

Magnesium Salicylate	Recovery Weight (g)	Sample Weight (g)
Sample Loading Phase	4.187	**4.234**
Hexane wash	0.158	
Hexane : Diethyl ether wash	0.150	
2-Butanone wash	0.026	
Methanol wash	0.204	**Recovery (%)**
Sum of Recovery	**4.725**	**111.60**

Table 8.6d Showing sample recovery magnesium salicylate.

8.3. Results and Discussions

8.3.1. Fourier Transform Infrared Spectrometry

Aliquots of individual eluent fractions from the SPE were diluted in a relevant solvent so a thin film can be produced between sodium chloride windows. The sample in between the sodium chloride plates was then placed into the instrument for FTIR

analysis. Between each sample the windows were cleaned with methanol and analysed to ensure cleanliness.

The SPE procedure results in least polar compounds eluting from the column first. The polarity of the compounds eluted should increase with the polarity of the eluents used.

Figure 8.7 shows the spectra obtained from the loading phase eluate, in which there is an intense peak in the region for O-H stretching. This peak is a bit odd for a mineral base oil; however, this could be a result of the carbonate core containing some calcium hydroxide. As expected we see large responses due to C-H, C-C and C=C bonds for aliphatic and aromatic compounds. For the experiments here the most interesting peak is found at $862cm^{-1}$, indicating the presence of carbonate. The spectrum in figure 8.8 shows the presence of some carbonate in the hexane wash. O-H stretch is not evident in this spectrum. Figure 8.9 shows the hexane : diethyl ether spectrum, indicating aliphatic compounds and some aromatics with peaks at $1610cm^{-1}$ and $1525cm^{-1}$. No carbonate peak is present suggesting that all the carbonate has been eluted, without the presence of any alkylsalicylate. The alkylsalicylate is not eluted in this phase and this result is expected.

Figures 8.10 and 8.11 show the spectra for the 2-butanone and methanol extracts respectively. The salicylate salt (COO^-) peak is present at $1550cm^{-1}$. The main inference from these spectra is that salicylate is present without the presence of any carbonate, indicating that the micelles are in fact being disrupted by the SPE stage for the clean up of the standards prior to CE.

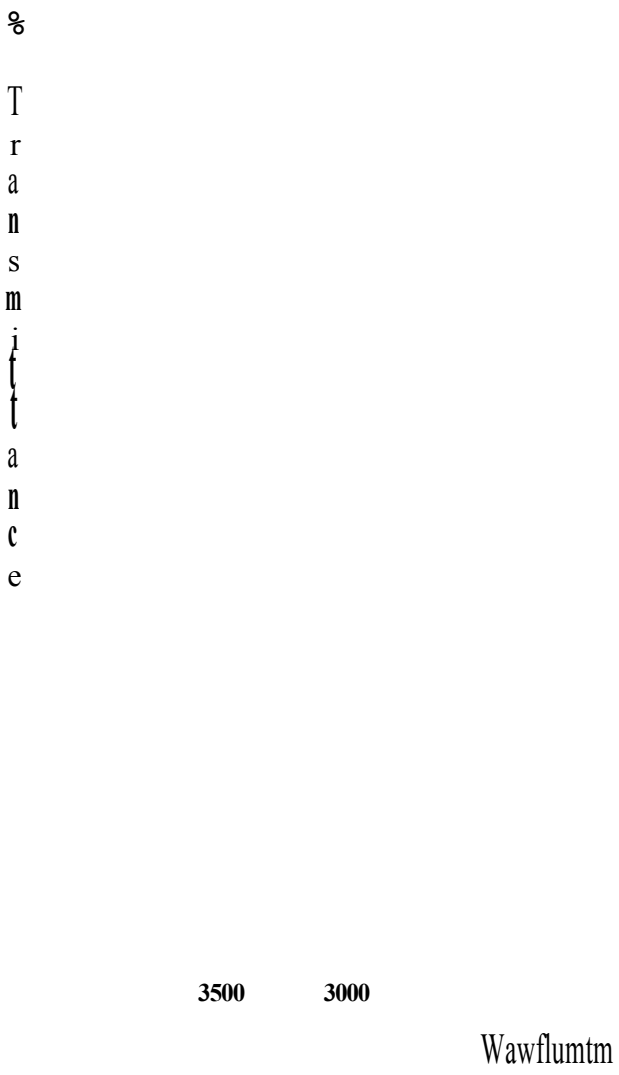

Figure 8.7. Infrared spectrum of the sample loading fraction. The carbonate peak (862cm l) is coloured red.

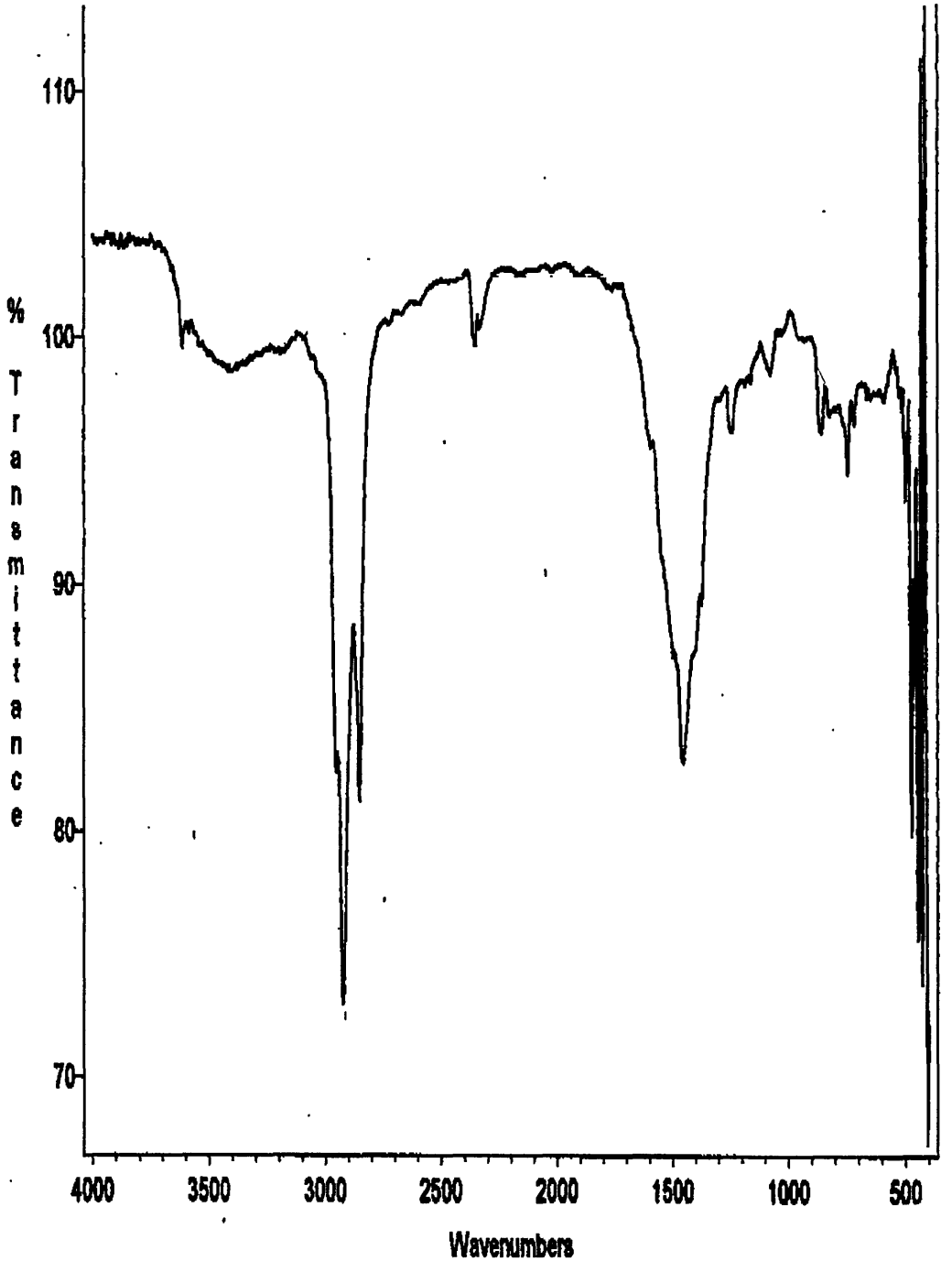

Figure 8.8. Infrared spectrum of the hexane wash fraction. The carbonate peak ($862cm^{-1}$) is coloured red.

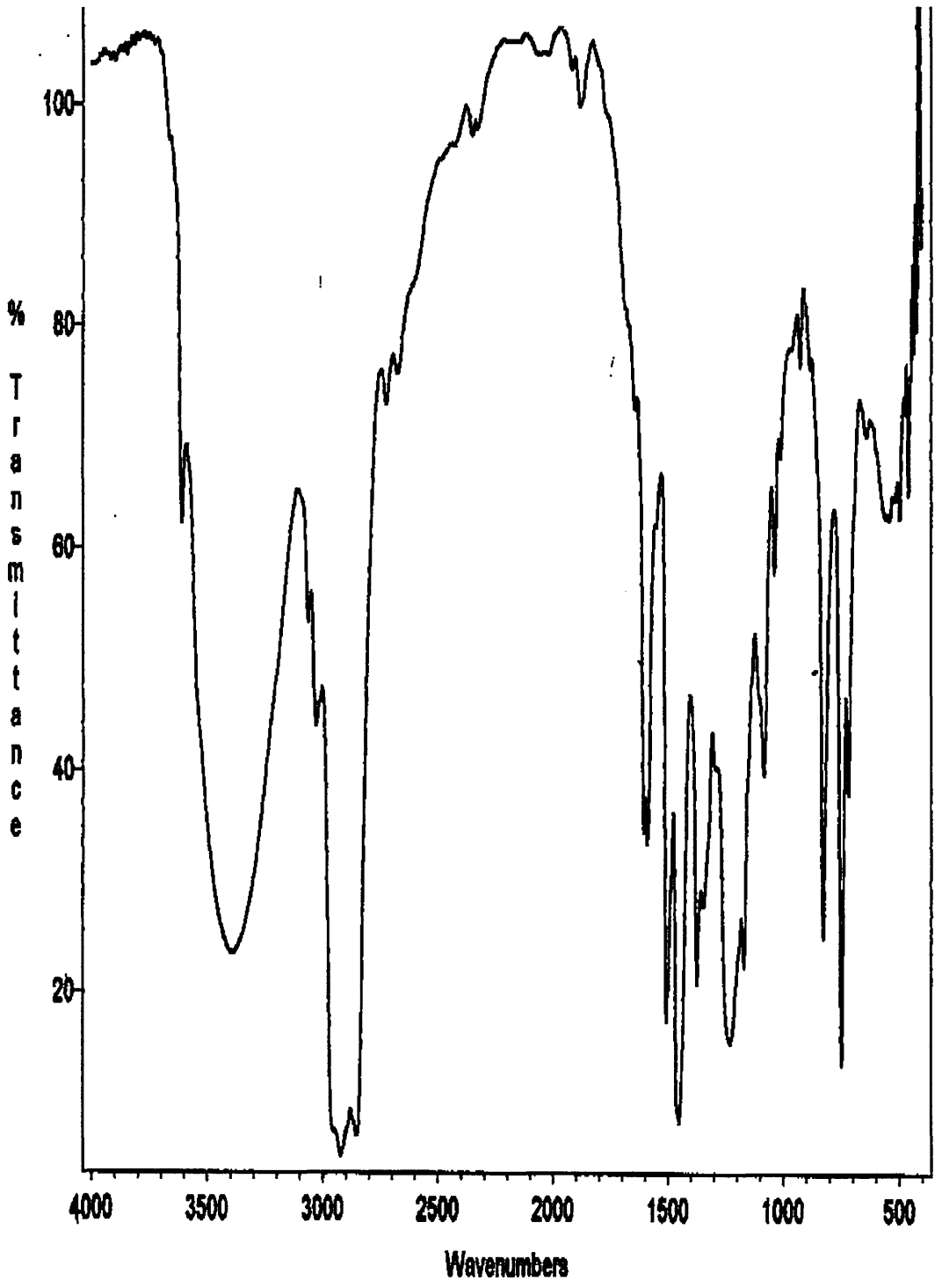

Figure 8.9. Infrared spectrum of the hexane:diethyl ether fraction.

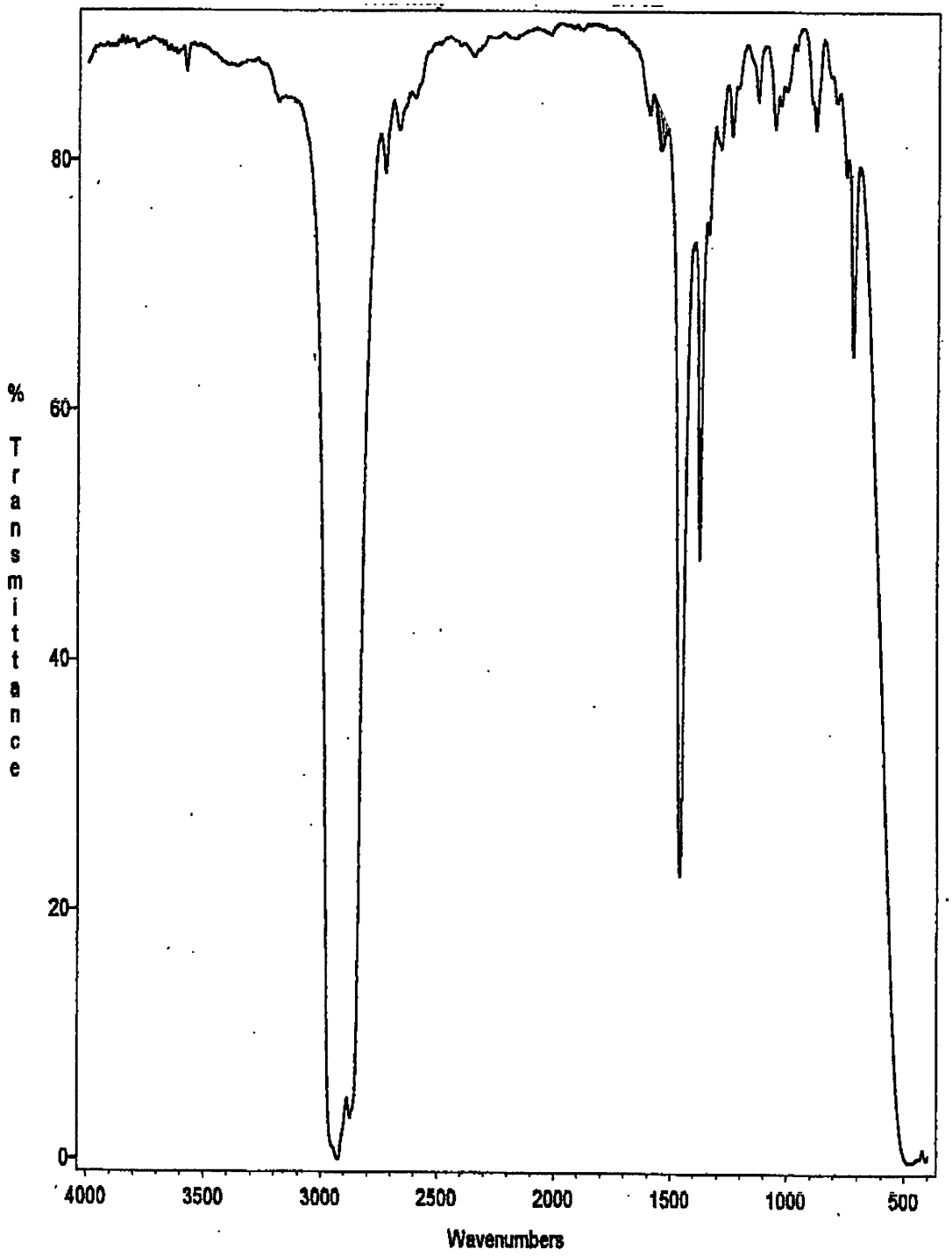

Figure 8.10. Infrared spectrum of the 2-butanone wash. Salicylate peak ((COO^-) 1550cm-1) is coloured blue.

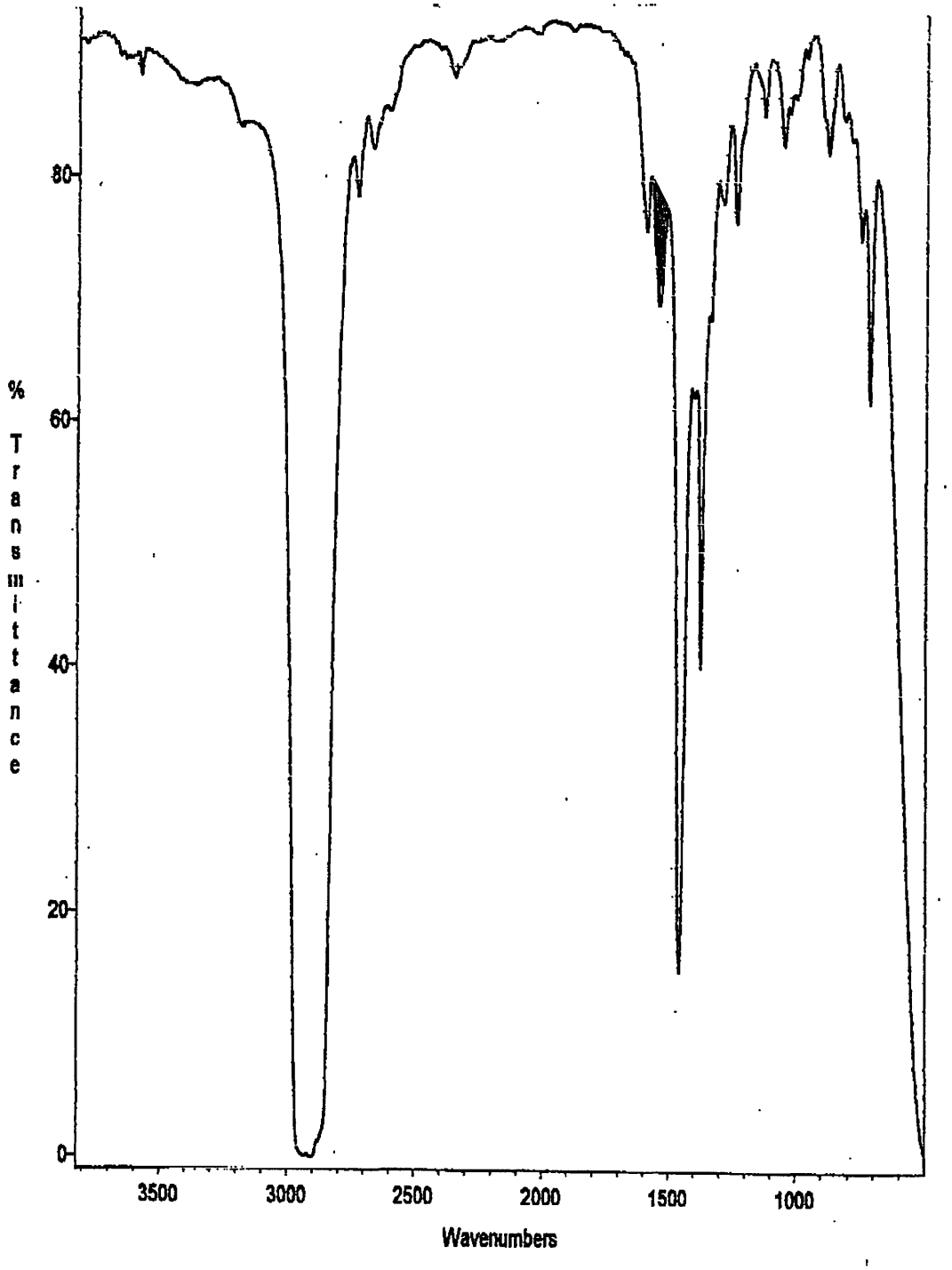

Figure 8.11. Infrared spectrum of the methanol wash. Salicylate peak ((COO^-) 1550cm^{-1}) is coloured blue.

8.3.2. Nuclear magnetic resonance spectrometry (NMR)

Aliquots of the individual clean up phases were diluted in deuterated chloroform and submitted for ^{1}H spectral recording.

Figures 8.12, 8.13 and 8.14 (pages 242 to 244) correspond to the first three fractions eluted from the column, being sample load, hexane wash and hexane : diethyl ether. Figure 8.12 shows clearly that the sample load consists mostly of aliphatic compounds. The aromatic proton signal was very weak, dwarfed by the aliphatic signal. Figures 8.13 and 8.14, the first two washes, again show the presence of aliphatic protons but with an increasing signal due to aromatic protons. Structural analysis is not really possible as mineral oils contain a variety of aliphatic linear and cyclic hydrocarbons as well as aromatic compounds, leading to a very complex spectrum of mixed components.

The spectra for the 2-butanone and methanol washes, figures 8.15 and 8.16 (pages 245 and 246) show many similarities. The FTIR results suggested the presence of salicylates in both the 2-butanone and methanol washes. In the methanol wash spectrum, the aliphatic protons (0-3ppm), when integrated from left to right give a ratio of 1:1:10:2 for the different environments. At 0.9ppm (a) (figure 8.15 & 8.16) we see signals due to methyl groups. From the ratios we can determine that the alkyl chain of the salicylate has a single branch. This is consistent with previous work that the alkyl chains of these types of metallic detergents are branched and in some cases highly branched, the branching being important for optimum performance and solvation of the micelles in lubrication oil.

In the aromatic region (6-8ppm), three less well resolved signals are present, with integration ratios of 1:1:1. This pattern fits exactly with the expected signals for the

salicylate. As stated the aromatic regions show low resolution, and the line broadening can be attributed to several factors. Sample viscosity will decrease the rate of sample relaxation causing broadening and loss of signal. The third region in the spectra is the carboxylic acid peak, which shows presence of free acid in addition to the salt. One signal that is not seen is the proton corresponding to the phenol. Comparison with the spectrum of salicylic acid (figure 8.17 page 247) shows it may not be seen.

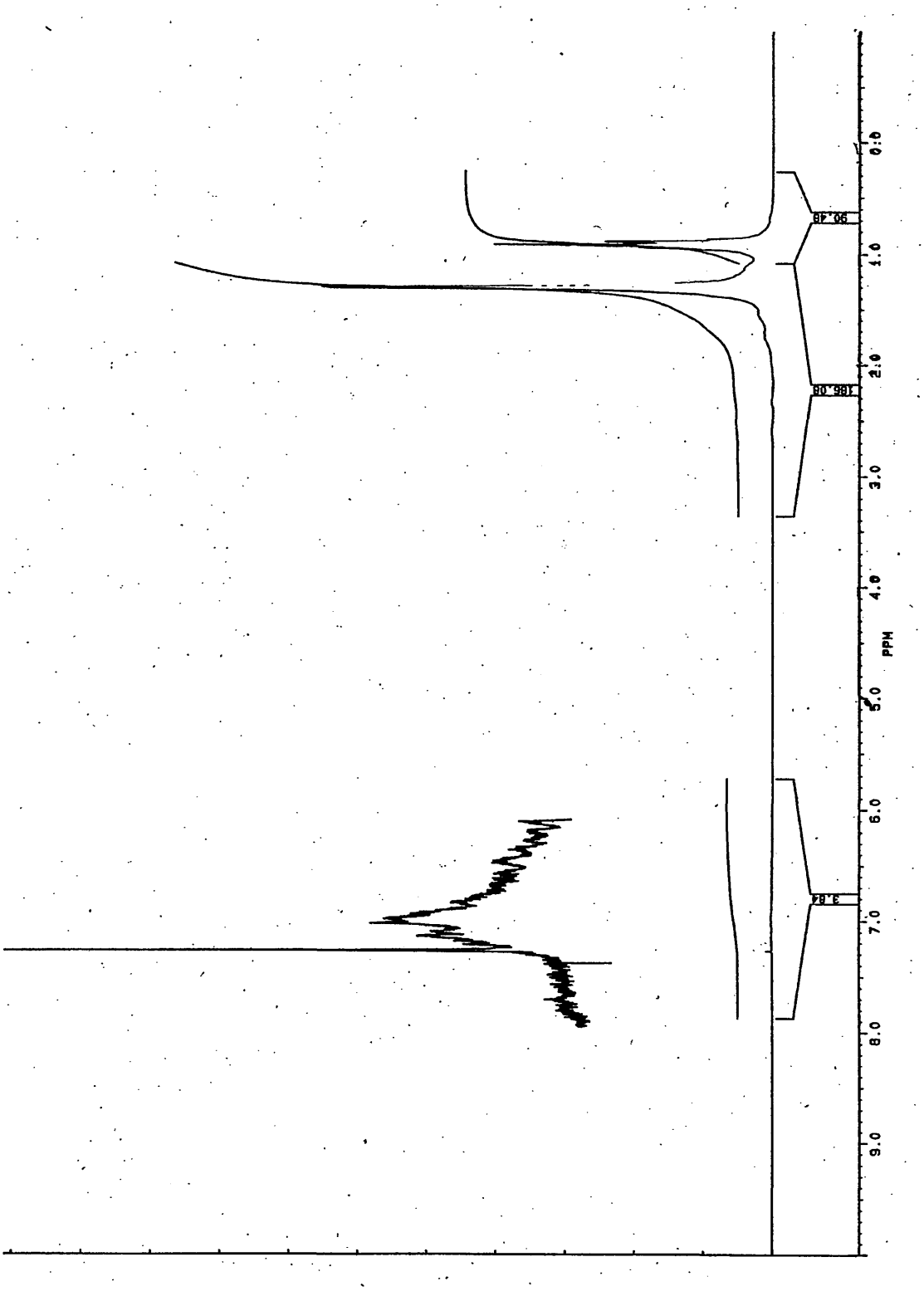

Figure 8.12. Proton NMR spectrum of the sample load from the SPE.

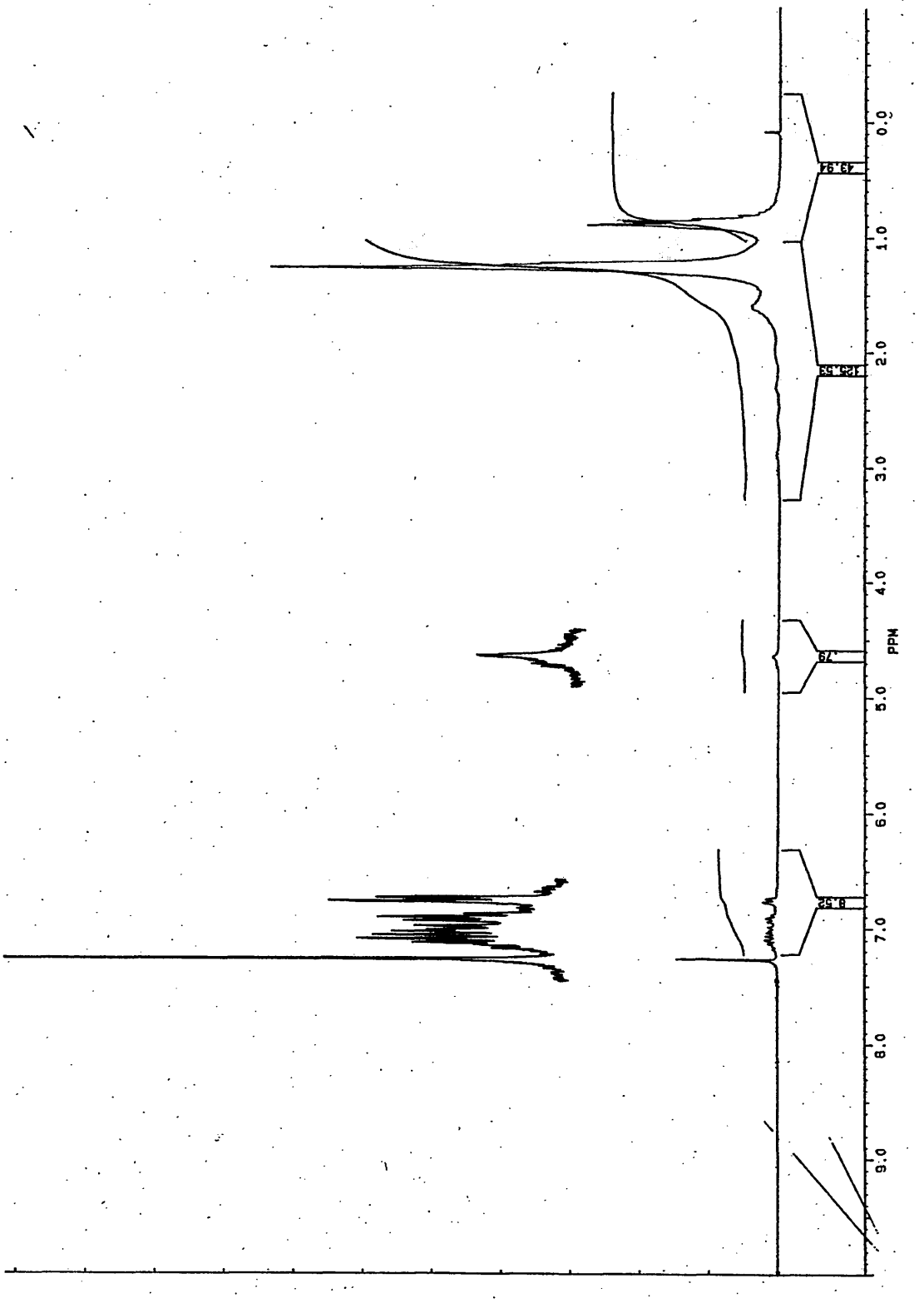

Figure 8.13. Proton NMR spectrum of the hexane wash from the SPE.

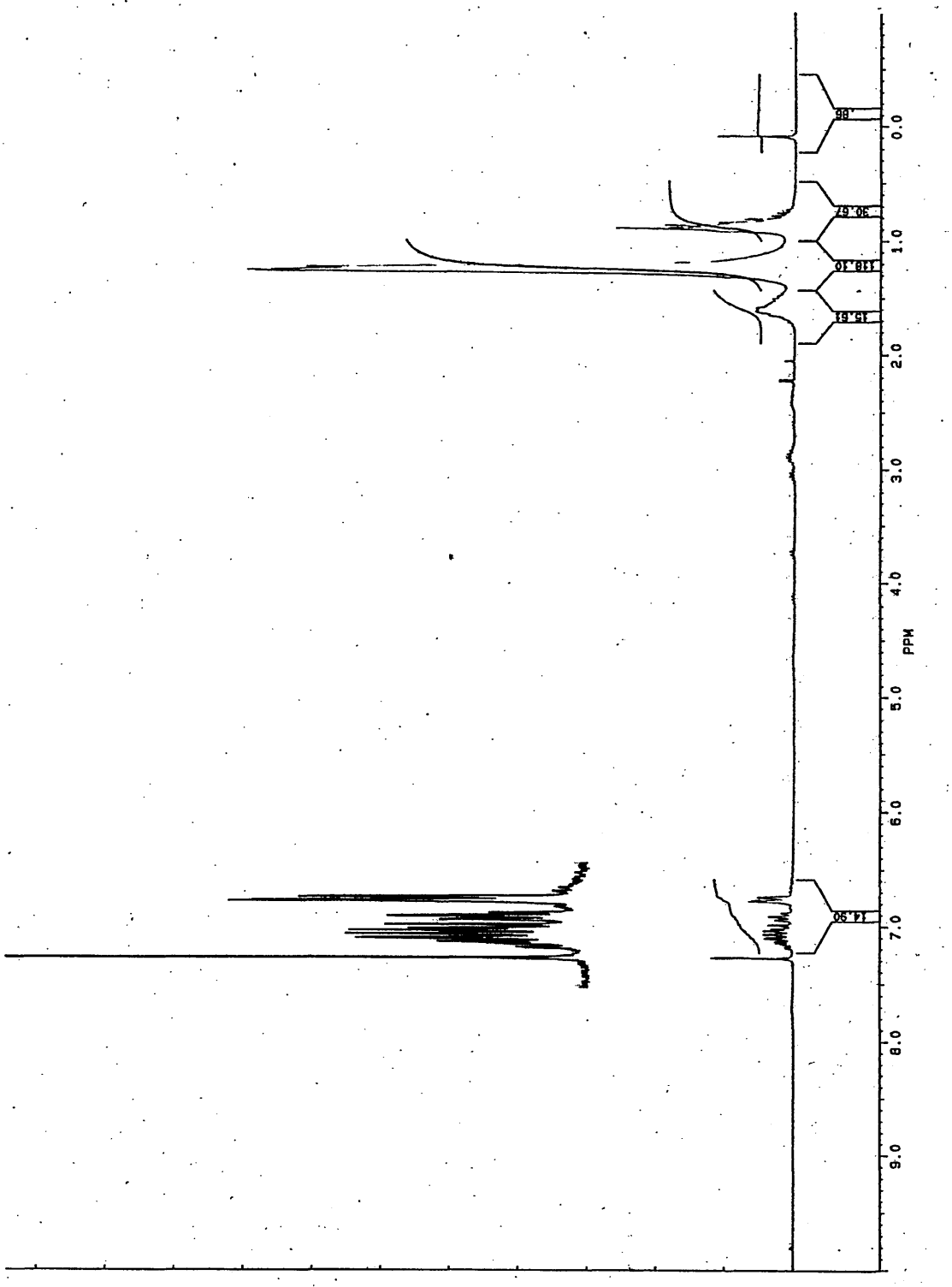

Figure 8.14. Proton NMR spectrum of hexane:diethyl ether wash from the SPE.

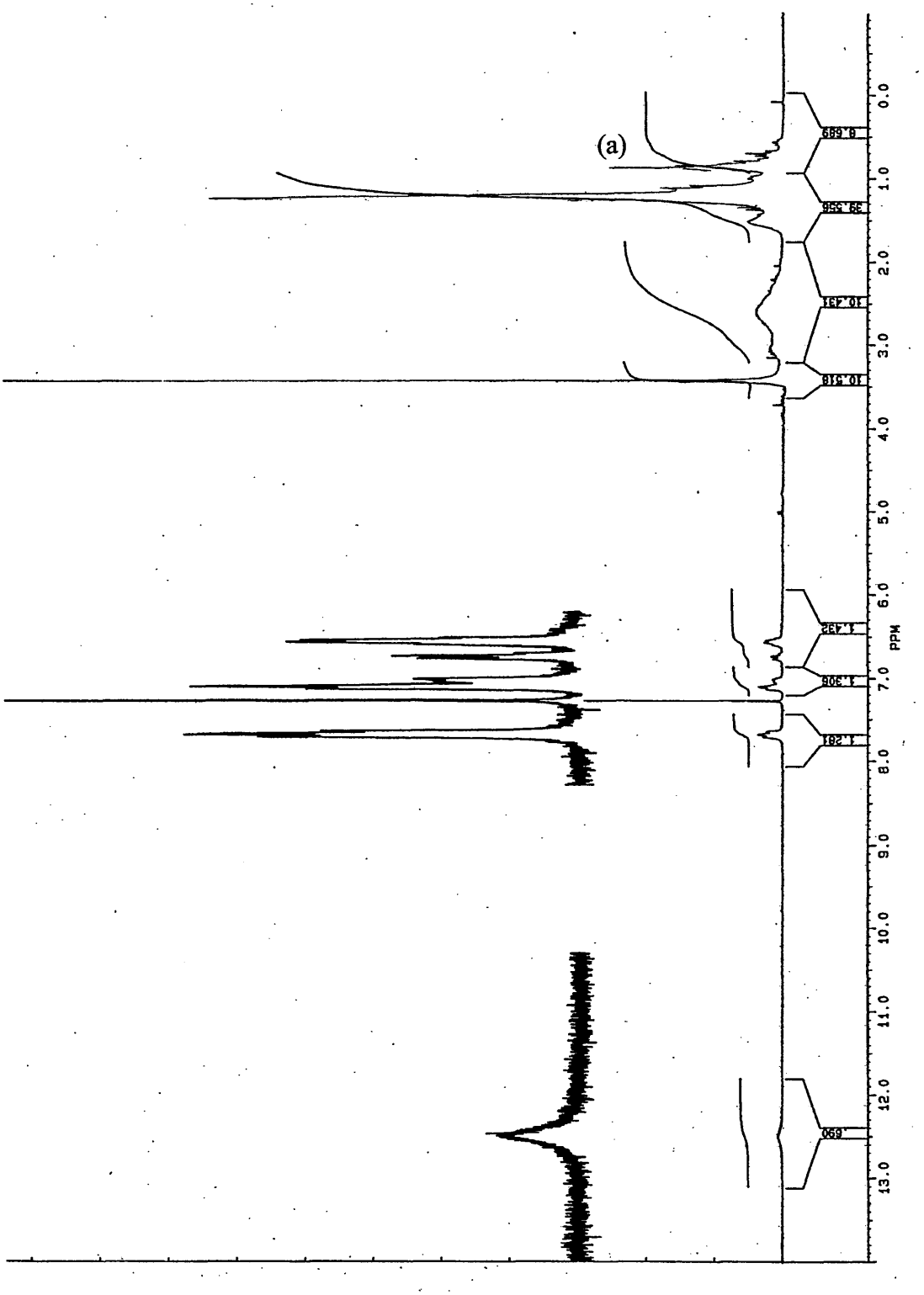

Figure 8.15. Proton NMR spectrum of 2-butanone wash from the SPE.

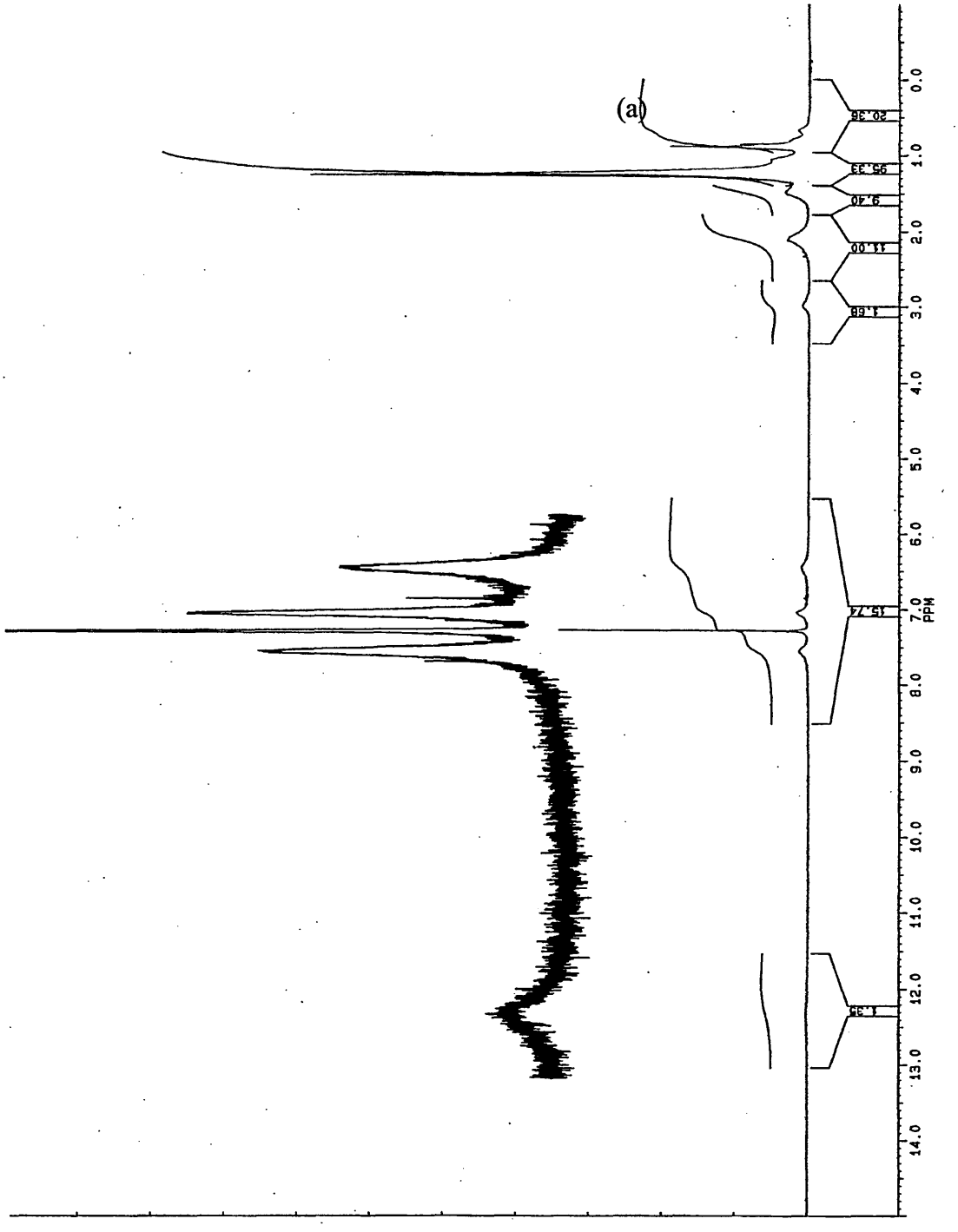

Figure 8.16. Proton NMR spectrum of the methanol wash from the SPE.

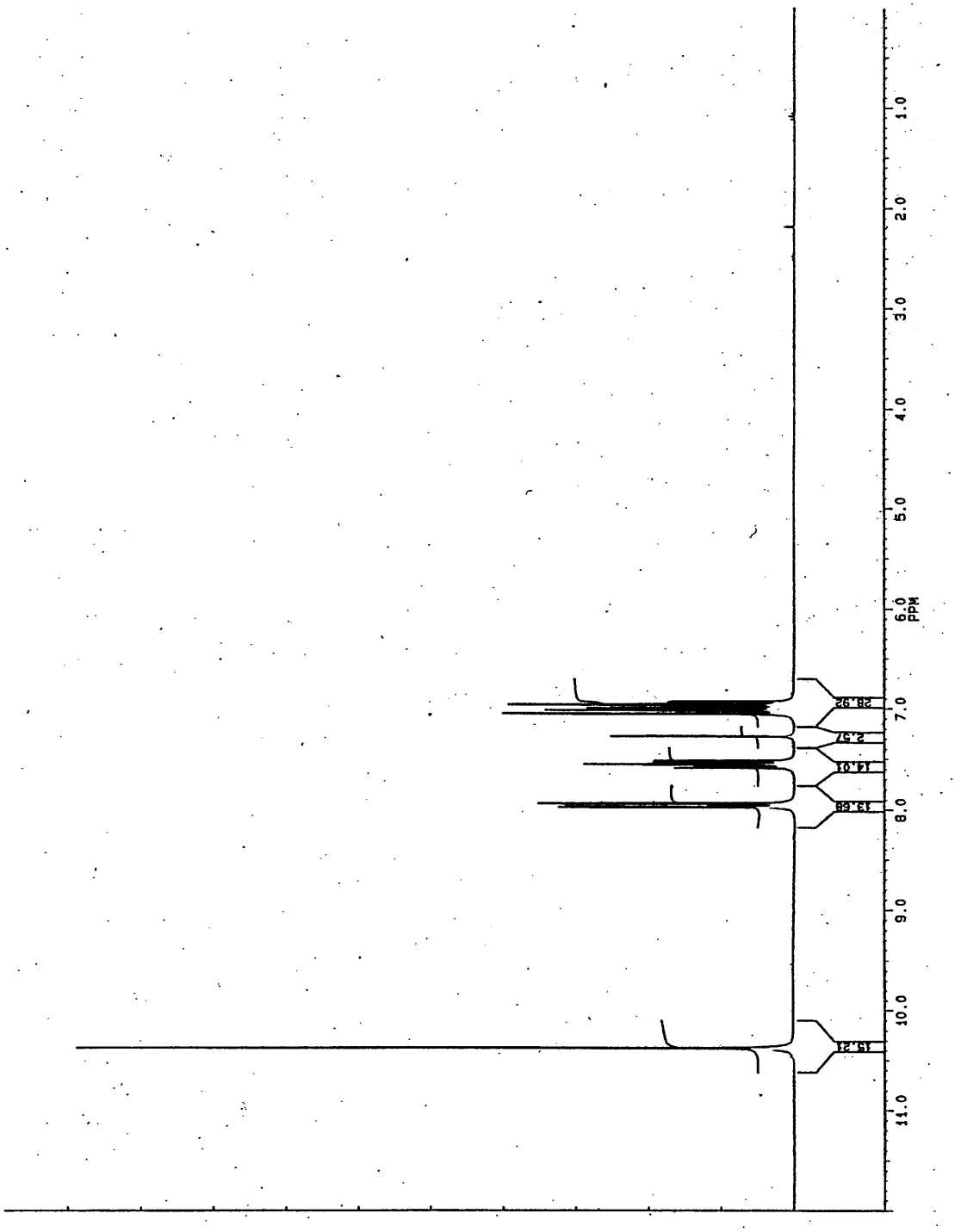

Figure 8.17. Proton NMR spectrum of salicylic acid.

8.3.3. Inductively coupled plasma optical emission spectrometry

Samples were prepared by wet digestion. A weighed quantity of sample was added to 5ml of cone, nitric acid in a beaker covered with a watch glass and gently heated. The end point of the reaction was determined by the cessation of gas evolution from the beaker. The remnants were then placed into a tube where they were diluted with deionised water (18MfI) so as to ensure that the results were within the instruments calibration range. The sample was then introduced into the plasma through the use of a peristaltic pump present on the ICP instrument.

Figure 8.18. Graph showing the elution trend of metals from the salicylate standards through SPE

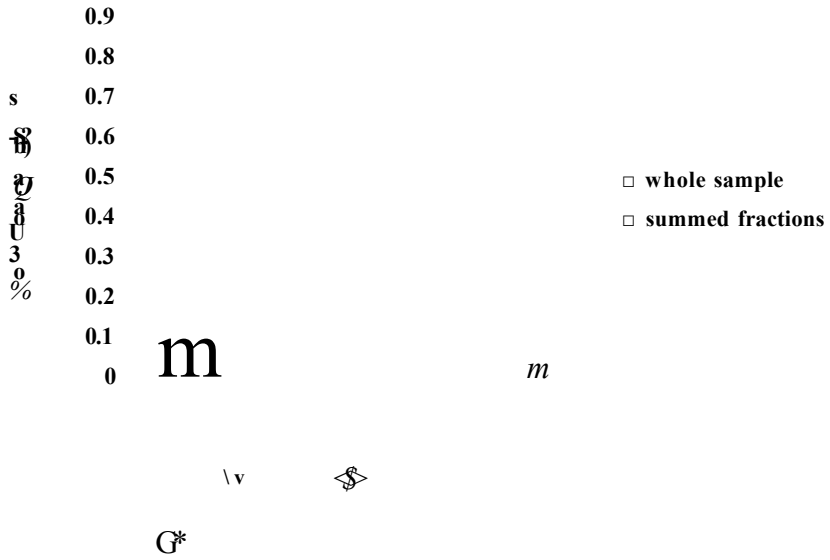

Figure 8.19. Comparison of the total metal content of the whole oil digest and with summed fraction digestions.

ICP-OES was carried out to determine the quantity of the metals calcium and magnesium eluted through each stage of the SPE process. As previously all the fractions were examined. Figures 8.18 and 8.19, show that the quantity of metal in the samples increased in line with the degree of overbasing.

It can also be seen that most of the metal was eluted in the loading phase, and thus the calcium was mostly unretained by the column. Knowing that most of the metals are associated with the carbonate, apart from those associated with the neutral salicylate, a correlation is evident with the results from infrared spectrometry in that most of the carbonate was present in the loading phase. Figure 8.18, shows that the content of magnesium in the magnesium salicylate is approximately the same as that of the calcium in the 64TBN salicylate.

Analysis of whole salicylate samples in a base oil show differences when compared to the SPE results (figure 8.19). The total mass of magnesium is seen to be similar to the 168 TBN rather than the 64 TBN. Also, the highest overbasing (calcium 280 TBN) showed much more calcium (210%) in the SPE than in the whole digest. This could be due to the inhomogeneity of the sample even after mixing, because of the high viscosity, although a more plausible explanation is that the wet digestion method used for this amount of sample was inadequate.

8.4. Conclusion

Results from FTIR spectrometry showed that most of the carbonate was eluted as soon as the sample was loaded and hence was not retained by the column. The salicylate was eluted partially in the 2-butanone fraction but mostly in the methanol wash, as evidenced by the peak at 1550cm^{-1} (COO^-). NMR spectrometry confirmed that the salicylate was eluted in the 2-butanone and methanol washes respectively, and also that some free acid was present. ICP-OES confirmed that most of the metal was eluted in the sample loading phase, in agreement with the FTIR results. From the alkyl salicylate structure (figure 8.1 page 223), most of carbonate and metal should be found in the inorganic core of the micelle.

Eluate	IR (Carbonate/Salicylate)	NMR (Salicylate)	ICP (Metal)
Sample load	Positive / Negative	Negative	High concentrations
Hexane wash	Positive / Negative	Negative	Trace concentrations
Hexanerdiethyl ether	Negative / Negative	Negative	Trace concentrations
2-Butanone	Negative / Positive	Positive	Trace concentrations
Methanol	Negative / Positive	Positive	Trace concentrations

Figure 8.20 Comparisons of analytical techniques used to identify contents of eluates.

It therefore seems that the SPE method disturbs the micelle and that the separation seen in CE is a separation of free salicylates, and not separation of micelles.

References

1 Griffiths, J.A., Bolton, R., Heyes, D.M., Clint, J.H., Taylor, S.E., Journal of the Chemical Society: Faraday transactions 1995, **91**, (4), 687-696.

2 Dong, J., Van DeVoort, F.R., Ismail, A.A., Lubrication Engineering 2000, **56**, (6), 12-20.

3. Stellman, C.M., Ewing, K.J., Bucholtz, F., Aggarwal, I.D., Lubrication Engineering 1999, **55**, (10), 45-52.

4 Baladincz, J., Vuk, J., Aver, J., Kis, G., Bartha, L., Hungarian journal of Industrial Chemistry 1998, **26**, 155-159.

5 Kutova, G.G., Ulanova, M.F., Fialko, M.M., Chemistry and Technology of Fuels and Oils 1998, **24**, (1-2), 15-17.

6 Kapur, G.S., Chopra, A., Sarpal, A.S., Ramakumar, S.S.V., Jain, S.K., Tribology Transactions 1999, **42**, (4), 807-812.

7 Inoue, K., Watanabe, H., ASLE Transactions 1983, **26**, (2), 189-199.

8 Sarma, A.S., Joshi, N.C., Journal of Scientific & Industrial Research 1998, **57**, 503-514.

9 Harrison, P.G., Brown, P., McManus, J., Wear 1992, **156**, 345-349.

10 Turunen, M., Peräniemi, S., Ahlgrén, M., Westerholm, H., Analytica Chimica Acta 1995, **311**, 85-91.

11 Al-Swaidan, H.M., Talanta 1996, **43**, (8), 1313-1319.

12 Escobar, M.P., Smith, B.W., Winefordner, J.D., Analytica Chimica Acta 1996, **320**, 11-17.

Overall conclusions

The objective of the work carried out was to investigate the usefulness of nonaqueous capillary electrophoresis, possibly in conjunction with mass spectrometry, in the analysis of lubricant additive systems.

NACE was used to analyse two additives, zinc dialkyldithiophosphates and alkylsalicylates. The use of NACE for the analysis of ZDDP has been reported previously; however, the work carried out here exploited the use of a reverse EOF and a simple buffer system, which is novel and a considerable improvement over previous methods. It has been possible to identify individual ZDDP products by the use of peak patterns and also relative migration times, although these are very close.

The use of NACE for the analysis of alkylsalicylates has shown this technique to be advantageous over TLC. TLC can take several hours to obtain results that show only that a surfactant is present within a formulated product. The use of NACE has shown it is possible to identify various alkylsalicylates by alkyl chain length. It has also been shown that it could be possible to identify the manufacturer of the alkylsalicylates by the use of peak patterns and relative migration times.

ICP, NMR and FTIR were used to determine whether the alkylsalicylates were analysed as monomers or as micelles. These analytical techniques have shown that the alkylsalicylates were separated as monomers.

The use of mass spectrometry as a detection technique for NACE was evaluated. Direct infusion was first used to identify the masses present for NACE-MS. NACE-

MS was difficult for the analysis of lubricant additives, because resolution was lost compared with uv detection and sensitivity was not adequate with the interface used.

The identification of formulated oil was attempted by NACE, NACE-MS and MS. In formulated oils where a large quantity of additives are present identification was successful with NACE, NACE-MS and MS. Identification problems occurred where formulated oils contained many additives in small quantities, especially for NACE-MS where a loss of resolution was seen along with a decrease in sensitivity. However NACE-MS was successful in the identification of some ZDDP degradation products, probably in the form of thiophosphates and phosphates and also nitrated alkylsalicylates in used oil.

NACE is a separation technique that could be a valuable tool for the lubricant industry, and has already shown improvements over thin layer chromatography. MS has been shown to be successful for the identification of lubricant additives. With future improvements NACE-MS could become an useful instrumental technique for analysis of lubricant additives.

Comparing this work to that of Thibon *et. al.*[1] improvements are seen, in that the separation is faster and the buffer is not as complex to make up. Using a reverse EOF allows this method to be compatible with mass spectrometry detection, unlike Thibon's method. Compared to the gas chromatography-mass spectrometry method utilised by Beechi *et. al.*[2], NACE has the advantage of not requiring any derivatization of the analyte to make it suitable for the separation, and the analysis time is quicker. Unlike gas chromatography NACE cannot separate isomers, but it does separate dialkyldithiophosphate groups for identification. Cardwell *et. al.*[3] provided a separation using normal phase high performance liquid chromatography, with an

adequate separation of ZDDPs that were eluted intact with the zinc complex. This does not seem to show any advantages to the NACE separation where only dialkyldithiophosphates groups are separated. Cardwell *et. al.*[4] used electrospray mass spectrometry for identification of ZDDP. However, their method required the addition of dimethylsulphoxide or dialkyldithiophosphate for the production of negative ions of dialkyldithiophosphates. The method here requires no excess of anions to produce identification of ZDDPs as sample standard or with the formulated oil products.

Compared to thin layer chromatography, the method developed here is far better in that identification of different alkylsalicylates with varying chain lengths can be carried out in under twenty minutes. Thin layer chromatography takes over an hour for the separation and staining, and the results are much less clear.

NACE therefore shows considerable promise for the analysis of lubricant additives.

References

1. Thibon, V.R.A., Bartle, K.D., Abbott, D.J., McCormack, K.A., Journal of Microcolumn Separations 1999, **11**, (1), 71-80.

2. Beechi, M., Perret, F., Carraze, B., Beziau, J.F., Michel, J.P., Journal of Chromatography A 2001, **905**, 207-222.

3. Cardwell, T.J., Lambropoulos, N., Caridi, D., Marriott, P.J., Journal of Chromatography A 1996, **749**, 87-94.

4. Cardwell, T.J., Colton, R., Lambropoulos, N., Traeger, J.C., Marriott, P.J., Analytica Chimica Acta 1993, **280**, 239-244.

Future work

Although the work carried out here has been successful and demonstrated that NACE is a viable analysis technique for the lubricant industry, there is room for improvement.

Further improvements may be brought about by the inclusion of additives to the buffer, such as ion pair agents or cyclodextrins that can act as pseudo-stationary phases with which lubricant additives interact. The lubricant additives will interact differently with the pseudo-stationary phase and therefore migrate through the capillary with greater differences in mobility. Capillary electrochromatography is another technique that might improve the separation by the use of a stationary phase packed within the capillary. The lubricant additives interact with the stationary phase altering their mobilities. Improvements to the separation will improve the results obtained by analysis using NACE-MS.

Analysing mixtures of additive standards will improve the understanding of working additives by identifying compounds resulting from possible interactions present in the formulated product. The products can then be attributed to certain additives leading to a greater understanding of formulated oils in how they function and degrade.

Research carried out here has opened up a whole new world of analysis techniques for lubricant additives, and years of future research.